General Disclaimer

One or more of the Following Statements may affect this Document

- This document has been reproduced from the best copy furnished by the organizational source. It is being released in the interest of making available as much information as possible.

- This document may contain data, which exceeds the sheet parameters. It was furnished in this condition by the organizational source and is the best copy available.

- This document may contain tone-on-tone or color graphs, charts and/or pictures, which have been reproduced in black and white.

- This document is paginated as submitted by the original source.

- Portions of this document are not fully legible due to the historical nature of some of the material. However, it is the best reproduction available from the original submission.

jpl

JET PROPULSION LABORATORY
CALIFORNIA INSTITUTE OF TECHNOLOGY
PASADENA, CALIFORNIA

750-73

SHUTTLE SYNTHETIC APERTURE RADAR IMPLEMENTATION STUDY

VOLUME I

March 8, 1976

John G. Mehlis

CONTRACT NAS7-100
(TASK ORDER NO. RD-164)

JET PROPULSION LABORATORY
CALIFORNIA INSTITUTE OF TECHNOLOGY
PASADENA, CALIFORNIA

LIST OF CONTRIBUTORS

JPL

T. Bicknell
W. Brown
J. Brown
E. Caro
E. Cohen
J. Granger
R. Gray
R. Jordan
J. Junkins
A. Laderman
A. Lawson
E. McMillan
J. Mehlis
D. Sedgwick
J. Wang

GOODYEAR AEROSPACE CORPORATION

R. Manning
L. Moyer

BALL BROTHERS RESEARCH CORPORATION

R. Munson
G. Sanford

ENVIRONMENTAL RESEARCH INSTITUTE OF MICHIGAN

G. Adams
I. Cindrich

GLOSSARY

S/N	Signal-to-noise ratio
PRF	Pulse repetition frequency
τ	Compressed pulse width
ΔF	Linear bandwidth
B	Linear bandwidth
T	Expanded pulse width
r_s	Slant range resolution
c	Speed of light
r_r	Ground range resolution
θ	Surface angle
α	Off-nadir angle
TBP	Time-bandwidth product
Δf_D	Doppler bandwidth
T_c	Coherent time
ρ_a	Azimuth ground resolution
v_s	Radar platform velocity
λ	Wavelength
R_s	Slant range
R_e	Radius of Earth
h	Altitude of radar
ψ	Angular displacement between radar platforms and target, measured at center of Earth
γ	Main response broadening
$(T\Delta f)_{AZ}$	Azimuth time bandwidth broadening
P_t	Peak transmitter power
P_{AV}	Average transmitter power
G	One-way peak antenna gain
σ°	Backscatter coefficient
K	Boltzman's constant

T_s	System noise temperature
T_a	Antenna noise temperature
T_r	Transmission-line noise temperature
T_e	Receiver noise temperature
NF	System noise figure
α_{AZ}	Azimuth beamwidth
η	Antenna efficiency
A	Aperture area
L_r	Transmission-line loss during reception
S/A	Signal-to-ambiguity ratio
S(f)	Doppler power spectrum
F	Doppler processing bandwidth
SW	Ground swath width
L_a	Antenna aperture length
n	Normalized sampling rate
T_{sw}	Imaged swath time
T_s	Width of transmitted pulse
T_d	Receiver recovery time
τ_d	Delay between nadir echo and center of swath
DR	Data rate
Q	Analog-to-digital quantization bits
M	Number of looks

TABLE OF CONTENTS

TABLE OF CONTENTS (contd)

TABLE OF CONTENTS (contd)

LIST OF TABLES

LIST OF FIGURES

LIST OF FIGURES (contd)

1.0 EXECUTIVE SUMMARY

1.1 FORWARD

This report is a required deliverable by the Jet Propulsion Laboratory (JPL) to the Lyndon B. Johnson Space Center (JSC) under the terms of the contract "Imaging Radar for the Shuttle - System and Subsystem Definition Study."

Described herein are the results of an implementation study for a Synthetic Aperture Radar for the Space Shuttle Orbiter. The report is in two volumes: the first being the system analysis study and preliminary hardware definition, the second being the cost estimates and management plan. The overall effort has been directed toward the determination of the feasibility and usefulness of a multifrequency, multipolarization imaging radar for the Shuttle Orbiter. The radar is intended for Earth Resource monitoring as well as oceanographic and marine studies.

From literature surveys (the results of the active microwave workshop and direct contact with scientists using radar imagery), a set of system guidelines was established for a Shuttle Synthetic Aperture Radar (SAR) with a broad applicability for Earth observations. These guidelines, listed in Section 2, have been discussed in earlier reports submitted during this program.[1,2]

Several candidate imaging radar systems were analyzed, studied, and evaluated as scientific sensors and their abilities to meet user requirements of such variables as wavelength, polarization, swath widths, calibration, off-nadir angles, etc. Various data handling schemes have been investigated and evaluated on the basis of user needs. The Hughes Aircraft Corporation conducted parallel studies based on the JPL-generated guidelines.

The particular choice of system has been dictated by JSC, based on the candidate system studies presented to JSC by JPL and the Hughes Aircraft Corporation in January 1975. The system (an X and L-band, dual-polarized SAR) represents a compromise which can provide high quality

radar imagery useful in a wide variety of significant applications and which is consistent with Shuttle constraints. In addition to the candidate system studies, several other reports have been delivered during the course of this effort which have contributed to the choice of the reported system. The system, however, is not necessarily the final choice of either JPL or JSC, and the implementation study given here should be regarded as an example based upon what is presently the most promising candidate system.

There are no options presented to the fully focused SAR system. The position is taken that the instrument must expand the capabilities of the SEASAT-A SAR. Analysis of other options have been required as part of the continuation of this effort and will be an output of the FY 1976 study.

1.2 REPORT SUMMARY

The shuttle SAR consists of a flight instrument for collecting the raw imaged radar data and a ground data processor system, used both for processing the radar data and for recording the resulting imagery on photographic and computer-compatible tape.

The flight sensor consists of two high-powered, dual-polarized coherent pulse radars; one operating at L-band, and the other at X-band. During data-taking operations, the receiver output signal is converted to digital form and then recorded on digital tape. Data on the digital tape can be either transmitted via a digital data link to a ground receiving terminal, or the digital tape can be delivered to the ground processing center after end of flight. In either event, the data tape is the source of imaged data inputs to the ground processor system, where the tape is processed. The ground processor system is designed to provide the users with the kinds of SAR data they need in a timely and convenient fashion. The data outputs available to users will be of two kinds: imaged computer-compatible tapes and an imaged photographic copy. These imaged outputs will have a maximum swath width of 100 km and a minimum resolution of 25 meters.

In summary, from user requirements and shuttle constraints, the proposed Shuttle SAR has the baseline characteristics shown in Table 1-1.

Table 1-1. Shuttle SAR Baseline Parameters

	Parameter	
1.	Altitude	185 km (nominal
2.	Frequency	L-band and X-band
3.	Polarization	Dual (HH, HV or VV, VH)
4.	RF Signal-to-Noise Ratio	≥10 dB
5.	Spatial Resolution	25 and 50 meters
6.	Imaged Swath Width	100 km (max), 40 km (min)
7.	Off-Nadir Angle	25, 38, and 50 degree capability
8.	Minimum Scattering Coefficient	-20 dB at 20°, -25 dB at 50°
9.	PRF Range	1615 to 1900 pulses/second
10.	System Bandwidth	17.38 MHz
11.	Transmitter Pulse Width	23 microseconds (L-band)
		21 microseconds (X-band)
12.	Peak Transmitter Power	6 kw (L-band)
		20 kw (X-band)
13.	Antenna Envelope	12 m by 3 m
14.	Multiple Looks	4 (min) to 32 (max) both in azimuth and range
15.	Image Dynamic Range	50 dB
16.	Image Gray Scale Resolution	1 dB
17.	Weight (flight SAR)	310 kg
18.	Volume (flight SAR)	1.72 m^3
19.	Power (flight SAR)	6.62 kw

1.2.1 Selection of Frequency and Antenna Envelope Frequency

Initially, three frequencies (L, X, and K_u) were considered on the basis of user inputs. The candidate systems which were studied in detail by JPL were single-frequency X and L-band systems, a dual-frequency X and L-band system, and a three-frequency L, X, and K_u-band system. JPL recommended that the study concentrate on the dual-frequency X and L-band system as the most promising compromise between total user satisfaction and ease of implementation. This recommendation was accepted by JSC, and JPL was directed to proceed with the implementation study. Subsequently, JPL was directed to investigate K_u-band as an alternative to X-band in the dual-frequency system. It was determined that the superiority of K_u-band in the vegetation resource area and its ability to identify small-scale roughness, such as capillary waves, was more than offset by difficulties in implementation. This is particularly true of the antenna which potential vendors regarded as a high-risk item.

Antenna Envelope

The selection of a planar array antenna length of 12 meters was determined as the required to give a 100 K_u swath width at the greater look angle length that could be accommodated on a pallet in its folded configuration. The 3-meter width was selected at a maximum that could be accommodated without folding on the pallet, as the length of each pallet is 3 meters.

1.2.2 Functional Requirements

Two functional block diagrams of the overall Shuttle SAR are shown in Figures 1-1 and 1-2 and are briefly described below.

Shuttle Orbiter SAR (Figure 1-1)

The antenna utilizes a rectangular array, with proper feeds coupled to a common aperture to generate three independent beams for each of the three off-nadir angles, and allows both horizontal and vertical polarization. The antenna will be positioned in the pallet area to obtain a compact launch profile and be deployed when in orbit. During orbit, the antenna will be mechanically positioned at the selected off-nadir

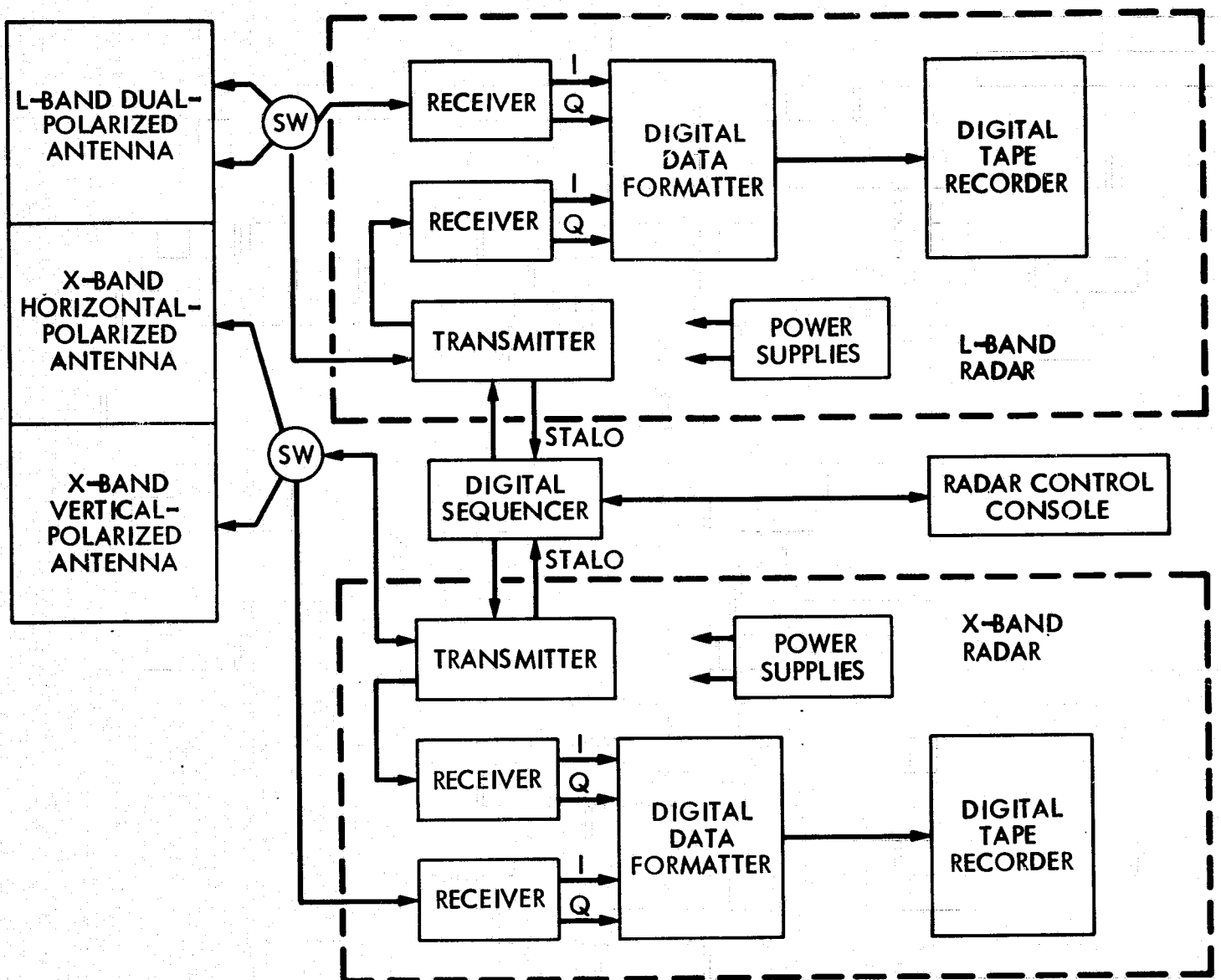

Figure 1-1. Shuttle SAR Functional Block Diagram (Shuttle Orbiter)

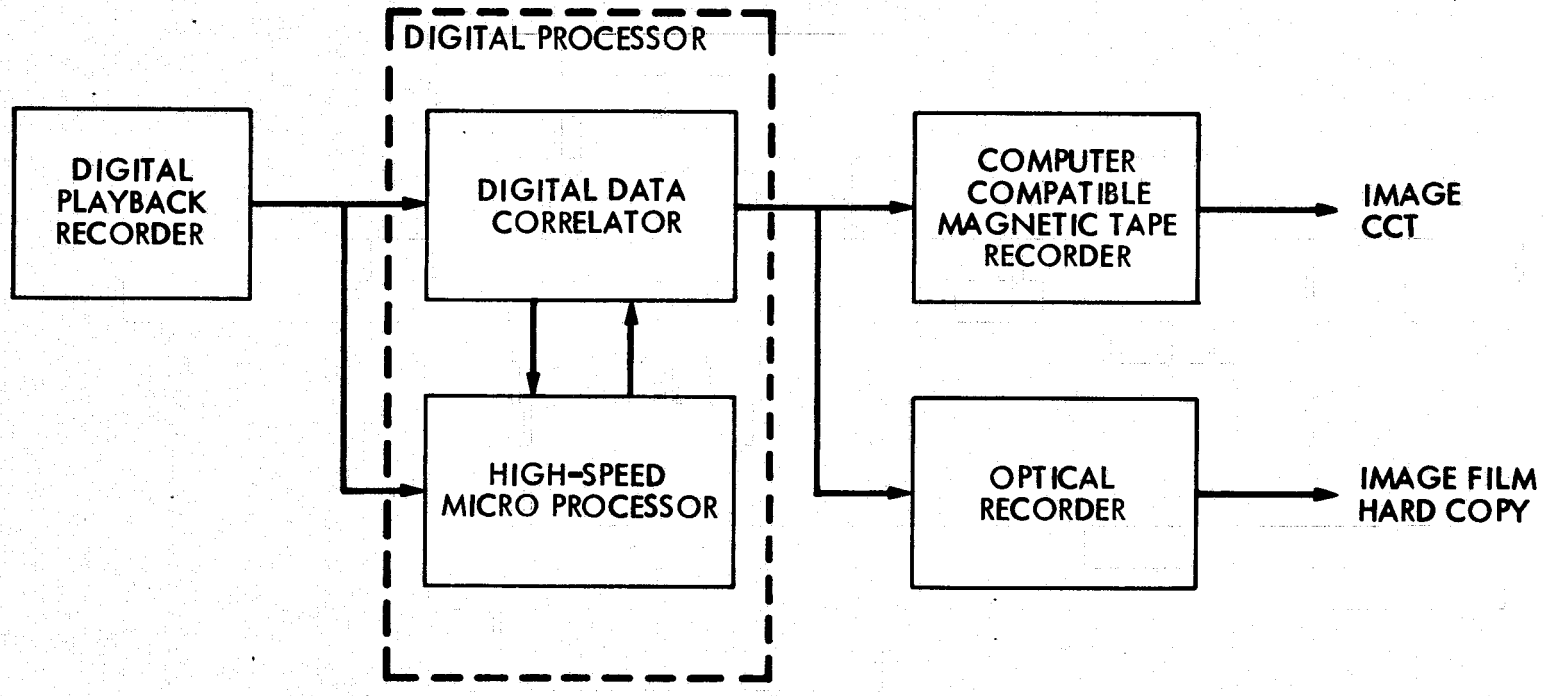

Figure 1-2. Shuttle SAR Data Center Functional Block Diagram

angles. The antenna consists of three deployable antennas. These are: one L-band dual-polarized antenna, and two X-band single-polarized antennas. Dual polarization at X-band is not feasible to attain on a single planar array antenna, as efficiency would be degraded.

Both frequencies utilize TWT transmitters to attain the required side-lobe control by minimizing phase amplitude deveiations. TWTs were selected because solid state devices currently are not capable of producing the necessary peak power outputs.

Low noise receiver front ends are used, transistor amplifiers at L-band and parametric amplifiers at X-band, for overall noise figures of 3 dB.

The STALO has been optimized for maximum reliability by deriving all timing and microwave sources from one primary source, utilizing frequency multipliers and dividers. Either the L- or X-band STALO frequency will be used as a master frequency standard for both radars.

The digital sequencer provides all logic and timing functions for the radar. From its connections with the control panel, it provides all the turn-on and mode-selection commands for the radar.

The digital data formatter is used for parallel/serial conversion and formatting of radar data prior to its insertion into the high-density digital tape recorder. Commands, timing, and logic functions will also be part of the digital data formatter.

The control console will be available to an operator, with the capability of selecting a number of radar functions described in Section 3.1.

High-density digital tape recorders will be used to record and store radar data that will be subsequently processed on the ground by the data system.

A power drain of less than 7 kw is indicated for the on-board Shuttle Orbiter SAR.

Shuttle SAR Data Center (Figure 1-2)

The digital playback recorder will be used to play back the stored radar data that was gathered by the Orbiter SAR.

The ground digital processor will perform the function to compress the radar data in range and azimuth. Weighting will be applied to the data to reduce sidelobe levels. Clutter tracking will be provided to remove the Doppler offset due to the Earth's rotation. Range walk and range curvature corrections will also be performed. This baseline processor will be capable of processing a 100-km range swath to azimuth and range-resolution elements 25m by 25m. The minimum system will have the capability of four azimuth multilooks and one in range.

The SAR data center will produce two kinds of data outputs available to users. These output are: digitized images on computer compatible tapes and hard copies in the form of photographic image strips. Both types of outputs will include calibration and navigational indexing.

1.2.3 Implementation Summary

Section 2 contains the results of the system tradeoff studies and gives the radar parameters and configuration of the selected L- and X-band imaging radar system. Radar parameters of a Ku-band radar system appear in the appendix.

Section 3 contains hardware specification details of the selected candidate radar subsystems. The results of a subcontractor antenna study are included as an appendix to this report.

Section 4 describes the ground data system and shows how data from a sortie mission will be processed into an image. Subcontractor reports on optical and digital processors are included as appendices to this report.

The environmental characteristics and acceptance tests, the reliability and quality assurance plans, and a suggested flight test program are given in Sections 5, 6, and 7 respectively.

1.3 SUPPORTING DOCUMENTATION

Reports dealing with applications studies adn image interpretability will be submitted at a later date. The Equipment Implementation Plan, Work Breakdown Structure, Schedule, cost estimate, and management plan for the radar development are presented as Part II and will be submitted separately as directed by JSC.

REFERENCES

1. J. G. Mehlis and E. A. Cohen, "Shuttle Imaging Radar Guidelines," submitted April 1974.

2. E. A. Cohen and J. G. Mehlis, "Shuttle Imaging Radar Study — System Definition Update," submitted November 1974.

   a. "Support of Imaging Radar for the Shuttle — System and Subsystem Definition Study," Texas A&M University, Remote Sensing Center, Report on Contract No. 141850, November 1974.

   b. "Applications of Imaging Radar" — A Bibliography, University of Kansas, Remote Sensing Laboratory, Report on Contract No. 141849, November 1974.

   c. "Bibliography of Imaging Radar Systems Design and Imaging Radar Data Processing," Environmental Institute of Michigan, Report on Contract No. 141848, November 1974.

2.0 RADAR SYSTEM ANALYSIS

2.1 RADAR RATIONALE AND DESIGN SUMMARY

The function of the Shuttle-borne radar is to provide imagery for use in Earth-resource and oceanographic applications.

The SAR has the capability of mapping the entire United States; the imagery, however, must have a high degree of resolution to be meaningful. The diverse users require a resolution on the order of 25 meters. Attaining this resolution at the Shuttle altitude is not feasible without signal processing, as opposed to simply relying on the track and cross-track dimension as determined by the antenna resolution and transmitted pulse width, respectively.

Pulse compression-processing techniques enable achievement of range resolutions by transmitting a pulse whose frequency is dispersed linearly. Upon reception, this pulse is compressed by passing it through a digital dispersive-delay line whose time delay is a function of frequency. All frequency components of the pulse then occur at the same time and the pulse is compressed to a fraction of its transmitted length, thus achieving a high resolution. Binary-coded waveforms can be used as a pulse compression technique; however, a linear FM pulse compression implementation is used as an example for this radar.

The along-track or azimuth resolution improvement is achieved by processing over the linearly changing doppler frequencies for each point target as the target passes through the antenna beam. This technique of matched filter-azimuth processing (known as Synthetic Aperture Radar (SAR)) provides a much finer along-track resolution than that permitted by the linear extent of the physical beam itself.

JPL's design approach is that the maps and imagery obtained are to be used for scientific evaluation of Earth resources and must be of high obtainable quality compatible with the diverse users requirements.

Imagery of the required quality can be achieved through the design approach in the following areas: antenna patterns, resolution, azimuth and range ambiguities, adequate signal-to-noise (S/N) ratio, multilook capability, off-nadir angle, and coordinated subsystem specifications to ensure overall system performance.

Ambiguites are a fundamental factor in the radar design (see Section 2.3.7). Specified values will be placed on them as they form tradeoff constraints on system design.

An image RF S/N greater than 10 dB is required for optimum calibrated backscatter coefficient measurements for a clutter cell of low reflectivity with a minimum value of -20 dB at 20° off-nadir angle and -25 dB at 50° off-nadir angle. The above S/N ratio should allow backscatter determination of poor reflectors.

Map quality is enhanced through the use of multilook techniques, which generate a single image from the average of spectrally independent images, thus, reducing the speckle caused by the statistical variation of the returns from each reflector. If other system parameters are constant, the number of looks attainable varies as the area of the resolution element. The proposed radar design has a 25-m resolution and is configured as a four- or eight-look system, depending on which off-nadir angle is used. Fifty-meter resolution is also available and would be configured as a 16- or 32-look system.

As each subsystem in the radar can introduce noise or sidelobes, tight coordinated subsystem specifications are necessary to hold their contribution to -30 dB or better of the primary target response. Preliminary specifications of major functional requirements and error tolerance allocated to each one is presented. These specifications are necessary to itemize estimates for such parameters as weight and power consumption to develop a credible system design. This is presented in Section 3.0.

As a baseline from Shuttle Orbiter an antenna length requirement of 12m x 3m was desired and realizable ambiguity levels will be determined from tradeoff studies.

A summary of the selected L- and X-band dual-frequency radar system and system parameters for an altitude of 185 km are given in Table 2.4.1 and is a result not only of system parameter tradeoffs and basis of radar design (see Section 2.3.6) but it is determined as the most acceptable minimum system that would satisfy most user requirements. Some of these parameters such as altitude, range resolution, frequency, signal-to-noise, noise figure and antenna dimensions were used as design criteria. Given the shuttle power constraints and the S/N

ratio, ambiguity level and resolution requirements, the design rationale was to maximize imaged swath width and minimize antenna area for each of the three off-nadir angles.

2.2 SYSTEM REQUIREMENTS

The radar system designs are heavily dependent upon such Shuttle parameters as altitude and velocity. A number of parameters influence image quality. These include signal-to-noise ratio, resolution, ambiguity levels, and number of looks.

System guidelines are given in Table 2.2.1. The Shuttle altitude is significant in that signal-to-noise ratio, swath width, and off-nadir angle are heavily affected by altitude. The 185 km orbital altitude indicated was selected as nominal for this study. The orbit characteristics affects mapped areas as well as the time per orbit. The eccentricity, Earth oblateness and local relief displacement affect the transmit/receive time. The on time/orbit is a rough estimate of the time that Shuttle will be above the continental United States. Unprocessed imaged data will be formatted on a on-board data storage system.

The antenna azimuth aperture dimension determines the return doppler spectrum which then is of significant interest in evaluating azmiuth ambiguities, resolution, number of azimuth looks and PRF. The elevation aperture is of concern in that it defines the elevation beam shape and the signal strength variation over the imaged swath. Further, the elevation aperture determines range ambiguities over the swath width for a given PRF. A common planar array antenna is configured such to produce three independent beams at the three off-nadir angles and frequencies.

A pre-processed RF image signal-to-noise requirement of greater than 10 dB is specified for optimum calibrated backscatter coefficient measurements for a clutter cell of low reflectivity with a minimum value of -20 dB at 20 deg off-nadir angle and -25 dB at 50 deg off-nadir angle. This S/N ratio should allow backscatter determination against poor reflectors. Another parameter which affects image quality is the number of looks. The more the number of looks, the less the image grainyness and better the image quality.

Table 2.2.1. System Guidelines

Shuttle Altitude

185 km (nominal)

Orbit Characteristic

Circular, 55 degree inclination angle

Orbit period

≈100 min

On Time/Orbit

12 minutes

Frequency

L-Band
X-Band

Antenna size

Planar array 12m x 3m

Polarization

Dual

Image RF signal-to-noise ratio

10 dB with σ° min = -20 dB at 20° off-nadir angle
σ° min = -25 dB at 50° off-nadir angle

Ground resolution

25m (nominal at beam center)

Imaged Swath width

100 km (max), 40 km (min)

Ambiguous Responses

<-18 dB

Off-Nadir Angle

20 - 50 degrees

An additional factor directly contributing to image quality is ambiguous responses. These responses result from such system imperfections as: linear distortion in amplitude or phase of system elements, improper selection of PRF after consideration of swath width and antenna patterns, and video limiting or nonlinear distortion. Inadequate suppression of these result in the appearance of false targets and poor map background. More than 30 dB suppression is desired.

2.3 DEVELOPMENT OF RADAR PARAMETERS AND TRADEOFFS

This section discusses how the various radar system parameters such as frequency, polarization, power, PRF, bandwidth, resolution, swath width, etc., were derived. To determine these, radar performance parameters such as signal-to-noise ratio, swath width and ambiguity suppression will be calculated. All parameters were derived under the system constraints and guidelines discussed in Section 2.2. The purpose of this section is to show what radar parameters are required to achieve given system performance.

2.3.1 Frequency

It would be desirable from the user viewpoint to observe the Earth at all microwave frequencies. Only certain frequencies can be implemented and two frequencies of broad user interest appear to be L- and X-bands. These are also desirable frequencies from the standpoint of accessibility of components such as transmitter tubes, low noise receiver front ends and antenna components.

2.3.2 Polarization

Users have indicated definite interest in observing the Earth at different polarizations simultaneously with multifrequency radars. Users interest is almost exclusively centered on comparing like and cross polarized imagery, i.e., transmit with horizontal polarization (H) and receive on both horizontal (H) and vertical (V) polarization. These are known as HH and HV. If transmission is with vertical polarization, the pair is VV and VH. A choice of these two will be provided by mechanizing the transmitter to transmit on either H or V and by mechanizing two receiver channels, one for H and one for V.

2.3.3 Resolution

Users indicated desired resolutions varying from 10m to 100m. As a guideline, 25m was given as a design goal resolution; this will be taken as the requirement for system tradeoffs. An additional resolution of 50m is also available.

The 25m resolution is defined as the 3 dB width of the resolution cell in both range and azimuth dimensions.

Range Resolution. In order to achieve high range resolution a linear frequency modulated or a chirped pulse is necessary. The transmitted/stalo generates an expanded pulse of width T with a linear bandwidth Δf. Upon reception, this expanded pulse is compressed to a pulse of width τ, where

$$\tau = 1/\Delta f = 1/B \tag{1}$$

Wf is the range bandwidth B. This compressed pulsewidth is related to range resolution by

$$r_s = c\tau/2 \tag{2}$$

where c = speed of light = 3×10^8 m/sec.

The compressed pulse is in the form of sin x/x with a -13.4 dB peak sidelobe level. If unsuppressed, these sidelobes can appear as false targets on the map. These sidelobes may be suppressed to any desired level by spectral amplitude weighting. In addition to suppressing sidelobes, the weighting broadens the mainlobe. This effect is shown in Figure 2.3.1. Assuming a Taylor weighting function that suppresses sidelobes to -30 dB, the main response of the compressed pulse will be broadened by 26 percent. The range bandwidth B must then be compensated with a resolution 26 percent better than the net desired resolution by

$$B = 1.26/\tau \tag{3}$$

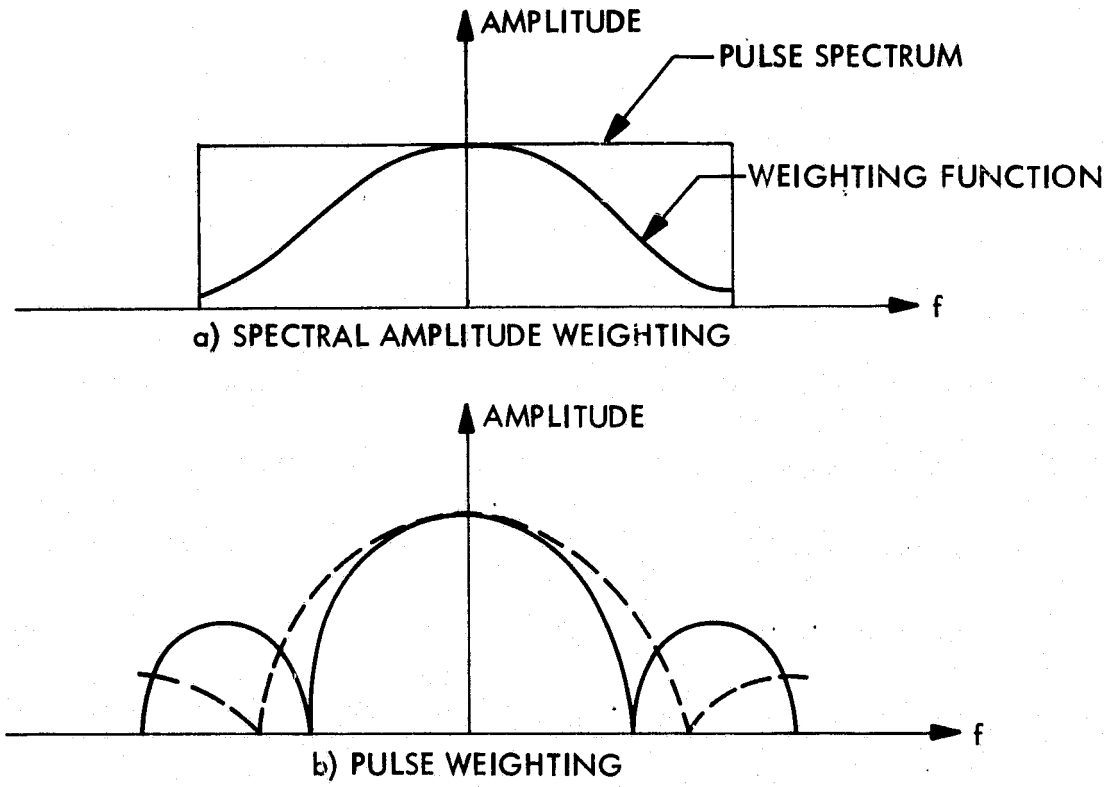

Figure 2.3.1. Pulse weighting

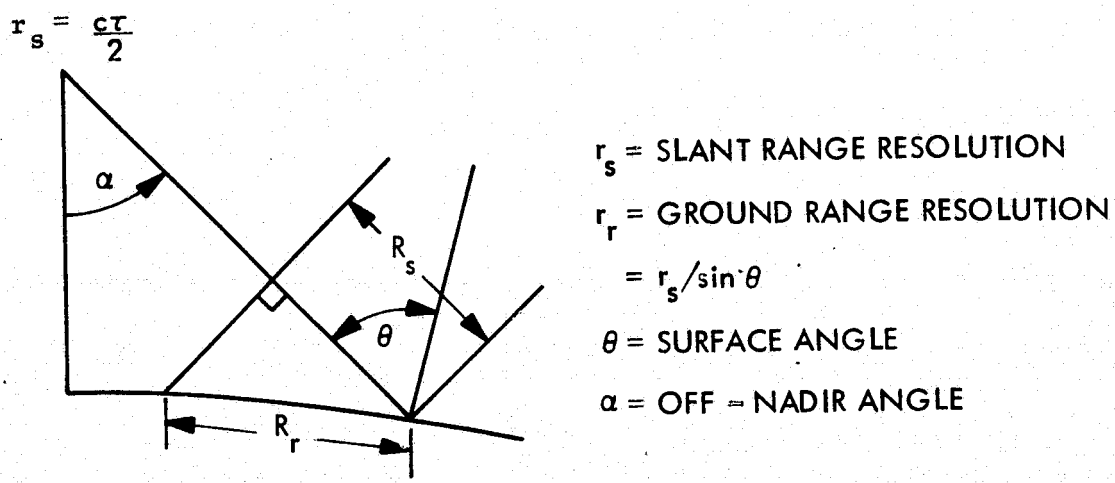

Figure 2.3.2. Slant and ground range resolution

Figure 2.3.2 depicts ground resolution geometry for circular Earth where the slant range resolution is:

$$r_s = c\tau/2 \tag{4}$$

From Figure 2.3.2 the ground range resolution is

$$r_r = r_s/\sin\theta = c\tau/2 \sin\theta \tag{5}$$

with the range bandwidth compensation equation 5 becomes

$$r_r = \frac{1.26\ c}{2\ B \sin\theta} \tag{6}$$

For a surface resolution of 25 meters and an off-nadir angle of 25 degrees the necessary bandwidth is 17.38 MHz.

The product of expanded pulsewidth T and bandwidth B is the range signal time — bandwidth product TBP.

$$TBP = TB = 400 \tag{7}$$

where T = 23.0 μsec.

A constant bandwidth of 17.38 MHz is assumed for each of the three off-nadir angles. This single bandwidth simplifies the processor design, complexity and cost. The respective ground resolution at the three off-nadir angles of 25, 38 and 50 degrees are 19.84, 13.62 and 10.95 meters, respectively.

Azimuth Resolution. In order to achieve the specified azimuth resolution, the synthetic aperture processor must be supplied with a minimum amount of Doppler information. This information can be expressed in terms of the Doppler bandwidth, Δf_D (i.e., twice the highest Doppler frequency considered in processing

the radar echoes) and the "coherent time", T_C, (the time required to collect information over the bandwidth Δf_D). The bandwidth and coherent time necessary to obtain a desired resolution ρ_a is given by the following equation and Figure 2.3.3.

$$\Delta f_D = \frac{\nu_s}{\rho_a} \left(\frac{R_e}{R_e + h} \right) \cos \Psi \tag{8}$$

and

$$T_C = \frac{\lambda R_s}{2 \nu_s \rho_a} \tag{9}$$

where

Δf_D = Doppler bandwidth
T_C = coherent time interval
ρ_a = azimuth ground resolution
ν_s = radar platform velocity relative to stationary target
λ = wavelength
R_s = slant range
R_e = radius of Earth

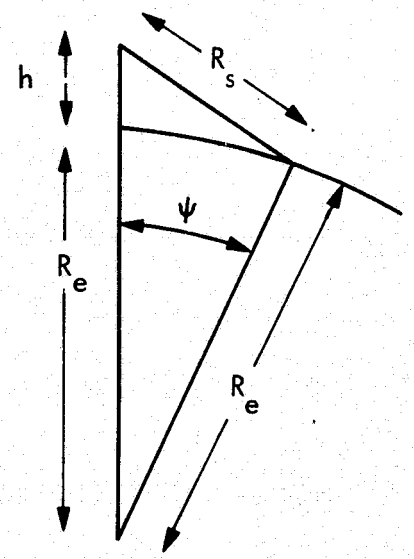

Figure 2.3.3. Radar geometry including Earth curvature

h = altitude of radar platform

Ψ = angular displacement between radar platform and target, measured at center of Earth

As in the case of range correlation, the compressed pulse in the azimuth dimension is of the form sin x/x. Again, spectral amplitude weighting is required to suppress peak sidelobe levels to -30 dB; this will suppress false targets on the radar map but will broaden the main response peak by about 26 percent. Expressions (8) and (9) can be modified to account for this effect as follows:

$$\Delta f_D = \gamma \frac{v_s}{\rho_a} \left(\frac{R_e}{R_e + h}\right) \cos \Psi \tag{10}$$

and

$$T_C = \gamma \frac{\lambda R_s}{2 v_s \rho_a} \tag{11}$$

letting $\gamma = 1.26$.

An expression for the azimuth time bandwidth product can be obtained by combining expressions (10) and (11):

$$(T\Delta f)_{AZ} = \left(\frac{\gamma}{\rho_a}\right)^2 \frac{\lambda R_s}{2} \left(\frac{R_e}{R_e + h}\right) \cos \Psi \tag{12}$$

2.3.4 Signal-to-Noise Ratio

Providing imagery that is of Earth resources quality requires RF signal-to-noise (S/N) ratios $\geq$ 10 dB for absolute backscatter calibrated measurements on a low reflectivity background. This is in accordance with the user requirements. These S/N ratios will insure that various terrain types, such as agricultural fields, may be readily identified and distinguished from one another and represent diffused targets rather than point targets.

This section will be addressed to the S/N equation and a description of important parameters that describe such equation. In the analysis below, the S/N equation is described for a single look operation and the effects of multi-look will be covered in Section 2.3.5.

The S/N ratio equation for any synthetic aperture radar, for a single look, is

$$\frac{S}{N} = \frac{P_t G^2 \lambda^2 \sigma^\circ \eta^2}{(4\pi)^3 R_s^3 k T_s B L} \left[\frac{cT \alpha_{AZ}}{2 \text{ Tan } (\theta)} \right] \tag{13}$$

where

P_t = Peak transmitter power

$P_t = P_{AV}/TPRF$

G = One-way peak antenna gain

λ = Transmitted wavelength

σ° = Backscatter coefficient

R_s = Slant range to target

k = Boltzman's constant

T_s = System noise temperature

$T_s = T_a + T_r + L_r T_e$

T_a = Antenna noise temperature = 290°K

T_r = Transmission-line noise temperature = $290°K(L_r - 1)$

T_e = Receiver noise temperature = L_r 290°K(NF - 1)

L_r = Transmission-line loss during reception

NF = System noise figure

B = Transmitter bandwidth

L = Total system losses

c = Speed of light

T = Transmitter pulse width

α_{AZ} = Azimuth beamwidth (-3 to +3 dB antenna pattern points)

θ = Surface angle

η = Antenna efficiency

Average Transmitter Power. In space operation, average power must be minimized and still be consistent with S/N requirements. This relaxes requirements on prime power generating capacity and eases the thermal energy dissipation problem. Peak power must also be minimized to avoid the large voltages associated with large peak powers and to increase transmitter reliability. Average and peak transmitter power are related by

$$P_{av} = P_t \cdot T \cdot PRF \tag{14}$$

The PRF was chosen on the basis of a given ambiguity suppression (Section 2.3.7) and is a variable due to altitude changes.

Initial analysis showed that the L-band radar requires 262 watts average power to achieve performance goals. Assuming a transmitter duty cycle of 4.3 percent, a peak power requirement of 6 kW, a maximum PRF of 1900 Hz and a maximum pulse width of 23.0 μsec are needed.

For the X-band radar, 800 watts of average power is required to achieve performance goals. This assumes a nominal transmitter duty cycle of 4 percent. The peak power, maximum PRF and maximum pulse width required are 20 kW, 1900 Hz and 21 μsec, respectively.

Antenna Gain. The peak one-way gain for an uniformly illuminated array is given by

$$G = \frac{4 \cdot \pi \cdot A}{\lambda^2} \tag{15}$$

where

A = aperture area

λ = wavelength.

The maximum antenna size in azimuth is 12m, the elevation dimension being a variable as shown below. The antenna gains for the three frequency radars are given in Table 2.3.1. The size of the elevation dimensions are derived in Section 2.3.6. Antenna efficiency is not included in determining antenna gain, but is included in the S/N ratio equation.

Table 2.3.1. Antenna gain

(12m azimuth dimension)

Frequency	Off-Nadir Angle		
	25°	38°	50°
L-Band, λ = 0.23m			
Elevation dimension, m	0.65	1.55	2.2
Antenna gain, dB	32.67	36.45	37.97
X-Band, λ = 0.036m			
Elevation dimension, m	0.12	0.24	0.36
Antenna gain, dB	41.4	44.46	46.2

Backscatter Coefficient. A plot of the minimum backscatter coefficient used for this study is plotted in Figure 2.3.4 as a function of surface angle. These minimum backscatter coefficients are in accordance with user requirements.

Noise Figure. A very low noise parametric amplifier is assumed at the receiver front end for both the X radar and a low noise transistor amplifier is assumed for the L-band radar. An overall noise figure of less than 3 dB is assumed for each.

System Losses. System losses consist of RF, atmospheric and field degradation. The RF losses consist of contributions from waveguide or coaxial structures, receiver protector and filters, flexible joint and switches. These losses are itemized in Table 2.3.2.

Range. The slant range to the target, earth in this case, is a function of antenna off-nadir angle or surface angle. Range is calculated for a spherical Earth using the geometry in Figure 2.3.5.

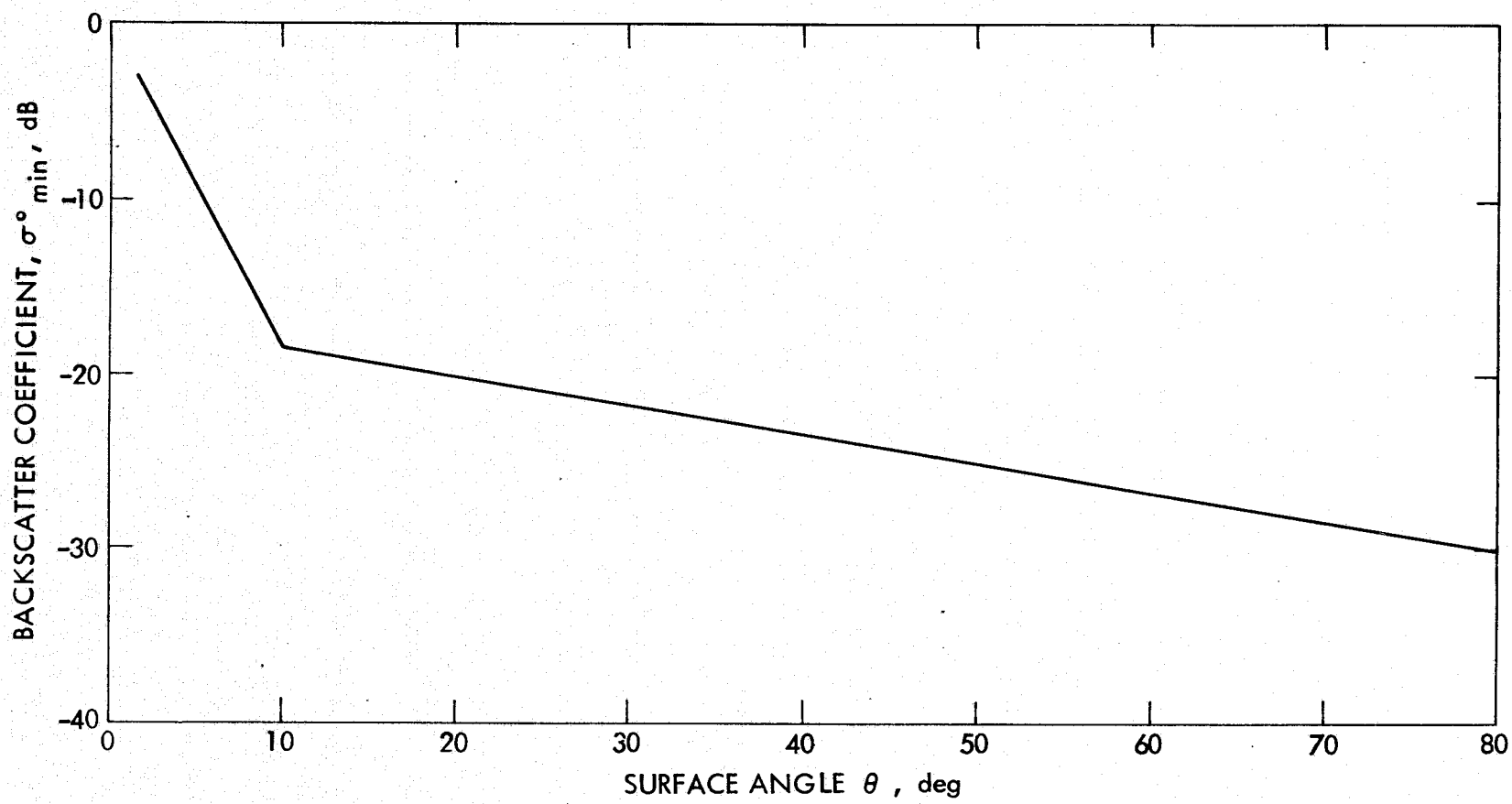

Figure 2.3.4. Backscatter coefficient vs surface angle

Table 2.3.2. System Losses

	Loss	L-Band	X-Band
1.	Field degradation, dB	1.0	1.0
2.	Atmospheric, dB	0.3	0.4
3.	RF		
	T/R switch (2-way), dB	0.6	0.6
	Dual directional coupler (2-way), dB	1.3	3.0
	Waveguide or coaxial structures (2-way), dB	0.4	0.6
	Flexible joint (2-way), dB	0.6	0.6
	RF switch (2-way), dB	0.4	0.4
	Antenna switch (2-way), dB	0.2	0.2
	TOTAL	5.4	7.4

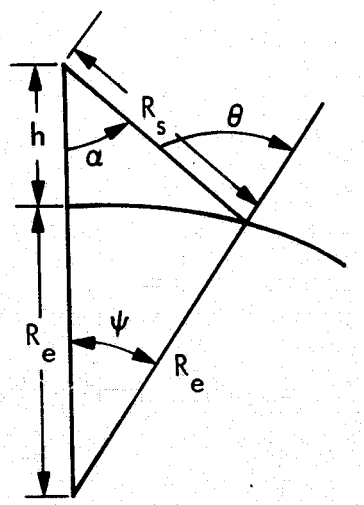

Figure 2.3.5. Spherical Earth Geometry

with α being the off-nadir angle, the surface angle θ is computed by

$$\theta = \arcsin\left[\left(\frac{h + R_e}{R_e}\right) \sin \alpha\right] \tag{16}$$

slant range is computed

$$R_s = \frac{R_e \sin \Psi}{\sin \alpha} \tag{17}$$

where

R_e = Earth radius

$\Psi = \theta - \alpha$

H = altitude

Net Single Look S/N Ratio. Figures 2.3.6 and 2.3.7 are plots of single look S/N as a function of surface angle for the three radar systems discussed at the three off-nadir angles and are the results of Section 2.3.6, basis of radar design and system parameters from Table 2.4.1.

Final S/N Ratios. As a further illustration of the radar systems performance capabilities, S/N as a function of backscatter coefficient σ° is plotted in Figures 2.3.9 and 2.3.10 for L-band X-band for various polarizations. S/N is shown for a 25m resolution cell size. Several terrain types such as desert, agricultural fields, and industrial sites are located on the σ° axis for convenience. The variations in σ° for a given terrain type allow for individual variations, such as different types of agricultural fields and forests of varying density and was done for surface angles varying from 55 degrees to 5 degrees. See also "A Survey of Terrain Radar Backscatter Coefficient Measurement Programs", University of Kansas CRES TR 2432, by King and Moore, December 1973.

The resultant S/N ratios are greater than 10 dB against weak backscatter target for all surface angles and systems considered. For strong

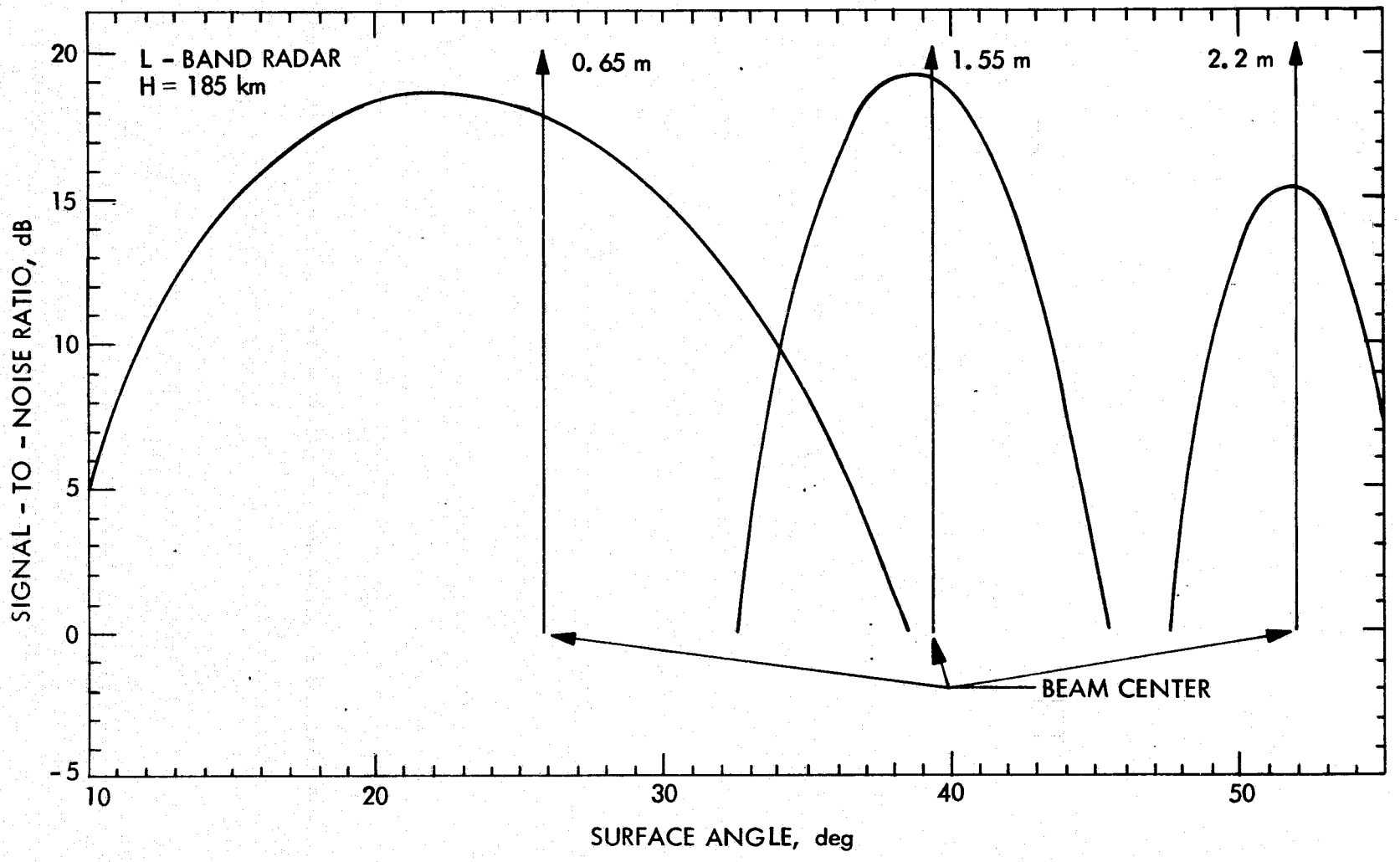

Figure 2.3.6. L-band radar signal to noise ratio

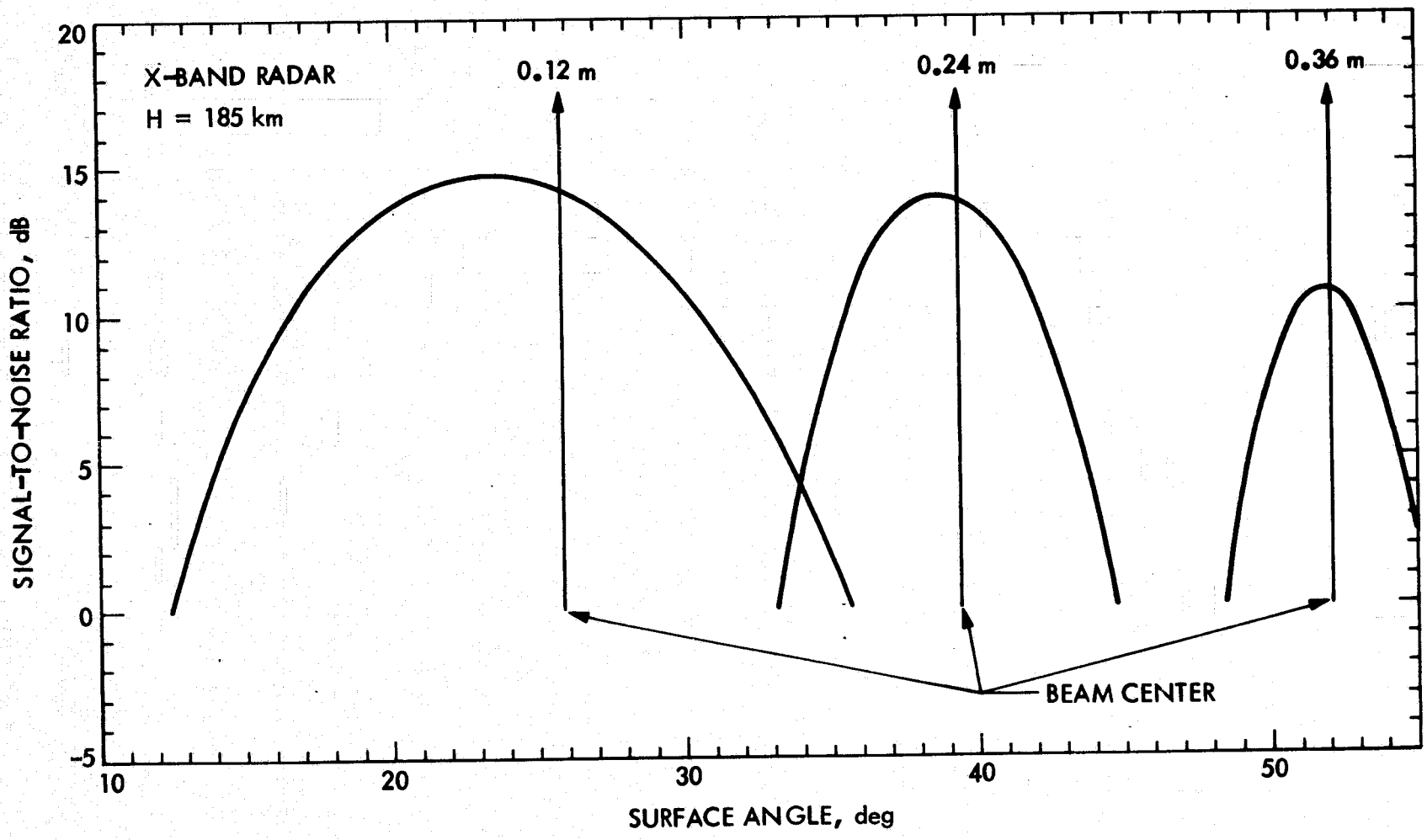

Figure 2.3.7. X-Band Radar Signal-to-Noise Ratio

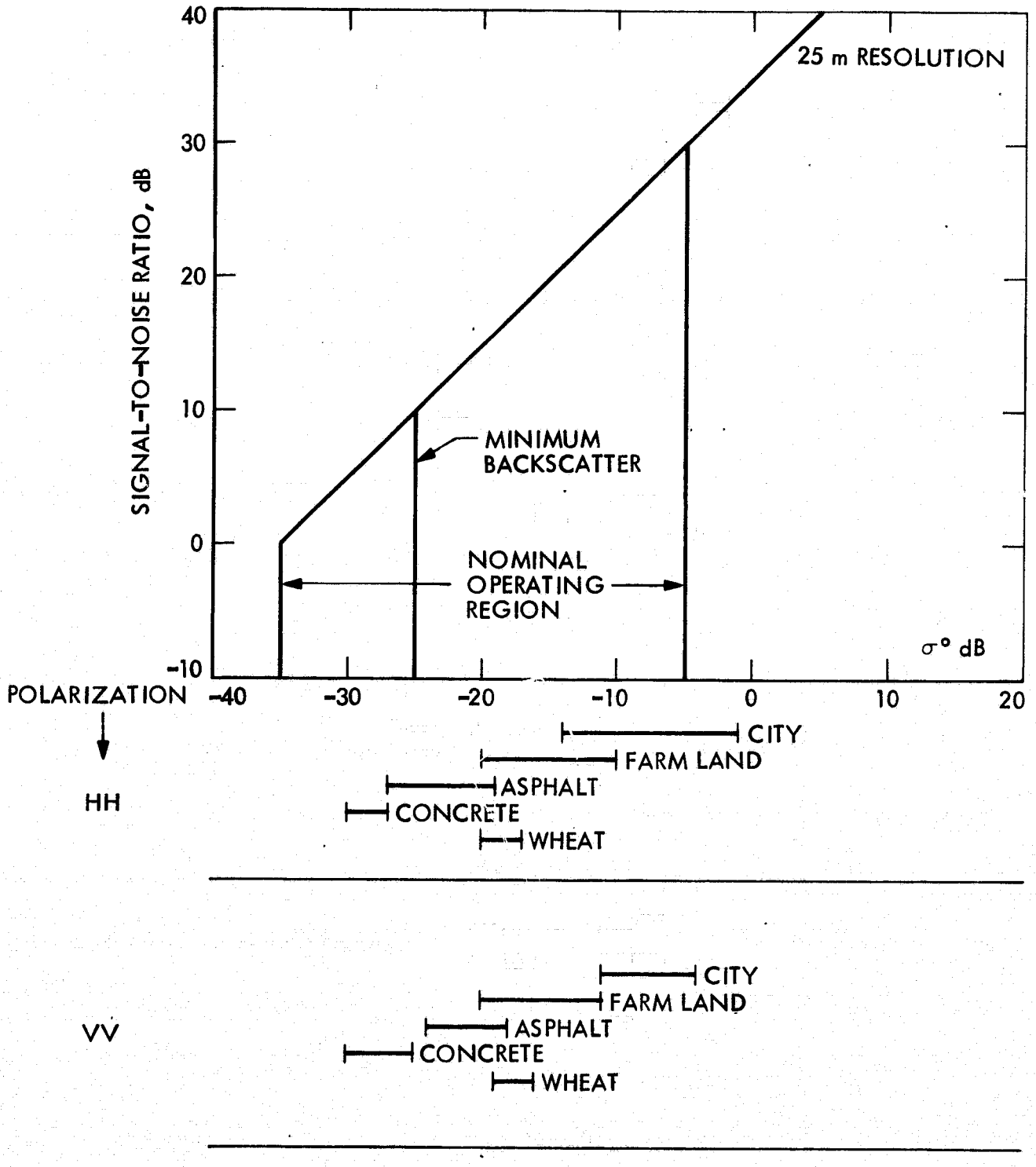

Figure 2.3.8. L-Band Radar Final S/N Ratio

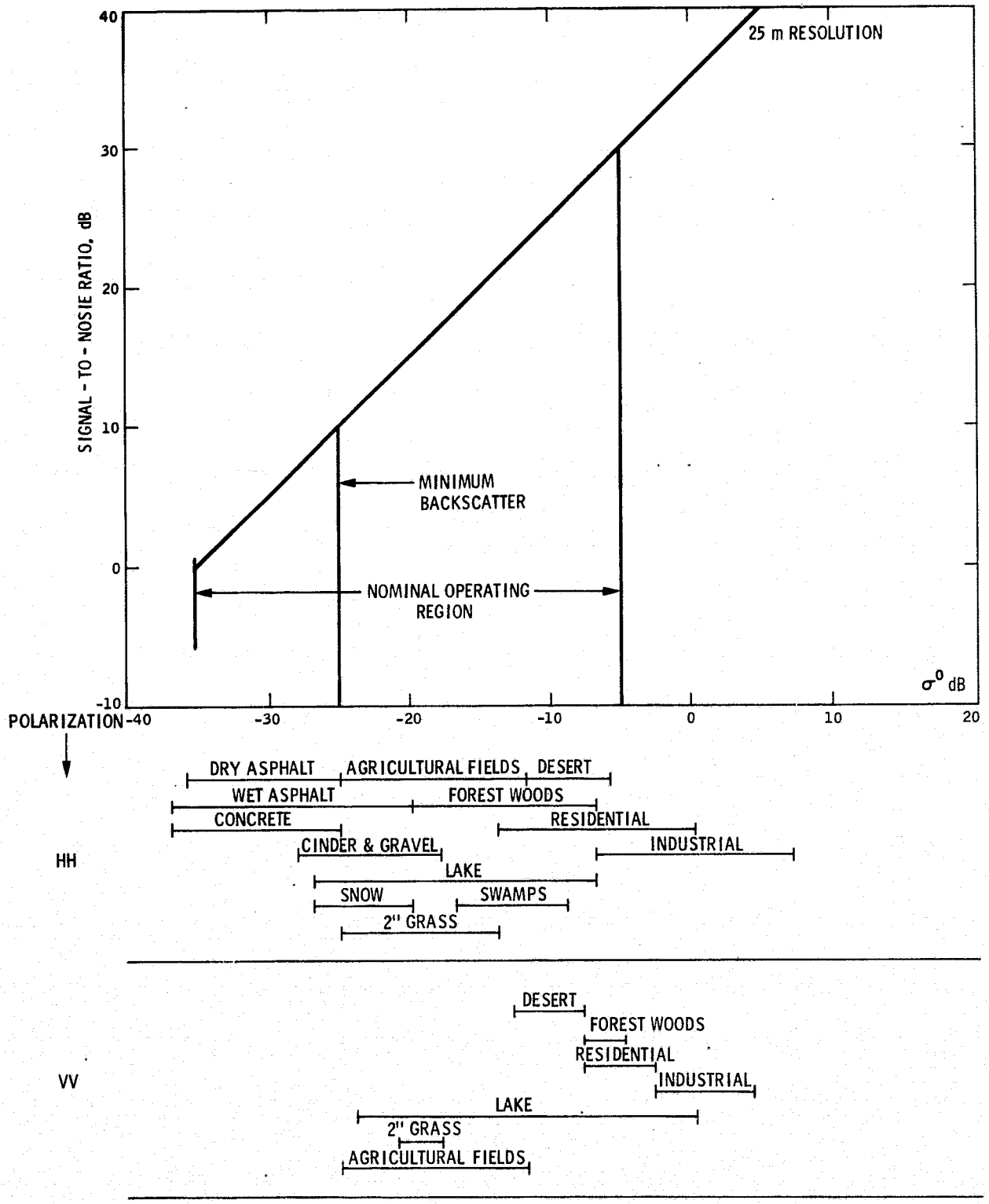

Figure 2.3.9. X-band radar final S/N ratio

backscattering target, S/N can easily be greater than 10 dB. These S/N ratios will readily provide the high quality imagery required for Earth resources applications.

2.3.5 Multiple Looks

The radar map is enhanced by the so-called "multiple-look" technique, the purpose of which is to reduce the "speckle" effect observed in coherent SAR imagery. Multiple-look processing consists essentially in: (a) the production of multiple independent images of the same target area and (b) the noncoherent averaging of the multiple images. Multiple-look processing may be performed in either the range dimension, the azimuth dimension or both. The choice of implementation is influenced by the overall system configuration and by user requirements.

Azimuth Multiple Looks. Multiple look processing may be accomplished by doing the non-coherent image averaging in the azimuthal direction only. It oftens happens that the additional Doppler bandwidth required for multiple azimuth looks is easier to obtain than the additional video bandwidth required for multiple looks in range. When this is so, the economics of the system strongly favor azimuth looks.

Range Multiple Looks. Multiple look processing may also be accomplished by non-coherent image averaging in the range dimension. As always, for information occupying a given bandwidth (whether video or Doppler) the number of looks may be increased only at the expense of degrading the resolution. Put another way, for a specified resolution the number of looks may be increased only at the expense of increasing bandwidth.

It is possible that some users might be willing to sacrifice some resolution to obtain further speckle reduction. This could be accomplished by further processing of the correlated radar image to effect a combination of range and azimuth looks. For example, if the output of the processor is an image with 25 meter resolution and four azimuth looks, that image can be further processed to obtain 50 meter resolution and, effectively, an end result of two looks in range and eight in azimuth. This would be the equivalent of averaging 16 independent images (looks) of the target area.

Multilook Signal-to-Noise Improvement. The signal-to-noise improvement realized by multiple-look processing is approximately equal to the square root of the number of looks. In the above example, the four-look image would have twice the image signal-to-noise ratio of a single-look image. Similarly, the 16-look, 50-meter image would have twice the S/N of the four-look image.

Obviously the S/N improvement afforded by multiple-looks must be paid for by increasing the information gathering capability of the radar system. This translates into changes in such basic parameters as antenna dimensions, power and pulse repetition frequency.

2.3.6 Basis of Radar Design

This section addresses the approach taken for the basis of radar design.

Average Power Requirements. Transmitter average power requirements were first determined to meet system guideline parameters (see Table 2.2.1) for an image S/N ratio equal or greater than 10 dB for the minimum backscatter coefficient σ° over a 100 km imaged swath width as shown in Figure 2.3.10. Results of average powers requirements for the above constraints and for each of the three frequencies are shown in Figure 2.3.11 as a function of off-nadir angles. Clearly,

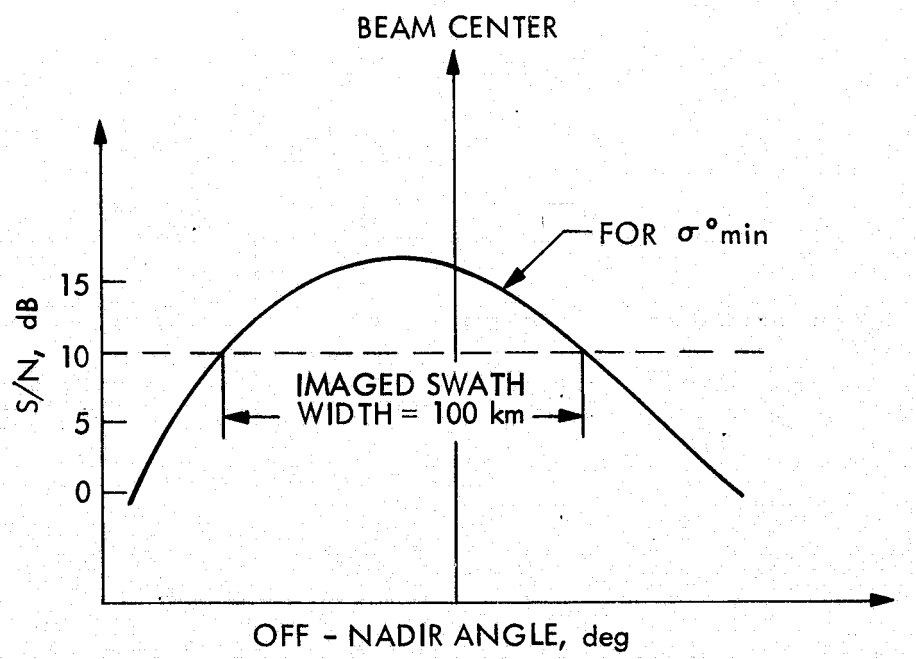

Figure 2.3.10. S/N vs off-nadir angle

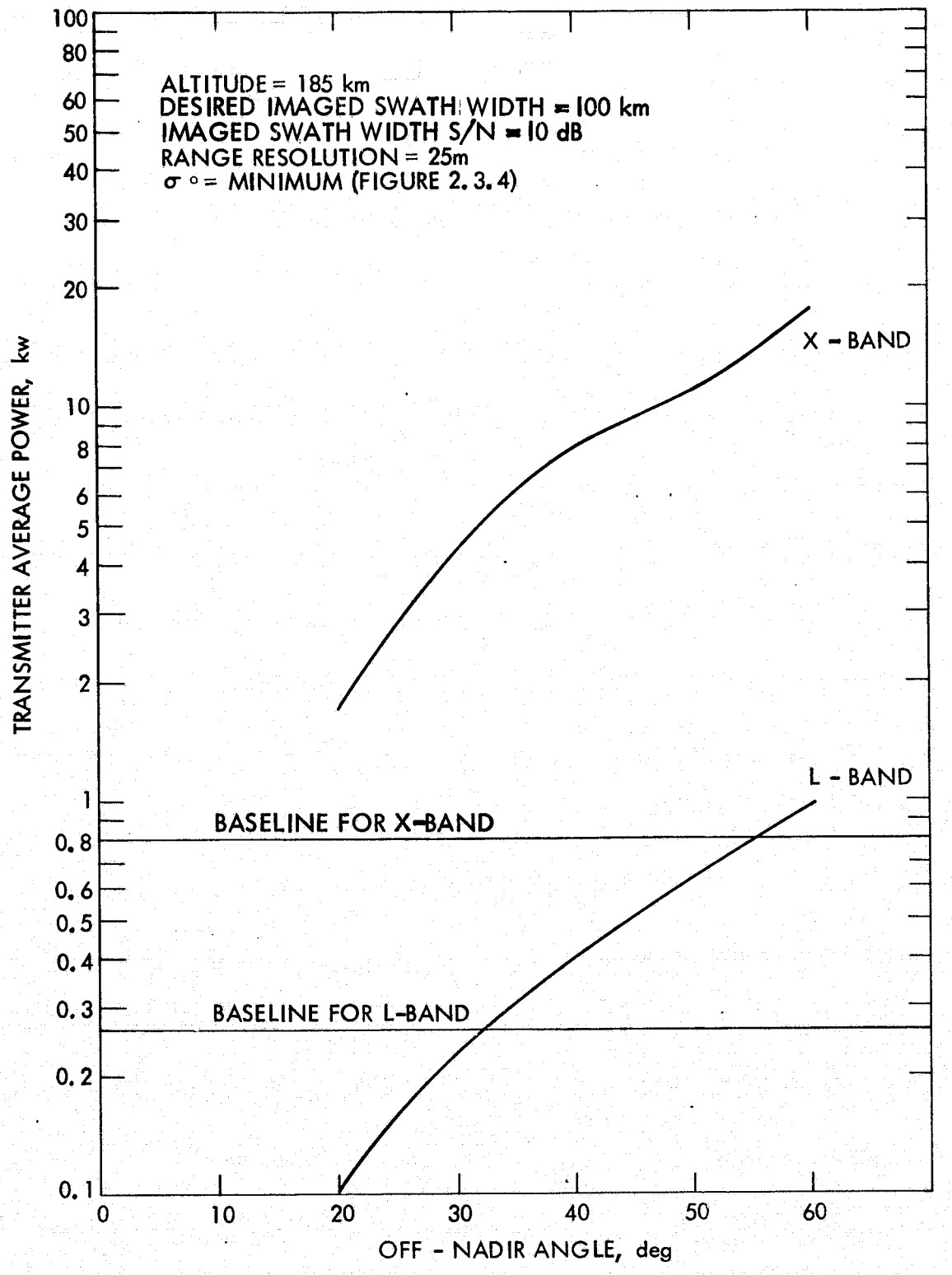

Figure 2.3.11. Transmitter average power vs off-nadir angle

it would be unreasonable to specify an average power requirement greater than 260 watts for the L-band radar and greater than 800 watts for the X-band radar due to basic hardware and system constraints.

Also, Figure 2.3.11 indicates that less than a 100 km imaged swath width for the minimum σ° is attainable for the X band radar. At off-nadir angles of 20 to 32° a 100 km imaged swath width for σ° (min) is realized for the L-band radar.

Antenna Requirements. With the limitations imposed by the transmitter average power constraints as described in the previous section, the second step then is to determine the elevation apertures at the various off-nadir angles. These elevation apertures will then determine what the imaged swath width will be for signal-to-noise ratios greater than 10 dB for the minimum σ°. An example is shown in Figure 2.3.12 for the X-band radar at 38 degrees off-nadir angle. Here the chosen aperture is 0.24 meters with its corresponding imaged swath width. Similarly, other off-nadir angles were selected for optimum range coverage, i.e., from 7° to 55°. These angles are 25°, 38° and 50°.

The antenna as defined in the system guidelines is assumed to be a planar array. Three beams can be derived from this common aperture with proper feeds coupled to it for the selected off-nadir angles. These sub-apertures are shown in Figures 2.3.13 and 2.3.14. The selected antenna elevation aperture dimensions for the three frequencies and three off-nadir angles are presented in Table 2.3.3.

Table 2.3.3. Antenna configuration

	L-Band			X-Band		
Off-Nadir Angle, deg	25	38	50	25	38	50
Antenna, aperture length						
Azimuth, m	12	12	12	12	12	12
Elevation, m	0.65	1.55	2.2	0.12	0.24	0.36

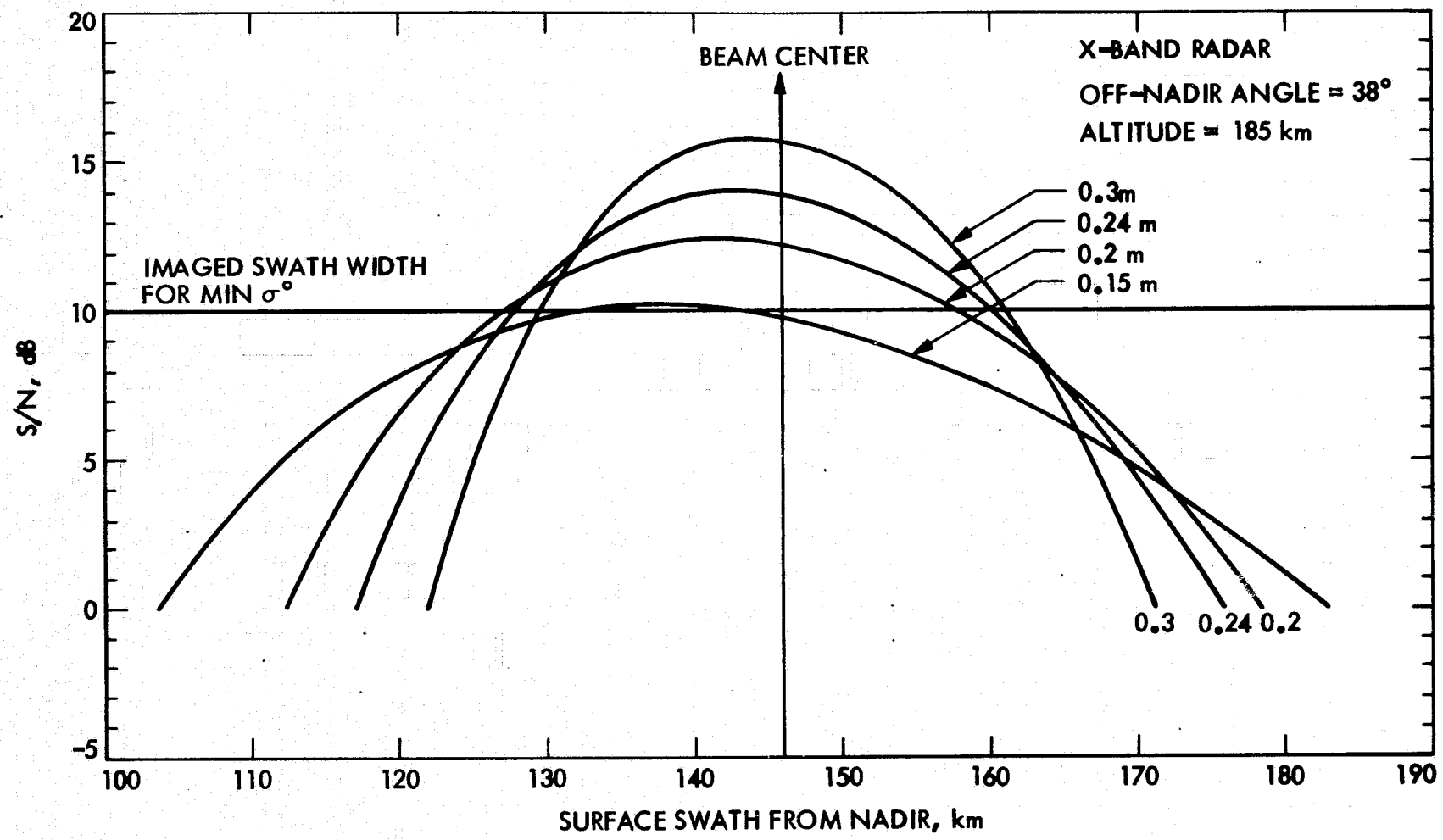

Figure 2.3.12. Antenna Elevation Aperture Determination

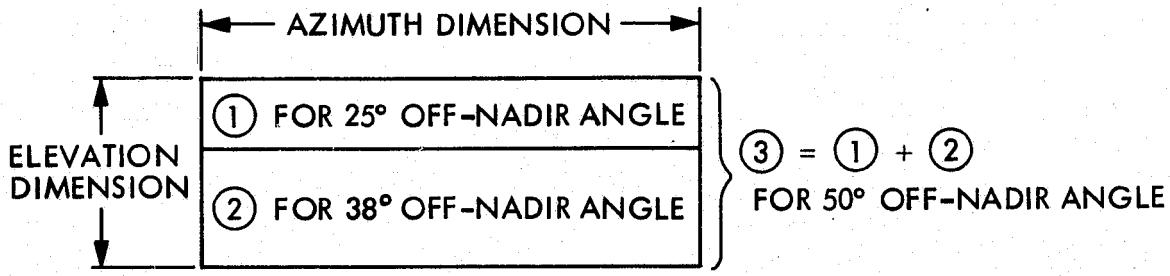

Figure 2.3.13. Planar array antenna aperture

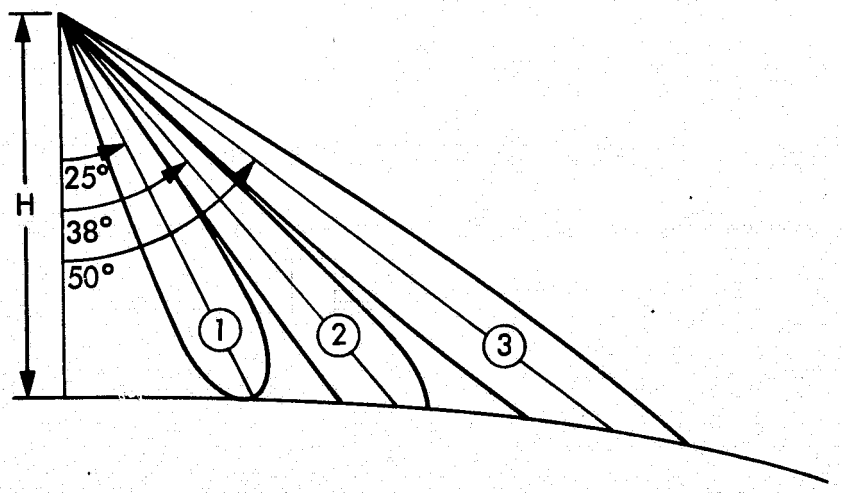

Figure 2.3.14. Off-nadir angle antenna beams

2.3.7 Ambiguity Suppression and Imaged Swath Width

A target can under certain circumstances appear on a map at its true position and also displaced in range and azimuth from its true position. These displaced images are ambiguous or false targets. If proper attention is not given to suppression of these ambiguities, they can result in poor imagery that will be difficult to interpret. Achievement of quality image requires that ambiguity in both range and azimuth dimensions be -18 dB or less.

After a minimum PRF is selected from azimuth ambiguities the selection of the imaged swath width is restricted by any one of four factors. These factors are:

1) Pulse interleaving constraints.

2) Range ambiguities.

3) Antenna swath width

4) Data processor maximum swath width.

Azimuth Ambiguity. Azimuth ambiguities are the result of aliasing or fold-over of the Doppler spectrum which occurs due to sampling the Doppler information at a rate of PRF samples per second. Qualitatively, Doppler ambiguities will cause the radar image of a single point target to appear as a series of several bright spots of varying intensity spaced periodically in the azimuthal direction. A quantitative measure of azimuth ambiguity is the integrated signal-to-ambiguity ratio (S/A) which is the ratio of the intensity of the true image to the combined intensities of the ambiguous images. The minimum overall S/A required for Shuttle is 18 dB for both range and azimuth ambiguities. If range ambiguities are kept at -20 dB or lower, the minimum allowable azimuth S/A ratio becomes 22.5 dB.

Figure 2.3.15 shows the one-way power pattern of the azimuthal antenna aperture for the 12m antenna. When the antenna beam is aligned with the zero Doppler plane, it is also the envelope of the Doppler spectrum. When the Doppler information is sampled at the rate PRF, energy present at frequencies $f \pm n$ PRF, $n = 1,2,3, \ldots$ is folded or aliased into the region $-PRF/2 < f < PRF/2$. The dashed curves in the figure represent the result of the first fold-over ($n = 1$). The case shown is for PRF = 1260 Hz so that the nulls of the

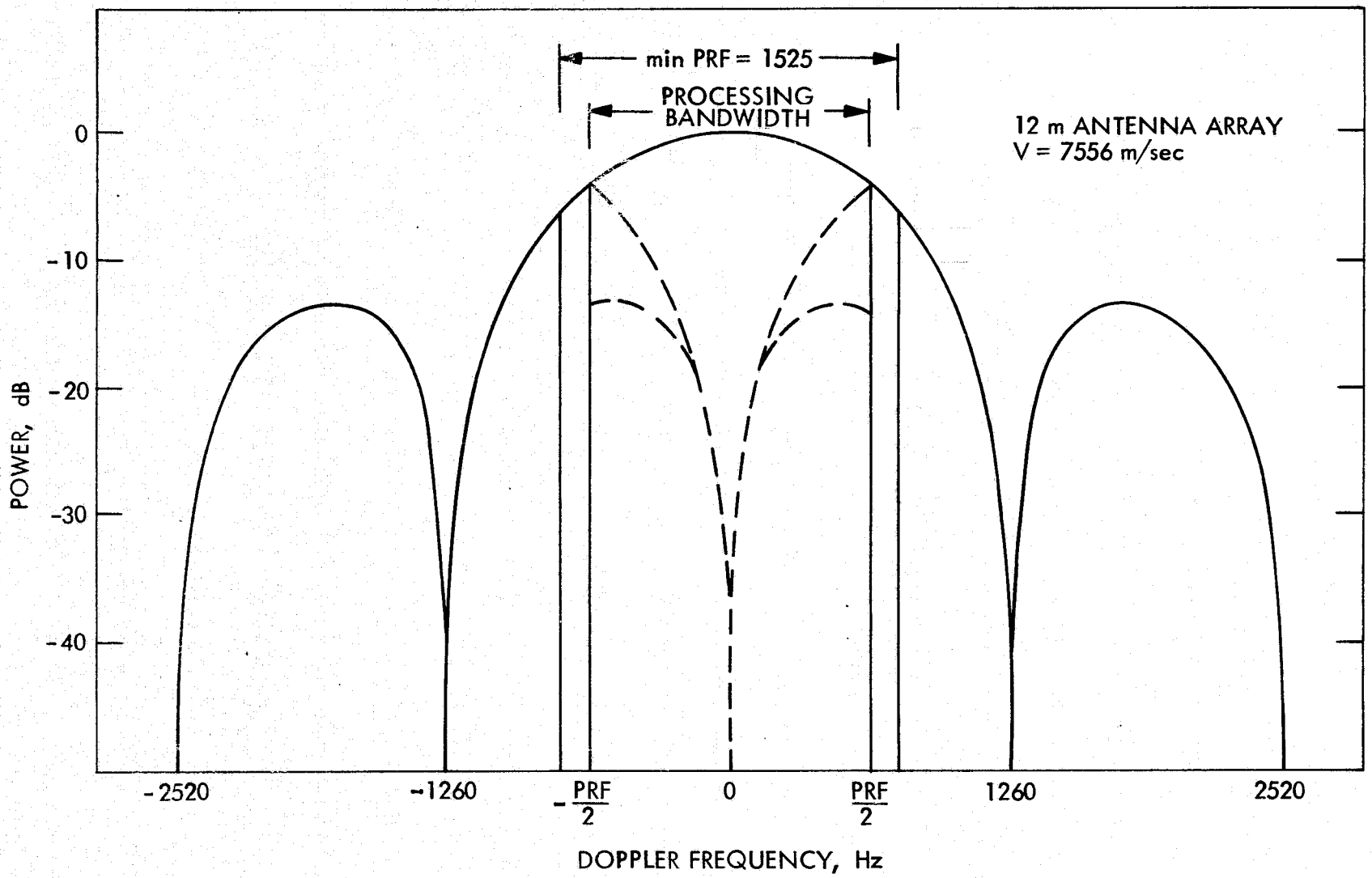

Figure 2.3.15. Doppler spectrum

spectrum are aliased to zero Doppler. The integrated signal-to-alias ratio is computed as follows:

$$\frac{S}{A} = \frac{\int_{-F/2}^{F/2} S(f)\,df}{\sum_{n=1}^{\infty} \int_{-F/2}^{F/2} \left[S(f + n \cdot PRF) + S(f - n \cdot PRF)\right] df} \qquad (18)$$

where S(f) is the Doppler power spectrum and F is the Doppler processing bandwidth.

Azimuth ambiguities are a function of antenna beam shape, Doppler processing bandwidth and PRF. For a uniform aperture antenna illumination and a Doppler processing bandwidth of 1260 Hz the integrated signal-to-ambiguity ratio S/A is plotted as a function of a normalized sampling rate n shown in Figure 2.3.16. The minimum PRF for an S/A ratio of 22.5 dB is computed to be 1525 Hz. This then becomes the minimum radar PRF.

Imaged Swath Width Determination. The selection and determination of the imaged swath width can be restricted by any one of four factors. These are:

1) Antenna swath width
2) Pulse interleaving constraints
3) Range ambiguities
4) Data processor maximum swath width

Antenna Swath Width. Ground swath width must be calculated using spherical Earth geometry as in Figure 2.3.17. For a given off-nadir angle α and satellite altitude h, a given elevation beamwidth $\Delta\alpha$ will intercept a ground swath SW

$$SW = \Psi R_e. \qquad (19)$$

The swath width is bounded by slant range R1 and R2 (angular separation $\Delta\alpha$). Ideally the interpulse period 1/PRF should match the angular separation $\Delta\alpha$.

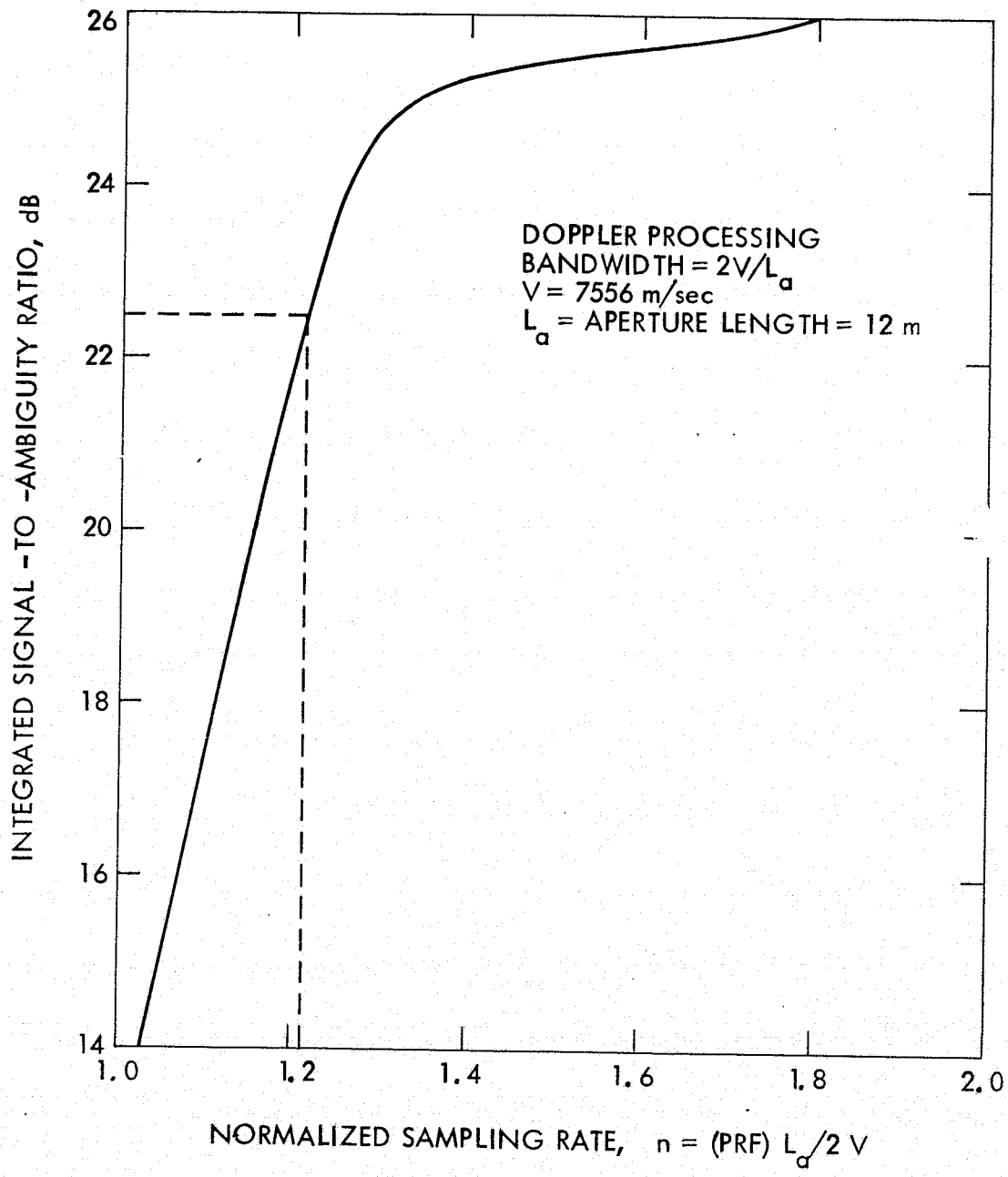

Figure 2.3.16. Azimuth integrated signal to ambiguity ratio

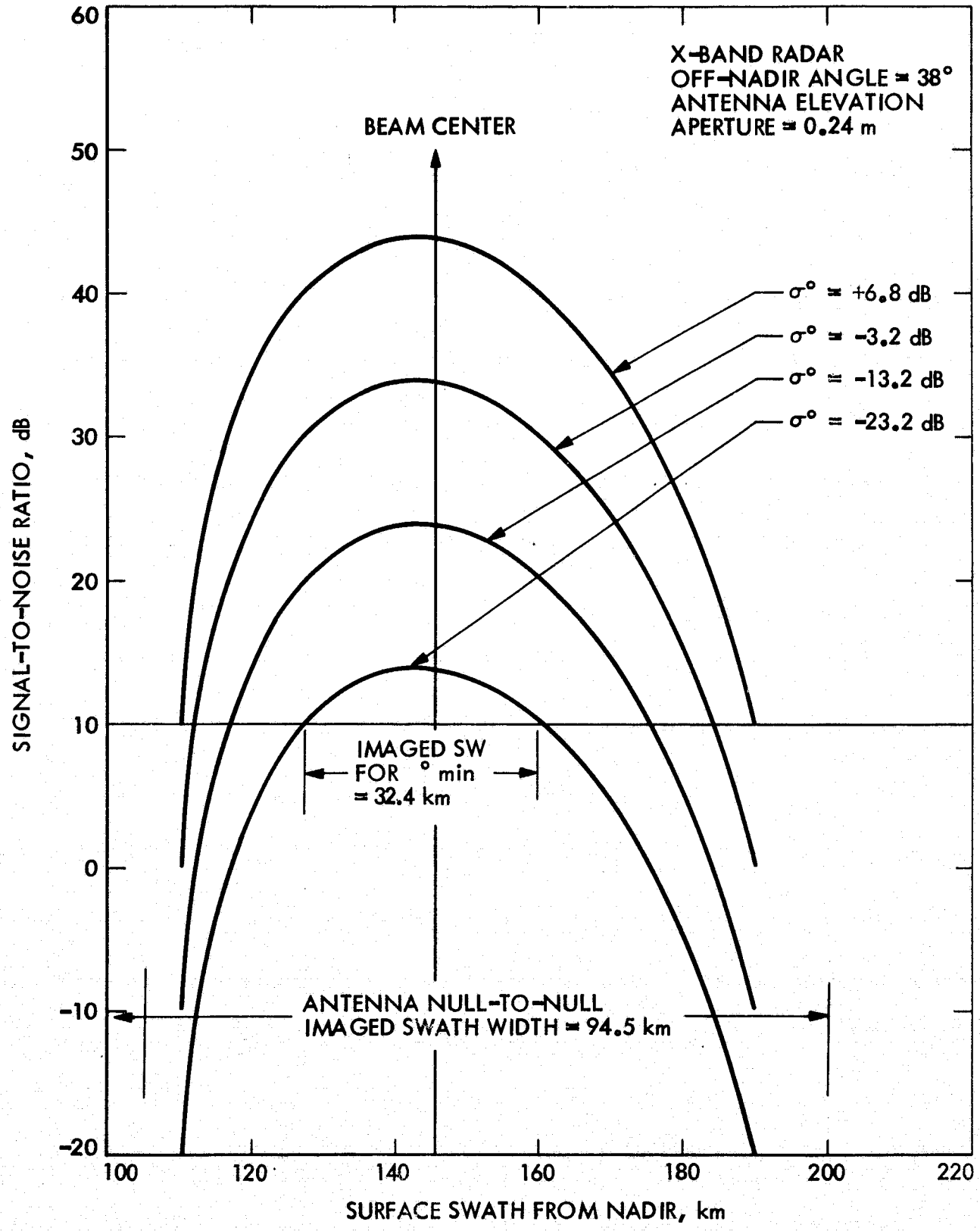

Figure 2.3.18. S/N ratio swath width determination

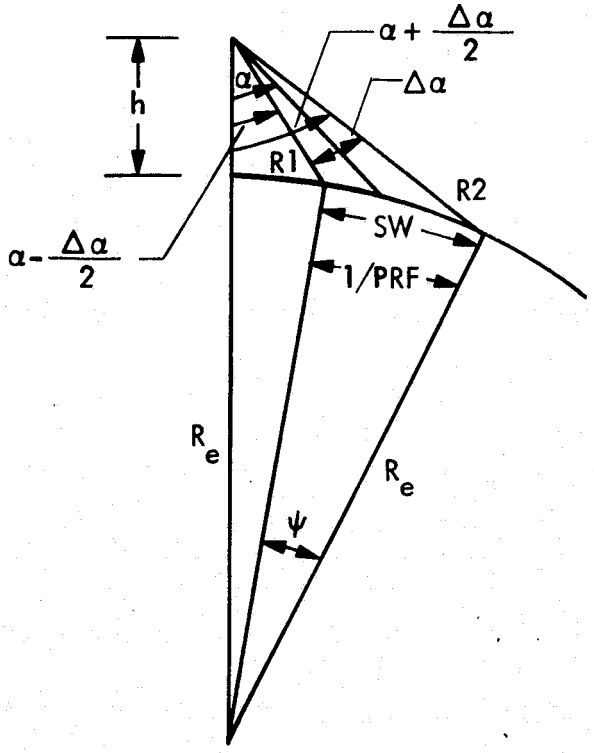

Figure 2.3.17. Swath width determination

As an example for the X-Band antenna elevation aperture length of 0.24m at 38ff-nadir angle, the antenna separation is 17.25 degrees, which gives a null to null imaged swath width of 94.5 km and an ideal PRF of 2469 Hz. For PRF's less than 2469 Hz, the SW becomes bounded by the angular separation slant ranges, which is the case, and is limited by range ambiguities, which is also the case.

A decrease in gain limits imaged swath width due to S/N requirements. S/N ratio values are usually calculated at swath center with peak antenna gain. At any other point in the swath, the antenna gain decreases with a S/N decrease. The maximum imaged swath width is then determined by how much S/N loss can be tolerated, regardless of how much unambiguous range may be provided. The antenna null-to-null swath width is presented in Figure 2.3.18 as a function of surface swath width from nadir for the above example. Also shown is the variation of S/N as a function of backscatter coefficients.

Pulse Interleaving Constraints. Pulse interleaving constraints place restrictions on the pulse repetition frequency at any given altitude. There are two requirements which must be met. The PRF is chosen such that:

1) A pulse is not being transmitted at the same time the data (the echo of an earlier pulse from the image swath) arrives at the antenna.

2) The nadir return of one pulse and the data return of another pulse do not overlap.

Figure 2.3.19 shows the timing of transmitted and received pulses, where

R_s = slant range to center of swath

T_{sw} = Imaged swath time

T_p = width of transmitted pulse

T_d = receiver recovery time

τ_d = delay between nadir echo and center of swath

H = altitude

C = speed of light

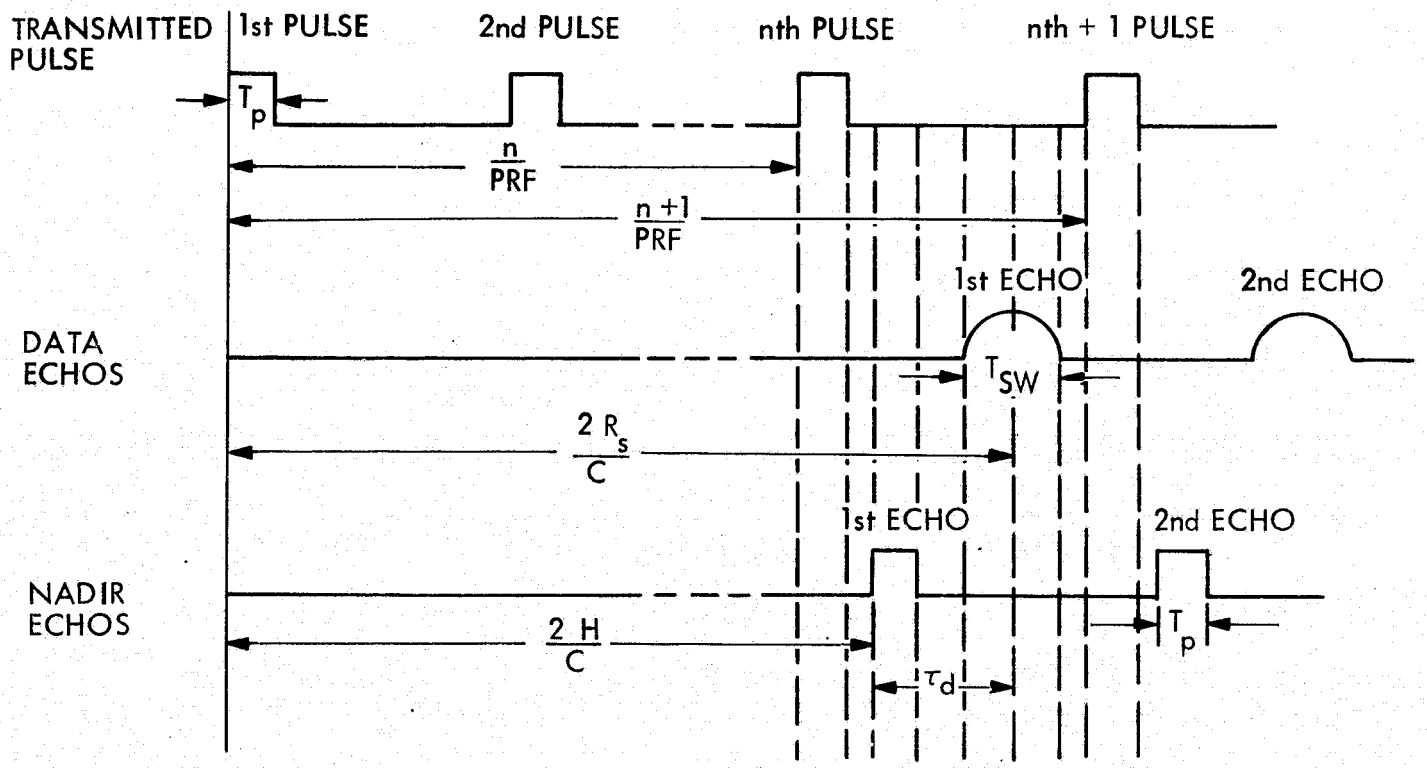

Figure 2.3.19. Pulse timing

The first interleaving requirement will be satisfied by:

$$\frac{n}{PRF} + T_p + T_d < \frac{2R_s}{C} - \frac{T_{sw}}{2} \tag{20}$$

$$\frac{n+1}{PRF} > \frac{2R_s}{C} + \frac{T_{sw}}{2} + T_p \tag{21}$$

Similarly, the second requirement is satisfied by:

$$\frac{N}{PRF} < \tau_d - \frac{T_{sw}}{2} - T_p \tag{22}$$

$$\frac{N+1}{PRF} > \tau_d + \frac{T_{sw}}{2} + T_p \tag{23}$$

Failure to meet the first requirement results in gap in the data swath. And failure to meet the second requirement would result in a streak in the data swath.

Figure 2.3.20 shows the allowable values of PRF over the altitude range of 185 km for the three off-nadir angles. Cross-hatched areas represent forbidden regions.

The values of swath time used to generate these curves represent an optimum swath width at the three off-nadir angles of 100, 85 and 75 km. To get larger swath width at the 38 and 50 degree off-nadir angles would narrow the non crossed-hatched areas to the extent of not meeting azimuth ambiguity considerations.

As the figure indicates, more than one PRF will be required to cover the full range of altitudes for the orbit. The choice of exact values for PRF are based on the azimuth ambiguity consideration.

The nadir-return for the 50 degree off-nadir angle is at a PRF of 1000 Hz and should not affect the data swath as its amplitude should be quite small.

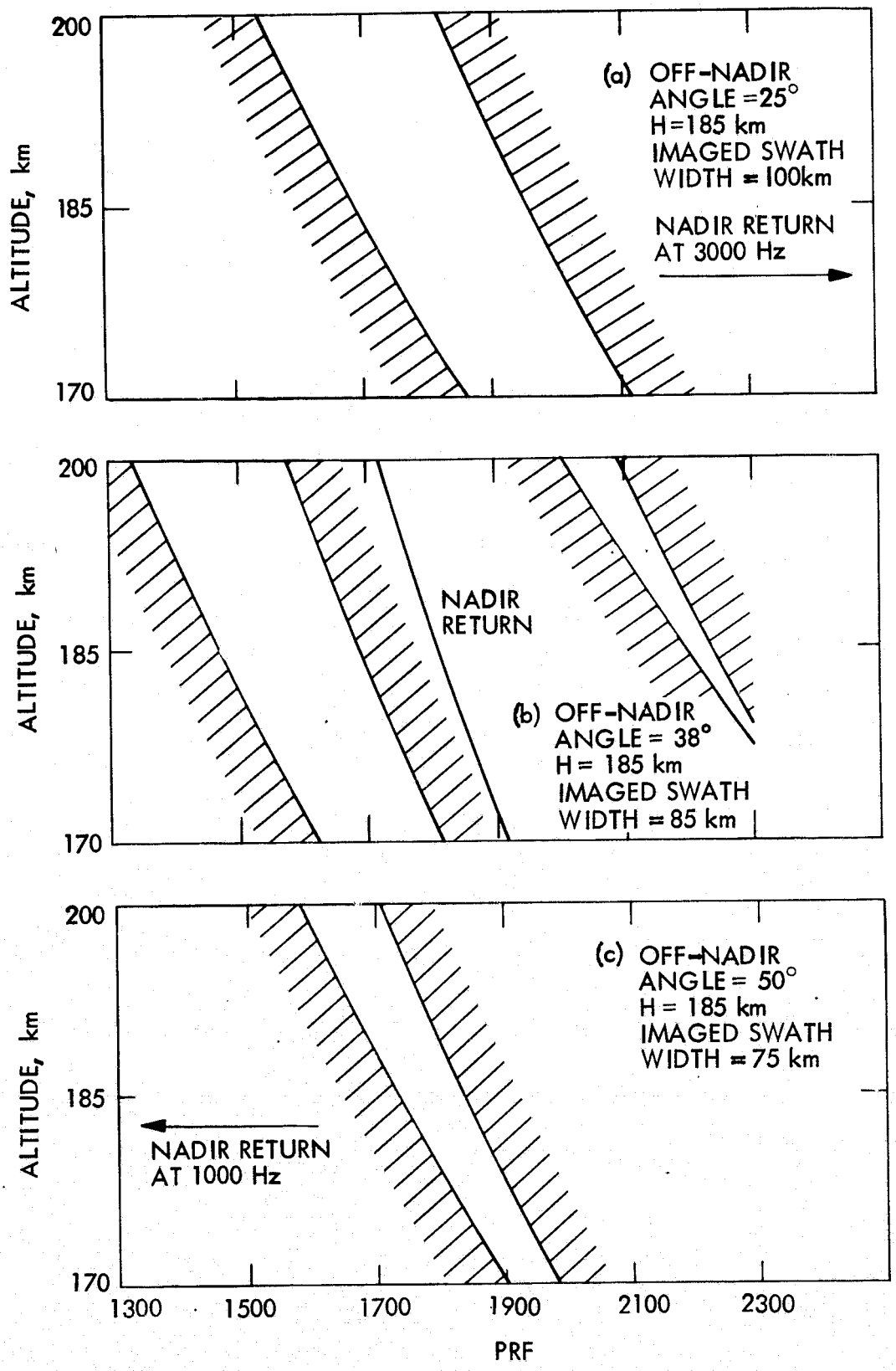

Figure 2.3.20. PRF configuration for various off-nadir angles

Range Ambiguities. As shown in Figure 2.3.21 range ambiguities are the result of ground point returns, separated by many IPP's, that are outside of the desired imaged swath width whose slant ranges are R_1 and R_N. These returns will arrive at the receiver simultaneously with the return from a point which lies on the desired swath R_s. Range ambiguities will cause the radar image of a single point target to appear as bright spots of varying intensity in the range direction. A quantitative measure of range ambiguity is the ratio of the desired swath image field power to the range ambiguous image field power. For this study the minimum allowable range S/A ratio is 20 dB.

Range ambiguity suppression is provided almost exclusively by the antenna elevation pattern. As shown in Figure 2.3.21 when peak gain is directed to a point at range R_s, the gain at ranges R_N are much less and the slant range to the ambiguous ranges is greater or less than the range to the desired swath. The resultant ambiguity suppression must also take into account the backscatter coefficient transfer function. This is done by multiplying the relative amplitudes of the range time history and the transfer function of the backscatter coefficient.

From the above the effective swath width can be determined for a S/A ratio of 20 dB. Figure 2.3.22 shows a plot of the range S/A ratio as a function of surface swath from nadir. Table 2.3.4 shows the effective swaths for a S/A ratio of 20 dB for the different off-nadir-angles and frequencies.

Maximum Data Processor Swath Width. For simplicity of processor design, complexity and cost, a constant processed swath time of 329 μsec is assumed for each of the three off-nadir-angles. The corresponding imaged or processed swath widths are 133, 78 and 63 km respectively at 25, 38 and 50 degree off-nadir-angles.

Results. Table 2.3.4 presents how the final selection of imaged swath widths are determined for the three frequencies and three off-nadir-angles. The four factors that restrict swath width are also shown.

2.3.8 Antenna Pointing Requirements

The items basic to the subject of antenna pointing are (a) the position of the antenna beam relative to the plane of zero Doppler and (b) the rate of

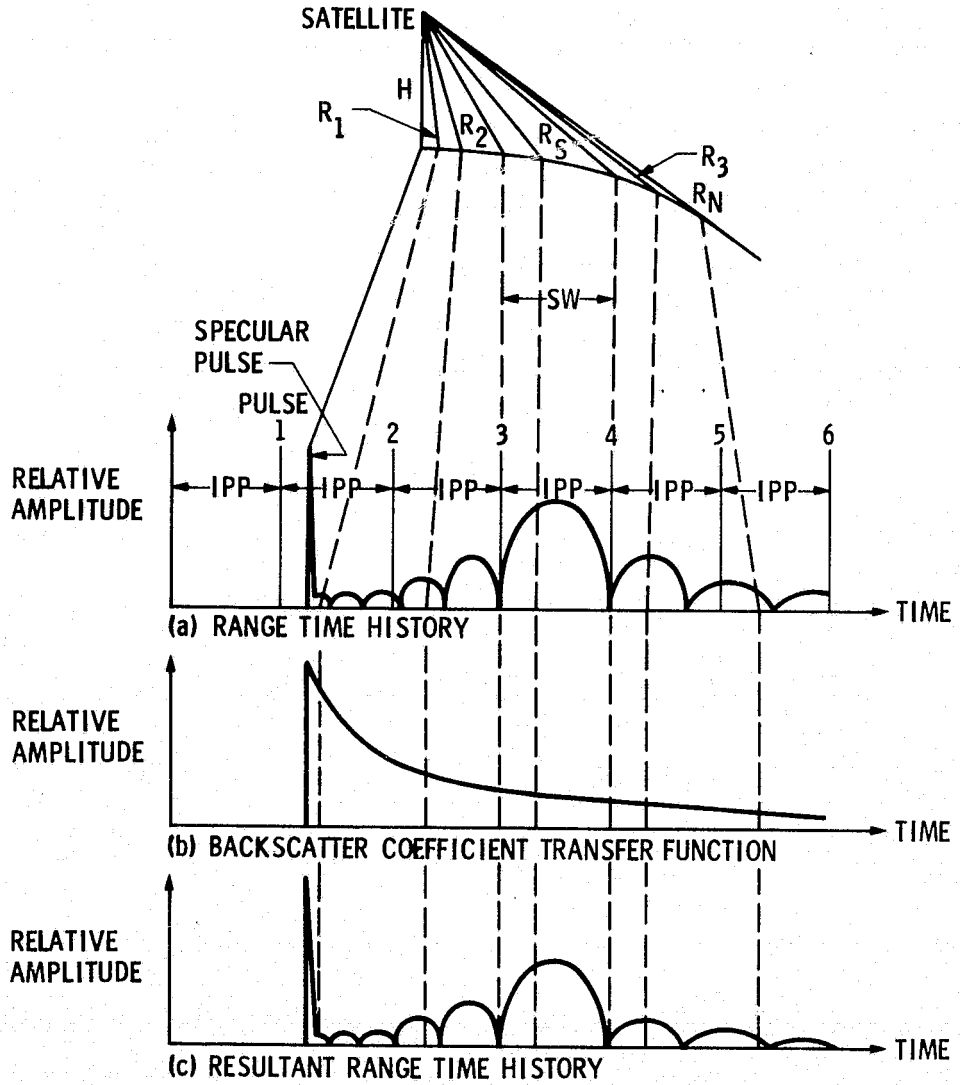

Figure 2.3.21. Range ambiguities

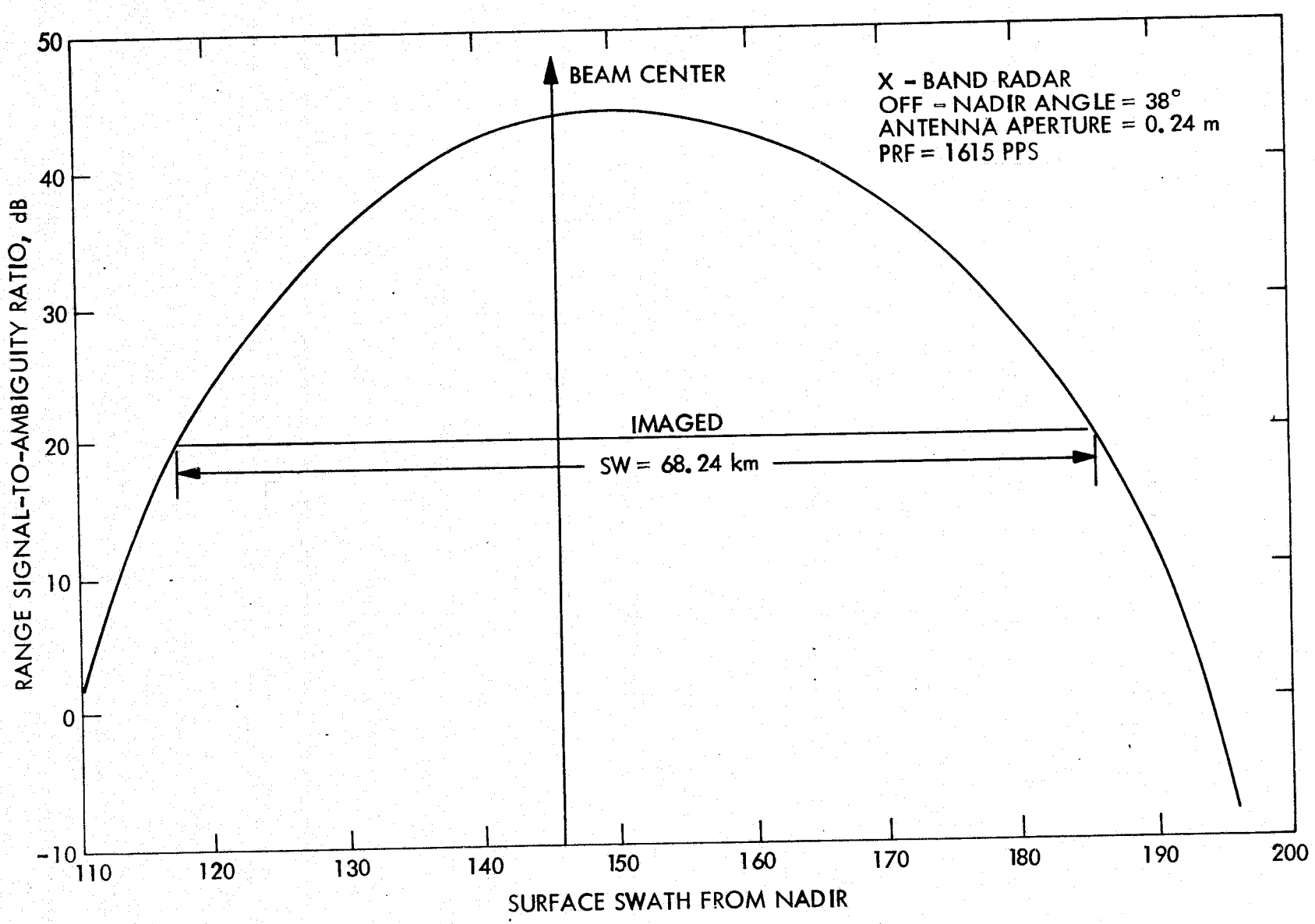

Figure 2.3.22. Range S/A ratio

Table 2.3.4. Imaged swath widths

Off-Nadir-Angle	L-Band			X-Band		
	25°	38°	50°	25°	38°	50°
Swath Width Factors						
1. Pulse interleaving constraints, km	100	85	75	100	85	75
2. Range ambiguities, km	96	69	66	88	69	63
3. Antenna null to null, km	178	94	103	147	95	98
4. Processor, km	113	78	63	113	78	63
Selected imaged swath width, km	96	60	63	88	69	63

change of that position. Even more basic to the pointing problem, then, is some knowledge as to the location of the zero Doppler plane (ZDP).

Orientation of the Zero Doppler Plane. The zero Doppler plane and other surfaces of constant Doppler frequency (isodops) are abstractions which are useful in the analysis of certain synthetic aperture problems. By definition, the zero-Doppler plane must be perpendicular to the velocity vector $\vec{V}_{net}$ which is the velocity of the real aperture with respect to the illuminated target. Thus the spatial orientation of the zero Doppler plane is determined by the direction of its normal, $\vec{V}_{net}$. The velocity $\vec{V}_{net}$ can be expressed as:

$$\vec{V}_{net} = \vec{V}_{sc} + \vec{\omega}_a \times \vec{r}_m - \vec{V}_{targ} \tag{24}$$

where

$\vec{V}_{sc}$ = orbital velocity vector of spacecraft

$\vec{\omega}_a$ = angular velocity vector of spacecraft (combined pitch, roll and yaw angular velocities)

$\vec{r}_m$ = position vector of center of antenna aperture relative to spacecraft center of mass

$\vec{V}_{targ}$ = velocity vector of target due to Earth rotation

Note that the velocity $\overrightarrow{V}_{sc}$ is a function of orbital location. $\overrightarrow{V}_{targ}$ is a function of target latitude and therefore a function of spacecraft latitude and altitude as well as antenna orientation.

The following remarks can be made concerning the orientation of the ZDP:

1) The ZDP is normal to the velocity vector $\overrightarrow{V}_{net}$. In order to determine its exact orientation, one must be able to determine the orbital velocity, target velocity and angular velocity of the spacecraft.

2) Even assuming absolute attitude stability (i.e., $\overrightarrow{\omega}_a = 0$), the ZDP tends to "wobble" with respect to the pitch, roll and yaw axes of the spacecraft. This is due to the combined effects of orbital eccentricity (changing $\overrightarrow{V}_{sc}$) and planetary rotation (changing $\overrightarrow{V}_{targ}$). Figure 3.2.23 illustrates this in terms of the angular displacement of the ZDP with respect to the S/C pitch and yaw axes for the following assumptions:

Nominal altitude = 185 km
Orbit eccentricity = 0.002
Inclination angle = 55°
Look angle = 25°
$\overrightarrow{\omega}_a = 0$
Non-steerable antenna beam

Alternate Solutions to Antenna Pointing Requirements. In the process of forming the synthetic aperture, it is necessary that any changes in the position of the antenna beam relative to the isodops be sensed and compensated. One way of doing this is to monitor the average Doppler shift of the radar data (in real time) and use this information to keep the beam centered about the required isodop. For a side-looking radar, this isodop would be the ZDP. This approach decreases the complexity of the correlator at the expense of precise beam steering.

A second approach is to monitor the Doppler content of the data during the correlation process and dynamically adjust the correlator to compensate for the effects described in the previous section. In effect, this moves the pointing

problem (and its solution) from the front end of the SAR system to the correlator. The correlator, therefore, must be made more sophisticated than in the steered-beam approach. The antenna pointing problem, on the other hand, is reduced to placing limits on the angular excursions of the antenna (pitch, roll and yaw) and on the rate of change of this angular motion.

Assuming the second method is chosen, it is possible to calculate the worst case allowable for ω_a, where $\omega_a = |\vec{\omega}_a|$. Two criteria must be satisfied which restrict the maximum allowable rotation rate, ω_{max}: (a) the position of the beam must be stable enough so that the target is illuminated for T, the time required to form the synthetic aperture, and so that amplitude modulation of the data due to antenna beam motion is minimized; and (b) the antenna motion should not produce an appreciable phase shift in the data during the time required to form the synthetic aperture. Requirements (a) and (b) are expressed more formally as:

$$\omega_{max} << \frac{\lambda}{L_a T} \tag{25}$$

and

$$\omega_{max} << \frac{\lambda}{r_m T} \tag{26}$$

where

$$T = \frac{\lambda R_S}{2V_{net}\ \rho_a}$$

λ = wavelength

R_S = slant range

ρ_a = azimuth resolution

L_a = azimuth dimension of antenna

r_m = moment area of center of antenna aperture relative to spacecraft CM

The restriction on ω_{max} may be re-written as:

$$\omega_{max} << \frac{2V_{net}\ \rho_a}{R \cdot \text{max of } \{L_a,\ r_m\}} \tag{27}$$

Substituting the values:

$$V_{net,\ min} = 7520 \text{ m/sec}$$

$$\rho_a = 25\text{m}$$

$$R_{max} = 326 \text{ km at } 50° \text{ off-nadir}$$

$$L_a = 12\text{m}$$

$$r_m = 10\text{m}$$

into expression (27) yields:

$$\omega_{max} << 0.096 \text{ rad/sec} = 5.5°/\text{sec}$$

This requirement will be met if the pitch roll and yaw rates are each limited to 0.01 degrees/second. This corresponds to a worst case phase distortion of 1.8 degrees over the synthetic aperture. Note that the worst contribution to the yaw rate resulting from Earth rotation and orbit eccentricity (see Figure 2.3.23) is approximately 0.004 degrees/second.

The limits on the maximum magnitude of pitch, roll and yaw angles are affected to some extent by the limitations of the correlator: the further the beam is allowed to swing away from zero Doppler, the more sophisticated the correlator must become.

In summary the recommended antenna pointing and stability limits are:

$\pm$0.5 degrees in pitch, roll, and yaw;

0.01 degrees/second maximum pitch, roll, and yaw rates.

2.3.9 Output Data Rates

Data outputs are presented for both a digital and analog radar outputs.

Digital Data Rate Outputs. Digital data rate outputs are presented for two configurations. The first configuration represents a single channel radar output data rate consisting of I and Q channel outputs at the receiver analog-to-digital converter (A/D). This data will be recorded and stored on a digital tape recorder and later correlated at the ground station. The second configuration represents fully correlated on-board imaged data that will be stored on a digital tape recorder and later processed at the ground station.

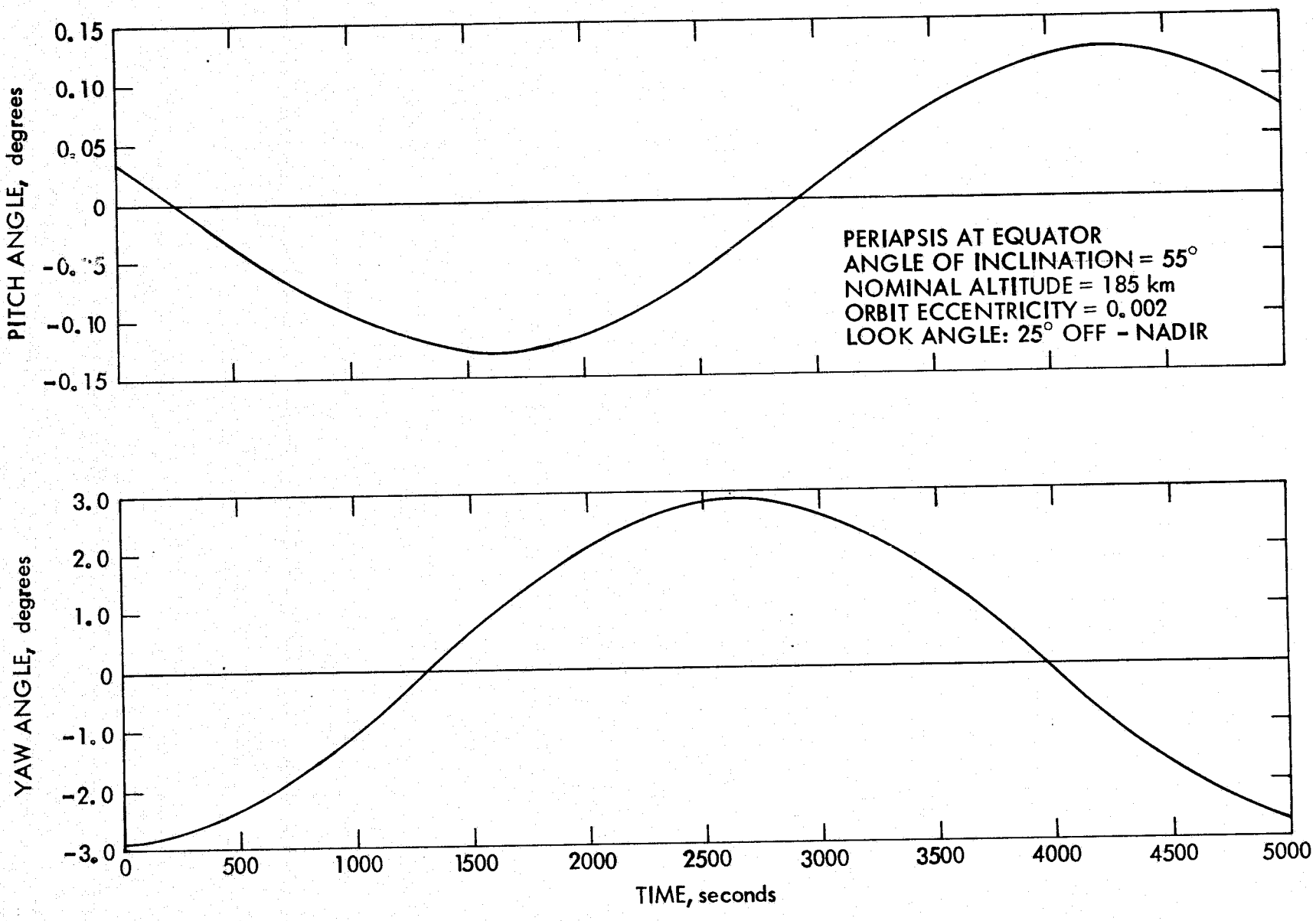

Figure 2.3.23. Pitch and yaw variation of zero doppler line

These data rate outputs are presented in Figure 3.2.24 as a function of imaged swath width. The three top curves represent unprocessed radar outputs for each of the three off-nadir angles. The last curve represents on-board correlated data rate outputs and shows a significant decrease in output data rates.

For unprocessed data rate outputs are computed by using the following equation:

$$DR = \left(\frac{SW}{r_r} + BT\right) \cdot 2 \cdot Q \cdot PRF \tag{28}$$

and the correlated or processed output rates are computed by

$$DR = \frac{SW}{r_r} \cdot Q \cdot \frac{PRF}{M} \tag{29}$$

where

SW = imaged swath width

r_r = range resolution

BT = range compression ratio = 400

Q = number of A/D quantization bits = 6

PRF = pulse repetition frequency = 1900

M = number of looks = 4

The above A/D (analog-to-digital) quantization bits represents a radar output dynamic range of 30 dB.

Analog Data Rate Outputs. An analog data rate output representing a single channel output of the receiver would require a 17.38 MHz bandwidth and a 30 dB radar output dynamic range. This data would then be recorded and stored on an optical recorder in the spacecraft and later correlated at the ground station.

2.4 SELECTED CONFIGURATION

The selected dual frequency radar system consists of L and X-Band radars and employs synthetic aperture and linear FM processing to achieve the desired resolution. Table 2.4.1 presents the radar parameters and is a result

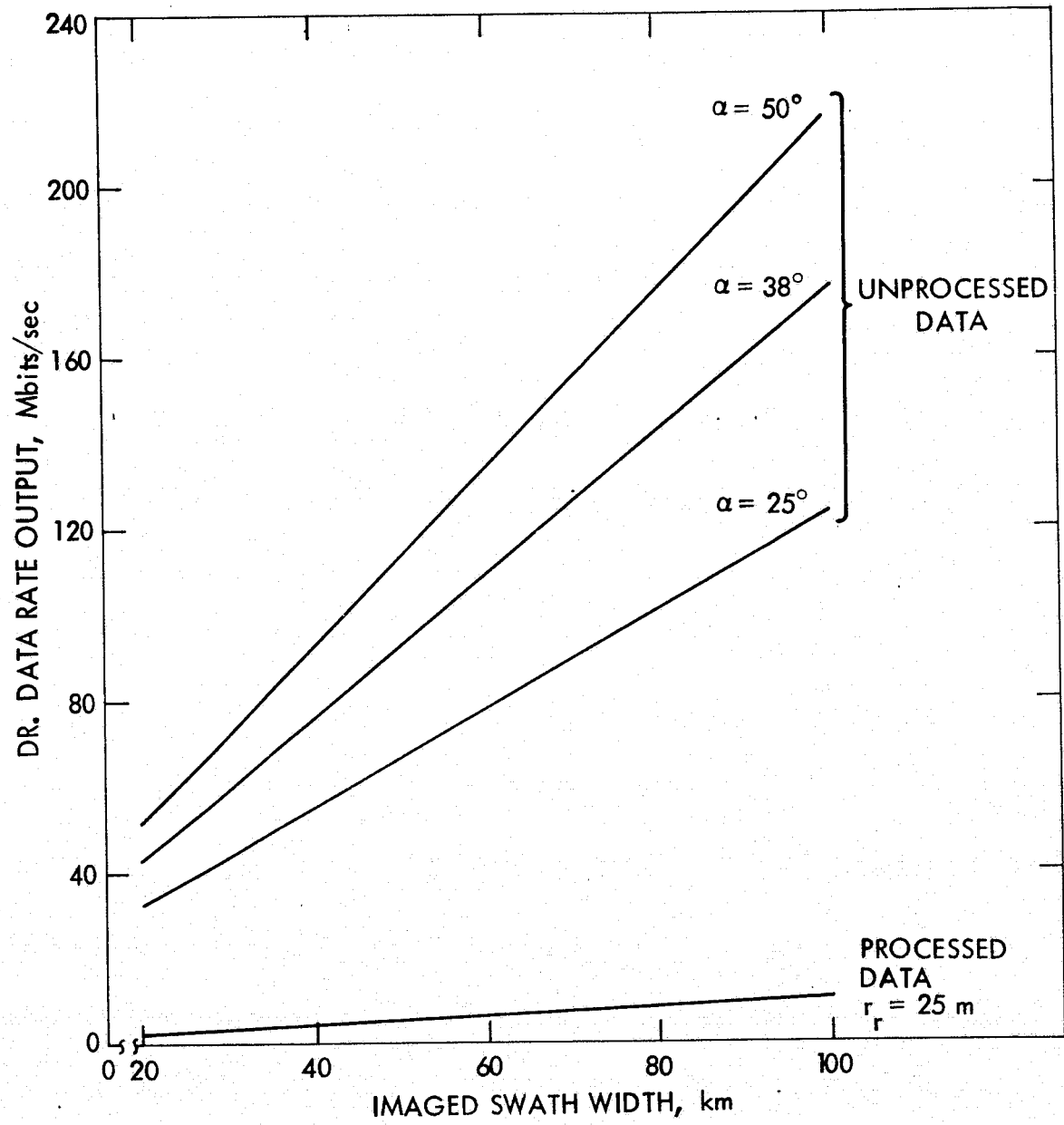

Figure 2.3.24. Digital data rate outputs

Table 2.4.1. Selected SAR System (h = 185 km)

Parameter	Radar System	
	L-Band	X-Band
1. Frequency, GHz	1.302	8.3328
2. Wavelength, m	0.23	0.036
3. Peak Transmitter Power, kW	6	20
4. Average Transmitter Power, kW	0.262	0.8
5. Transmitter Duty Cycle, %	4 - 6	3 - 5
6. Transmitter Efficiency, %	40	40
7. Transmitter Pulse Length, μsec	23	21
8. Antenna Polarization	HH, HV or VV, VH	HH, HV or VV, VH
9. Antenna Efficiency, %	70	70
10. Antenna Azimuth Dimension, m	12	12
11. Antenna Azimuth P-N Beamwidth, deg	1.1	0.172
12. Radar Output Quantization, buts	6	6
13. System Noise Figure, dB	≤ 3	≤ 3
14. System Losses		
RF, dB	4.1	6.0
Field Degradation, dB	1.0	1.0
Atmospheric, dB	0.3	0.4
15. System Noise Temperature, °K	1079	1630
16. Ambiguity (Overall), dB	<-18	<-18
Range, dB	-20	-20
Azimuth, dB	-22.5	-22.5
17. Spatial Resolution, m	25 and 50	25 and 50

Table 2.4.1. Selected SAR System (h = 185 km) (contd)

Parameter	Radar System					
	L-Band			X-Band		
18. Image Dynamic Range, dB	50			50		
19. Image Gray Scale Resolution, dB	1			1		
20. Weight, kg } See Note	Total = 310 kg					
21. Volume, m^3 } See Note	Total = 1.72 m^3					
22. Prime Power, kW } See Note	Total = 6620 watts					
23. Off-Nadir Angle, deg	25	38	50	25	38	50
24. Antenna Elevation Dimension, m	0.65	1.55	2.2	0.12	0.24	0.36
25. Antenna Elevation P-N Beamwidth, deg	20.8	8.5	6.0	17.45	8.63	5.74
26. Antenna Gain, dB	32.67	36.45	37.97	41.4	44.46	46.2
27. Minimum Scattering Coefficient, dB	-21	-23.2	-25.3	-21	-23.2	-25.3
28. System Bandwidth, MHz	17.38	17.38	17.38	17.38	17.38	17.38
29. Range Compression Ratio	400	400	400	365	365	365
30. Altitude, km	185	185	185	185	185	185
31. Signal-to-Noise Ratio, dB	17.98	19.13	15.33	14.2	13.8	10.7
32. Imaged Swath Width, km	96	69	63	88	68.2	62.2
33. Azimuth Compression Ratio	59.8	69.2	85.9	9.36	10.83	13.4
34. PRF, Hz	1810 1860	1615 1570	1700, 1790, 1870, 1900	1810 1860	1615 1570	1700, 1790, 1870, 1900

Table 2.4.1. Selected SAR System (h = 185 km) (contd)

Parameter	Radar System					
	L-Band			X-Band		
35. Multiple Looks (Total)	4, 16	8, 32	8, 32	4, 16	8, 32	8, 32
Azmiuth	4, 8	4, 8	4, 8	4, 8	4, 8	4, 8
Range	1, 2	2, 4	2, 4	1, 2	2, 4	2, 4
NOTE: Weight, volume and power estimates include: console, recorders, power supplies, transmitters, receivers. Does not include antenna.						

not only of system parameter tradeoffs but is determined as the most acceptable minimum system that would satisfy most user requirements.

The antenna for the L-Band radar consists of a single dual polarized planar array 12m by 2.2m. The X-Band radar antenna consists of two single polarized arrays, one horizontal and one vertical, 12m by 0.36m each. The total antenna dimensions being 12 x 2.92m. Each of the elevation arrays will be capable of generating different beams for each of the three off-nadir angles.

Table 2.4.2 presents a list of weight and power estimates of the selected configuration.

Table 2.4.2. Weight and Power Estimates

L, X-Band Radars	Weight (kg)	Power (W)
Transmitter	96	3708.3
Receiver	8	45.6
Digital	14	337.0
Power Supplied	59	1874.0
Console Instruments	16	55.0
Console Tape Recorders	55	600.0
Other	62	
TOTAL	310	6620.0

3.0 RADAR DESCRIPTION

This section contains a description of the design concept and hardware subsystem specification details of the selected candidate L and X-Band radars which reflect those parameters presented in Table 2.1.2.

3.1 DESIGN CONCEPT

The dual frequency Shuttle Synthetic Aperture Radar will generate a high resolution radar image of selected earth surfaces at one of three selectable off-nadir angle modes. This will generate a large amount of data which has to be recorded and processed.

The radar system and data handling capabilities of this study are projected to the 1978 state-of-the art hardware technology.

An operator, via the control panel, will have the capability of selecting the following radar functions as shown in Table 3.1.

Table 3.1. Radar functions

1.	Selection of any one of three off-nadir angles.
2.	Power on-off.
3.	Standby power on-off.
4.	Orbital altitude designation.
5.	PRF selection.
6.	Selection of data swath bounds.
7.	Manual/automatic receiver gain settings.
8.	Initiate calibration sequence.
9.	Antenna polarization selection
10.	Tape recorder selection and speed.
11.	Monitor return signal amplitudes by means of a CRT.
12.	Monitor system status by means of a CRT.
13.	STALO selection.
14.	Operate-Run (Data Taking).

The selected candidate L and X-Band radar system consists of the following: (See Figure 3.2.1)

1) A very stable oscillator which drives both L and X-Band transmitters, the logic and serves as a coherent reference for the return signals.

2) Logic which controls the system.

3) Two frequency chirp blocks to provide the frequency dispersion of the pulses to be transmitted.

4) Two TWT transmitters.

5) Switches, driven by logic, which allows the use of the same antenna for transmission and reception for two different polarizations.

6) Three deployable antennas, one L-Band dual polarized antenna and two X-Band single polarized antennas.

7) Switches, driven by logic, which allows the use of any one of the three different antenna apertures corresponding to the selection of any one of the three off-nadir angles.

8) Four receiver channels with corresponding receiver protectors to avoid high transmitter power leakage into the receiver.

9) Two receiver low-noise transistor amplifiers for the L-Band radar and two receiver low-noise parametric amplifiers for the X-Band radar.

10) Four quadrature mixers and Eight analog-to-digital converters.

11) Digital data formaters and magnetic tape/recorders.

12) Control panel for initiating the various radar functions.

The data processing configuration will be presented in Section 5. This entails storage of raw data on board Shuttle. The processing will be done by the ground station to produce a hard copy image.

3.1.1 Hardware Design Philosophy

The hardware design philosophy adopted for this study consists of meeting several requirements. These requirements which are described below are in keeping with the concept of a high reliability system design.

1) Single point failures will be minimized at a minimum cost. This in turn will maximize the probability of success.

2) The utilization of a redundant design in those critical areas at a minimum cost. Redundancy will be incorporated in those areas where single point failures are most likely to occur and are identified as the TWT transmitter and high voltage power supply.

3) Parts with known reliability history will be used.

4) Existing NASA or DOD hardware will be used whenever possible.

5) Construction and packaging will be of modular form as distinct functions will be individual replacable packages for ease of repair and accessibility.

6) Provisions for adequate base plate temperature control will be done to minimize temperature constraints on hardware design.

7) All RF interconnections will be done by means of semirigid coax for maximum shielding.

3.1.2 Radar Calibration

The instrument calibration approach is that of determining what the radar gains and transmitted power are so that the receiver power and ground reflectivity may be determined. As receiver gain varies with AGC, it is desirable to have calibrated image output density strips. This is achieved by initiating calibration tests prior to the data acquisition time across the desired swath.

These calibrated image density strips will appear on the film and reflect system conditions prior to the data acquisition time. The precise time location and amplitude of the actual image is compared with the calibrated image density strips which allow reflectivity calculations to be made upon a map coordinate designation as well as direct visual density comparisons.

Reflectivity Determination. The reflectivity or backscatter coefficient is basically determined by comparing the received with transmitted power. Detailed examination of the measurement indicates that a variety of radar parametric factors must be accurately known in order to make a determination.

Examination of the equation for the reflectivity or backscatter coefficient indicates areas of concern. The equation is given below.

$$\sigma^o = \frac{P_r \, 2(4\pi)^3 \, R_s^3}{P_t \, G^2 \lambda^2 C \, T \, \alpha_{AZ}} \tag{1}$$

where

P_t = Peak transmitter power.

P_r = Received power

σ^o = Backscatter coefficient (unit cross-section)

G = One-way antenna gain

λ = Transmitted wavelength

R_s = Slant range.

θ = Surface angle

C = Speed of light

T = Transmitter pulse width

α_{AZ} = Azimuth beamwidth

The above equation serves to indicate the salient parameters that must be considered.

Calibration Technique. A calibrated series of pulses over a 42 dB dynamic range decreasing in magnitude in steps of 3 dB are generated for this technique. These pulses are derived from the transmitter output power out of the 30 dB coupler through the precision attenuator and injected into the directional couplers of the receiver front end by the calibration sequencer. As the antenna is excluded in this calibration technique, the antenna gain patterns

must be measured accurately prior to installation on Shuttle. These calibration pulses pass through the entire radar/processor system, ultimately appearing on the output or map film. These calibration pulses are then compared in density with the map imagery. As the attenuation between the transmitter and receiver is known, the fractional received to transmit power can be determined. Thus a stable, accurate calibration technique is available with an assumed accuracy of better than 3 dB.

Continuous system monitoring of such parameters as transmit power, receiver gain via the AGC voltage as well as other parameters will be monitored and recorded along with the data. This will provide a measure of general system status as well as an independent verification of reflectivity calculations.

The calibration signal injection block diagram is shown in Figure 3.1.1. The transmitter pulse is taken out of the 30 dB coupler through the precision step attenuator, directional couplers and injected into both horizontal and vertical polarized receiver channels.

The calibration sequencer will produce appropriate timing such that 20 pulses per IPP interval are generated for the entire calibration sequence time. This is shown in Figure 3.1.2.

The procedure for the proposed calibration scheme is as follows:

1) Calibration sequence will be commanded prior to data taking.

2) The receiver AGC will be set to maximum gain.

3) Test pulses for the maximum input power will be injected into the front end directional couplers for a simulated image integration interval by the calibration sequencer.

4) Step 3 will be repeated 14 times and will range over a 42 dB dynamic range that is decreased in magnitude in steps of 3 dB.

5) The AGC will then be set at maximum gain minus 3 dB.

6) Step 4 will be repeated 14 times.

7) The AGC will be set to its next gain setting until a total of a 42 dB dynamic range is covered. Step 3 will be repeated each time.

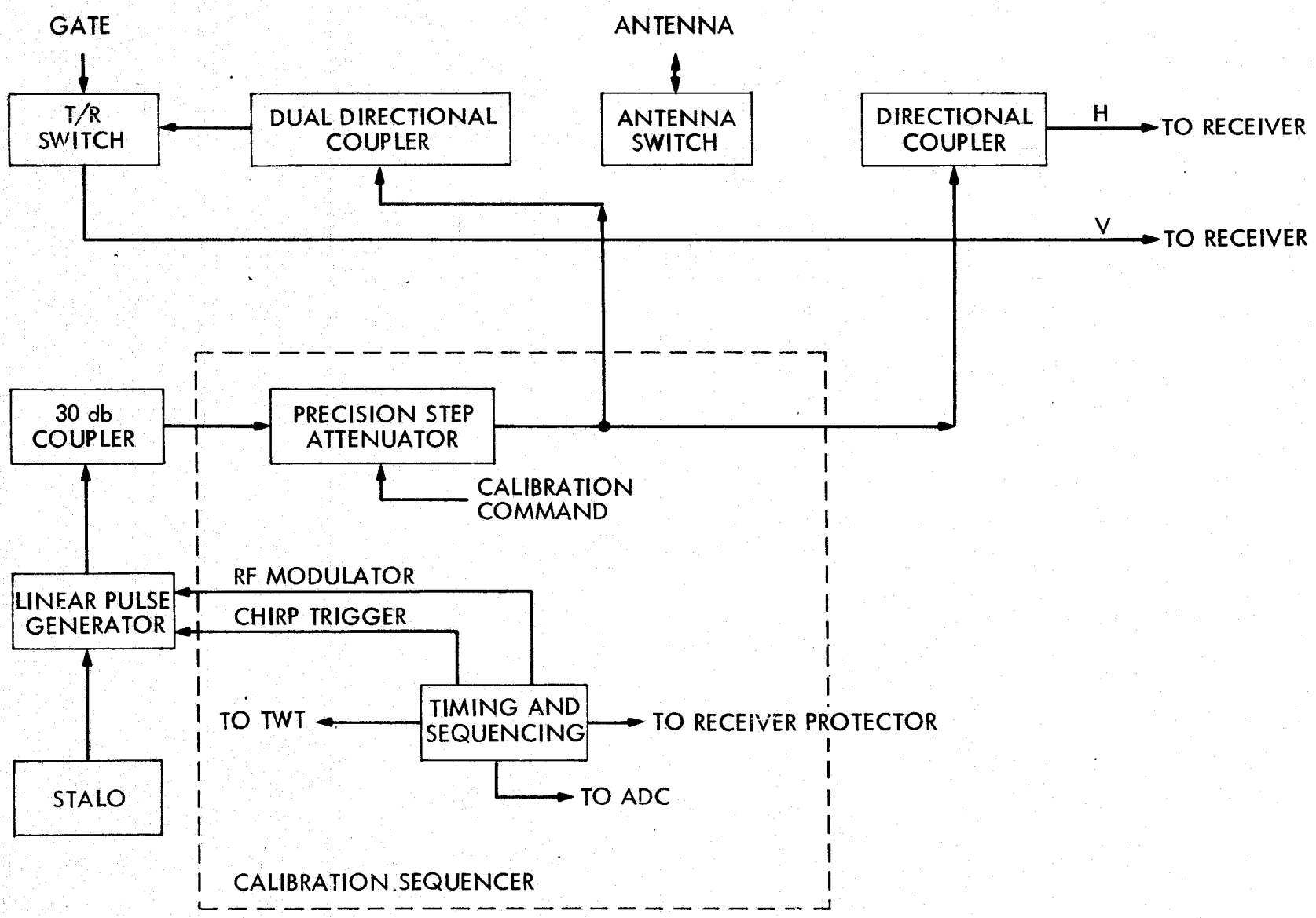

Figure 3.1.1. Calibration signal injection

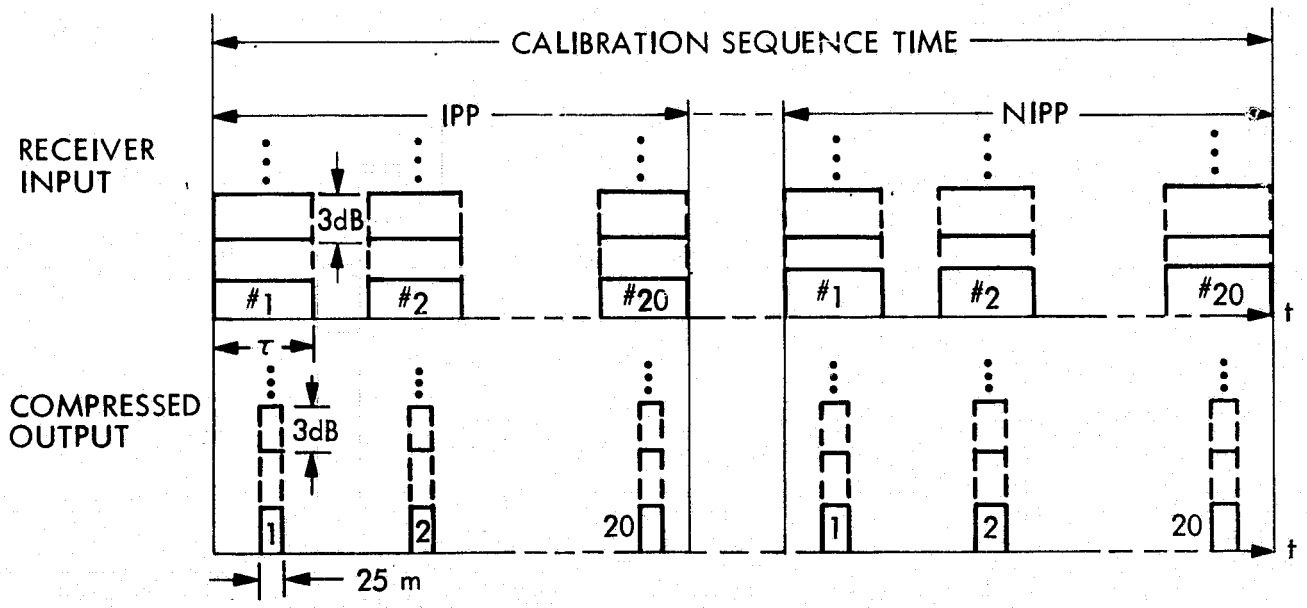

Figure 3.1.2. Calibration pulses

8) After the last AGC step, control will be returned to normal operation.

The entire calibration sequence will produce 196 different calibrated image density strips. These strips will represent 25 meter resolution bands across the range interval. The total calibration sequence will vary from 5 sec to 50 sec, depending which off-nadir angle and radar is being calibrated. Since this calibration system does not calibrate the antenna, it is suggested that a separate transponder be implemented at some location on the ground to allow calibration of the antenna system.

3.2 OVERALL RADAR BLOCK DIAGRAM

The Shuttle Synthetic Aperture Radar, consists of four basic system blocks, as shown in Figure 3.2.1. These are:

1) Radar Control Console
2) L-Band Radar System
3) X-Band Radar System
4) Antenna Subsystem

The Radar Control Console provides all the control and data-handling functions for both radars. An operator, via the control console, will turn-on the radars, select their operating modes, and record data on two magnetic tape recorders. Section 3.8 contains a detailed description of the Control Console. The digital tape recorders are discussed in Section 4.

The L-Band radar system consists of a transmitter, two receivers, a digital data formatter, a digital sequencer, and a power conditioning subsystem. A switch at the output of the transmitter selects the antenna polarization to be transmitted. The digitized outputs of the data formatter, and the outputs of the digital sequencer are routed to the interface panel of the control console. Commands from the console are routed to the digital sequencer, where they are decoded and executed. The transmitter and receiver portions of the L-Band radar are described in detail in Section 3.4. The digital sequencer and digital data formatter are described separately in Section 3.6. The power subsystem is discussed in Section 3.7.

Implementation of the X-Band radar is basically the same as for the L-Band radar. It, consists of a transmitter, two receivers, a digital data

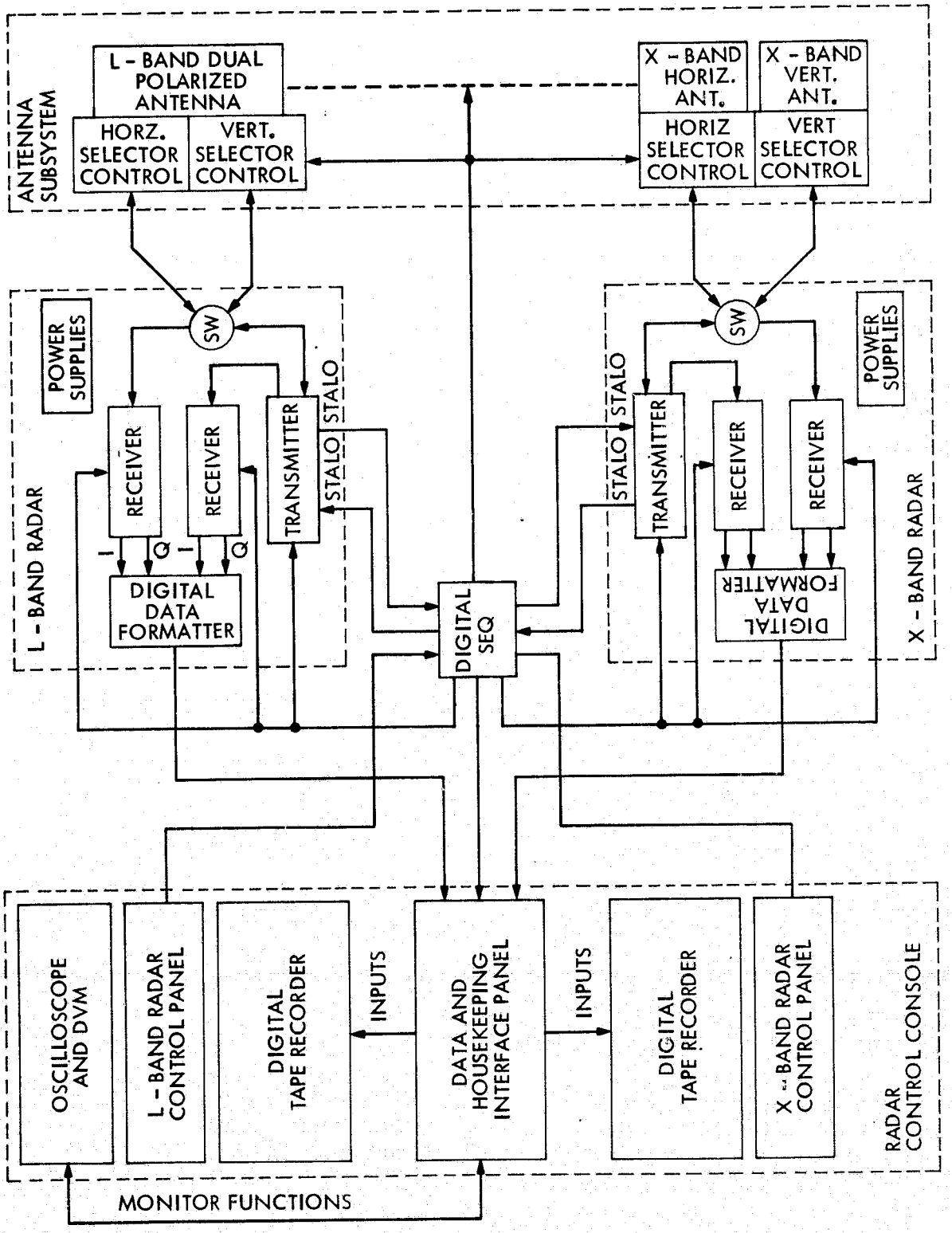

Figure 3.2.1. Overall radar block diagram

formatter, a digital sequencer, and a power conditioning subsystem. A detailed description of the X-Band transmitter and receivers can be found in Section 3.5. The digital data formatter, digital sequencer, and power subsystems are discussed separately in Sections 3.6 and 3.7.

Each radar operates independently of each other. A stalo from one of the radars can be used as a reference for the other. When this is done, the radars operate in coherence with one another.

Selection of transmitting antenna polarization is accomplished on command from the console.

The Antenna subsystem is comprised of one L-Band, dual-polarized antenna and two X-Band, singly-polarized antennas. The off-nadir angle is selected by command from the console. A detailed description of the antenna subsystem can be found in Section 3.3.

3.3 ANTENNA SYSTEM

This section reflects the selected L and X-Band radar system. Three antennas are required, each of which will consist of a rectangular array with proper feeds couples to a common aperture to generate three independent beams at the three off-nadir angles as shown in Figure 3.3.1. The L-Band antenna will consist of a common dual polarized rectangular aperture. Each of the X-Band antennas will consist of a single polarized (H and V) rectangular aperture. The salient parameters are given in Table 3.3.1. The total dimension of the antenna being 12 m by 2.92 m.

3.3.1 Antenna Characteristics

The antenna characteristics are given in Table 3.3.1. These characteristics reflect the major system constraints of maximizing gain and minimizing range and azimuth ambiguities.

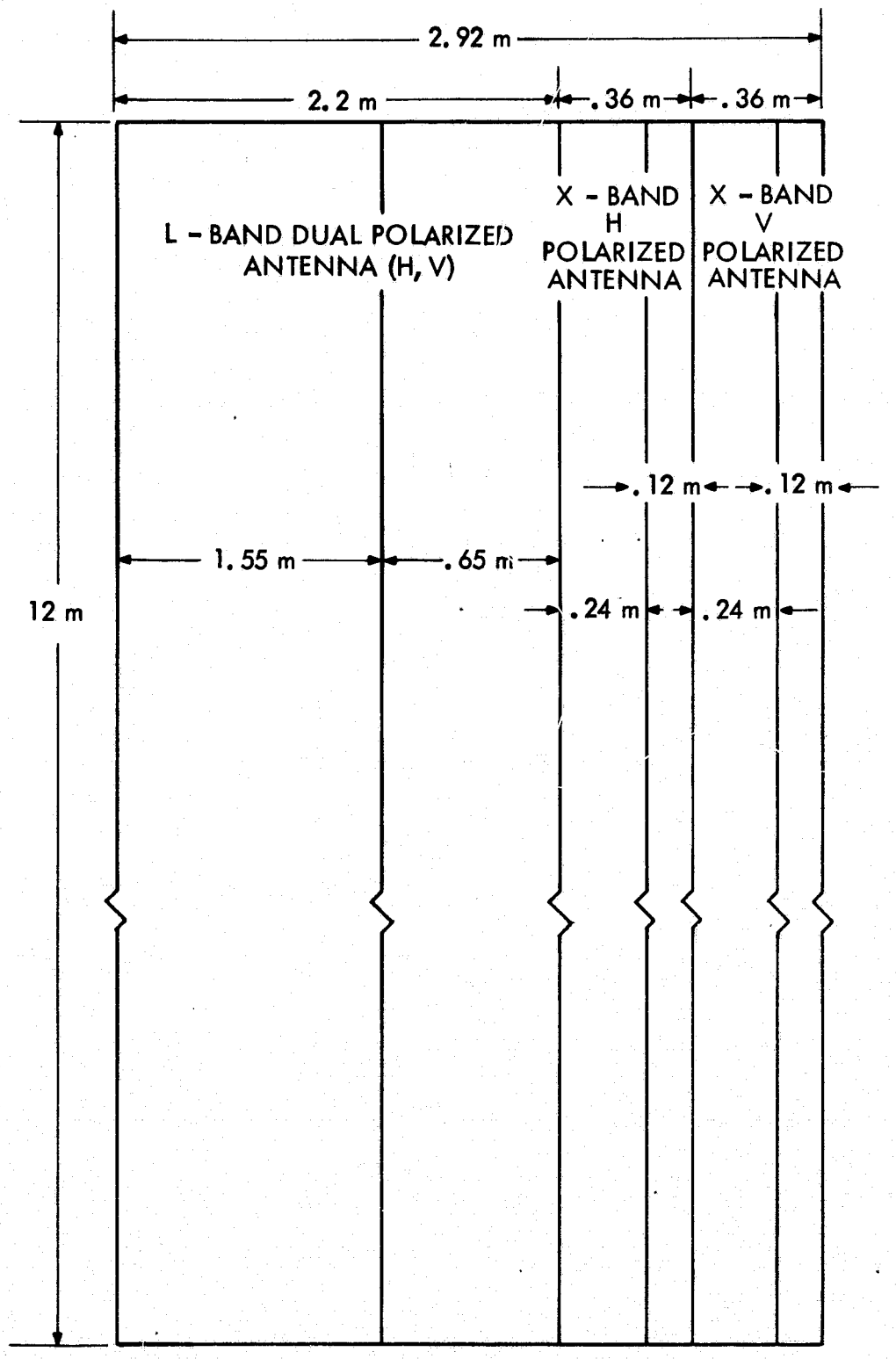

Figure 3.3.1. Arrangement of L-band and X-band antenna aperture

Table 3.3.1. Antenna characteristics

Frequency	L-Band (1.302 MHz)			X-Band (8.33 MHz)			X-Band (8.33 MHz)		
Polarization	Dual (H and V)			Single (H)			Single (V)		
Azimuth dimension, m	12			12			12		
Azimuth Peak-to-Null beamwidth, deg	1.1			0.172			0.172		
Efficiency, %	≥70			≥70			≥70		
Peak power rating, kW	6			20			20		
Pointing accuracy, deg	±0.5			±0.5			±0.5		
Peak sidelobe level									
Azimuth (one-way), dB	≤13.5			≤13.5			≤13.5		
Elevation (one-way), dB	≤13.5			≤13.5			≤13.5		
Off-nadir angle, deg	25	38	50	25	38	50	25	38	50
Bandwidth, ±0.1 dB, MHz	17.38	17.38	17.38	17.38	17.38	17.38	17.38	17.38	17.38
Peak Gain, dB	32.67	36.45	37.97	41.4	44.46	46.2	41.4	44.46	46.2
Elevation dimension, m	0.65	1.55	2.2*	0.12	0.24	0.36*	0.12	0.24	0.36*
Elevation Peak-to-Null beamwidth, deg	20.8	8.5	6.0	17.45	8.63	5.74	17.45	8.63	5.74

*The 25° and 38°, panels are combined to form the 50° panel (see Figure 3.3.1)

The mechanical design goals consists of meeting several requirements, namely:

1) Lightweight design, to facilitate the launch and orbiting processes, deployment and redeployment processes.
2) Material and components that do not deform under high thermal gradients or during outgassing.
3) The design must be strong enough to resist the shock and vibration loads encountered in service.
4) Antenna material must not outgas so slowly as to present a corona problem.

3.3.2 Antenna Pointing and Stabilization

The antenna pointing and stabilization requirements were derived in Section 2.3.8. These limits are:

±0.5 degrees in pitch, roll and yaw;

0.01 degrees/sec maximum pitch, roll and yaw rates.

3.3.3 Antenna Deployment System

The antenna will be stowed in the pallet area for launch and landing. For ease in deployment and to minimize losses the number of folds must be kept small. The present design assumes two folds resulting in a stowed package of approximately 4 x 3 m . In the fully deployed position the antenna will appear as shown in Figure 3.3.2. Should the deployment mechanism fail to retrieve the deployed antenna, the antenna will be jettisoned. No EVA's will be attempted to salvage the antenna.

The details of the deployment mechanism and antenna supporting structure are not included in this report. However, a tentative design is sketched in Figure 3.3.3.

3.3.4 Antenna Study

JPL has subcontracted an antenna study to the Ball Brothers Research Corporation. The purpose was to determine the feasibility of a large microstrip antenna for space SAR application. It was assumed that alternative approaches to the antenna design were pursued in a parallel study by Hughes Aircraft Corp. for JSC and that the alternatives need not be investigated by JPL at this time. The significant results of the BBRC report are included in this report as Appendix B.

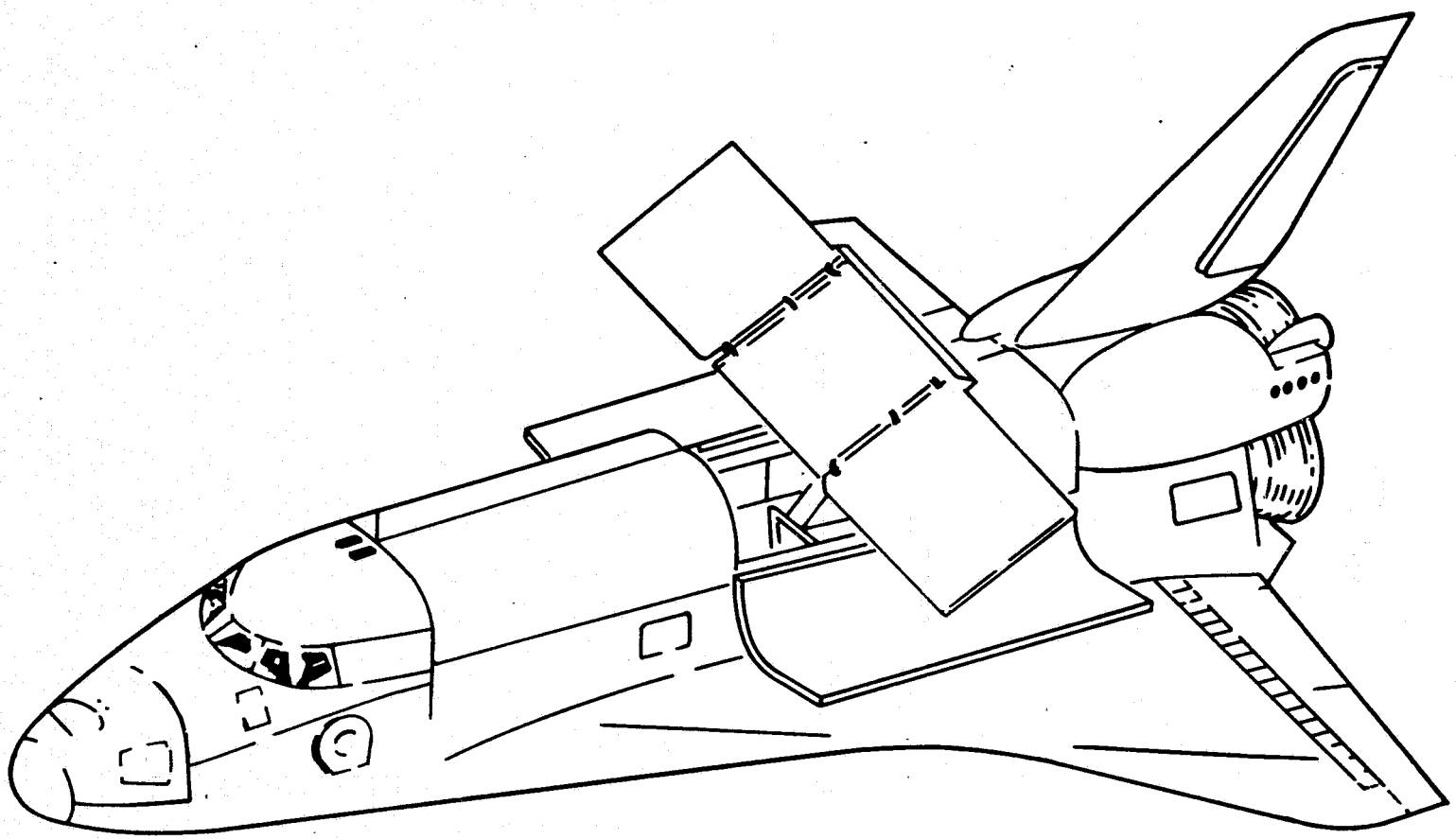

Figure 3.3.2. Array Unfolds from Pallet on Shuttle

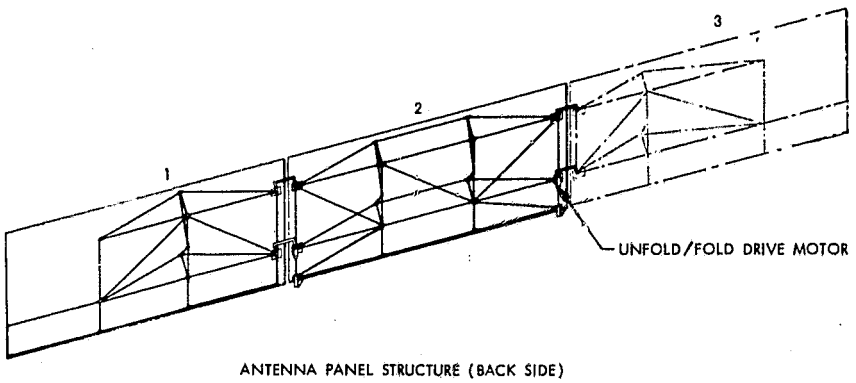

ANTENNA PANEL STRUCTURE (BACK SIDE)

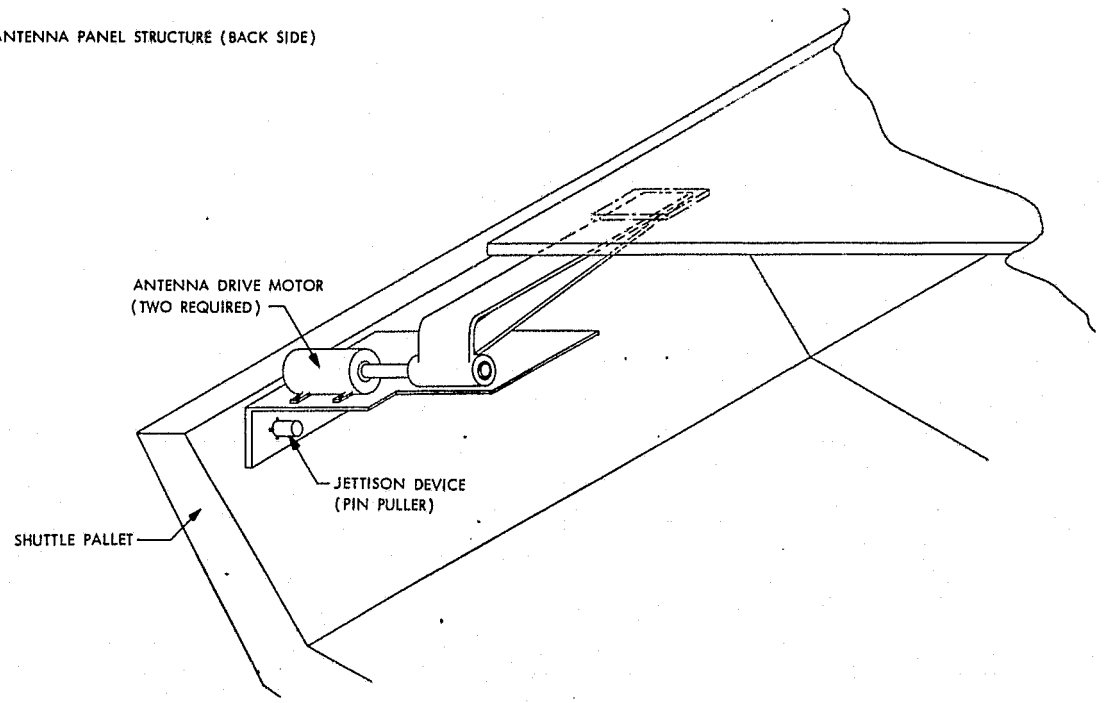

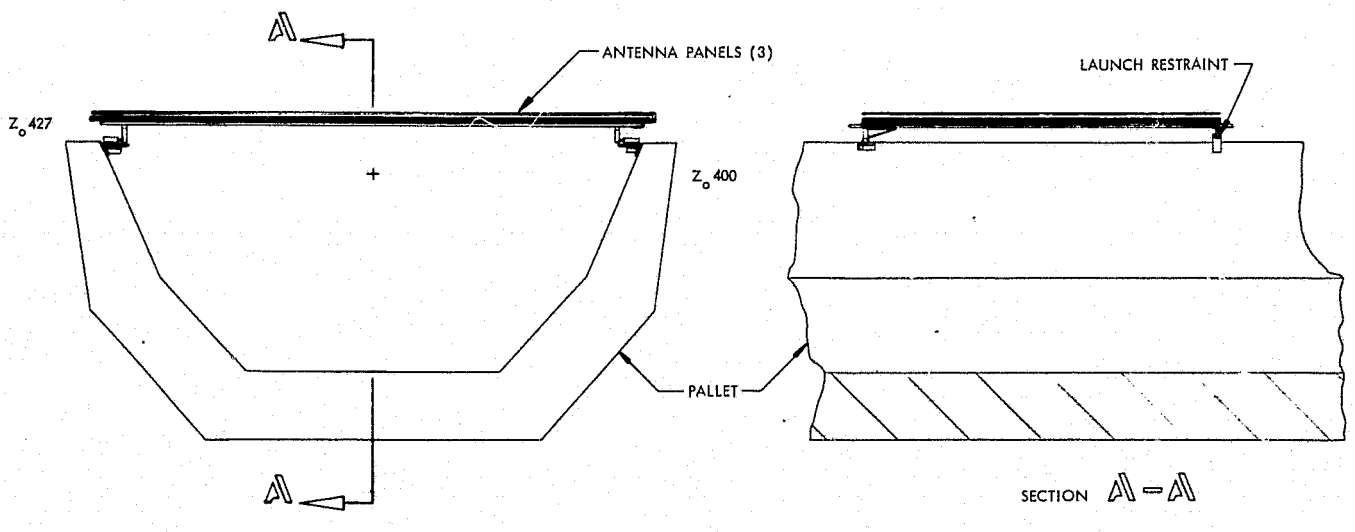

STOWED CONFIGURATION

Figure 3.3.3. Antenna Supporting Structure

3.4 L-BAND SYSTEM

3.4.1 L-Band System Block Diagram

The Shuttle L-Band Imaging Radar, Figure 3.4.1, consists of four subsystems:

1) Transmitter Subsystem
2) Receiver Subsystem
3) Digital Sequencer and Digital Data Formatter
4) Power Conditioning Subsystem

The Transmitter Subsystem consists of a stable local oscillator, a linear FM pulse generator, and a Traveling-Wave-Tube final amplifier. The transmitter pulse is 23 microseconds wide with a peak power of 6 kilowatts and a maximum repetition frequency of 1900 Hertz.

The Receiver Subsystem consists of one double-sideband, singly-het heterodyned receivers - one for each antenna polarization. Each receiver is comprised of a low-noise, front-end amplifier followed by a variable-gain amplifier and a quadrature mixer. The quadrature mixer produces two video signals 90° out-of-phase with each other. The video signals are amplified to produce ± 1 volt peak-to-peak signals at the inputs of the analog to digital converters (ADC). The noise figure of each reciever is less then 3.0 dB referred to its input. Its center frequency is 1302 MHz with a bandwidth of 17.4 MHz, and its overall gain is programmable from 40 dB to 80 dB.

The Digital Sequencer portion of the Digital Sequencer and Data Subsystem provides all the logic and timing functions for the radar. From its connections with the control panel, it provides all the turn-on and mode selection commands for the radar. Also, it provides the signals for initiating and executing the calibration sequence. The Digital Data Formatter consists of high-speed Analog-to-Digital converters and accept the four receiver video signals and converts them to a digital format for recording on magnetic tape. A further description of the Digital Sequencer and Data Subsystem can be found in Section 3.6.

The power supply subsystem consists of dc-to-ac and dc-to-dc converters, which provide all the voltage levels required by the radar. Some of the dc outputs are unregulated, and supply power to those circuits which have "on-board" regulators. Efficiency of dc-to-ac conversion is better than 80%,

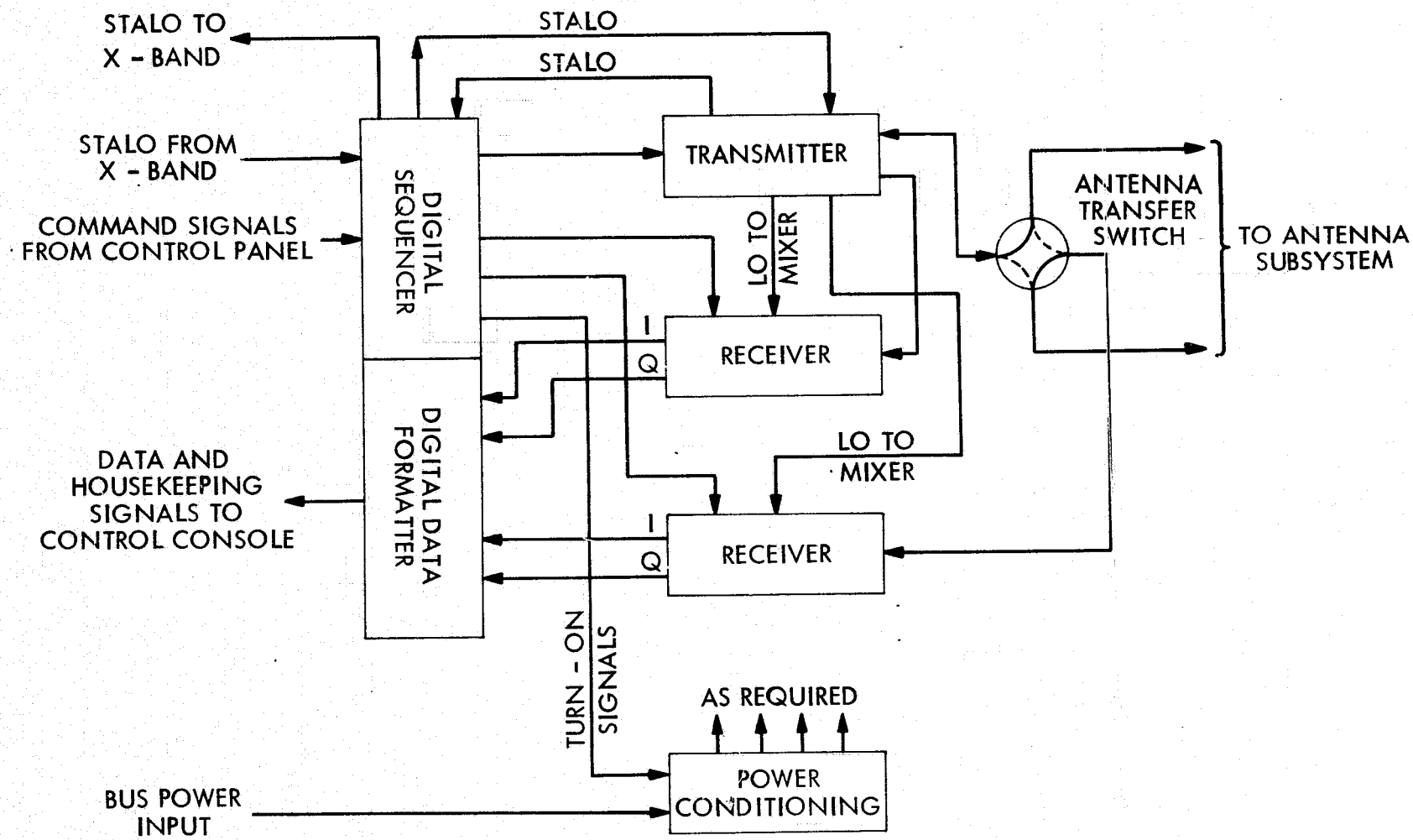

Figure 3.4.1. L-band radar block diagram

and dc-to-dc converstion is better than 70%. An estimate of the power requirements for the L-Band radar can be found in Section 3.11. A move complete description of the power supply subsystem can be found in Section 3.7.

3.4.2 L-Band Transmitter Subsystem

General Description. A block diagram of the transmitter subsystem is shown as part of Figure 3.4.2. A 86.8 MHz signal from the stable local oscillator is routed to the stalo distribution system. On command from the digital sequencer, the stalo distribution system selects either the L-Band stable oscillator or the X-Band stable oscillator to be used as the master frequency standard for the radar. The selected oscillator signal is amplified and fed to the data system and frequency multiplier.

The frequency multiplier accepts the 86.8 MHz signal and multiplies it times 15 to produce the L-Band fundamental carrier frequency of 1302 MHz. The 1302 MHz signals are routed to the chirp generator and the local oscillator ports of the quadrature mixures in the receiver subsystem.

The chirp generator uses the 1302 MHz signal as a reference for creating a linear frequency modulated signal for the transmit event. A voltage-controlled oscillator (VCO) operating at the fundamental carrier frequency is phase locked with the reference signal. When triggered by the Digital Sequencer, the phase-locked-loop is opened, and a linear voltage ramp is applied to the VCO. At the end of the sweep, the loop is closed, and the VCO reacquires the reference signal.

The output of the chirp generator is fed to the RF modulator, which accurately gates the FM waveform to produce the required sidelobe levels in the transmitted signal.

The output of the RF modulator is fed through a bandpass filter and a 30 dB coupler to the input of a transistor power amplifier. The 30 dB coupler picks out a portion of the transmitted waveform signal, which is passed through a precision step attenuator and used as a calibration signal for the receivers.

The transistor driver amplifier amplifies the low-level FM signal to a level sufficient to drive the TWT final amplifier into saturation.

The Traveling-Wave-Tube amplifier is a PPM-focused, conduction-cooled type having a minimum gain of 40 dB and a peak output power of 6 kilowatts. DC

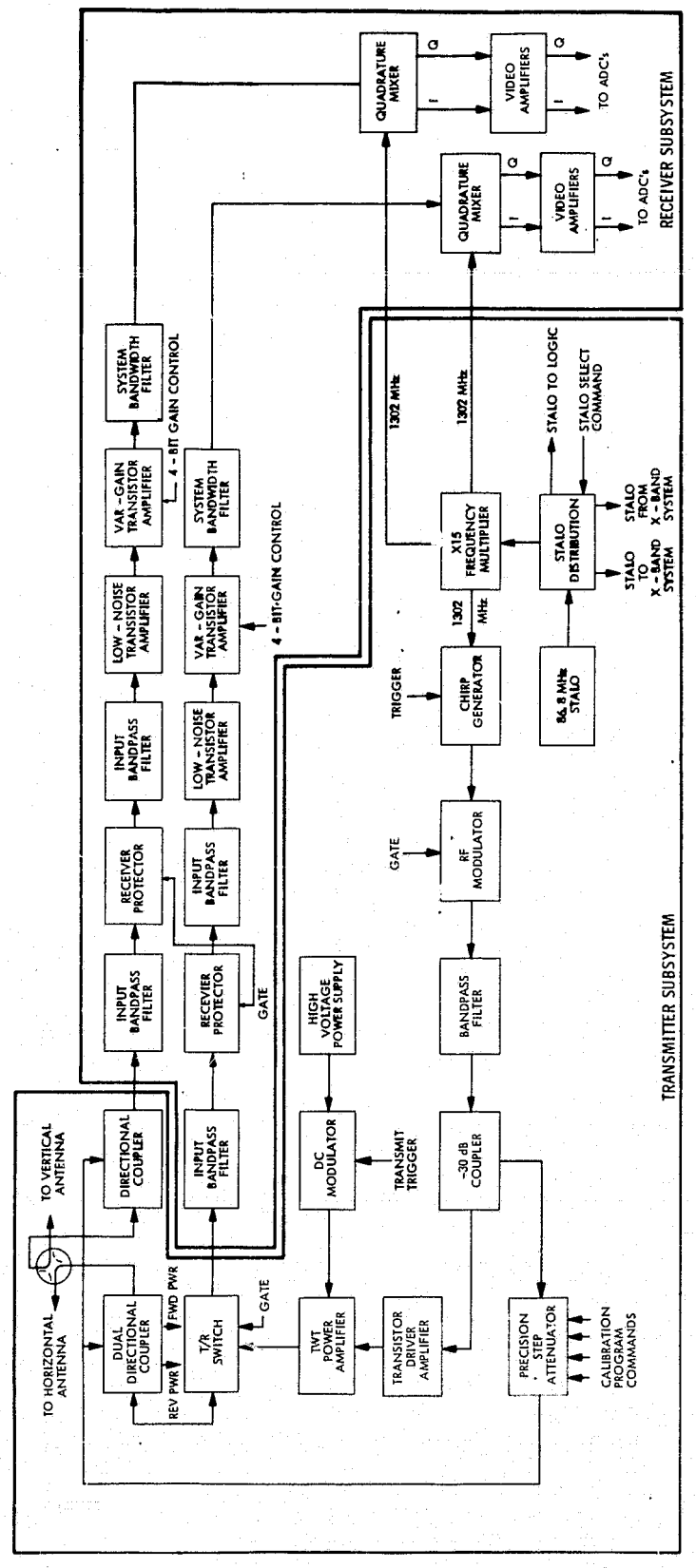

Figure 3.4.2. Block diagram of L-band transmitter and receiver

to RF efficiency of the tube is expected to be 30% and its maximum duty cycle is 4.37%. Conduction cooling of the tube is facilitated by heat pipes strategically placed around its body.

The high-power RF pulse is routed through a T/R switch, a dual-directional coupler, and the antenna switch before finally reaching the antenna.

The Transmit/Receive Switch is a PIN-diode SPDT switch with low insertion loss and moderate isolation. The dual directional coupler provides a measurement of forward and reflected power as well as coupling the calibration signal into the receiver. The antenna switch is a low insertion loss, mechanical, coaxial switch with two positions.

The transmitter electrical characteristics are presented in Table 3.4.1.

Stalo. The STALO is the master frequency standard in the radar system. Both the X-Band and L-Band systems have STALOs operating at 86.8 MHz. Provision is made in the STALO distribution systems of both radars to select the source to be used in each radar. Consequently, each radar can be operated independently or in coherence with each other.

Extreme stability is of the STALO achieved by temperature control of the oscillator circuit using a proportional oven.

Stalo Distribution System. The stalo distribution system selects the reference oscillator to be used as the frequency standard and distributes it to the rest of the radar. Either the L-Band stalo or the X-Band stalo can be selected to run the radar. If the X-Band stalo is selected to run both radars, the L-Band stalo will be turned off to eliminate the possibility of interference. Conversely, if the L-Band stalo is selected to run both radars, the X-Band stalo will be turned off by the X-Band control system.

A hybrid power divider will provide the basic signal splitting function. Buffer amplifiers will provide additional isolation and gain for each output circuit.

Chirp Generator. This subassembly generates a linear FM signal to be used as the transmitted chirp. The rate of frequency sweep is 0.7557 MHz/microsecond.

Table 3.4.1. L-Band transmitter electrical characteristics

1	STALO	
	Frequency	86.8 MHz
	Frequency Stability	$\pm 10^{-4}$ ppm/sec
	Temperature Stability	$\pm 10^{-6}$ ppm/°C
	Power Consumption:	3 watts
	Warm Up Time	20 minutes
2	STALO DISTRIBUTION SYSTEM	
	Input Frequency	86.8 MHz
	Input Level	10 milliwatts
	Output Level	10 milliwatts/port, 2 ports
	Isolation, port-to-port	40 dB minimum
	Power Consumption	1.5 watts
3	CHIRP GENERATOR	
	Input Reference Signal	1302 MHz, 10 milliwatts
	Output Frequency Sweep	0.7557 MHz/microsecond
	Output Power Level	10 milliwatts
	Trigger Input	TTL level pulse
	Power Consumption	3 watts
4	RF MODULATOR	
	Input	FM signal from chirp generator; 10 milliwatts
	Insertion Loss (switch closed)	1.0 dB maximum
	Isolation (switch open)	50 dB minimum
	Trigger Gate	TTL level, 23 micro-seconds wide
	Power Consumption	1.5 watts
	Frequency Sweep after gating	1293.31 MHz to 1310.69 MHz

Table 3.4.1. L-Band transmitter electrical characteristics (contd)

5	BANDPASS FILTER	
	Center Frequency	1302 MHz
	Bandwidth	±50 MHz
	Insertion Loss	0.3 dB maximum at 1302 MHz
	Flatness of Passband	±0.1 dB
	Out of Band Rejection	50 dB down at ±300 MHz
6	PRECISION STEP ATTENUATOR	
	Input	4-bit binary coded word
	Attenuation	16 steps
	Power Consumption	1.5 watts
7	TRANSISTOR DRIVER AMPLIFIER	
	Gain	20 dB nominal
	Bandwidth	1252 MHz to 1352 MHz
	Saturated Power Output	200 milliwatts
	Power Consumption	2.4 watts
8	TRAVELING-WAVE-TUBE FINAL AMPLIFIER	
	Saturated Gain	50 dB
	Bandwidth	1250 MHz to 1350 MHz
	Peak Power Output	6 Kilowatts
	Maximum Duty Cycle	5%
	Nominal Beam Voltage	11 Kilowatts
	Nominal Beam Current	1.82 amps peak
9	DC MODULATOR ELECTRICAL CHARACTERISTICS	
	Input Trigger	TTL level gate
	Filament and Bias Supply Power Consumption	48 watts

Table 3.4.1. L-Band transmitter electrical characteristics (contd)

10	TRANSMIT/RECEIVE SWITCH	
	Insertion Loss, Antenna to Transmitter or Receive port	0.3 dB
	Isolation, Transmitter to Receiver port	25 dB minimum
	Frequency	1250 MHz to 1350 MHz
	Power Rating	6 kW peak pulse, 23 microseconds wide
	Input Trigger	TTL gate
	Power Consumption	4.5 watts
11	TRANSMITTER POWER MONITOR	
	Power Rating	6 kW peak pulse, 23 microseconds wide at 1900 pps
	Calibration Power Input	Less than -20 dBm
	Mean Coupling, Calibration Signal to T/R switch port	-30 dB
	Output	Calibrated DC signals proportional to foreward and reflected peak powers.
12	ANTENNA SWITCH	
	Insertion Loss	0.1 dB maximum
	Operating Frequency	1250 MHz to 1350 MHz
	Power Rating	6 kW peak pulse, 23 microseconds wide at 1900 pps
	Power Consumption (during switching)	4.8 watts

A block diagram of the chirp generator is shown in Figure 3.4.3. A voltage controlled oscillator, operating at the fundamental carrier frequency of 1302 MHz, is phase locked to the reference signal from the frequency multiplier. When triggered by a signal from the Digital Sequencer, the loop is opened and a linear-voltage ramp is applied to the VCO.

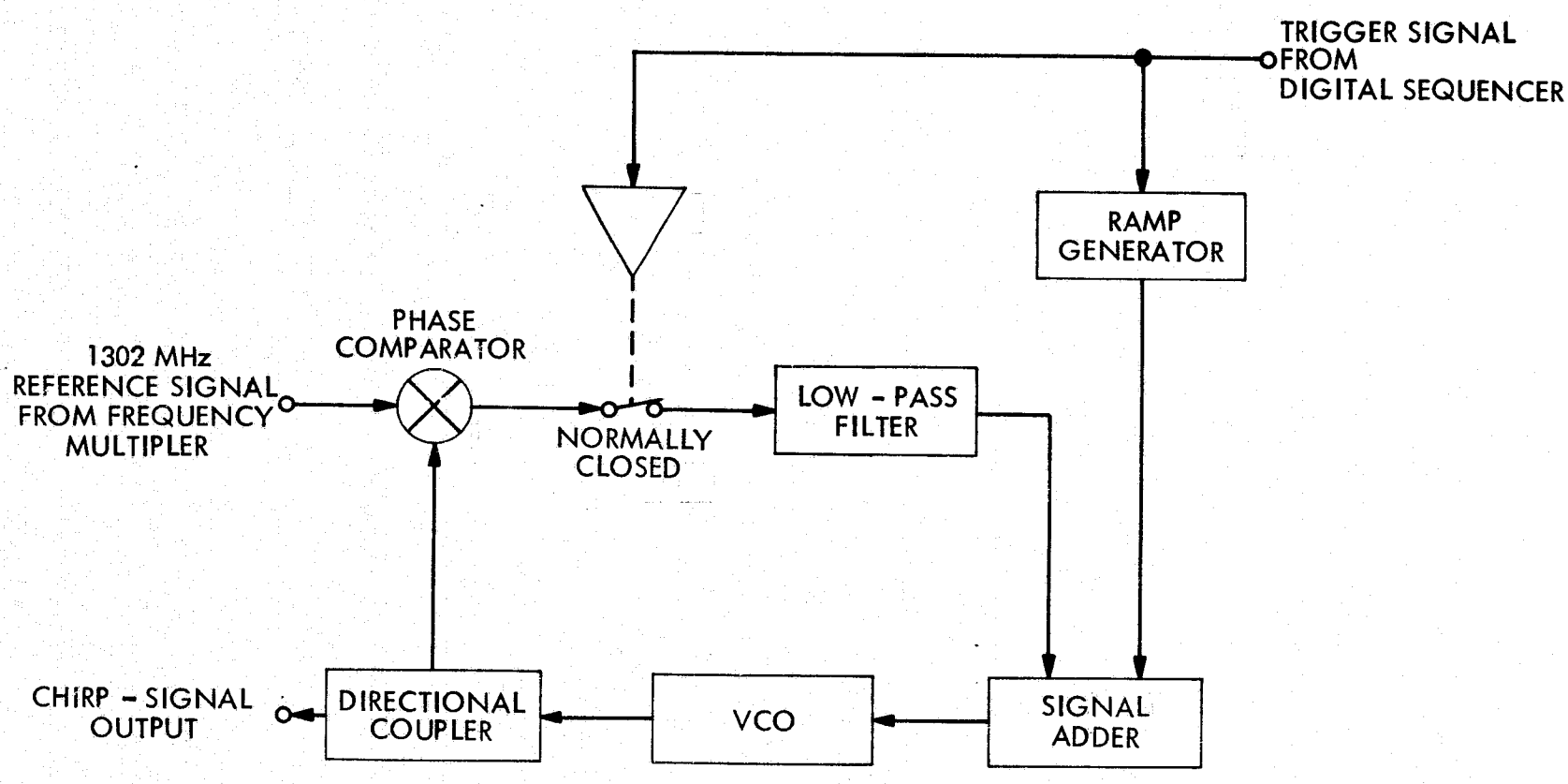

Figure 3.4.3. Chirp generator block diagram

At the end of the sweep, the loop is closed, and the VCO reacquires the reference signal. In this manner, the same starting phase is guaranteed for each linear sweep.

Provision is made within the chirp generator for sensing an out-of-lock condition in the loop and automatically initiating a reacquisition sequence.

RF Modulator. The RF modulator accepts the linear FM signal from the chirp generator and accurately gates a 23 microsecond segment corresponding to the desired frequency range. The transmitter pulse width and its rising and falling edges are established at this stage. Proper tayloring of the pulse's rising and falling edges can minimize the sidelobes of the transmitted signal.

The modulator is basically a PIN diode switch with driver circuitry to obtain proper edge shaping from an input TTL level pulse.

Bandpass Filter. The bandpass filter limits the input frequencies to the transistor driver amplifier. It prevents out-of-band signals from the chirp generator when it is in a reacquisition sequence. It also limits spike leakage at the rising and falling edges of the RF modulator switch transistions.

Gain Calibration Subsystem. A portion of the gated chirp signal is routed through a precision step attentuator and injected into the antenna ports of both receivers to be used as a calibration signal. The signal is taken from the exciter chain with a 30 dB coupler at the output of the bandpass filter. After passing through the precision attenuator, it is injected into the antenna ports of both receivers through separate directional couplers. The directional coupler in the transmitter antenna leg also serves as a power monitor.

Transistor Driver Amplifier. The transistor driver amplifier raises the signal to a level sufficient to drive the TWT final amplifier into saturation.

Traveling-Wave-Tube Final Amplifier. The TWT final amplifier is a PPM-focused conduction-cooled type operated in a grounded-anode configuration. Biasing and gating of the grid is performed by the DC modulator. DC-to-RF efficiency is expected to be 30%. Conduction cooling of the tube is facilitated by heat pipes strategically placed around the body of the tube.

Transmit/Receive Switch. The Transmit/Receive Switch transfers the antenna connection from the transmitter output to the receiver input in synchronism with the transmit and receive events. The switch is comprised of series and shunt PIN diodes in a SPDT configuration. Circutry to drive the diodes at high speed interfaces the switch with a TTL level input pulse.

Transmitter Power Monitor. The transmitter power monitor consists of a dual directional coupler and detector diodes operated as peak power detectors. This allows monitoring of transmitter power delivered to the antenna and reflected power due to mismatch. In addition, the calibration signal for the receiver is injected at this point.

Antenna Switch. The antenna switch transfers the transmitter output to either the horizontally-polarized or vertically-polarized antenna. Simultaneously, it switches the input of one of the receivers to the other antenna polarization. This switch is a low-loss, mechanical, latching switch with a 4-port transfer switching configuration.

3.4.3 Receiver Subsystem

General Description. A block diagram of the receiver subsystem is shown as part of Figure 3.4.2. It consists of two separate, singly-heterodyned receivers. One receiver is permanently connected to the T/R switch, and receives radiation at the same polarization as transmitted. The second receiver is connected to receive cross-polarized radiation from the antenna. When the antenna polarization of the transmitter is switched, the antenna polarization of both receivers is also switched.

The two receivers are identical in every respect. Each begins with an input bandpass filter followed by a receiver protector switch and another bandpass filter. The filters act as preselectors for the receiver and protect the input amplifiers from high-voltage switching transients caused by the receiver protectors.

The low-noise transistor amplifier has specially selected transistors to obtain a noise figure of 2.0 dB. Overall gain of the amplifier is approximately 35 dB.

The low noise amplifier is followed by a variable-gain amplifier. The gain of the amplifier is controlled by a 4-bit input command in 16 steps from 0 dB to 40 dB.

The system bandwidth filter limits the signal and noise to ±8.7 MHz about the center frequency of 1302 MHz.

The quadrature mixer beats the amplified L-Band signal with an LO-signal at 1302 MHz to obtain two signals 90 degrees out-of-phase with each other. Both of these signals contain the upper and lower 8.7 MHz sidebands of the received signal. The quadrature signals are amplified by video amplifiers to obtain approximately ±1 volt of signal at the input to the ADC's.

The overall noise figure of each L-Band receiver is 3.0 dB relative to the input of the first bandpass filter. Its overall gain is adjustable from 40 dB to 80 dB. The receiver electrical characteristics are presented in Table 3.4.2.

Input Filters. The input filters preselect the range of frequencies to be amplified by the receiver. In addition, they serve to protect the low-noise amplifier from switching transients in the receiver protector and transmit receive switch.

Receiver Protector. The receiver protector provides further isolation of the low-noise amplifier from the transmitter during the transmit event. It is essentially a single-pole, single-throw switch which is open during transmit, and closed all other times.

The receiver protecter consists of two assemblies. One assembly is the switch itself, which consists of series and shunt PIN diodes with appropriate isolation capacitors and RF inductors. The second assembly drives the switch and serves as an interface between the TTL level signal from the Digital Sequencer and the high-current pulse necessary to drive the switch.

Table 3.4.2. L-Band receiver electrical characteristics

1	INPUT FILTERS	
	Center Frequency	1302 MHz
	Bandwidth	±50 MHz
	Insertion Loss	0.3 dB maximum at center frequency
	Flatness of Passband	±0.1 dB
	Out of Band Rejection	50 dB down at ±300 MHz
	Peak Power Rating	6 kW
2	RECEIVER PROTECTOR	
	Isolation (switch open)	25 dB minimum
	Insertion Loss (switch closed)	0.3 dB maximum
	Center Frequency	1302 MHz
	Bandwidth	±50 MHz
	Peak Power Rating	6 kW
	Switching Speed	1 μsec minimum
	Power Consumption	1.5 watts
3	LOW-NOISE AMPLIFIER	
	Gain	35
	Noise Figure	25 dB maximum, 2.0 dB desired
	VSWR	2:1 maximum
	Center Frequency	1302 MHz
	Bandwidth	±100 MHz
	Saturated Power Output	0 dBm
	Power Consumption	1.5 watts
4	VARIABLE GAIN AMPLIFIER	
	Gain	4-bit digitally controlled in 16 steps from 0 dB to 40 dB
	Noise Figure	4.5 dB
	VSWR	1.5:1 maximum
	Center Frequency	1302 MHz
	Bandwidth	±100 MHz

Table 3.4.2. L-Band receiver electrical characteristics (contd)

4	VARIABLE GAIN AMPLIFIER (contd)		
	Saturated Power Output	0 dBm	
	Power Consumption	1.5 watts	
5	SYSTEM BANDWIDTH FILTER		
	Center Frequency	1302 MHz	
	Bandwidth	±8.7 MHz	
	Insertion Loss	3.0 dB maximum at center frequency	
	Flatness of Passband	±0.5 dB	
	Out of Band Rejection	50 dB down at ±60 MHz	
6	QUADRATURE MIXER		
	Signal Input Frequency	1302 MHz ±8.7 MHz	
	Local Oscillator Input Frequency	1302 MHz	
	Video Output Frequency	DC to 8.7 MHz	
	Conversion Loss (SIG input to one VIDEO output)	10 dB maximum	
	VSWR at SIG and LO parts	1.5:1 maximum	
	VIDEO amplitude imbalance	±0.5 dB maximum	
	VIDEO phase difference	90 degrees ±2 degrees	
	LO rejection at SIG inputs	15 dB	
	LO rejection at VIDEO outputs	30 dB	
7	VIDEO AMPLIFIERS		
	Gain	Matched to ±0.2 dB, 100 Hz to 9 MHz	Matched pair
	Phase	Matched to ±2 degrees 100 Hz to 9 MHz	Matched pair
	Gain	20 dB	Single Amplifier
	Frequency response	±0.1 dB, 100 Hz to 9 MHz	Single Amplifier
	Phase linearity	±2 degrees, 100 Hz to 9 MHz	Single Amplifier
	Saturated output voltage	±1 volt peak	Single Amplifier
	Power consumption (per pair)	4.5 watts	Single Amplifier

Low-Noise Amplifier. The first stage of amplification in this receiver will be the major contributor to the overall noise figure. The amplifier used here shall have transistors specially selected for low-noise and high gain. The design goal for the amplifier is an input noise figure of 2.0 dB at a gain of 35 dB.

Variable Gain Amplifier. The second stage of amplification consists of a transistor amplifier with a gain controlled by a 4-bit digital command. The digital command controls the amplifier gain in 16 steps from 0 dB to 40 dB.

System Bandwidth Filter. The system bandwidth filter sets the system noise bandwidth to 17.4 MHz.

Quadrature Mixer. The quadrature mixer is basically a dual balanced mixer with its video outputs in phase quadrature. The usual means of obtaining two outputs in phase quadrature is shown in Figure 3.4.4. Adding an extra length of quarter-wave line to either an output of the signal hybrid or an output of the local oscillator hybrid will produce the desired phase shift.

Video Amplifiers. The video amplifiers raise the level of the quadrature-mixer outputs to approximately ±1 volt peak-to-peak. The amplifiers are constructed in matched pairs.

3.5 X-BAND SYSTEM

3.5.1 X-Band System Block Diagram

The Shuttle X-Band system is similar to the L-Band system in most respects. It, too, is comprised of four subsystems (see Figure 3.5.1).

1) Transmitter Subsystem
2) Receiver Subsystem
3) Digital Sequencer and Digital Data Formatter
4) Power Conditioning Subsystem

C.2

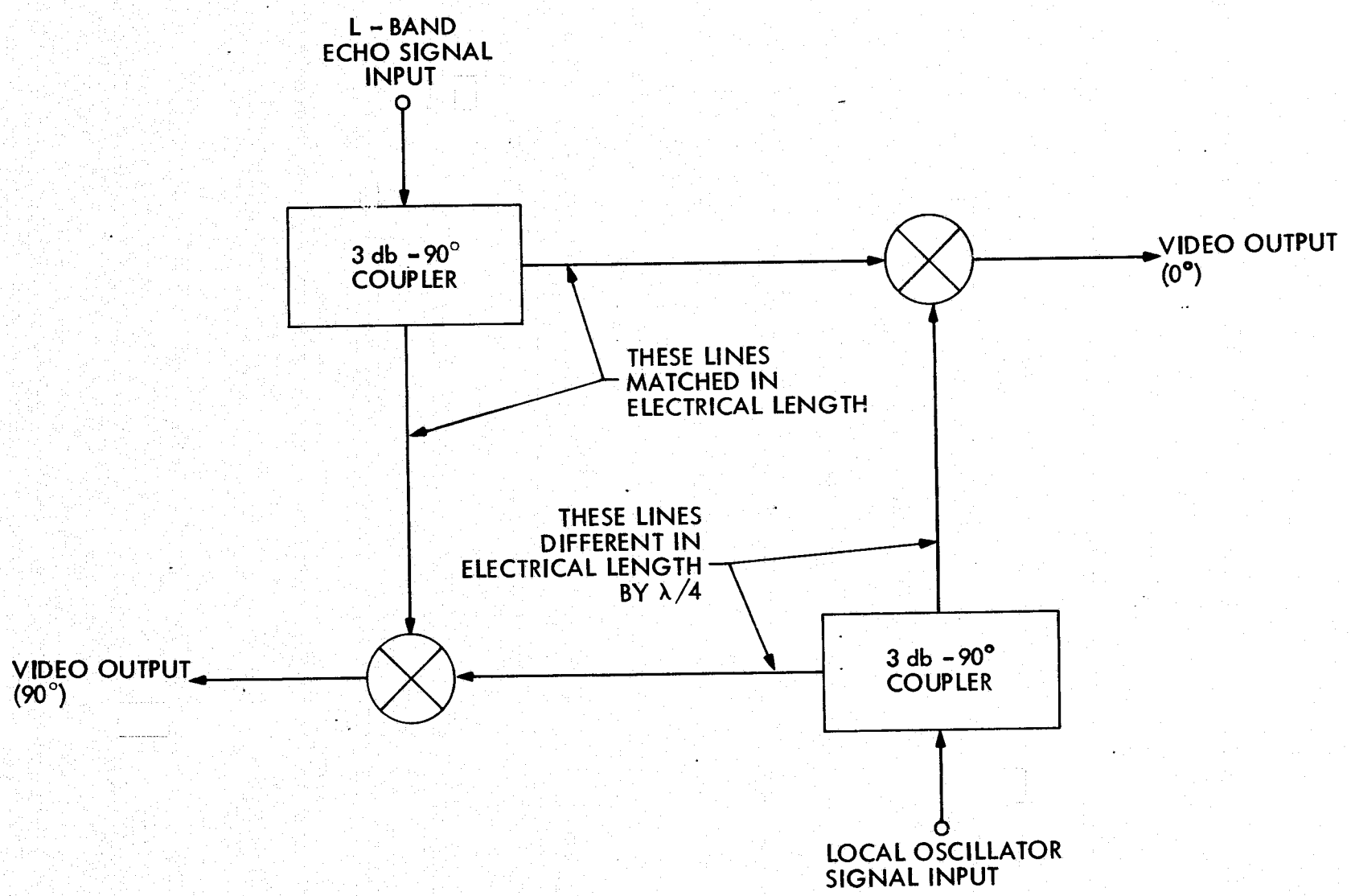

Figure 3.4.4. Quadrature mixture

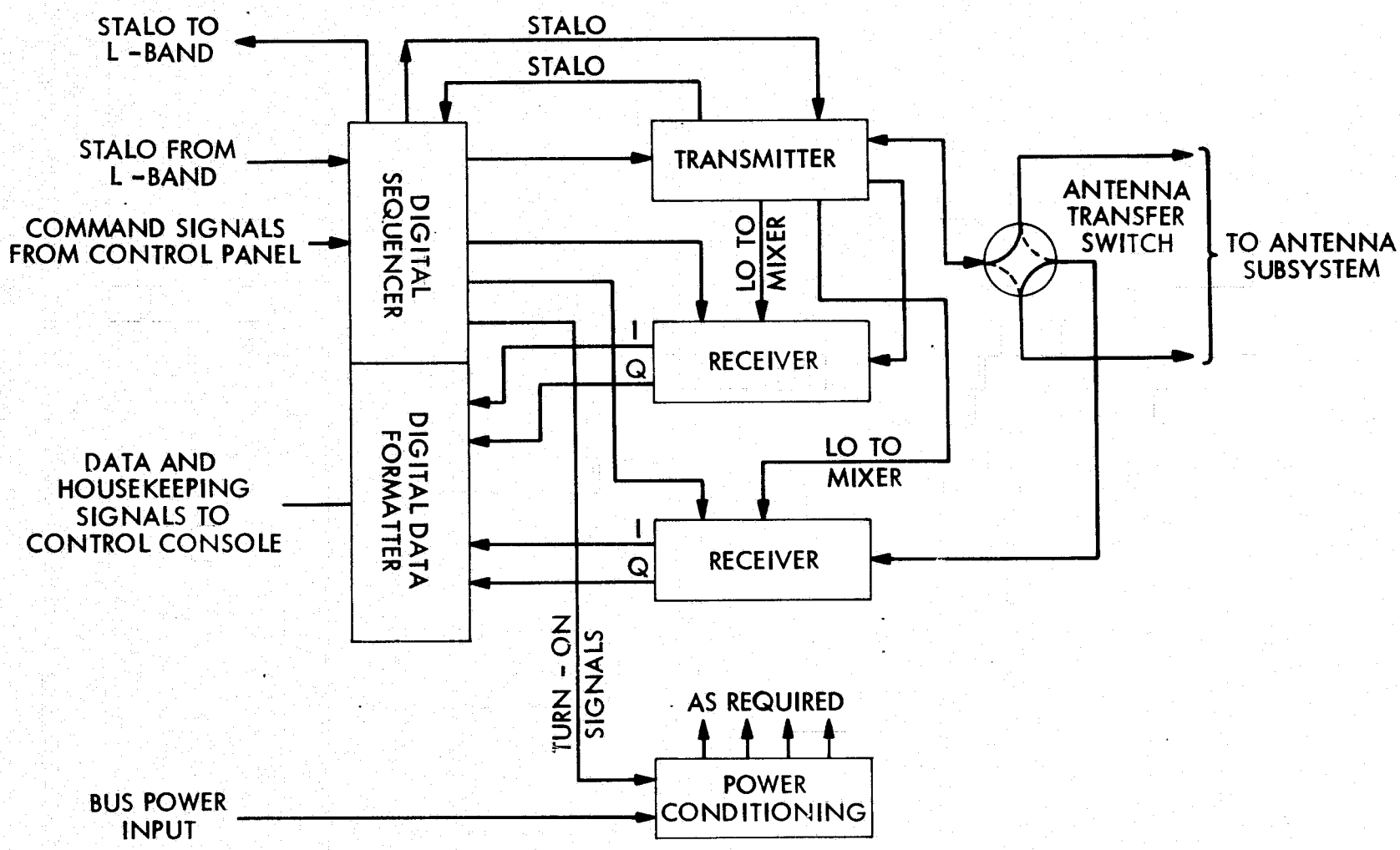

Figure 3.5.1. X-band radar block

The Transmitter Subsystem consists of a stable local oscillator, a linear FM pulse generator, and a Traveling-Wave-Tube final amplifier. The transmitter pulse is 21 microseconds wide with a peak power of 20 kilowatts and a maximum repetition frequency of 1900 Hertz.

The X-Band Receiver Subsystem also consists of one double-sideband, singly-heterodyned receiver for each antenna polarization. The front-end of each receiver has a parametric amplifier with a noise figure of 1.5 dB and a gain of 15 dB. The paramp is followed by two transistor amplifiers, one of which has a programmable gain. Single down-conversion to video frequencies is accomplished in a quadrature mixer. The quadrature video signals are amplified to produce ±1 volt peak-to-peak signals at the inputs of the ADC's. The noise figure of each receiver is less than 3.0 dB referred to its input. Its center frequency is 8332.8 MHz with a bandwidth of 17.4 MHz, and its overall gain is programmable from 40 dB to 80 dB.

The X-Band system has a Digital Sequencer and Digital Data Formatter completely separate from that of the L-Band radar. The Digital Sequencer portion provides all the logic and timing functions for the radar. It also provides the signals for initiating and executing the calibration sequence. The Digital Data Formatter consists of high-speed Analog-to-Digital converters that accept the four receiver video signals, samples and converts them to a digital format for recording on magnetic tape. The DDF also contains circuitry for monitoring and correcting the telemetry signals to a digital format.

The power supply subsystem consists of dc-to-ac and dc-to-dc converters, which provide all the voltage levels required by the radar. Some of the dc outputs are unregulated, and supply power to those circuits which have "on-board" regulators. Efficiency of dc-to-ac conversion is better than 80%, and dc-to-dc conversion is better than 70%.

3.5.2 Transmitter Subsystem

General Description. Except for the operating frequencies, the block diagram of the X-Band transmitter, Figure 3.5.2, is quite similar to that of the L-Band system. A 86.8 MHz signal from the stable local oscillator is routed to the

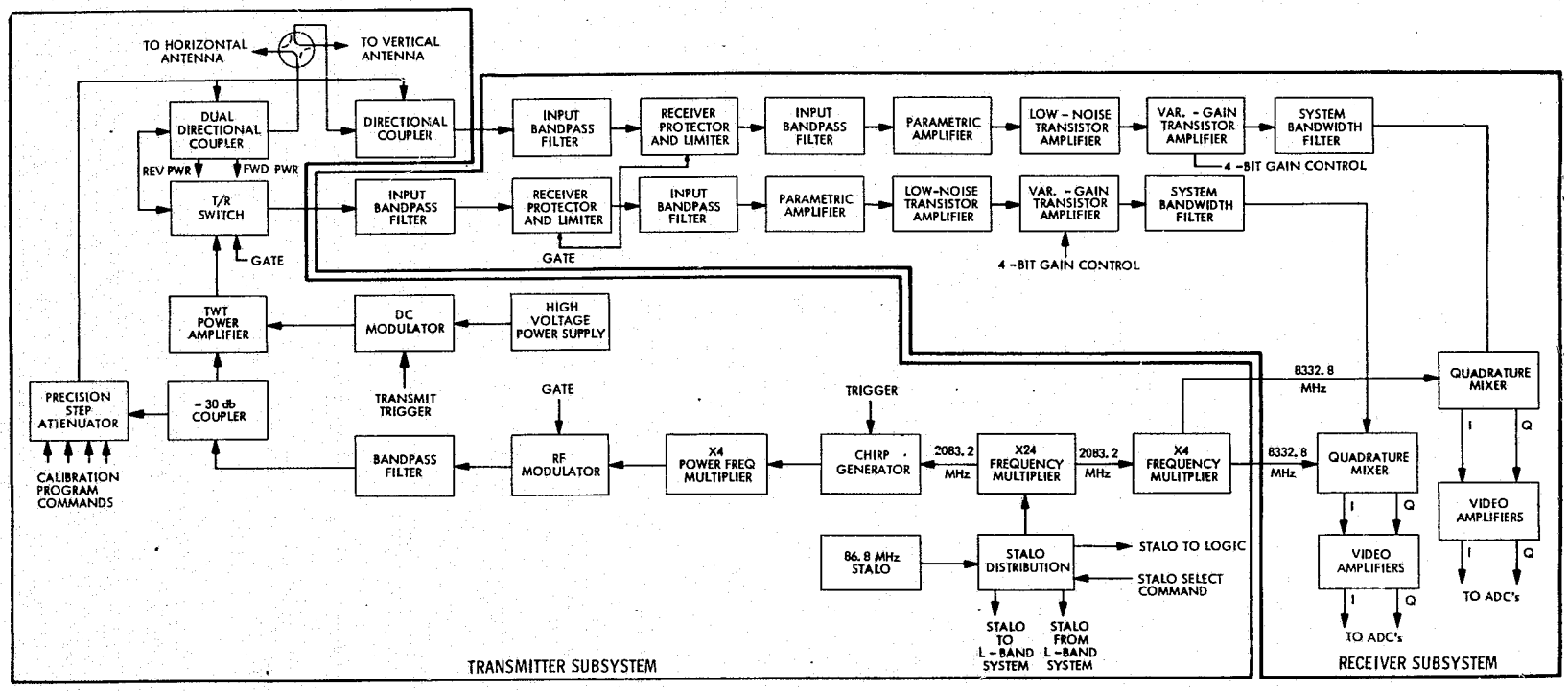

Figure 3.5.2. Block diagram of X-band transmitter and receiver

stalo distribution system. On command from the data sequencer, the stalo distribution system selects either the X-Band STALO or the L-Band STALO to be used as the master frequency standard for the radar. The selected oscillator signal is amplified and fed to the data system and frequency multipliers.

The X-Band system uses two frequency multipliers. The first multiplier accepts an 86.8 MHz signal and multiplies it times 24 to obtain a signal at 2083.2 MHz. One 2083.2 MHz signal is routed to the chirp generator to be used as a reference signal. Another is routed to the second frequency multiplier which multiplies times 4 to obtain the X-Band center frequency of 8332.8 MHz. Two X-Band signals are routed to the quadrature mixers to be used as LO-signals.

The chirp generator uses the 2083.2 MHz signal as a reference for creating a linear frequency-modulated signal. A voltage-controlled oscillator operating at 2083.2 MHz is phase locked with the reference signal. When triggered by the Digital Sequencer, the phase-locked-loop is opened, and a linear ramp is applied to the VCO. At the end of the sweep, the loop is closed, and the VCO reacquires the reference signal. In this manner, the phase at the start of each linear sweep is the same.

The output of the chirp generator is fed to an amplifier and a times-four frequency multiplier, which converts the linear FM-sweep signal at 2083.2 MHz to a FM-swept signal at 8332.8 MHz. The power output of the multiplier is sufficiently high to drive the TWT into saturation after passing through the RF modulator, bandpass filter, and calibration-signal coupler.

The RF modulator accurately gates the FM waveform to produce minimum sidelobes in the transmitted signal.

The output of the RF modulator is fed thru a bandpass filter and a 30 dB coupler before reaching the TWT. The 30 dB coupler picks out a portion of the transmitted waveform signal, which is passed through a precision step attenuator and used as a calibration signal.

The Traveling-Wave-Tube amplifier is a PPM-focused, conduction-cooled type having a minimum gain of 50 dB and a peak output power of 20 kilowatts. DC to RF efficiency of the tube is expected to be 30% and its maximum duty cycle is 4%. Conduction cooling of the tube is facilitated by heat pipes strategically placed around its body.

The high-power RF pulse is routed through a Transmit/Receive switch, a dual-directional coupler, and the antenna switch before finally reaching the antenna.

The Transmit/Receive Switch is a PIN-diode SPDT switch with low insertion loss and moderate isolation. The dual directional coupler provides a measurement of forward and reflected power as well as coupling the calibration signal into the receiver. The antenna switch is a low insertion loss, mechanical, coaxial switch with two positions.

The transmitter electrical characteristics are presented in Table 3.5.1.

Stalo. The stalo for the X-Band system is identical to that used in the L-Band system.

Stalo Distribution System. The stalo distribution system used in X-Band radar is identical to that used in the L-Band radar.

Frequency Multiplier (24x). Two frequency multipliers are used to convert the stalo frequency to the higher frequencies used in the X-Band radar. The first of these has a multiplication factor of 24 and two RF output ports. One of the outputs is used as a reference for the phase-locked chirp generator. The other output drives a times-four multiplier, which supplies the LO-signal to the receiver quadrature mixers.

Frequency Multiplier (4x). The second frequency multiplier takes the 2083.2 MHz signal output of the first multiplier and converts it to an X-Band center frequency signal at 8332.8 MHz. The multiplier has two outputs to drive the quadrature mixers in the receivers.

Chirp Generator. This subassembly generates a linear FM signal to be used as the transmitted chirp. The rate of frequency sweep generated shall be 0.2069 MHz/microsecond. This sweep rate, when multiplied by the times-4 frequency multiplier that follows, will become 0.8276 MHz/microsecond. After gating by the RF modulator, the frequency sweep becomes 8324 MHz to 8341 MHz.

Except for the sweep rate and center frequency, the operation of the X-Band chirp generator is identical to that of the L-Band chirp generator.

Table 3.5.1. X-Band transmitter electrical characteristics

1	STALO	
	Same as table 3.4.1	
2	STALO DISTRIBUTION SYSTEM	
	Same as table 3.4.1	
3	FREQUENCY MULTIPLIER (24x)	
	Input signal	86.9 MHz, 10 milliwatts
	Output signal Chirp-reference port	2083.2 MHz, 10 mw
	Output signal to 4x multiplier	2083.2 MHz, 100 mw
	Spurious Signals	40 dB down, minimum
	Power Consumption	9.6 watts
4	FREQUENCY MULTIPLIER (4x)	
	Input Signal	2083.2 MHz, 100 milliwatts
	Output Signal both ports	8332.8 MHz, 10 milliwatts
	Spurious Signals	40 dB down, minimum
5	CHIRP GENERATOR	
	Input Reference Signal	2083.2 MHz, 10 milliwatts
	Output Frequency Sweep	0.2069 MHz/microsecond
	Output Power Level	10 milliwatts
	Trigger Input	TTL level pulse
	Power Consumption	3 watts
6	POWER FREQUENCY MULTIPLIER (4x)	
	Input Signal	2083.2 MHz center frequency, 10 milliwatts
	Input Bandwidth	±3 MHz
	Output Signal	8332.8 MHz center frequency, 250 mw
	Output Bandwidth	±9 MHz
	Power Consumption	3.6 watts

Table 3.5.1. X-Band transmitter electrical characteristics (contd)

7	RF MODULATOR	
	Input	FM signal from 4x multiplier, 250 mw
	Insertion Loss (switch closed)	1.0 dB maximum
	Isolation (switch open)	50 dB minimum
	Trigger Gate	TTL level, 21 μsec wide
	Power Consumption	1.5 watts
	Frequency Sweep after gating	8324.11 to 8341.49 MHz
8	BANDPASS FILTER	
	Center Frequency	8332.8 MHz
	Bandwidth	±50 MHz
	Insertion Loss	0.3 dB maximum at 8332.8 MHz
	Flatness of Passband	±0.1 dB
	Out of Band Rejection	50 dB down at ±300 MHz
9	PRECISION STEP ATTENUATOR	
	Input Code	4-bit binary coded word
	Attenuation	16 steps
	Power Consumption	1.5 watts
10	TRAVELING-WAVE-TUBE FINAL AMPLIFIER	
	Saturated Gain	50 dB
	Bandwidth	8230 to 8430 MHz
	Peak Power Output	20 kW
	Maximum Duty Cycle	4%
	Normal Beam Voltage	25 kilovolts
	Nominal Beam Current	2.67 amps peak
11	DC MODULATOR	
	Input Trigger	TTL level gate
	Filament and Bias Supply Power Consumption	48 watts

Table 3.5.1. X-Band transmitter electrical characteristics (contd)

12	TRANSMIT/RECEIVE SWITCH	
	Insertion Loss, Antenna to transmitter or receiver port	0.3 dB
	Isolation, transmitter to receiver port	25 dB min.
	Frequency	8230 to 8430 MHz
	Power Rating	20 kW peak pulse, 21 μsec wide at 1900 pps
	Input Trigger	TTL level pulse
	Power Consumption	4.5 watts
13	TRANSMITTER POWER MONITOR	
	Power Rating	20 kW peak pulse, 21 μsec wide at 1900 pps
	Calibrated Power Input	Less than -10 dBm
	Mean Coupling, Calibrated Signal to T/R Switch Port	-40 dB
	Output	Calibrated DC signals proportional to forward and reflected peak powers.
14	ANTENNA SWITCH	
	Insertion Loss	0.1 dB maximum
	Operating Frequency	8230 to 8430 MHz
	Power Rating	20 kW peak pulse, 21 μsec wide at 1900 pps
	Power Consumption (during switching)	4.8 watts

Power Frequency Multiplier (4x). The output of the chirp generator is fed to a times-four multiplier which amplifies and converts the 2083.2 MHz FM signal to a 8332.8 MHz FM signal of sufficient amplitude to drive the TWT amplifier into saturation. The easiest way to accomplish this is to amplify the signal with a transistor amplifier while it is still at L-Band. The amplified signal is then fed to a high-power, step-recovery-diode multiplier followed by a filter to select the desired signal.

RF Modulator. The RF modulator accepts the linear FM signal from the multiplier and accurately gates a 21 microsecond segment corresponding to the desired frequency range. The transmitter pulse width and its rising and falling edges are established at this stage. Proper tailoring of the pulse rising and falling edges can minimize the sidelobes of the transmitted signal.

The modulator is basically a PIN diode switch with driver circuitry to obtain proper edge shaping from an input TTL level pulse.

Bandpass Filter. The bandpass filter limits the input frequencies to the TWT final amplifier. It also limits spike leakage at the rising and falling edges of the RF modulator switch transistions.

Gain Calibration Subsystem. A portion of the gated chirp signal is routed through a precision step attenuator and injected into the antenna ports of both receivers to be used as a calibration signal. The signal is coupled from the exciter chain with a -30 dB coupler at the output of the bandpass filter. After passing through the precision attenuator, it is injected into the antenna ports of both receivers through separate directional couplers. The directional coupler in the transmitter antenna leg also serves as a power monitor.

Traveling-Wave-Tube Final Amplifier. The TWT final amplifier is a PPM-focused, conduction-cooled type operated in a grounded-anode configuration. Biasing and gating of the grid is performed by the DC modulator. DC-to-RF efficiency is expected to be 30%. Conduction cooling of the tube is facilitated by heat pipes strategically placed around the body of the tube. The output of the tube is protected from operation into high VSWR loads with a built-in isolator.

Transmit/Receive Switch. The Transmit/Receive switch transfers the antenna connection from the transmitter output to the receiver input in synchronism with the transmit and receive events. The switch is comprised of series and shunt PIN diodes in a SPDT configuration. Circuitry to drive the diodes at high speed interfaces the switch with a TTL level input pulse.

Transmitter Power Monitor. The transmitter power monitor consists of a dual directional coupler and detector diodes operated as peak power detectors. This allows monitoring of transmitter power delivered to the antenna and reflected power due to mismatch. In addition, the calibration signal for the receiver is injected at this point.

Antenna Switch. The antenna switch transfers the transmitter output to either the horizontally-polarized or vertically-polarized antenna. Simultaneously, it switches the input of one of the receivers to the other antenna. This switch is a low-loss, mechanical, latching switch with a 4-port transfer switching configuration.

3.5.3 Receiver Subsystem

General Description. Like the L-Band radar, the X-Band radar has two receivers (see Figure 3.5.2). One receiver is permanently connected to the T/R switch, and the other is connected to the cross-polarized antenna. When the antenna polarization of the transmitter is switched, the antenna polarization of both receivers is also switched.

The two receivers are identical in every respect. Each begins with an input bandpass filter, followed by a receiver protector switch and another bandpass filter. The filters act as preselectors for the receiver and protect the paramp from high-voltage switching transients caused by the receiver protector.

The parametric amplifier is the main noise-figure determining element in the X-Band receiver. The paramp to be used here will operate at ambient temperatures, and be pumped with a Gunn-diode oscillator. Its expected noise figure is 1.5 dB with a gain of 15 dB.

The paramp is followed by two stages of transistor amplification. The second amplifier is controlled by a 4-bit input command in 16 steps from 0 dB to 40 dB.

The system bandwidth filter limits the signal and noise to ±8.7 MHz about the center frequency of 8332.8 MHz.

The quadrature mixer beats the amplified X-Band signal with an LO-signal at 8332.8 MHz to obtain two signals 90 degrees out-of-phase with each other. Both of these signals contain the upper and lower 8.7 MHz sidebands of the received signal. The quadrature signals are amplified by video amplifiers to obtain approximately ±1 volt of signal at the input to the ADC's.

The overall noise figure of each X-Band receiver is 3.0 dB relative to the input of the first bandpass filter. Its overall gain is adjustable from 40 dB to 80 dB. The receiver electrical characteristics are presented in Table 3.5.2.

Input Filters. The input filters preselect the range of frequencies to be amplified by the receiver. In addition, they serve to protect the low-noise amplifier from switching transients in the receiver protector and transmit-receive switch.

Receiver Protector and Limiter. The receiver protector provides further isolation of the parametric amplifier from the transmitter during the transmit event. It is a single-pole, double-throw switch which connects the antenna input to a termination during transmit and to the paramp all other times. Following the switch is a diode limitation module which further limits high power spike leakage to ±10 dBm peak.

The receiver protector switch consists of two assemblies. One assembly is the switch itself, which consists of series and shunt PIN diodes with appropriate isolation capacitors and RF inductors. The second assembly drives the switch, and serves as an interface between the TTL level signal from the Digital Sequencer and the high-current pulse necessary to drive the switch.

Parametric Amplifier. A solid-state, minature, parametric amplifier provides the first stage of amplification in the X-Band receivers. The pump oscillator for the amplifier is a Gunn-effect diode. The units are temperature stabilized with heaters to assure undegraded performance over the expected temperature extremes.

Low-Noise Transistor Amplifier. Because of the limited gain of the parametric amplifier, the stage immediately following it can significantly add to the overall receiver noise figure, unless its own noise figure is kept low. Commercially

Table 3.5.2. X-Band receiver electrical characteristics

1	INPUT FILTERS	
	Center Frequency	8332.8 MHz
	Bandwidth	±50 MHz
	Insertion Loss	0.3 dB min at center frequency
	Flatness of Passband	±0.1 dB
	Out of Band Rejection	50 dB down at ±300 MHz
	Peak Power Rating	20 kW
2	RECEIVER PROTECTOR AND LIMITER	
	Isolation (switch open)	50 dB min.
	Insertion Loss (switch closed)	2.7 dB max.
	Maximum Spike Leakage	+10 dBm
	Center Frequency	8332.8 MHz
	Bandwidth	±50 MHz
	Peak Power Rating	20 kW
	Switching Speed	1 μsec min.
	Power Consumption	1.5 watts
3	PARAMETRIC AMPLIFIER	
	Gain	15 dB min.
	Noise Figure	1.5 dB max.
	VSWR	1.5:1 max.
	Center Frequency	8332.8 MHz
	Bandwidth	±10 MHz
	Pumping Oscillator	Gunn-effect diode
	Power Consumption	4.8 watts
4	LOW-NOISE TRANSISTOR AMPLIFIER	
	Gain	20 dB min.
	Noise Figure	7.5 dB max
	VSWR	1.5:1 max
	Center Frequency	8332.8 MHz

Table 3.5.2. X-Band receiver electrical characteristics (contd)

4	LOW-NOISE TRANSISTOR AMPLIFIER (contd)	
	Bandwidth	±100 MHz
	Saturated Power Output	0 dBm
	Power Consumption	1.5 watts
5	VARIABLE GAIN AMPLIFIER (INCLUDING DAC)	
	Gain	4-bit digitally controlled in 16 steps from 0 to 40 dB
	Noise Figure	9.0 dB
	VSWR	1.5:1 max.
	Center Frequency	8332.8 MHz
	Bandwidth	±100 MHz
	Saturated Power Output	0 dBm
	Power Consumption	1.5 watts
6	SYSTEM BANDWIDTH FILTER	
	Center Frequency	8332.8 MHz
	Bandwidth	±8.7 MHz
	Insertion Loss	3.0 dB max at center frequency
	Flatness of Passband	±0.5 dB
	Out of Band Rejection	50 dB down at ±60 MHz
7	QUADRATURE MIXER	
	Same as table 3.4.2	
8	VIDEO AMPLIFIERS	
	Same as table 3.4.2	

available GaAs FET amplifiers operating at this frequency typically have noise figures of 7.5 dB and gains of 20 dB. A noise figure of 7.5 dB adds 0.43 dB relative to the input of a paramp having 15 dB gain. Such an amplifier would be suitable for this application.

Variable Gain Amplifier. The second transistor amplifier has its gain controlled by a 4-bit digital command. The digital command controls the amplifier's gain in 16 steps from 0 dB to 40 dB.

System Bandwidth Filter. The system bandwidth filter sets the system noise bandwidth to 17.4 MHz.

Quadrature Mixer. Except for the difference in input frequencies, the X-Band quadrature mixers are the same as the L-Band mixers.

Video Amplifiers. The video amplifiers are the same in every respect to those used in the L-Band system.

3.6 DIGITAL DATA FORMATTERS AND DATA SUBSYSTEMS

The timing and control logic is provided by the digital data sequencer. This sequencer provides basic clock signals to the entire radar system. The digital data formatter (DDF) converts parallel raw radar data into a serial stream of digital video data which is sent to the tape recorders. The DDF also multiplexes housekeeping data into the serial stream of digital video data.

3.6.1 Data Sequencer

The SAR Data Sequencer provides TTL logic level clock signals to the analog-to-digital converters, digital data formatters, the data and housekeeping interface panel, the radar control panel, and the digital tape recorders for both the X-Band and L-Band radars. The clock signals are derived from a logic timing chain which is driven by a stable local oscillator from either the L-Band or X-Band system. The choice is made based on serial coded commands and direct commands received by the command decoder (Figure 3.6.1). The functions defined by the commands are shown in Table 3.6.1. The state of the command decoder at any given time depends on the sequence of commands which has been received since power turn-on. The state is monitored by the housekeeping data formatter (Figures 3.6.1 and 3.6.2) which time multiplexes this status data into the serial stream of digital video data sent to the tape recorders.

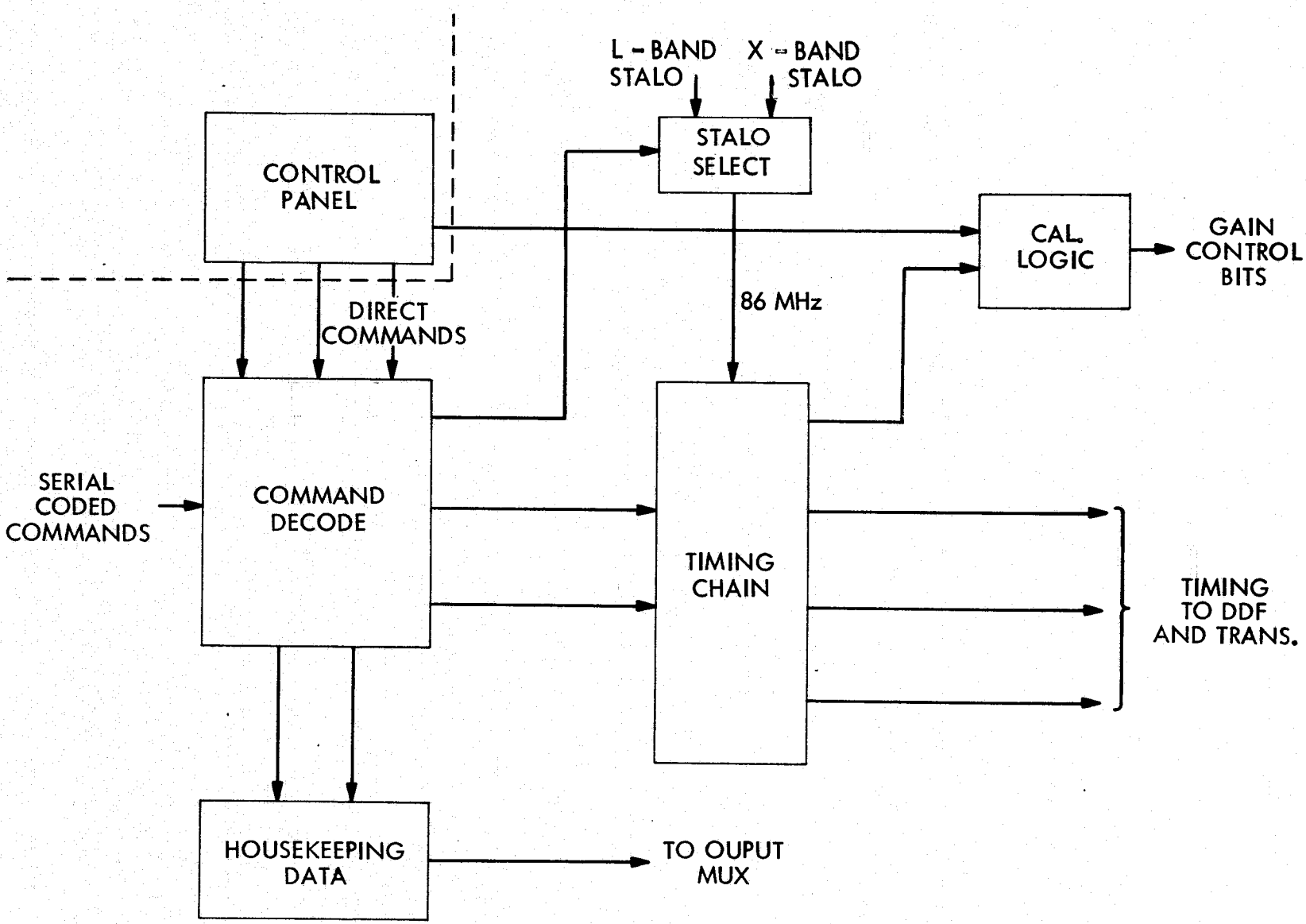

Figure 3.6.1. Data sequence

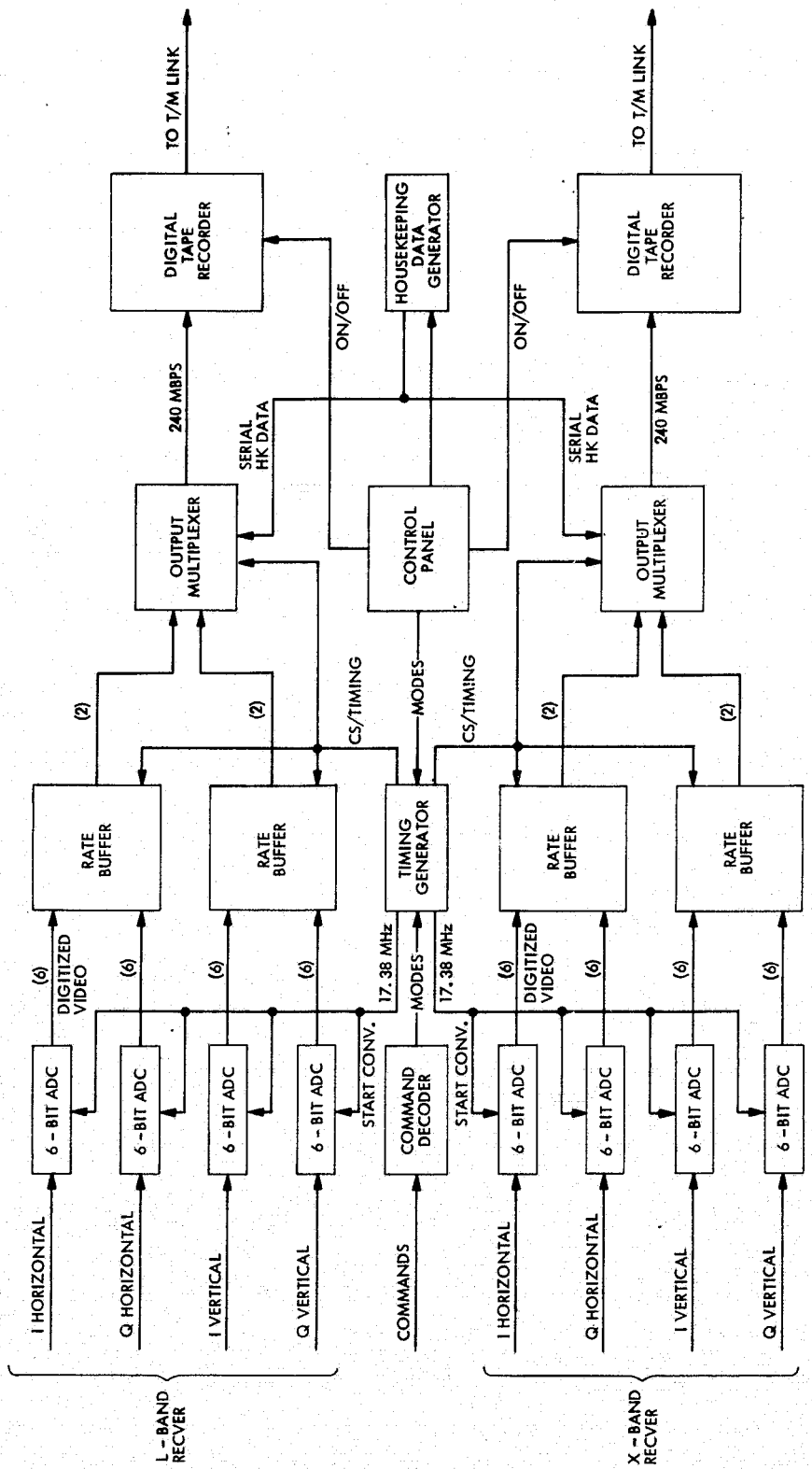

Figure 3.6.2. SAR data system block diagram

Table 3.6.1. Functions defined by command inputs

1. From Control Panel
   a. Off Nadir Angle
   b. Orbit Altitude
   c. Standby Power On
   d. Main Power On
   e. Full Power On
   f. Manual/Auto Receiver Gain Mode
   g. Manual Receiver Gain
   h. Antenna Polarization
   i. Calibrate Initiate
   j. DTR Selection and Speed
   k. CRT Display and Parameter Select
   l. Range Delay Over-ride and Select
   m. PRF Over-ride and Select
2. From Serial Coded Command
   a. Altitude
   b. Ground Velocity
   c. Range Delay
   d. PRF

The hardware estimates for the timing and control logic are:

Integrated Circuits:	215
Discrete Parts:	159
Boards:	3
Interface Lines:	180
Power:	31 watts

3.6.2 Digital Data Formatters

Analog-to-Digital Converters. (Figure 3.6.3) Each of eight ADC's receives a bi-polar analog input signal of 50 ohm input impedance from the SAR Receivers (L-Band/X-Band; I/Q; Vertically Polarized/Horizontally Polarized). Each of the eight signals varies from a maximum of +1.0 volt to a minimum of -1.0 volt and is bandlimited to 17.38 MHz. The ADC's are 6-bit converters with the output data encoded in offset binary (Table 3.6.2). The conversions are controlled by a digital waveform called Sample Strobe which is a 50% duty cycle waveform. At the trailing edge of Sample Strobe the instantaneous (within 1.5 nsec) analog input signal is held by a sample and hold network. Seven parallel comparators are used to encode the held signal to 3 bit resolution (Figure 3.6.4). These bits comprise the 3 MSB's of the final result. A digital-to-analog converter then converts the 3 bits to an equivalent analog voltage. This analog signal is

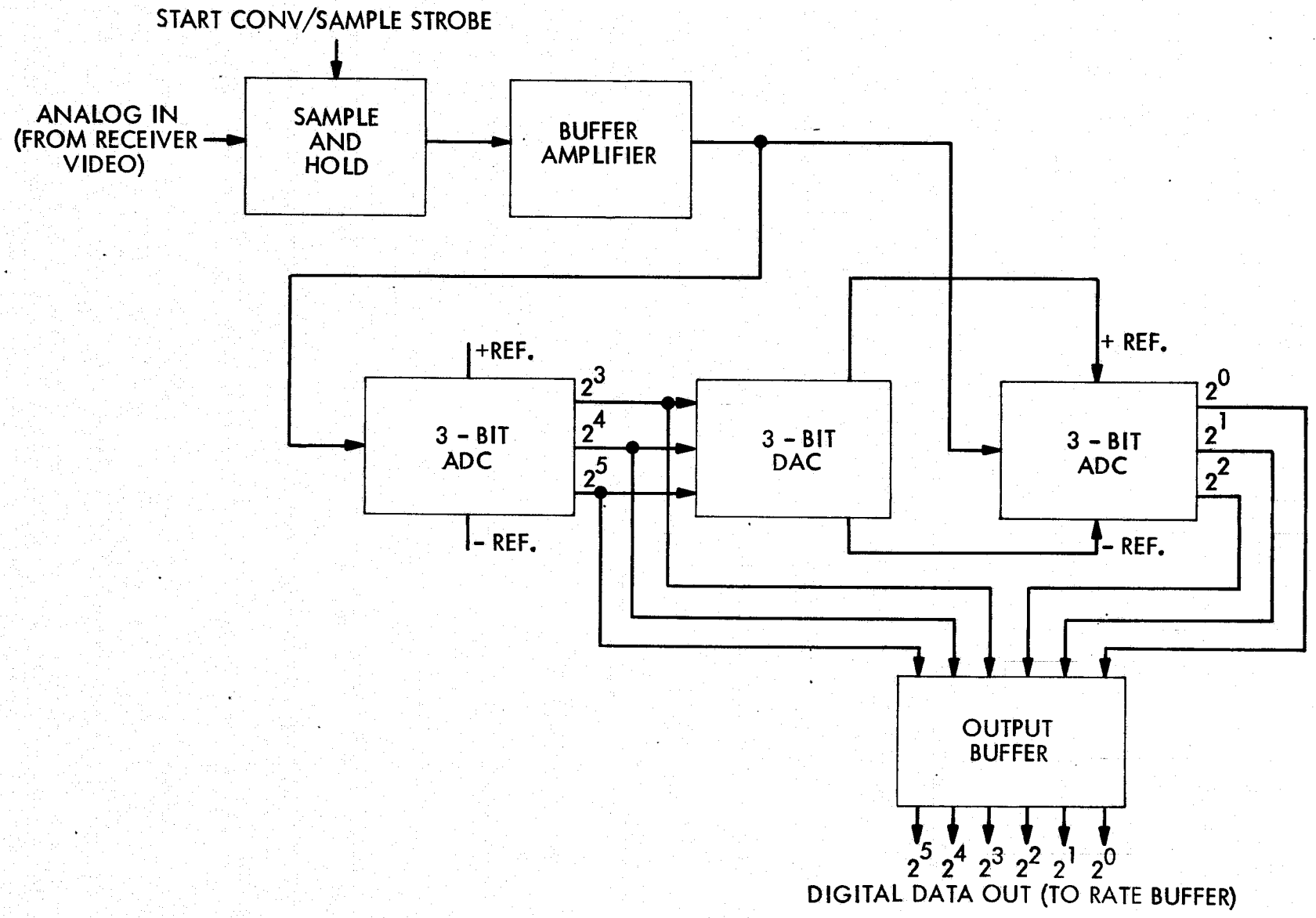

Figure 3.6.3. Six-bit ADC block diagram

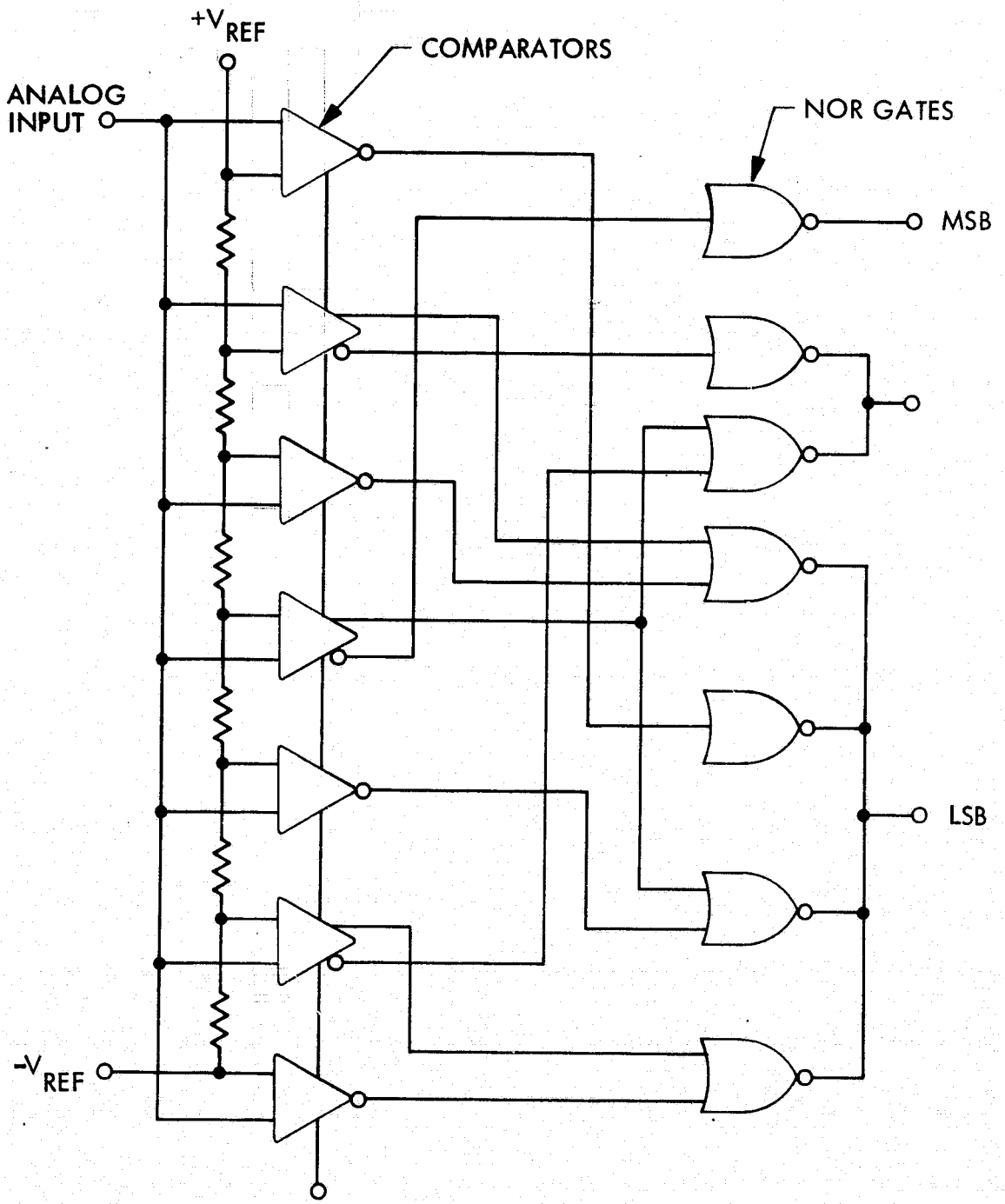

Figure 3.6.4. Three-bit ADC block diagram

Table 3.6.2. Offset binary notation

Location on scale	Analog voltage	Digital word
Maximum	+1.000 volts	111111
.	.	.
.	.	.
.	.	.
Mid positive +	+0.501 volts	110000
Mid positive -	+0.499 volts	101111
.	.	.
.	.	.
.	.	.
Mid scale +	+0.001 volts	100000
Mid scale -	-0.000 volts	011111
.	.	.
.	.	.
.	.	.
Mid negative +	-0.499 volts	010000
Mid negative -	-0.501 volts	001111
.	.	.
.	.	.
.	.	.
Minimum	-1.000 volts	000000

used to set the reference voltage for a second set of seven parallel comparators are used to encode the 3 LSB's of the final result. The total of 6-bits are then stored in a holding register until 54 nsec later when the next 6-bit sample is stored. The ADC's function continuously when Main Power is on, even though the summing buffers don't continuously utilize data. The output of the ADC's TTL logic compatible.

Rate Buffers. Each of four rate buffers handles the outputs of two of the 6-bit analog-to-digital converters. A 6-bit digital word is clocked into the Fanout and Hold Register (Figure 3.6.5) which accepts a 6-bit word every 57 nsec. The

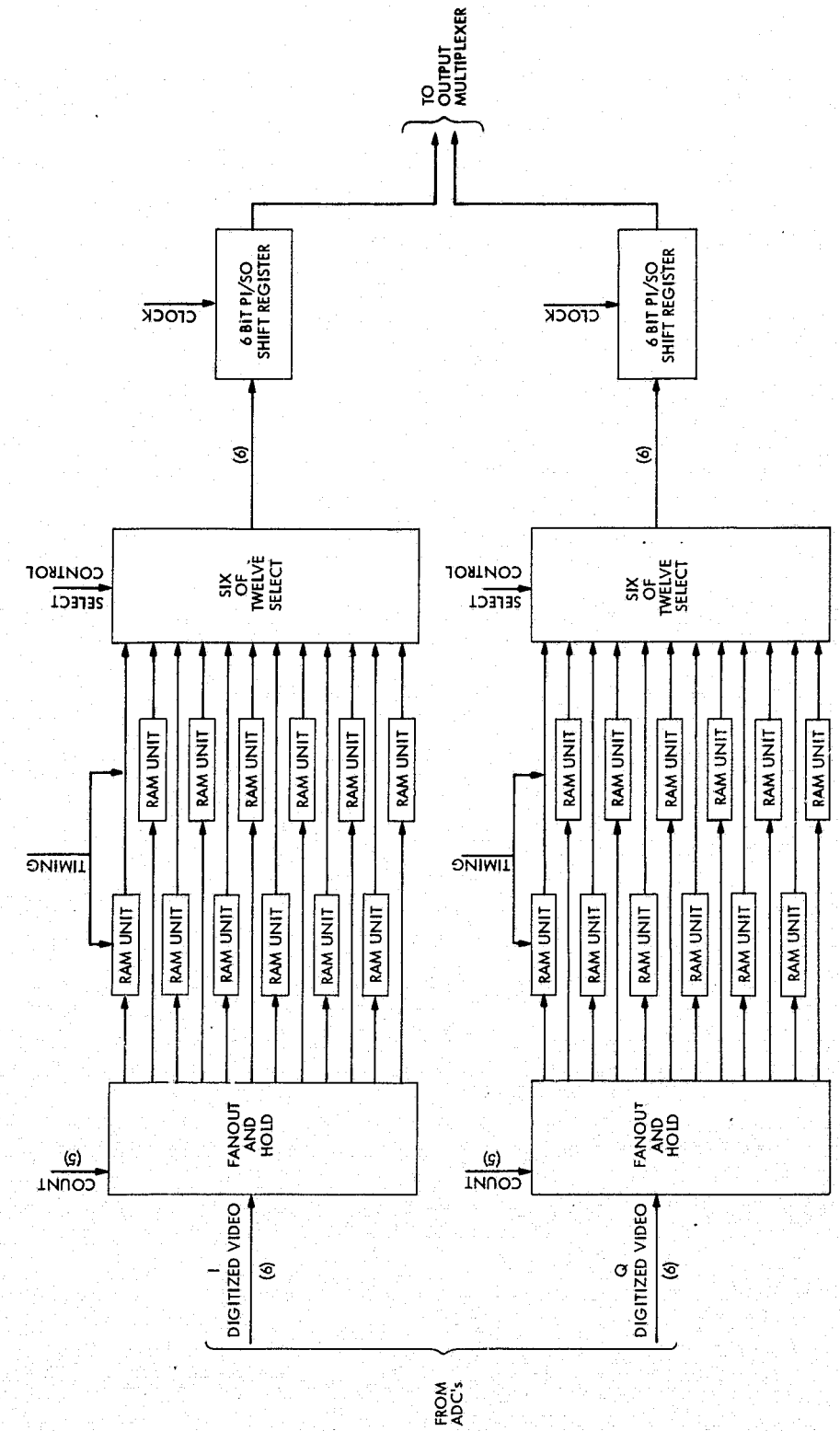

Figure 3.6.5. SAR data system rate buffer

timing logic counts out groups of three 6-bit words and then loads the full 18-bits into the RAM units every 171 nsec.

The timing signals for the rate buffers include Range Cell Count, Ram Chip Select, RAM Address Count, RAM Output Select Control, Output Shift Register Clock and Output Shift Register Dump. These timing signals are generated within a timing chain in the Timing and Control Logic (Figure 3.6.1). The 24 RAM units housed within each Rate Buffer contain six 1 K TTL RAM's (random access memories) each. The particular RAM's being loaded or unloaded at any given time are determined by the chip select signals from the Timing Generator. One-half of the RAM's in the rate buffer are loaded while the other half are unloaded during each PRF interval.

There are a total of 576 1 K RAM's in the Digital Data Formatters. A possible device which could be used for this is the Fairchild 93L415 low power Schottky RAM. If the total power consumption is of high concern, CMOS RAM's could be used depending on the technology cut-off date. At present the CMOS RAM's available are too slow to implement the approach outlined here.

Output Multiplexers. Each of two output multiplexers (one for X-Band data, the other for L-Band data) receives five separate serial data inputs which are time multiplexed to form a continuous output data stream. The timing chain provides the gates with which each of the separate data stream are combined to form the single digital data stream (one for each radar). The form of data sent to the digital tape recorders is NRZ-space accompanied by a 50% duty cycle bit sync. The DTR input electronics converts the NRZ-space format to a format appropriate for magnetic recording. The hardware estimate for the Digital Data Formatters is shown in Table 3.6.3.

Table 3.6.3. Digital data formatter hardware estimate

Integrated Circuits (SSI, MSI)	440
RAM's	576
ADC's	8
Discrete Parts	470
Boards	16
Interface Lines (doesn't include internal)	190
Power	260 watts

3.7 POWER SUPPLY SUBSYSTEMS

The power supply subsystems for both the L-Band and X-Band radars will take the form shown in Figure 3.7.1.

DC bus power from the shuttle passes through high-current, RFI filters before being distributed to several current-limiting circuits. The current-limit circuits provide short-circuit protection and serve as power on-off switches for the inverters.

One of the inverters converts the bus DC to an audio-frequency sinewave signal. This signal is applied to the filament transformer of the TWT, which has an additional secondary winding to supply power for biasing the TWT grid.

Another inverter is part of a closed-loop regulator that supplies high-voltage for the TWT. This inverter, because of its high-power output, must be carefully heat sunk.

The rest of the inverters convert the bus DC to audio-frequency square wave signals. These signals are converted to the required DC voltages using transformers and rectifiers.

Most of the high-current DC outputs will be unregulated. Regulation of these voltages will be accomplished at the load, if necessary.

Low current DC outputs that require regulation will be supplied through high efficiency switching regulators.

All outputs, whether regulated or unregulated, will be passed through additional filters before being applied to their loads.

Power conversion efficiency from bus DC to unregulated DC is expected to be greater than 80%. Conversion efficiency from bus DC to regulated DC is expected to be greater than 70%. The high-voltage power supply shall have an efficiency better than 70%, and the sine-wave supply better than 80%.

An estimate of the voltages and currents to be supplied by the power conditioning systems of both radars can be found in Section 3.11.

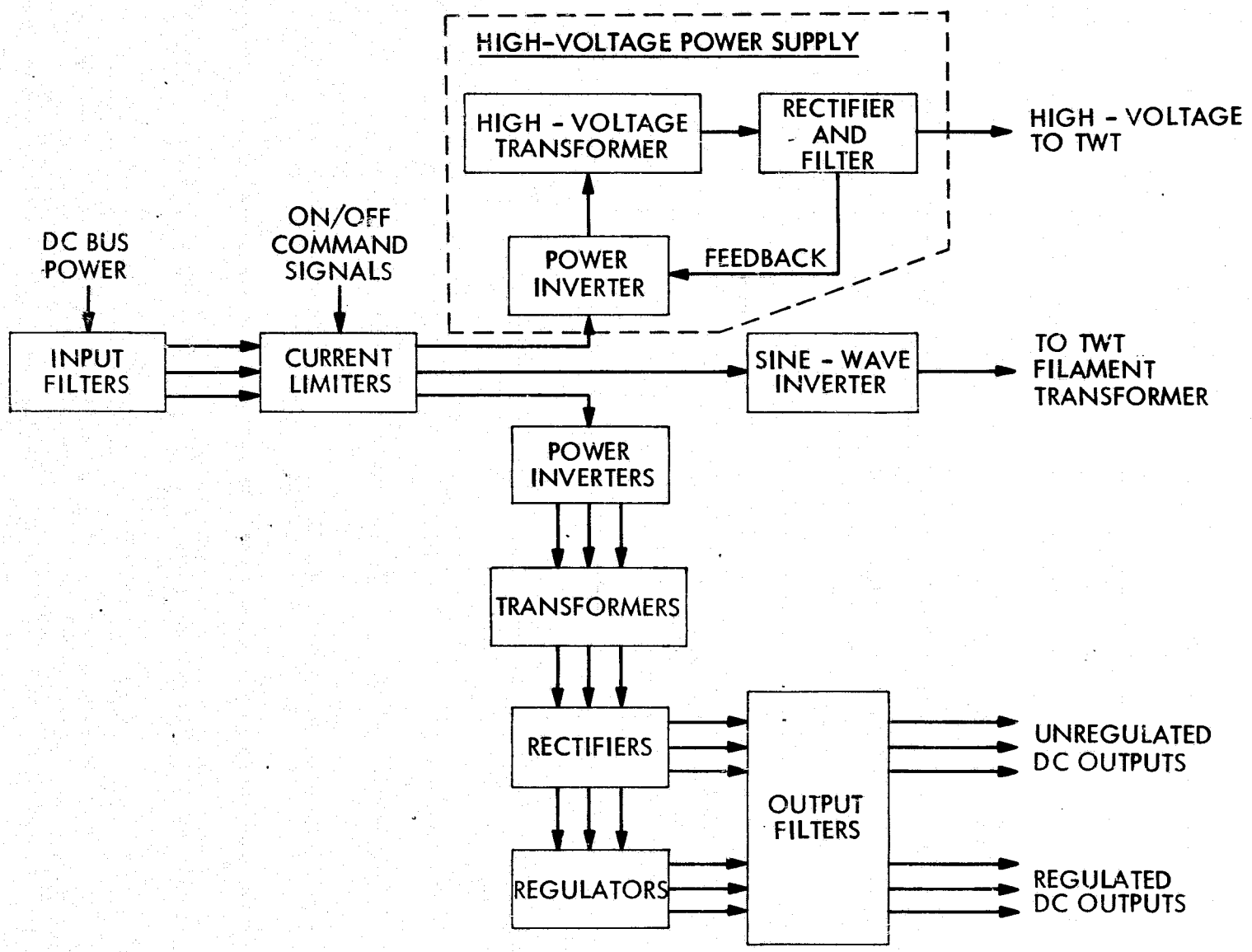

Figure 3.7.1. Power supply subsystem block diagram
(typical of both radars)

3.8 RADAR CONTROL CONSOLE - CRT DISPLAY

The Radar Control Console, Figure 3.8.1, is comprised of the following sections:

1) An oscilloscope and Digital multimeter (DVM)
2) An L-Band Radar Control Panel
3) An X-Band Radar Control Panel
4) Two high-speed digital tape recorders
5) A data and housekeeping interface panel

Together, these five sections provide all the control and data-handling functions for both radars. An operator, via the console, will have the capability of performing those functions listed in Table 3.1.

In addition, an operator may perform the following monitoring functions to determine proper radar operation or verify proper selection of data processing modes.

1) Monitor the return signal amplitudes on the oscilloscope (A-scope display).
2) Monitor housekeeping parameters on the DVM.
3) Monitor data-swath width and its placement within the return signal.

3.9 SHUTTLE INTERFACE REQUIREMENTS

This section presents a listing of interface requirements between the imaging radar system and Shuttle. These requirements are shown in Figure 3.9.1 as Shuttle command and control input/outputs, thermal control, attitude controls and power.

3.9.1 Shuttle Interface Listing

Table 3.9.1 through 3.9.4 presents respectively the interface listing of command and control input/outputs, thermal control input, power input and attitude control inputs.

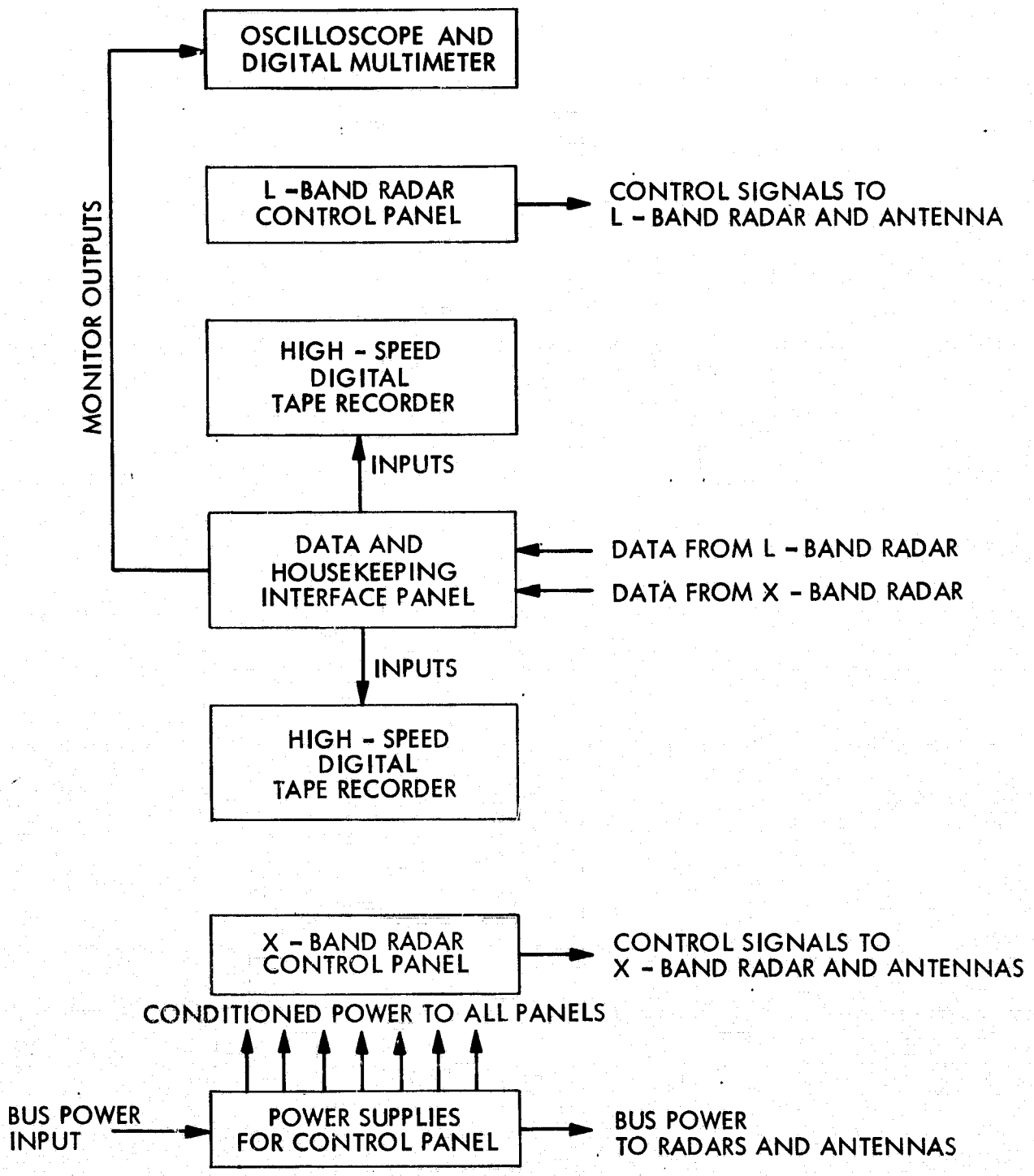

Figure 3.8.1. Radar control console

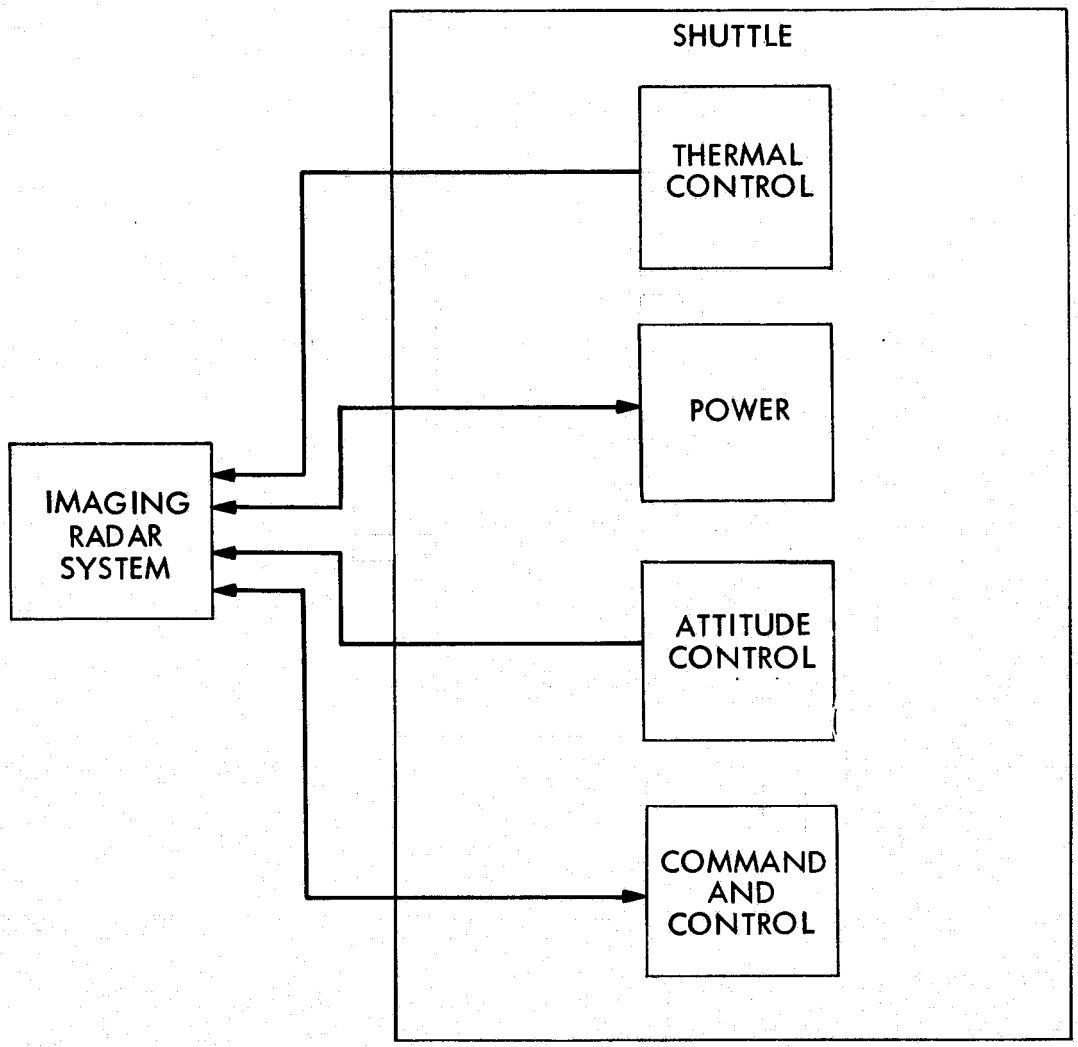

Figure 3.9.1. Shuttle and radar interfaces

Table 3.9.1. Command and control input/output

Parameter	Frequency
Power-On	Once/data track
Power-Off	Once/data track
Time	1/100 sec

Table 3.9.2 Thermal control

Parameter	Frequency
Radar Thermal	Once/data track
Cooling-On	Once/data track

Table 3.9.3. Power

Parameter	Frequency
Prime Power Bus	Once/data track

Table 3.9.4. Attitude control

Parameter	Frequency
Ground Velocity	1/10 sec.
Altitude	1/10 sec.

3.10 MECHANICAL AND ELECTRONIC PACKAGING

The components of the Shuttle Imaging Radar Experiment will be located in the pressurized module and on the pallet. The antenna, transmitters, receivers and associated power supplies will be located on the pallet. Cabling will be provided to interconnect with those inside the spacelab. Pressurized bulkhead connectors are assumed to be installed in the pressurized module, with JPL cabling attached to those connectors.

The components inside the pressurized module will be mounted in a console and in the cooled thermal rack.

The total heat dissipation from the Shuttle radar equipment is estimated to be 6.62 kW as shown in Table 3.10.1, which is less than the Shuttle bay heat rejection capability of 8.4 kW with doors open in the warmest orbit. Any other instruments on simultaneously with the radar will have to fall within the total heat rejection capability, or may have to be time shared with the radar or may have their own radiator capability.

The pallet temperature is assumed to be from 0°F to 50°F for the intended orbit. For a worst ease orbit, the temperature of the pallet is assumed to be from -30°F to 106°F. In order to permit the maintenance of a minimum temperature of 0°F of the pallet mounted electronics, the capability of 30 watts

Table 3.10.1. SAR heat dissipation

Pressurized Module		
Data Storage		600 watts
Power Supply		270 watts
Other		392 watts
Pallet (unpressurized)		
Transmitter		3708.3 watts
Receiver		45.6 watts
Power Supply		1604.0 watts
Total	=	6620 watts

of heating in the transmitter, 30 watts of heating in the power supply and 20 watts of heating in the receiver will be included. The oscillator in the receiver will also be mounted in an oven containing a small heater for frequency stability.

The pallet mounted equipment will contain thermal blankets, so that cooling of the equipment will use the pallet heat exchanging capability.

3.11 WEIGHT, POWER AND VOLUME ESTIMATES

Estimates of the volume and weight of the Shuttle Radar Subsystems are in Table 3.11.1. The majority of the weight contained in both transmitters is due to their Traveling-Wave Tubes. The majority of the weight in the Radar Power Subsystems is due to their TWT high-voltage power supplies. Most of the weight of the Control Console is due to the tape transports.

Estimates of the input power to the Shuttle Radar Subsystems are in Table 3.11.2. The input powers given for each subsystem's power conditioner refers to its dissipation due to conversion losses.

Figure 3.11.1 presents a preliminary view of the Shuttle equipment layout.

Table 3.11.1. Radar weight and volume estimates

Item	Size (cm)	Volume (M^3)	Weight (kg)
Control Console Instruments	50 x 43 x 44.0	0.086	16
Control Console Tape Recorders	50 x 43 x 152.4	0.328	55
Control Console Power Supplies	50 x 43 x 31.8	0.068	19
Total for Control Console	50 x 43 x 224.8	0.482	90
L-Band Transmitter	90 x 40 x 20	0.072	48
L-Band Receiver	25 x 20 x 20	0.010	3
L-Band Digital	10 x 20 x 20	0.004	7
L-Band Power Supplies	55 x 20 x 20	0.022	19
Total for L-Band System	90 x 60 x 20	0.108	77
Plus Heat Exchanger	90 x 60 x 2	0.0108	1
Total with Heat Exchanger	90 x 40 x 22	0.1188	78
X-Band Transmitter	80 x 40 x 20	0.064	48
X-Band Receiver	20 x 20 x 20	0.008	5
X-Band Digital	10 x 20 x 20	0.004	7
X-Band Power Supplies	50 x 20 x 20	0.020	19
Total for X-Band System	80 x 60 x 20	0.096	79
Plus Heat Exchanger	80 x 60 x 2	0.0096	1
Total with Heat Exchanger	80 x 60 x 22	0.1056	80

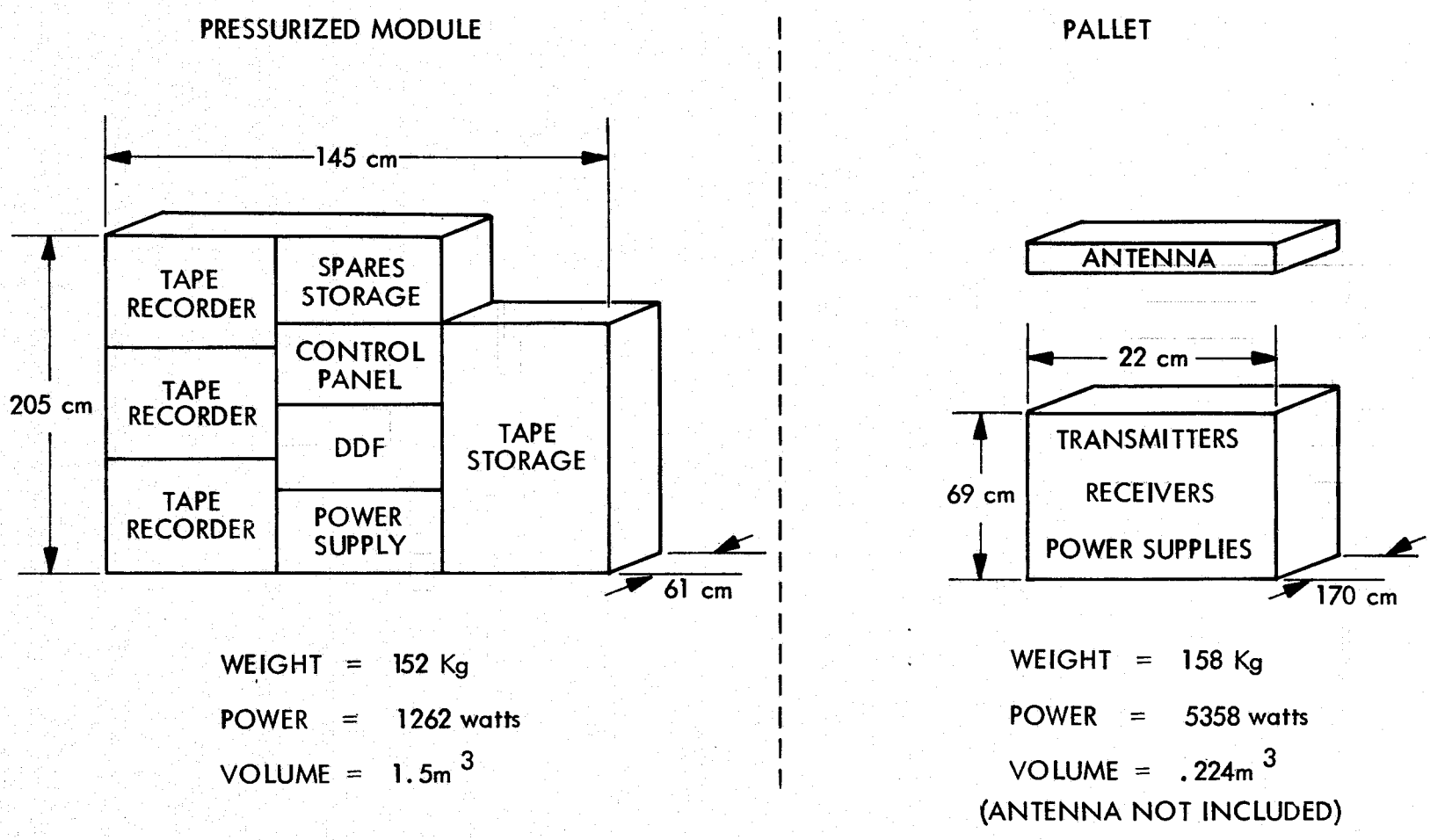

Figure 3.11.1. Shuttle equipment layout

Table 3.11.2. Radar power estimates

Item	Power (watts)
Digital Formatters and Data Subsystem	290
Control Console Instruments	55
Control Console Tape Recorders	600
Control Console Power Supplies (due to conversion losses)	270
Total for Control Console	1215
L-Band Transmitter	960
L-Band Receiver	18
L-Band Digital	23.5
L-Band Power Supplies (due to conversion losses)	417
Total for L-Band Subsystem	1418.5
X-Band Transmitter	2748.3
X-Band Receiver	27.6
X-Band Digital	23.5
X-Band Power Supplies (due to conversion losses)	1187
Total for X-Band Subsystem	3986.4
TOTAL POWER	6620 watts

3.12 ENGINEERING MEASUREMENTS

Engineering measurements will be recorded during a data track. These are presented in Table 3.12.1.

Table 3.12.1. Engineering measurements

Parameter	Frequency
Stalo output level	1/10 sec.
Freq. multiplier output level	1/10 sec.
Chirp VCO error output	1/10 sec.
Chirp phase lock	1/10 sec.
RF driver amp current	1/10 sec.
RF driver amp voltage	1/10 sec.
RF driver amp output level	1/10 sec.
TWT power amp 6 each — current and voltage monitors	1/10 sec.
	1/10 sec.
	1/10 sec.
	1/10 sec.
	1/10 sec.
	1/10 sec.
	1/10 sec.
RF power amplifier output	1/10 sec.
DC modulator-PRF presence	1/10 sec.
Coupled forward power	1/10 sec.
Coupled reverse power	1/10 sec.
Calibration Ref. voltage	1/10 sec.
Calibration Attenuator setting	1/10 sec.
Calibration delay setting	1/10 sec.
Receiver protector current	1/10 sec.
Variable gain amp setting	1/10 sec.
ADC detected volts	1/10 sec.
Data formatter volts	1/10 sec.
Data formatter current	1/10 sec.
PRF	1/10 sec.
PRF setting	1/10 sec.
DDF normal	1/10 sec.
DDF special	1/10 sec.
DDF data flow	1/10 sec.

Table 3.12.1. Engineering measurements (contd)

Parameter	Frequency
Power volts in	1/10 sec.
Power current in	1/10 sec.
Altitude	1/10 sec.
Ground speed	1/10 sec.
Off-nadir angle select	1/10 sec.
Longitude	1/10 sec.
Latitude	1/10 sec.

3.13 GROUND SUPPORT EQUIPMENT (GSE)

The purpose of GSE is to support the Factory Test Equipment (FTE) and the Portable Checkout Unit (PCU). The FTE will be used to test and calibrate the radar and determine its performance. The PCU will be used to support pre-launch testing of the radar.

3.13.1 Factory Test Equipment (FTE)

The purpose of FTE is to test, verify and calibrate the SAR radar. The following represents a list of hardware parameters that will be tested over specified environmental limits.

Transmitter. Peak Power - Measure output of antenna terminal to determine if transmitter is working within specified limits.

VSWR - Measure output of antenna terminal as a function of load VSWR at various phase angles.

Pulsewidth - Measure output of antenna terminal to determine the pulsewidth, rise time, fall time and chirp bandwidth.

PRF - Measure output of antenna terminal to determine that PRF is within specified limits.

Transmitter Spectrum - Using spectrum analyzer look at spectral content of waveform and determine if sidelobes are within specified limits.

STALO Frequency/Stability - Output of STALO will be counted as a function of time, temperature and power. Determine short and long term stability.

Chirp Phase Lock - Verify that chirp generator is in phase lock with the reference STALO.

Power Dissipation - Measure input current vs. voltage. Compute total DC power at DC prime power bus with transmitter on.

Receiver. Noise Figure - Measure receiver noise figure at antenna port with radar in receive mode.

Sensitivity and Gain - Determine receiver gain and sensitivity by means of internal or external calibrated signal.

Bandwidth - Determine 1 dB and 3 dB bandwidths of the receiver.

Receiver Protection Isolation - Measure the attenuation from antenna port to receiver protection gate.

Input VSWR - Measure VSWR at antenna port in receive mode.

Power Dissipation - Measure input current vs. voltage. Compute total DC power at DC prime power bus with transmitter off.

Digital Data Formatter. Built-In Test and Calibration Programmer - Verify all test and calibration function.

Clock, Sync and Data - Verify presence of clock, data and sync.

ADC Output - Verify frequency, stabilization and clock.

Digital Recorder. Generate serial data stream, record, and playback.

Digital Correlator. Correlate a synthesized two dimensional test of simulated radar signals.

Power. Input Current - Measure total prime power bus current vs. voltage, time and temperature with radar ON.

Required FTS Hardware. Table 3.13.1 lists required FTS test equipment to perform the above tests.

3.13.2 Portable Checkout Unit (PCU)

The purpose of the PCU is to support pre-launch testing of the Shuttle SAR. The following represents a list of functions that will be tested on a GO/NO GO basis.

1) Test and verify all SAR functions.

2) Simulate spacecraft interface and the following functions will be verified.

   a) Turn-on sequence

   b) Calibrate sequence

   c) Transmitter - verify peak power, PRF, phase lock loop.

   d) Receiver-verify sensitivity/gain.

   e) Digital Data Format - verify clock, data, sync.

   f) Digital Recorder - verify all functions.

Required PCU Hardware. Table 3.13.2 lists required PCU test equipment to perform the above tests.

Table 3.13.1. Required FTE hardware

Hardware	Number	Hardware	Number
Test Equipment			
a. Power Meter	4 ea	k. VSWR meter	1 ea
b. Hi Power Attenuator	10 ea	l. Noise Figure Meter	1 ea
c. Hi Power Loads	2 ea	m. Primary Power Supply	2 ea
d. Directional Couplers	2 ea	n. ±5V Supply	1 ea
e. Oscilloscope		o. ±15V supply	1 ea
(400 series)	2 ea	p. Stripchart	
(7000 series)	1 ea	Recorder	1 ea
f. Spectrum Analyzer	1 ea	q. Pulse Generator	2 ea
g. Counter/Printer	1 ea	r. STALO; Freq. Mult.	
h. Sign. Gen. L-Band	2 ea	RF Mod.	2 ea
i. Sign. Gen. X-Band	2 ea	s. Mixer, Preamp	2 ea
Miscellaneous Components			
a. Lower Power Attenuator	10 ea	a. Racks	2 ea
b. Low Power Loads	6 ea	b. Control Panels	as req.
c. COAX Switches	6 ea	(vendor fab)	
d. Meters and Readouts	10 ea	c. Cooling Fans	as req.
e. Thermistor Bridge	2 ea	d. Interconnect Cables	as req.

Table 3.13.2. Required PCU hardware

a. Power Meter	h. Step Attenuator
b. PRF Counter	i. Loads
c. DVM	j. Dir. Coupler
d. STALO and Freq. Mult., Pulse Mod.	k. Cabinet - 2 each
e. Digital Delay Generator	l. Control Panel - 2 each
f. Power Supply	m. GSE Cables
g. COAX Switches	n. Instruction Manual

4.0 DATA SYSTEM

4.1 INTRODUCTION

The two imaging radars, operating at two polarizations will, in 12 minutes gather enough data to image 5.5×10^5 square kilometers four times. The total number of resolution elements imaged in one 12 minute pass is 3.5×10^9 pixels. The method utilized to convert the raw radar video data into a format which the user can use must be efficient and able to be completed in a short period of time. Thus the criteria used to evaluate any processing method is as follows:

1) A continuous image strip of all data must be generated within 15 days of return of the Shuttle from orbit.

2) The processed data will be available to the users in computer compatible tapes within one week after selection of areas specified by the user.

3) All data from a single pass must be capable of being converted to processed computer compatible tapes within 3 days.

4) Each resolution pixel of one image from any radar system and polarization must be relatable to a corresponding pixel on the image of any other radar system and polarization.

The two processing methods which were seriously considered - optical processing and the digital convolution processor - can meet the expediency requirements and the convolution processor could meet the relative pixel identification requirement. It is realized that the relative pixel identification requirement is of great importance to the user which utilizes the simultaneous measurements at different frequencies and polarizations to infer physical properties of the area being imaged. Consequently the convolutional processor was investigated in spite of its higher cost.

4.1.1 Data Processing Objectives

The present data gathering objectives of the Shuttle Imaging Radar is to gather data based on 10 data passes of 12 minutes each on four channels. Two channels will be L-band data for H and V polarization and two will be X-band data of two polarizations.

The important output products of the processor are the images, to be sent to the users. These outputs will consist of the following:

1) Processed film strips will be continuous with 64 shades of gray levels.

2) Image data computer compatible tapes will be quantized to a 1 dB quantization level.

3) Images of selected areas will be supplied to users upon request. The imaged data outputs will have the following characteristics:

4) Image pixel-to-pixel registration will be to within one resolution element.

5) The geographic location accuracy will be within one kilometer.

6) The absolute radar cross-section measurement accuracy will be within 3 dB.

7) The relative radar cross-section measurement accuracy will be within 1 dB.

In forming the output products to users a number of parameters must be tagged as part of the output imaged film and computer compatible tapes. These parameters are time and Shuttle ephemeris data-latitude, longitude, altitude, velocity.

4.1.2 Data Processing Implications

Based on the total data taking time of 120 minutes per mission a substantial amount of imaged data will be available to the Users.

The total imaged data output available to users per mission is 1.3×10^{11} six-bit words which represents an imaged area of 2.1×10^{7} Km^2 or 5.25×10^{6} Km^2 per channel.

The processed 9 inch image film output to users will consist of one roll 1200 feet in length with a 20 by 20 micron spot per resolution element.

There will be approximately 3640 rolls of computer compatible tape per mission for users. Each roll will be 2400 feet with a packing density of 1600 bits/inch.

Since there would be a great number of tapes per mission, it is suggested that users review the imaged film for those areas of interest, then computer compatible tapes of those areas will be supplied.

4.1.3 Data System Requirements

In order for the overall system to yield output data consistent with the system guidelines outlined in section 2.2 of this report, the ground data center must have the capability to accomplish the following functions.

1) Play-back the digital tape recorded on the Shuttle orbiter.
2) Perform a range compression operation on the data to compensate for the dispersed pulse transmitted waveform.
3) Compute the range migration, or data path taken by each resolvable element, characteristics of the data.
4) Perform an azimuth compression operation compensating for the range migration of the separate resolvable elements.
5) Non-coherently add the separate images generated by each look (steps 2 to 4) after appropriate registration.
6) Print on photographic film the resultant images generated.

These steps must be accomplished in a timely manner for the users. The requirements of the processor is tabulated in Table 4.1.

Table 4.1. Data Center Functional Requirements

Parameter	Requirement
Radar Wavelengths	L and X-Bands
Number of Looks in range	1 to 4
Number of Looks in azimuth	4 and 8
Range Compression Ratio	365 and 400
Number of Azimuth Channels	1704
Range Pixel Registration	50 nanoseconds
Azimuth Pixel Registration	25 meters
Separate Look Registration	5 meters
Processor Integrated Sidelobe Level	18 dB
Output Image Scale Factor	500,000 to 1

4.2 SELECTED END-TO-END DATA SYSTEM

The selected data system for the Shuttle Imaging Radar, as shown in Figure 4.2.1, consists of a digital recording system on board the Shuttle and a Digital Correlator on the ground. The data flow sequence is as follows: The Imaging Radar bi-polar video is first converted to a digital format in the radar electronics for both direct and cross-polarized echoes. The digital stream is next buffered in the data formatter of the tape electronics and combined with the Shuttle Ephemerides data from the Shuttle computer. After buffering, the data is recorded in a high density multi-track tape recorder. Each tape will have sufficient capacity to store the data gathered by one frequency Imaging Radar for a duration of 12 minutes. Thus the number of tapes required equals the number of 12 minute passes per system. These tapes are stored aboard the Shuttle and their installation on the recorders require operator interaction. Upon completion of the mission, these tapes are returned to the ground central processor station where they are digitally processed. The output of the digital radar processor is then converted into photographic images by an optical recorder and computer compatible tapes by a high density tape recorder.

4.2.1 Justification of Selected Data System.

A digital signal processor offers many advantages over optical processing methods, among these are flexibility, in accommodating multiple modes and wide parameter variations, ease of operation, reliability, precise control of processing parameters, adaptability to nearly real time operation, and built-in test capabilities. Flexibility and ease of operation are of particular value in the present applications since the processing parameters will be varied to satisfy the needs of different users. This includes, for example, parameters such as spatial resolution, and number of looks can be changed by changing the initial set-up of the processing system.

The digital system is capable of providing pixel to pixel registration because the data storage is impervious to the dimentional stability of the storage medium. This is not the case with optical recording/processing systems.

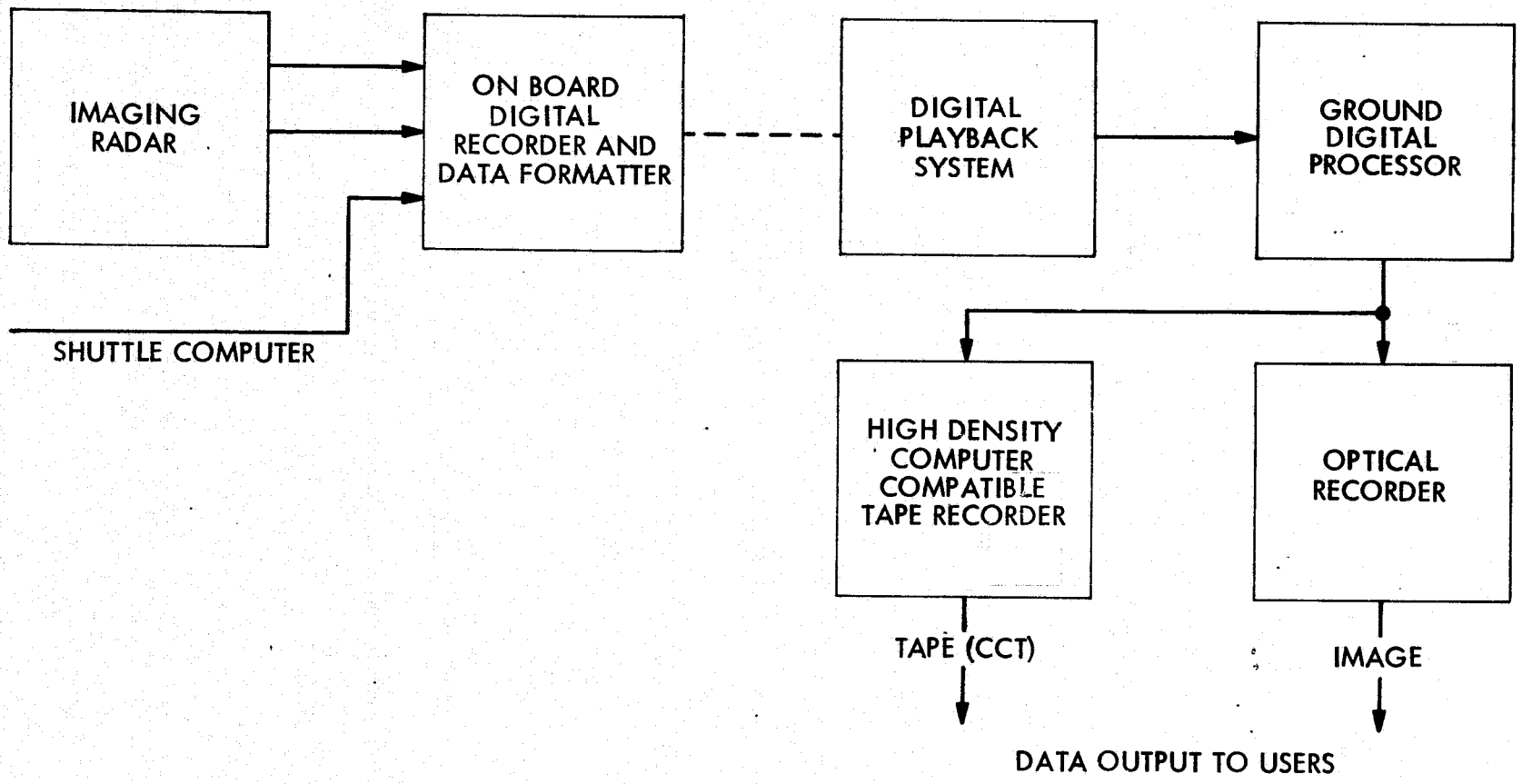

Figure 4.2.1. Selected end-to-end data system

4.3 DIGITAL HIGH CAPACITY, HIGH DATA RATE TAPE RECORDER

4.3.1 Requirements

The high capacity and data rate tape recorders must be capable of recording 240 Mbits/sec data from each of the two radar outputs; i.e., L-band and X-band. This recording rate represents a 120 Mbit/sec data rate for one independent channel of radar returns taken at a different antenna polarization and will be processed separately.

The recorder bit error rate will be specified as one in 10^6 bits.

The tape recorder must be capable of recording continuous 240 Mbits/sec for 12 minutes twice a day for five days. Two tape recorders are required, one for the L-band radar and one for the X-band radar. A third machine should be on line and ready to record in case of a breakdown in one of the prime machines.

4.3.2 Proposed Tape Recorder

As an example the proposed digital tape recorder needed for achieving the above requirements is the HRDM-240S that is currently being developed by RCA. These requirements are shown in Table 4.3.1.

A total of 20 tapes are needed to store data taken twice a day from both radars for five days. Five more tapes are required to be used as spares.

4.4 DATA CENTER SYSTEM DESCRIPTION

In order to process the large volume of data acquired by the radar sensor a suitable data center must be combined into a working system. Data received from the radar sensor will be stored in a high density tape, whose recording characteristics are presented in Section 4.3. The tape will be played back, split into its respective radar channel outputs and processed into a final image. The data system capable of meeting the above requirements is shown in Figure 4.4.1. Its major components are: a) a digital playback system, b) a ground digital processor, c) a high density computer compatible tape recorder, and d) an optical recorder for the generation of a hard copy image.

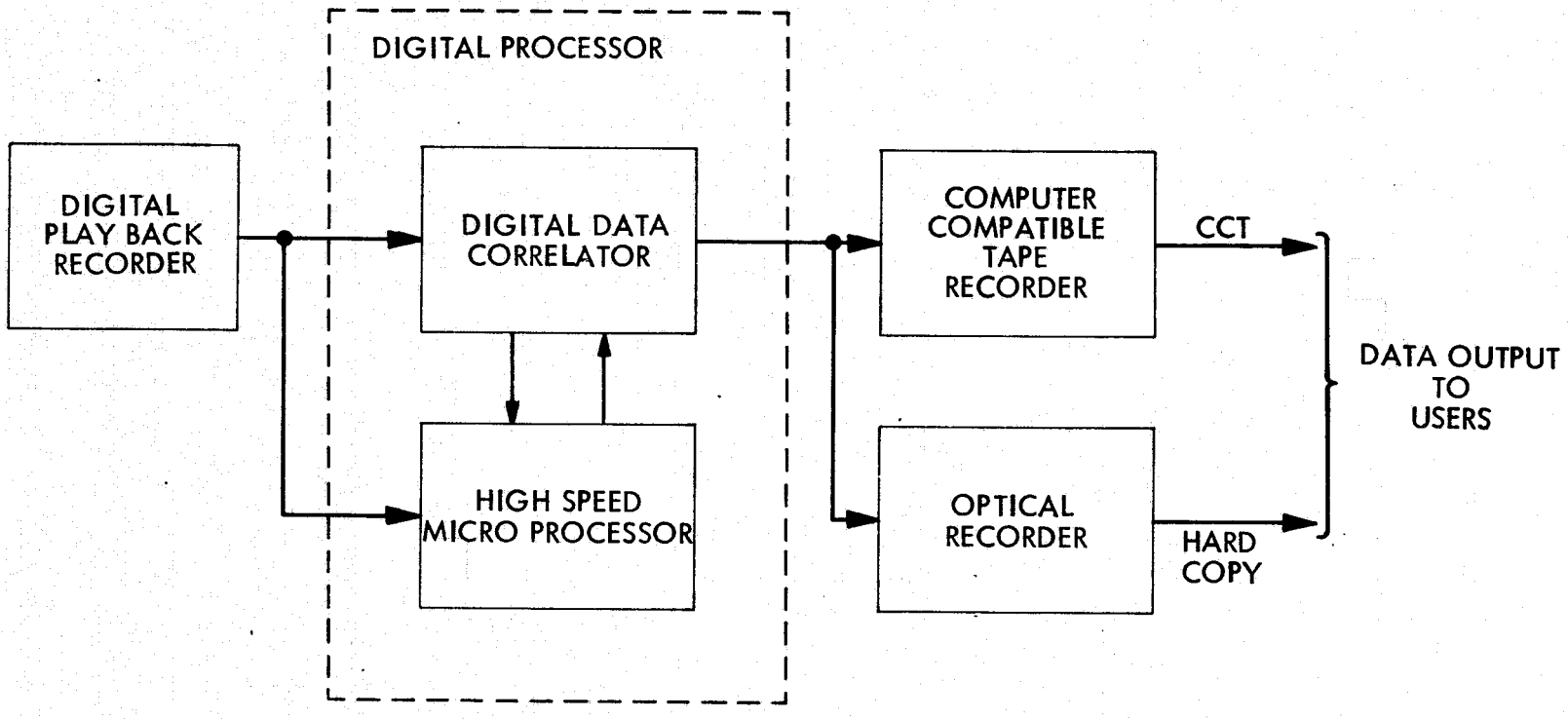

Figure 4.4.1. Data center subsystem

Table 4.3.1. HRDM-240S digital tape recorder

Parameter	Value
Data Rate	Record 240 Mb/s Reproduce 240 Mb/s to 15 Mb/s (min)
Data Format	Serial NRZ-L in/out
Auxiliary Data Inputs	6 lines at 2Mb/sec digital
Record time	12 minutes
Error Rate	1×10^{-6} maximum
Magnetic Tape	2-inch on NAB reel 7000 feet maximum
Packing Density	20,000 BPI in-track density $1.2 \times 10^{6} b/in^{2}$
Total Storage Capacity	1.728×10^{11} bits/tape
Head Life	2000 hrs
Size	5.3 cubic feet
Power	270w peak
Number of Tracks	120 data, 14 EDAC, 6 AUX
Tape Speed	100 in/sec at 240 Mb/s

4.4.1 Digital Playback System

The digital playback system will consist of the same digital high capacity, high data rate tape recorder described in Section 4.3, with the exception that it will be played back at a reduced rate.

4.4.2 Ground Digital Processor Requirements

The ground digital processor will perform the function to compress the radar data in two dimensions, i.e., range and azimuth. Weighting will be applied to the data to reduce sidelobe levels. Clutter tracking will be provided to remove the doppler offset due to the earth's rotation. Range walk and range curvature corrections will also be performed.

The baseline processor will be capable of processing a 100 kM range swath width to azimuth and range resolution elements 25m x 25m. Under the above

conditions the system will have four azimuth multilooks and one in range. Table 4.4.1 presents the baseline processing parameters.

Table 4.4.1. Baseline processing parameters

Parameters	L-Band			X-Band		
1. Off-Nadir Angle, deg	25	38	50	25	38	50
2. Antenna Elevation Dimension, m.	.65	1.55	2.2	.12	.24	.36
3. PRF, Max	1860	1615	1900	1860	1615	1900
4, Swath Width, km	100	78.1	62.6	100	78.1	62.6
5. Range compression ratio	400	400	400	365	365	365
6. Length of Azimuth Channels, m.	1188	1414	1704	186	221	267
7. Bandwidth, MHz	17.38	17.38	17.38	17.38	17.38	17.38
8. A/D bits	S+5	S+5	S+5	S+5	S+5	S+5
9. Pressure number	1	1	1	1	1	1
10. Antenna azimuth dimension, m.	12	12	12	12	12	12
11. Image grayscale resolution, dB	1	1	1	1	1	1
12. Image dynamic range, dB	50	50	50	50	50	50
13. Spatial resolution m.	25,50	25,50	25,50	25,50	25,50	25,50
14. Total number of looks	4,16	8,32	8,32	4,16	8,32	8,32
Range	1,2	2,4	2,4	1,2	2,4	2,4
Azimuth	4,8	4,8	4,8	4,8	4,8	4,8

Digital Processor Study. A study contract was given to Goodyear Aerospace Corporation to determine the feasibility of a digital signal processor for Space Shuttle. The report is presented in Appendix D and includes pertinent digital processing theory, a description of the proposed system, size, weight, power and scheduling.

4.4.3 Optical Recorder and Computer Compatible Tape (CCT) Requirements

The film recorder, which is the only means of seeing the processed data, is a key element to the overall system. This film recorder is composed of an accurately controlled and compensated Laser beam, an accurate film drive, optics and servo loops. The characteristics of this optical recorder and CCT recorder are presented in Table 4.4.2 by the way of an example.

The writing rate of the laser beam, its spot size, the speed of the film and the maximum enlargement must be determined. Thus for a system with a 100 km swath, a spacecraft velocity of 7.5 km/sec, a recording overlap of 50% and a recorder slow down factor of eight will generate 75.5 records/second. Selecting a nine inch film of which only 160 mm is usable will give a spot size of 20 microns. The film motion is 75.5 records/sec times spot size = 1.51 mm/sec. The writing rate of the laser beam becomes 12080 mm/sec. With this data generated, how many CCT tapes will be made.

Table 4.4.2. Processing - Output parameters

1.	Film size	9 inch
2.	Picture Aperture	160 mm
3.	Spot size	20 microns
4.	Film motion	1.51 mm/sec
5.	Writing rate	12080 mm/sec
6.	Tape Recording density	1600 bytes/inch
7.	Inter-record gap	1 inch
8.	Tape Type	9 track
9.	Tape Read Speed.	12.5 inch/sec
10.	Recording overlap	50%
11.	Number of tapes/10 passes	3640

Each record consists of 8000 words or range cells each of 6 bits. Thus for a 9-track tape each record is 8000 bytes long and a tape packing density of 1600 bytes/inch represents 5 inches of tape for one record or 6 inches, including one inch as interrecord gap. For a 12 minute data gathering time, there is a total of 4.35×10^5 records in one file times 0.5 feet/record gives a total of 2.175×10^5 feet/file. Assuming that the tape length/reel is 2400 feet, there will be 91 reels/file or 364 reels/pass or 3640 reels/10 passes.

4.5 TELEMETRY CONSIDERATIONS AND SYSTEM REQUIREMENTS

As shown in Section 2.3.9, the radar data rate output per channel can be in excess of 100 Mbits/sec. For a four-channel system, the required data rate output for transmission from orbit is almost one-half Gigabits/sec.

For a Shuttle sortie mission the data is to be recorded on board and carried down after each mission. An alternate solution to this is to telemeter the recorded data or raw data to a dedicated radar satellite which will relay the data to ground. As presently configured the Tracking and Data Relay Satellite System (TDRSS) would be unsatisfactory as it does not have this capability.

The expected TDRSS data links available during the 1980's are shown in Table 4.5.1. The return link TDRSS to GROUND for the Ku-band single access will have the capability of handling the data generated by the four channel radar, only if the radar data is played back at a reduced speed. From Table 4.5.1, the problem is that the projected single access return link between Shuttle and TDRSS is at a very reduced rate of 10 Mbits/sec for Ku-band. The radar data could be played back at a reduced rate to accommodate this low link rate. It is suggested that a much higher data rate link capability be incorporated between Shuttle and TDRSS and should be in the order of 50 Mbits/sec or higher.

Table 4.5.1. Tracking and data relay satellite system (TDRSS)

Return link (TDRSS to GROUND)
S-band (single access) at 2 Mbits/sec
Ku-band (single access) at 300 Mbits/sec
Return link (Shuttle to TDRSS)
S-band (single access) at 62 Kbits/sec
Ku-band (single access) at 10 Mbits/sec

4.6 OPTICAL SYSTEM STUDY

A study contract was given to ERIM to determine the feasibility of an optical system for Space Shuttle. The report is presented in Appendix C and includes design parameters of an on-board optical recorder and an associated optical ground-based processor. The following two sections present a summary and recommendation of the ERIM Study.

An optical system provides an alternate way to process data at a low cost. Because it does not have the capability of pixel to pixel registration it is not a recommended system.

4.6.1 Justifications for Optical System

The primary justifications for an optical processing system are the reliability and cost. The use of existing correlator optics combined with additional correction systems required for processing Shuttle data should be considerably less expensive than a full digital correlator, especially with the swath length of 5800 elements is taken into account. The size of buffer memory and central processor could lead to reliability problems in the digital processor. The major cost in the optical system is the implementation of the optical recorder. However, a similar device (with one channel instead of four) would be required at the output of the digital processor anyway. A four-channel, 5800 element per channel recorder is a very complex and expensive device and is the key problem to be solved for optical processing system for Shuttle.

4.6.2 Film Storage

Latent image decay will occur in photographic film during the time between exposure and development unless the film is stored at near 0° centigrade temperatures. Two basic techniques can be employed to account for this problem. The first technique is to store the film at the freezing temperature immediately after exposure until it is developed. The second method requires calibration of the image decay for the expected time stored at the expected temperature. Increased exposure and/or different processing can be used to obtain the desired photometric properties of the signal film. In any case, it is recommended that calibrations be performed on the film to determine the effects of storage temperature, time, vacuum, or whatever conditions will exist aboard Shuttle. These conditions can then be used for the calibration of the optical recorder/processor system. The total quantity of film (if it is 9 or 10 in. wide) should be less than 1000 ft and would require less than 1 cu. ft. of storage space.

5.0 ENVIRONMENTAL CHARACTERISTICS AND ACCEPTANCE TESTS

5.1 ENVIRONMENTAL CHARACTERISTICS

This section describes the natural and induced environments that the Imaging Radar may be exposed to during operation with the Spacelab system. The induced environment data is preliminary and will be updated as Orbiter and Spacelab test results become available. At the design stage, appropriate design margins will be imposed.

The environments that the Imaging Radar will be exposed to depend upon the equipment location and the mission phase. The radar equipment electronics will be located in the pressurized module. The transmitter, power supply, receiver and the planar array antenna will be pallet mounted in the aft section of the payload bay which will be open or closed with a clam-shell-type door. The space environments of the payload bay will vary significantly from an open to a closed configuration. In a typical mission, the radar will experience various environmental stresses from launch through re-entry and during ground operations. The stresses due to the different types of environments will be grouped and briefly discussed under three categories: (1) Module Equipment/Flight Environment, (2) Pallet Equipment/Flight Environment, and (3) Ground Operations Environment.

5.1.1 Module Equipment/Flight Environment

Vibration.

1) Sine Vibration

Events such as gust loading, engine ignition and cutoff, separation and docking will induce low frequency transient design requirements in the frequency range from 3 to 35 Hz at an acceleration amplitude of plus or minus 0.25g peak.

2) Random Vibration

Equipment will be subjected to wideband random vibration arising from the overall acoustic level inside the payload bay, and to a lesser degree from vibration transmitted through the Orbiter/Spacelab mounting fixtures into the module structure. The

vibration levels' duration is 6 seconds per mission at an overall level of 10g rms.

Acoustic. The estimated acoustic spectrum inside the cargo bay produces an effective overall sound pressure level of 145 dB (re 20 $\mu n/m^2$). The maximum acoustic level occurs at the timeof liftoff. The Spacelab module shell and insulation will attenuate the acoustic vibration level down to 138 dB.

Shock. The shock environment consists of the following:

1) Pyro Shock — TBD

2) Landing Shock — The 'g' levels are relatively low in comparison to the handling shock described in 5.1.3.

3) Crash Safety Shock — The equipment design goal should be based on a 40g $\pm$ 6g sawtooth for an 11 millisecond duration. The equipment must survive the crash safety shock without creating hazards to the flight personnel.

Acceleration. The estimated maximum total acceleration acting on the center of gravity of the Imaging Radar in any direction during all the mission phases is $\pm$4g or less.

Spacelab and payload equipment must be capable of surviving the "crash" landing acceleration loads of 9g's with sufficient physical integrity to preclude hazards to the flight personnel.

Temperature. The module air temperature may be adjusted within the range 18°C to 27°C.

Atmosphere. During normal operations, pressure within the Spacelab module is maintained at 1.013 $\pm$ 0.013 bar (1 atmosphere). The relative humidity is controlled within 25% to 70%.

Cleanliness. All equipment surfaces shall be capable of being cleaned to a visible clean level. During operation of the Spacelab module the cleanliness shall be maintained by using circulated air filtered by 5 micron HEPA filters.

Electrical.

1) Orbital Radiated Emission. At the Orbiter S-band transmission frequencies, preliminary calculations show an expected level of approximately 3.4 v/m within the forward portion of the cargo bay, decreasing to 0.7 v/m in the aft section of the cargo bay. The module structure is expected to provide an attenuation of at least 20 dB to electrical fields.

2) Conducted Emissions. The conducted interference levels on the primary power line interface (+28 vdc nominal) is 1.8 volts peak-to-peak 30 Hz to 7 KHz, decreasing to 0.6 volts peak-to-peak at 50 KHz, then flat at 0.6 volts peak-to-peak 50 KHz to 400 MHz.

Magnetic Environment.

Orbiter Emissions. Orbiter contribution to the payload magnetic environment will not exceed the following levels:

DC Magnetic Field = TBD

AC Magnetic Field = 120 dB above a picotesla at 30 Hz decreasing to 20 dB above a picotesla at 10 KHz.

5.1.2 Pallet Equipment/Flight Environment

Vibration.

1) Sine Vibration = Same as module equipment.

2) Random Vibration. For equipment less than 15 kg in mass, the overall level is 26.4g RMS. For equipment greater than 15 kg in mass, the overall level is 12g RMS.

Acoustic. The overall acoustic level is 145 dB.

Shock and Acceleration. Same as module equipment.

Temperature. While the Orbiter payload bay doors are closed, the radiative coupling with pallet equipment is dependent on the inside door surface

characteristics and temperature which in turn is determined by the attitude mode of the Orbiter. With the payload bay open, the radiative environment for pallet mounted equipment is determined by the Orbiter altitude, the equipment shadow/ illumination configuration, and the incoming fluxes (nominal) given below:

Solar Radiation: 1352.2 W/m^2

Earth Global Albedo: 30% of Solar Radiation

Earth Thermal Radiation: 236.4 W/m^2

Space Sink Temperature: 2.7°K

Atmosphere. The Orbiter payload bay is vented during the launch and entry phases and is unpressurized during the orbital phase of the mission. During ascent, the payload bay internal pressure will decrease from 1 atmosphere to vacuum in 130 seconds. During re-entry andlanding the payload bay pressure will be increased to the landing site pressure by using filtered atmospheric air (50 microns absolute). The vent opens at 70,000 feet. The pressure will increase to 1 atmsophere in 350 seconds.

Cleanliness and Contamination. During entry, no control of humidity or concentration of other gases will be provided by the Orbiter.

Electrical and Magnetic. The electrical environment described in 5.1.1 is generally applicable also for pallet mounted equipment. The significant difference between the two environments is that the pallet mounted equipment can be expected to encounter S-band RF field strengths of approximately 3.4 volts/meter due to the absence of any module shielding. The magnetic environment is similar to the module environment in 5.1.1.

Thermal. The thermal environment of the Shuttle Imaging Radar during entry consists of the shuttle bay wall temperature, the pallet or bay floor temperature and the bay air temperature. The temperature of the Radar will depend upon the thermal control provided by the Orbiter and the Radar while the Radar is being subjected to the thermal environment.

Based on the information in Space Shuttle System Payload Accommodations, JSC 07700, Vol. XIV, Rev. D, 1975, the transient thermal environment during entry, but before the initiation of ground purge, has been conservatively estimated to be as follows.

	Temperature (°F)	Duration (Minutes)
Shuttle Wall	170°F	40
Pallet	160°F	40
Bay Air	150°F	25

The above temperature estimates are for the worst case condition. These temperatures could nominally be 30°F to 40°F less than the worst case temperatures.

5.1.3 Ground Operations Environment

Vibration/Shock.

1) Transportation. The dynamic loads should be controlled to be lower than flight operations.

2) Handling. The shock environments experienced by the payloads during handling are represented by 20g terminal sawtooth pulses of a 10 millisecond duration in both directions of each axis.

Temperature and Humidity. The temperature will be controlled to room temperature of 20° ± 3°C (70 ± 5°F). The temperature may vary from 7.2°C to 48.8°C (45 - 120°F)in the extreme cases during purging. The humidity will be controlled to 50% RH in general with some exceptions.

5.2 ENVIRONMENTAL ACCEPTANCE TEST PHILOSOPHY

The objective of the acceptance test is to demonstrate that the instrument (Imaging Radar) will function in a prescribed, satisfactory, and understood manner in its intended mission. This will be accomplished by developing a comprehensive environmental test program formulated early in the development stage of the instrument and updated as the instrument design and knowledge of the mission and the Space Shuttle environmental program mature.

Criteria shall be established for the environmental qualification, acceptance and other environmental testing which may be required by the NASA Project Management Center (PMC). The Environmental Test Program and documentation requirements for instrument testing are specified in the Environmental Requirements Document prepared for the instrument, and will be tailored to the individual requirements of the appropriate NASA PMC and the Space Shuttle interface requirements. However, certain baseline policy described herein will form the framework for the JPL environmental program requirements.

5.2.1 Types of Testing

1) Qualification Testing. Qualification (Qual) tests are required for the formal instrument environmental qualification of the instrument. Qualification environmental testing includes appropriate performance and margin tests as defined in the test specifications.

   Qual tests are not intended to be destructive, although the levels are intentionally more severe than Flight Acceptance (FA) conditions. The Qual tests are intended to provide a confidence in the instrument design for the expected environmental mission exposure and will be performed on hardware designated for the qualification test program.

2) Flight Acceptance Testing. Flight Acceptance (FA) tests are required for the formal environmental certification of flight acceptability for flight and flight spare instruments. Inspections, functional tests, etc., provide confidence that the flight instrument is representative of the design qualified by the Qual tests.

3) Protoflight Testing. Protoflight tests, under certain circumstances, may be used to replace qualification tests. The test levels are intermediate between qualification test and flight acceptance test. Protoflight test is intended to a certain degree to qualify the instrument design and to assure that the instrument still remains in flight quality after test.

5.2.2 Environmental Documentation

1) Environmental Requirements Document. The Environmental Requirements Document (ERD) is the top-level requirements document for the Environmental Test Program. The ERD presents a melding of the NASA PMC — furnished environmental program requirements, interface requirements, environmental estimates, and other pertinent environmental information or requirements with JPL environmental program and policy requirements, and program constraints (i.e., funding, schedule, and resources). The ERD then defines and establishes the Environmental Test Program requirements for the instrument which will form the basis for the environmental test specifications.

2) Instrument Environmental Test Specifications. These specifications define in detail the environmental Qualification and Flight Acceptance (FA) test requirements and the necessary performance evaluation for the science instrument. They include the appropriate performance criteria, and pre- and post-test performance checks (where applicable) by which the acceptance or rejection of the science instrument under the applied environment may be determined.

5.2.3 Environmental Testing Standards

Any facility used to perform environmental testing shall meet certain minimum standards in the General Environmental Test Standards. These standards shall be met whether the facility is at JPL, at the plant of a subsystem contractor, or at a test laboratory under contract with JPL or the contractor. The minimum standards will vary to some degree, depending upon the requirements of the particular science instrument.

6.0 RELIABILITY AND QUALITY ASSURANCE

6.1 INTRODUCTION

This Reliability and Quality Assurance (R&QA) section establishes the Quality assurance and Reliability criteria and activities to be implemented during the design, fabrication, test, and delivery of the Shuttle Synthetic Aperture Radar (SAR) Proto/flight and flight instruments.

6.2 RELIABILITY ASSURANCE PROGRAM

6.2.1 SAR Reliability Assurance Objectives

The objective of the detailed reliability assurance actions defined in this section is to provide a coordinated reliability assurance effort directed toward ensuring, insofar as practicable, maximum reliability for Shuttle mission performance consistent with SAR Project requirements and constraints.

Specific objectives include:

1) Emphasis and priority on reliability assurance efforts and actions that support and participate in design decisions and tradeoffs throughout the design process, from conceptual design to mission completion.

2) Identification and elimination of possible sources of unreliability during the design and development phases.

3) Development of comprehensive knowledge of hardware item functional failure modes using an abbreviated fault tree technique, and their sequential functional relationship to instrument output.

4) SAR reliability assurance efforts planned and implemented to be cost-effective in supporting SAR design and development.

5) Activities consistent with the "Safety Policy and Requirements for Payloads Using the National Space Transportation System" as applicable to this instrument.

The Reliability Assurance Program of the instrument will include design and development support, parts, material and processes control, problem/ failure reporting, and subcontractor/supplier reliability activities.

6.2.2 Design and Development Support

Documentation of reliability assurance activities and of the design/ development, fabrication, and test efforts pertinent to instrument reliability will be accomplished only to the extent that is effective and timely in support of these efforts.

The interface communications by SAR Reliability Assurance will be primarily accomplished through direct participation during design/development activity, and the continuing exchange of design/development documentation (technical and management memos, study reports, analyses, test results, etc.).

Reliability reviews and audits, as contrasted with formal engineering design/hardware reviews, will be conducted (as appropriate) by Reliability Assurance in conjunction with the JPL Cognizant Engineer to evalute and coordinate the status, effectiveness, accomplishments, and plans for the continuing reliability assurance activities.

Audits of Contractor's reliability assurance activities will be conducted by Reliability Assurance in conjunction with the JPL Cognizant Engineer to assess the effectiveness of activities and the extent of compliance with Plan requirements and objectives.

6.2.3 Reliability Analyses

Reliability analyses involving quantitative and probabilistic techniques will be limited to those which are timely and effective in support of design concept selection, optimization, and design/development decisions and tradeoffs. Specifically, numerical analysis techniques will be utilized in support of design decisions and tradeoffs only where comparative analyses are valid and a meaningful contribution to the design or tradeoff decision.

Design evaluation efforts, while requiring prior completion of some design configuration as a basis, will be accomplished as early as possible during the design phase. Evaluation efforts (initiated early in the design process and followed by recheck or updating as the design progresses) will provide maximum assurance of desired reliability, fault protection, and minimum residual unrealibility.

6.2.4 Design Assessment Analyses

Designs of flight hardware and critical support equipment will be evaluated by implementing a prudent selection and application of assessment-type analyses (e.g., worst-case, nominal stress, tolerance, and fault free analysis).

6.2.5 Review of Documentation

Design, fabrication, procurement, and test documentation will be reviewed for reliability considerations. Primary emphasis will be placed on determining the completeness and effectiveness of documented provisions in establishing requirements critical to maintaining inherent design reliability during procurement and fabrication, and in detecting and precluding faults and sources of unreliability.

6.2.6 Formal Design/Hardware Reviews

Formal design reviews will be accomplished by an Instrument Review Board, convened whenever a review will be most effective in the design/development effort. Board findings shall be consolidated and published in the Design Review Summary Report, which includes its findings and recommendations.

Preliminary Design Review (PDR). The PDR is an instrument and component-level review which is intended to assure that the proposed designs satisfy the experiment and mission requirements and are within existing technologies.

The following items are considered typical to a PDR:

1) Functional requirements

2) Block diagrams

3) Preliminary parts list (with parts status information)

4) Enviromental requirements document

5) Experiment performance analysis (including an analysis of the instrument system accuracy requirements)

6) Design parameters, restraints, and constraints

7) Preliminary stress analyses (as applicable)

8) Flow plan and schedule

9) GSE design data

10) Preliminary data reduction plans

Critical Design Review (CDR). The purpose of the CDR is to examine the design for final compatibility and consistency with Project requirements and to establish that existing mechanisms are adequate to assure that these requirements are satisfied. It will also determine the degree to which design and reliability meet the provisions of the system design characteristics and constraints and other controlling requirements. This review shall include an evaluation of detail mechanization, parts application, parts reliability, packaging, electronic circuitry, mechanical design, testing approach, engineering documentation, and other disciplines critical to the adequacy of the flight equipment.

The following items are considered typical of the CDR:

1) Parts lists

2) Environmental test specification status

3) Screening specifications and results

4) Flow plan and schedule

5) Materials and processing specification status

6) Detailed design parameters and restraints

7) Stress analyses

8) Details of design construction and packaging

9) Detail circuit drawings

10) Quality assurance and reliability considerations

11) GSE design data

12) Developmental test results

13) Calibration plan

14) Configuration control plan

15) Interface details

16) Data reduction plans

Pre-Shipment Review. Before the flight hardware is delivered, a Pre-Shipment Review shall be held at JPL to evaluate flight readiness and to assess the extent to which flight qualifications criteria were attained.

All test results, reports, Problem/Failure Reports (P/FR's), ECRs, Material Review Board (MRB) actions, and Inspection Reports (I/R's) discrepancies shall be dispositioned prior to this review, which will cover (but not be limited to) the following areas:

1) Review of hardware status and documentation to assure that the latest chieanges have been incorporated in affected hardware.

2) Review of the test documentation status and determination of the adequate and proper testing of hardware.

3) Review of the Problem/Failure reporting documentation to determine its status and to evaluate its program impact.

4) Review of the Quality Assurance history to ensure that necessary inspections have been performed and all discrepancies properly corrected as reflected in summaries of Inspection Reports and MRB actions.

5) Review of the results of the Instrument Calibration Report to ensure compliance with the Functional Requirements and the Calibration Plan.

6) Shipping and handling requirements and plans.

6.2.7 Parts, Materials, and Processes Control

A significant part of overall efforts to achieve the necessary high performance and reliability for the instrument is the control of selection, application, and use of parts, materials, and processes during the design and fabrication of all flight-type hardware and critical support equipment items.

This paragraph defines requirements, procedures, and responsibilities for a program of activities to accomplish the desired control of parts, materials, and processes. The scope of the design items to be controlled during instrument activities (and covered by requirements of this document) includes the following categories:

1) Electronic and electromechanical parts

2) Packaging parts

3) Fasteners

4) Mechanical parts

5) Purchased devices

6) Materials (metallic and nonmetallic)

7) Processes

Selection Requirements. To the degree practicable, only Parts, Materials, and Processes (PM&P) of the highest available reliability (as demonstrated by existing evaluation/qualification data, through previous satisfactory space flight experience or verified performance) shall be selected for application in the instrument flight-type hardware and critical support equipment.

Control of Parts, Materials, and Processes. It is required that the parts, materials, and processes used on the instrument be controlled as defined in this section. The control effort coordinated by Reliability Assurance will provide

Management with full visibility of parts, materials, and processes status, including selection, application, control provision documentation, and classification regarding acceptability for the intended flight application.

Electronic and Electromechanical Parts Control. The primary goal of the electronic parts control activities is to ensure the use of high reliability electronics parts, consistent with Quality and Reliability guidelines, and compatibility with the technical requirements of the experiment and available resources.

Specific control actions will ensure that the electronic parts chosen for the instrument are (1) appropriate for the specific applications, and (2) properly evaluated/qualified and verified to possess proven performance margins and functional capabilities.

Parts Selection. Electronic parts shall be selected according to three general criteria:

1) The part is on the JPL Preferred Parts List (PPL).

2) The part is known to have been successfully used in other space flight programs or is very similar to a JPL PPL part.

3) Parts not on JPL qualified parts list will be reviewed by the JPL parts specialist.

Screening. All electronic parts used in the instrument will be screened by burn-in at the subassembly, component, or installment level in lieu of individual part screening. However, critical individual parts may be screened on an individual part basis.

6.2.8 Redundancy

The following steps will be taken to insure the maximum instrument probability of success.

1) Incorporate high reliability design to minimize single point failures at a minimum cost.

2) Utilize redundant design in critical areas to enhance reliability at a minimum cost.

3) Incorporate functional redundancy as a design technique wherever feasible.

6.2.9 Failure Reporting System

A comprehensive, closed-loop, failure reporting system will be a primary effort in ensuring that the instrument hardware delivered for Shuttle operations will provide maximum instrument success. Emphasis and control effort will be placed upon (1) complete coverage of reportable incidents, (2) timeliness, completeness, and accuracy of actions and reporting, (3) adequacy, completeness, and depth of analysis, and (4) adequacy and verification of corrective actions.

During the appropriate phases of instrument design/development, test, and operation, three types of documentation will be used: Log Books (begun during early design/development activity); JPL Problem/Failure Reports (P/FR's); and JSC Malfunction Reports (MR's).

JSC Malfunction Reports. JSC Malfunction Reports will be submitted to JSC for use in the JSC failure reporting system by JPL at initiation and final closeout of the report.

Log Books. JPL will maintain separate Log Books per unit throughout the development, inspection, testing and operational phases while the Proto/flight and Flight units are under JPL cognizance. The JPL FSE Unit History Log provides a chronological history of the instrument, including operating time, starting with the first power application after assembly.

6.2.10 Subcontractor/Supplier Reliability

Reliability Plan. Subcontractor(s) shall develop appropriate Plans or documentation to define requirements, responsibilities, detail procedures, and data submittals to JPL. Subcontractor/supplier reliability efforts will be defined in the contractor's Plan or in an appropriate subcontractor/supplier

documentation (e.g., Plan, letter of agreement, purchase order attachment, or incorporated purchase order provisions). The JPL Reliability Assurance Plan is the controlling document for all in-house and subcontractor reliability efforts on instrument tasks.

6.3 QUALITY ASSURANCE PROGRAM

A Quality Assurance Program will be implemented by JPL and its subcontractors using NASA Publication NHB-5200.4(1C) as a baseline for requirements.

6.3.1 General

It will be the joint responsibility of the supplying JPL Technical Division and the JPL Quality Assurance organization to establish the Quality Assurance Plan for the JPL related activites.

Subcontractors and suppliers of special devices will be required to submit QA plans for their activities.

Inspection of protoflight/flight equipment will be based on engineering requirements and when appropriate will be defined by detailed Quality Assurance Instructions.

7.0 FLIGHT TEST PROGRAM

7.1 PURPOSE

It is essential to flight test the Prototype instrument as early as possible to verify instrument design, alignment, calibration and to correlate viewed images with ground truth with digital output data. It is also essential to flight test and calibrate the Flight Unit instrument after environmental testing over the same geographical areas as the Protoflight. Digital output data from the Flight Unit will be compared to Protoflight data as part of the calibration requirements. It is most feasible to flight test the Imaging Radar instruments, under continuous human control and surveillance, onboard a turbojet aircraft such as the Convair CV990 operated by Airborne Sciences of NASA/Ames Research Center. The CV990 provides a reasonably stable platform with convenient in-flight access to all radar equipment. The CV990 is fast enough (with an operational range of about 3500 nautical miles) to acquire a variety of suitable imagery targets within a short period of time.

7.2 FLIGHT TEST EQUIPMENT

The flight equipment will consist of:

1) Synthetic Aperture Radar (SAR) Protoflight and/or Flight Unit.

2) Antenna system.

3) Support equipment.

4) Recording equipment.

7.2.1 Synthetic Aperture Radar

The Shuttle flight configured units, both L and X bands, will be mounted in special designed racks located in the aircraft's rear baggage compartment in the immediate vicinity of the hermetically sealed antenna connectors.

7.2.2 Antenna System

Since the aircraft nadir distance to earth will be considerably less than that of Shuttle, antenna gains will not have to be as great permitting physical sizes suitable for aircraft application.

The L-band will use two slotted antennas (one vertically and one horizontally polarized) mounted on the outside of the aircraft's aft baggage door viewing the right side. Horizontal, vertical and cross-polarization will be employed as required.

The X-band will use two antennas (both viewing the right side) mounted on stabilized gimballed platform. The systems will be enveloped in a fiberglass radome affixed to the aircraft keel in line with aft baggage door.

Both antenna systems will view from nadir to 45° from nadir.

7.2.3 Support Equipment

Support equipment will consist of power supplies, SAR control command unit, absolute altimeter, signal patch panel, oscilloscopes, aircraft signal interface unit and aircraft Inertial Navigational System display.

7.2.4 Recording Equipment

High speed magnetic tape recorders will record digital video data from both SAR's. All recorders will record a mutual timing code derived from aircraft timing generator. All records will display tape footage counts to tag geographical locations and events logged with parameters provided by Inertial Navigation System.

All SAR electrical monitoring functions, timing signals and SAR video will be displayed on oscilloscopes and photographed with polaroid and 16 mm movie cameras.

7.3 PRE-FLIGHT TESTS

During the post equipment aircraft installation phase, prior to flight, SAR and aircraft systems testing will be accomplished to assure proper flight instrument and compatible systems operations. The following on-ground aircraft pre-flight tests will be made:

1) Measure all support equipment parameters to verify proper operation

2) Measure and record all SAR monitor test points

3) Measure and record antenna systems VSWR

4) Measure and record transmitter output power

5) Measure and record receiver sensitivity threshold

6) Photograph oscilloscope patterns of all SAR and applicable aircraft signals (i.e., PRF, clock, timing, transmitted pulse, etc.).

7) Insert a series of analog signal levels into the input of the digital data system and record on magnetic tape recorder and analyze for proper operation.

8) Measure dynamic receiver and recorder calibration, using both SAR and digital recorders. The chirped output from the RF modulator will be inserted into SAR receiver input via a pad attenuator programmed in 3 dB steps from saturation over dynamic range. The digital recordings will be analyzed prior to first flight.

7.4 FLIGHT TEST PROCEDURE

7.4.1 Flight Plan

Just prior to each flight, suitable radar target sites will be selected and appropriate flight plans will be filed to achieve maximum usefulness of target zones. Each flight plan will also include a SAR operational plan as outlined in SAR Flight Test Procedure. The Flight Plan will be a part of the SAR Flight Log.

7.4.2 Pre-Data Requirement

At least 30 minutes warm up time on each flight, prior to taking data, will be required on recorders and support equipment. The SAR temperature will be monitored for proper warm up before applying full power, since aircraft ambient temperature could be over a rather large range.

A dynamic receiver and recorder calibration will be made prior to data run on each flight.

7.4.3 Flight Data Requirements

Specular Targets. A minimum of 15 minutes duration (7.5 minutes each side of target) is required at a constant aircraft velocity, attitude, altitude and track. The optimum radar altitude varies with target, but usually 25,000 feet.

On multi-flights over a given specular target, four runs will be made within echo recording swath at each site; two on reciprocal headings at zero drift angle and two on reciprocal headings perpendicular to upwind/downwind headings.

Zonal Targets. Zonal runs, such as coast lines, will be flown on a straight track in a manner such that most of the areas of interest will be imaged in the recorder swath. Aircraft heading changes should be minimized, while velocity and altitude remain as constant as practical.

Secondary Targets. Secondary targets will be assigned for each flight in the event of unforeseen, forbidding or undesirable circumstances which could prevail at the primary target area (i.e., severe turbulence, zone becoming restricted, air traffic control constraint, etc.)

Target Reruns. Ascertain by aircraft tracking and oscilloscope video display if target was within recording sweep swath. If practical, data reruns should be made to capture desired targets.

Photographs. Whenever practical, multiple aircraft aerial photos will be taken at required intervals and overlap to sufficiently aid the final SAR data reduction.

7.5 ENGINEERING FLIGHTS

Two modes of flights are necessary for each SAR model; Engineering and Calibration Data flights. The first flight after equipment installation on the aircraft will be used for engineering purposes since overall system test cannot be accomplished on the ground. The engineering flight will employ the use of laboratory test equipment and additional technical personnel not normally used

on Data flights. Each engineering flight will last approximately 6 hours in duration and will be used to align and adjust the SAR over specific target areas.

7.6 FLIGHT DATA OBJECTIVES

The SAR, like any other flight instrument, must have its output data calibrated and correlated with all types and classes of sensed images or sources. The SAR instrument will be tested, calibrated and correlated to determine the characteristic features of each of the following images:

1) All types of ice and ice flows. Each type of ice and ice boundary is expected to present a unique and discrete effect on both L and X band energy.

2) Coastal Zone effects, both beach and inlet, at various ocean wave angle intercepts. This can best be accomplished by imaging the entire west coast of U.S.A. and Canada.

3) Dry sand dune desert area for surface penetration and surface layering effects.

4) Farmland, open fields and forests properly identified and calibrated. The farm belt of the U.S.A., the wheat fields of U.S.A. need to be imaged prior to and after harvests. The forests across the northern U.S.A. from coast to coast also require imaging.

5) Sea states of various wave heights, patterns and currents. In some instances, a specular target in an accurately measured and correlated sea state will be employed. Whenever practical, corresponding surface truth data will be acquired from independent means (i.e., instrumented buoys, ships, laser profilometer). Wave Pattern data will be acquired from North Pacific and North Atlantic Oceans during different surface conditions.

APPENDIX A

SHUTTLE Ku-BAND RADAR SYSTEM PARAMETERS

Table A-1. Summary of Ku-Band SAR System (H = 185 km)

Parameter	
1. Frequency, GHz	15.0
2. Wavelength, m	0.02
3. Peak Transmitter Power, kW	20
4 Average Transmitter Power, kW	0.8
5. Transmitter Duty Cycle, %	3 - 5
6. Transmitter Efficiency, %	40
7. Transmitter Pulse Length, μsec	21
8. Antenna Polarization	
9. Antenna Efficiency, %	60
10. Antenna Azimuth Dimension, m	12
11. Antenna Azimuth P-N Beamwidth, deg	0.095
12. Radar Output Quantization, bits	6
13. System Noise Figure, dB	3.0
14. System Losses	
RF, dB	7.4
Field Degradation, dB	1.0
Atmospheric, dB	0.5
15. System Noise Temperatures, °K	2152
16. Ambiguity (overall), dB	<-18
Range, dB	-20
Azimuth, dB	-22.5
17. Spatial Resolution, m	25 and 50
18. Image Dynamic Range, dB	50
19 Image Gray Scale Resolution, dB	1
20. Weight	150 kg
21. Power	4670 watts

Table A-1. Summary of Ku-Band SAR System (H = 185 km) (contd)

Parameter			
22. Off-Nadir Angle, deg	25	38	50
23. Antenna Elevation Dimension, m	0.11	0.2	0.31
24. Antenna Elevation P-N Beamwidth, deg	10.7	5.7	3.7
25. Antenna Gain, dB	46.1	48.7	50.7
26. Minimum Scattering Coefficient, dB	-21.0	-23.2	-25.3
27. System Bandwidth, MHz	17.38	17.38	17.38
28. Range Compression Ratio	365	365	365
29. Azimuth Compression Ratio	5.2	6.0	7.5
30. Signal-to-Noise Ratio, dB	13.2	12.0	9.0
31. Imaged Swath Width, km	63	50	46
32. PRF, Hz (Max)	1860	1615	1900
33. Multiple Looks (Total)	4, 16	8, 32	8, 32
Azimuth	4, 8	4, 8	4, 8
Range	1, 2	2, 4	2, 4

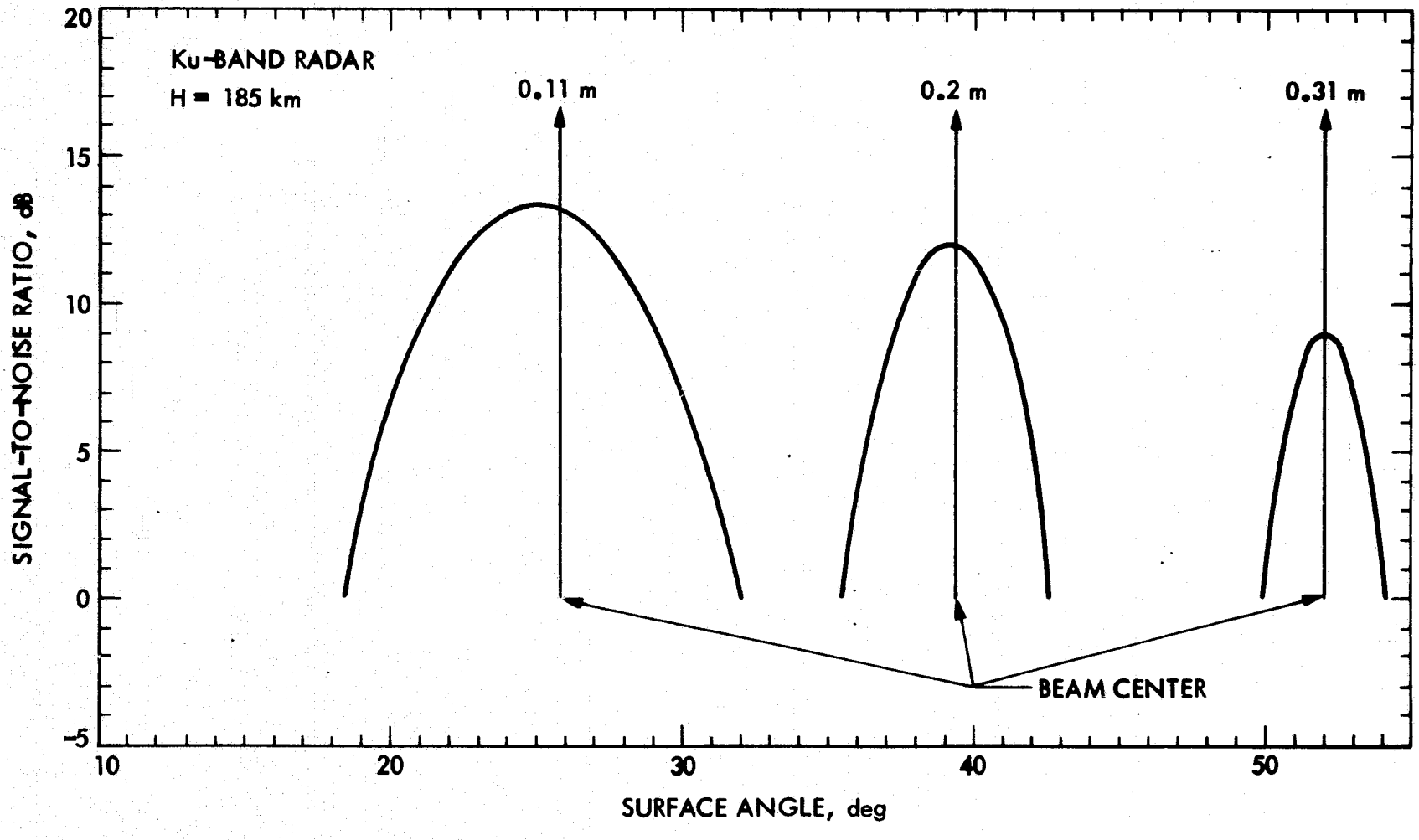

Figure A-1. Ku-Band Radar Signal-to-Noise Ratio

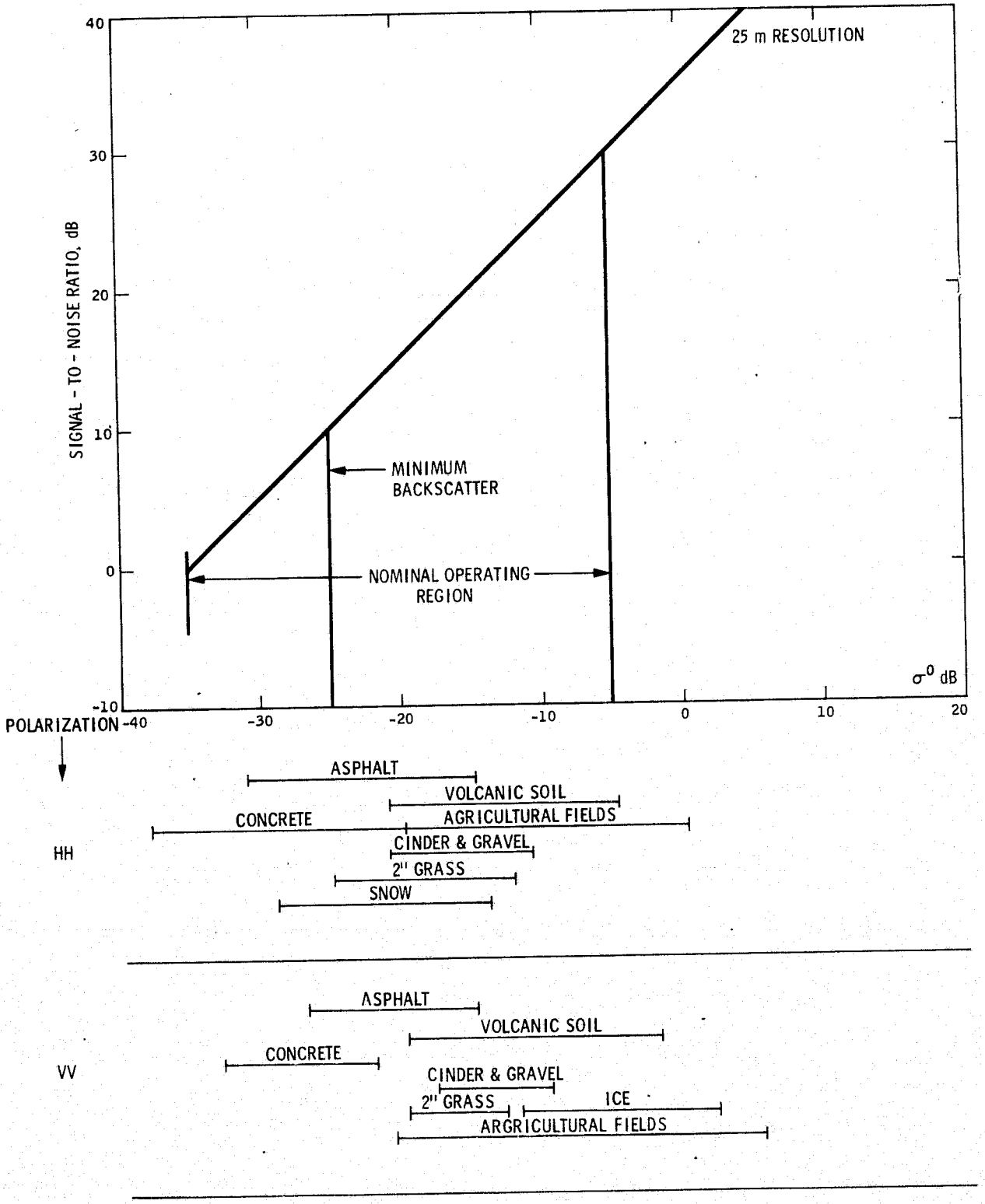

Figure A-2. Ku-Band Radar Final S/N Ratio

APPENDIX B

BALL BROTHERS RESEARCH CORPORATION
ANTENNA STUDY RESULTS

B1.0 SUMMARY

A study is described in which the feasibility of a dual polarization, dual frequency, microstrip antenna for the synthetic aperture radar on Shuttle is demonstrated. Subarrays were designed and fabricated at L-Band and X-Band; both had efficiencies of 95%. For the full arrays the efficiencies can be projected to 80% at L-Band and 60% at X-Band. A dual feed network was developed at L-Band to obtian the required dual polarization. Three different materials were studied for the X-Band array, and a maximum substrate thickness of 1/8 inch was established. Detailed projections for all significant array specifications are included.

B2.0 INTRODUCTION

Specifically, Ball Brothers Research Corporation was required to conduct a study which would lead to the development of a dual polarization, dual frequency microstrip array antenna for the Shuttle Imaging Radar system. Such an array would be unfolded from a pallet on the Shuttle. BBRC was to demonstrate the efficiency of L and X-Band microstrip arrays by designing, fabricating and testing subsections of the arrays so that the total antenna performance can be projected with confidence. Array subsections should show an efficiency of 95% at L-Band and 90% at X-Band. A typical 1.2 meter square panel should weigh less than 5 pounds.

It was understood that the dual frequency operation was to be achieved by using separate apertures for L and X-Bands. Furthermore the dual polarization of the X-Band array was to be accomplished using dual apertures for vertical and horizontal polarizations. This is made necessary by the limited space for the feed network on the X-Band panels.

However, at L-Band these two polarizations must be combined in a single aperture.

B3.0 MAJOR STUDY RESULTS

Each of the following items begins with a restatement of a task specified in the statement of work. This is followed by a description of the actual work and the results.

1. Apply results of high efficiency L-Band array development to the L-Band shuttle array design. Establish potential gain and efficiency.

   This Task was combined with the development of the dual-polarization feed in Task 2, since the feed technique influenced the ultimate efficiency. Six different configurations were designed, fabricated, and tested. Figure B1.1 shows one of these configurations, a two by four array. It has a maximum theoretical gain of 18.7 dB and a measured gain of 18.5 dB, resulting in a 95% efficiency. The array was dual polarized but did not work equally well in both polarizations. A more symmetrical array provided good efficiency in both polarizations, this array is shown in Figure B1.2. The theoretical gain of this array is 21.3 dB, and the measured gain is 21.1 dB in both polarizations. The resulting efficiency is 95%. These results show that the element proportions and spacing necessary for the dual polarized design do not compromise the high efficiency of the array. The potential gain of the L-Band subarray panels is 0.95 times the maximum theoretical gain for the subarray on its aperture dimensions.

2. Study at least two different techniques for incorporating a dual polarized feed system into the high efficiency L-Band array. Select most promising technique(s).

   Both corporate and series feed networks were considered. The corporate feed design, of which Figure B1.3 is typical, suffers from lack of space for the feedlines. Possibly these feedlines could be located on a separate substrate, but to keep the design simple, series feeds were favored in this study. Figures B1.1 and B1.2 show two of the series feeds that were actually fabricated and tested. The more symmetrical configuration in Figure B-1.3 had the better performance and is recommended as the most promising approach. The patterns for this array, Figures B1.4 and B1.5, shown that the aperture is fairly well controlled, although the side lobe structure suggests the need for some further improvement. The measured cross-polarized component for the array was

Figure B-1.1. L-Band Array Efficiency Better Than 95%

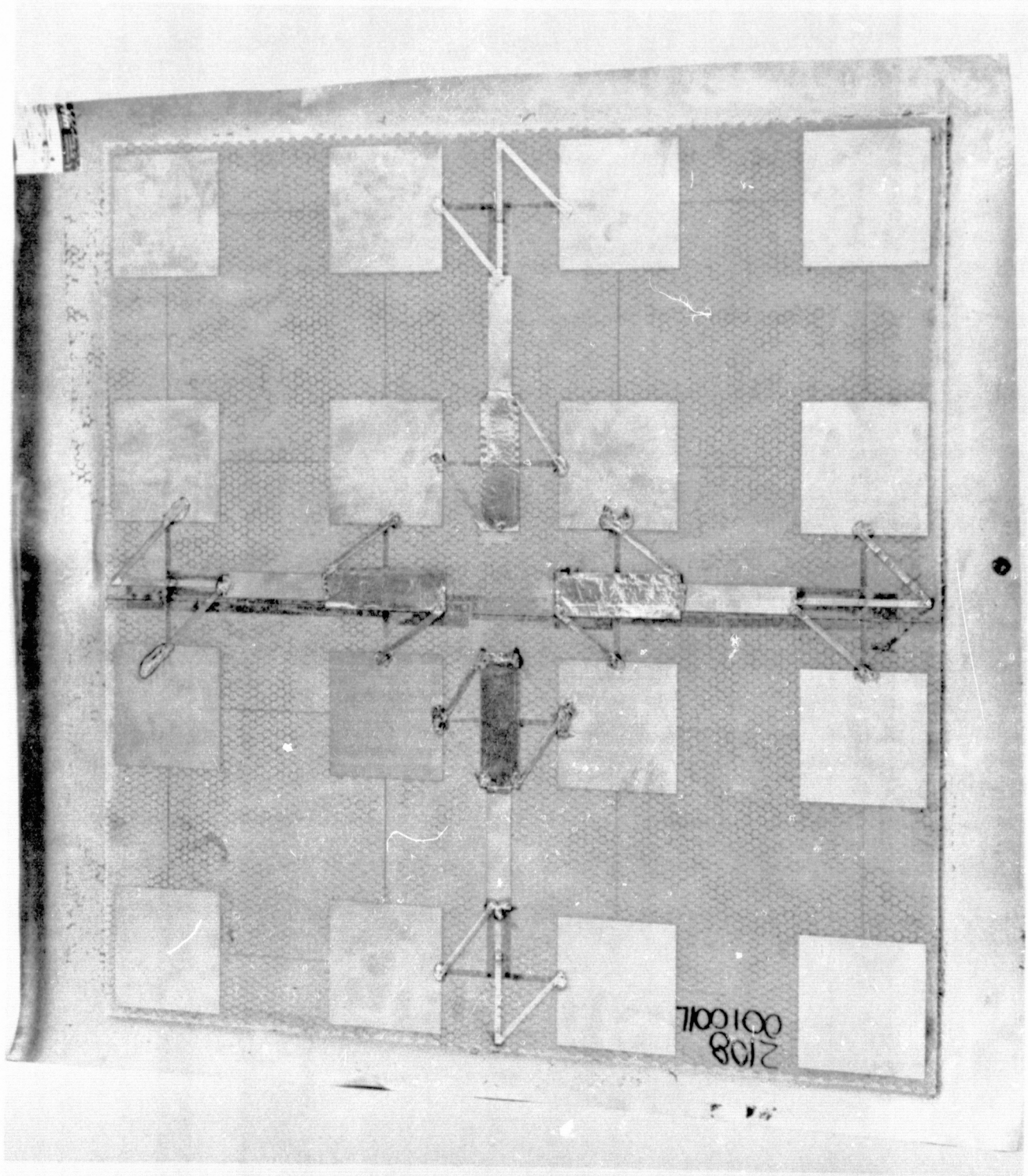

Figure B-1.2. Four Element by Four Element L-Band Array with 95% Efficiency

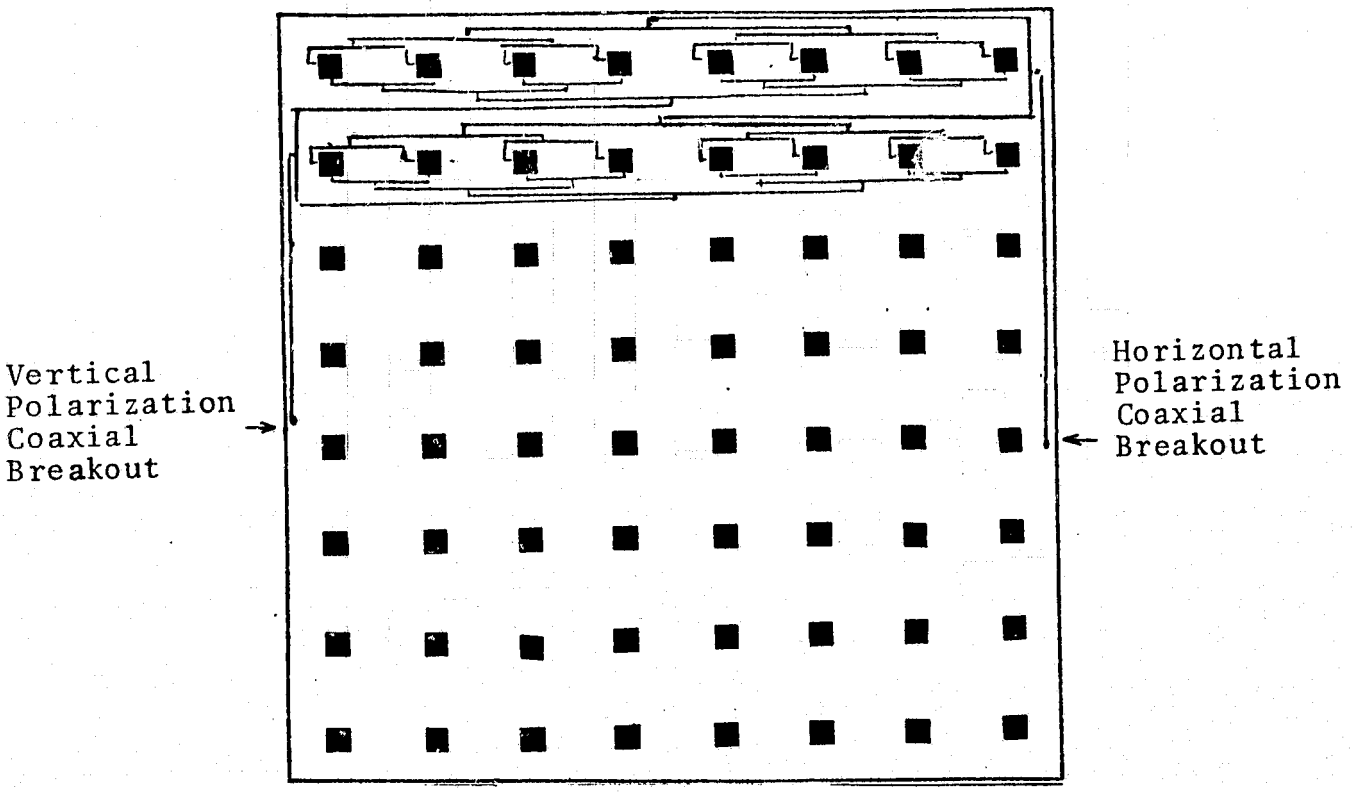

Figure B-13. Dual Polarization Layout with Corporate Feed

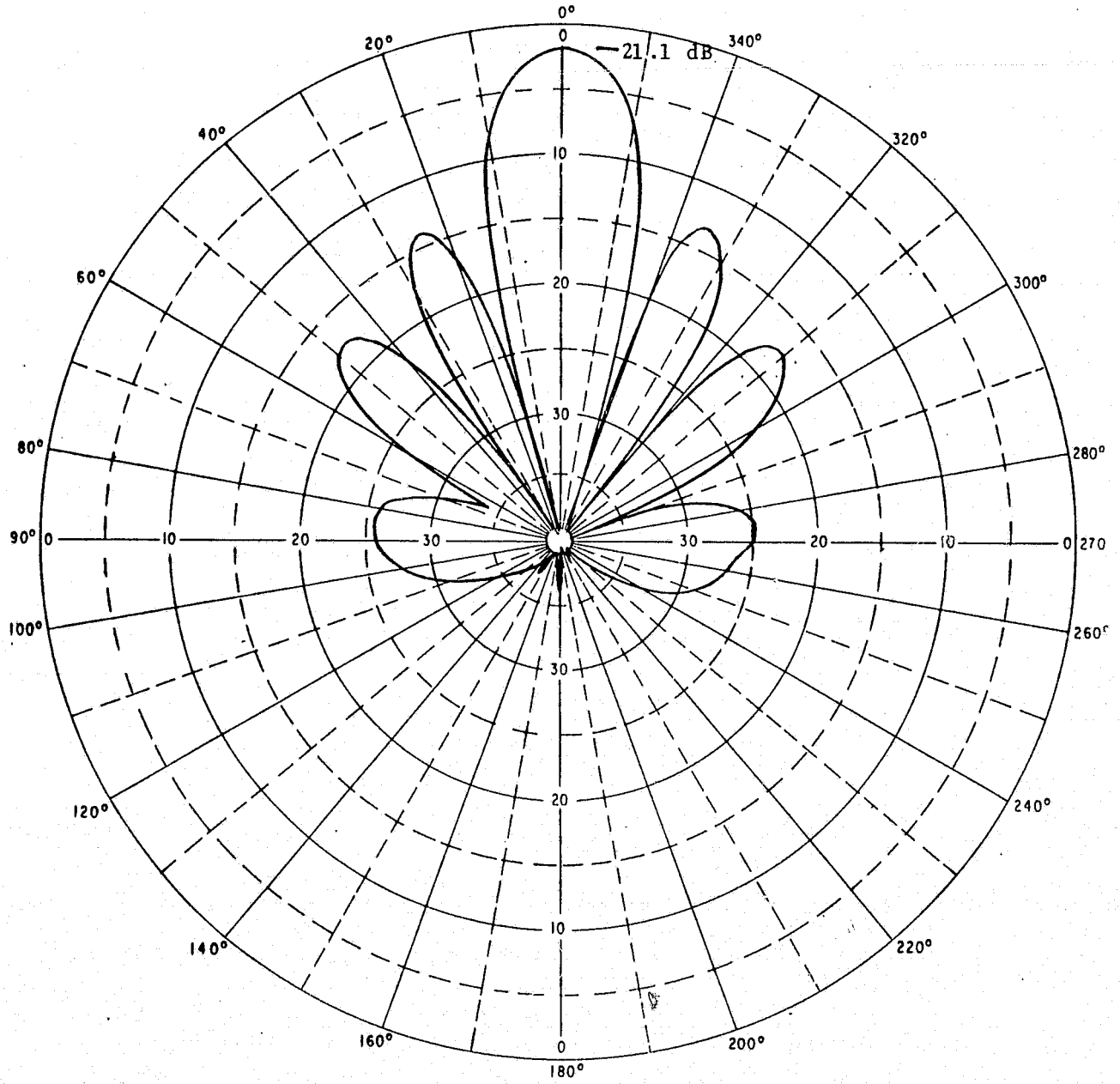

Figure B-1.4. H-Plane Pattern of 4 x 4 L-Band Array

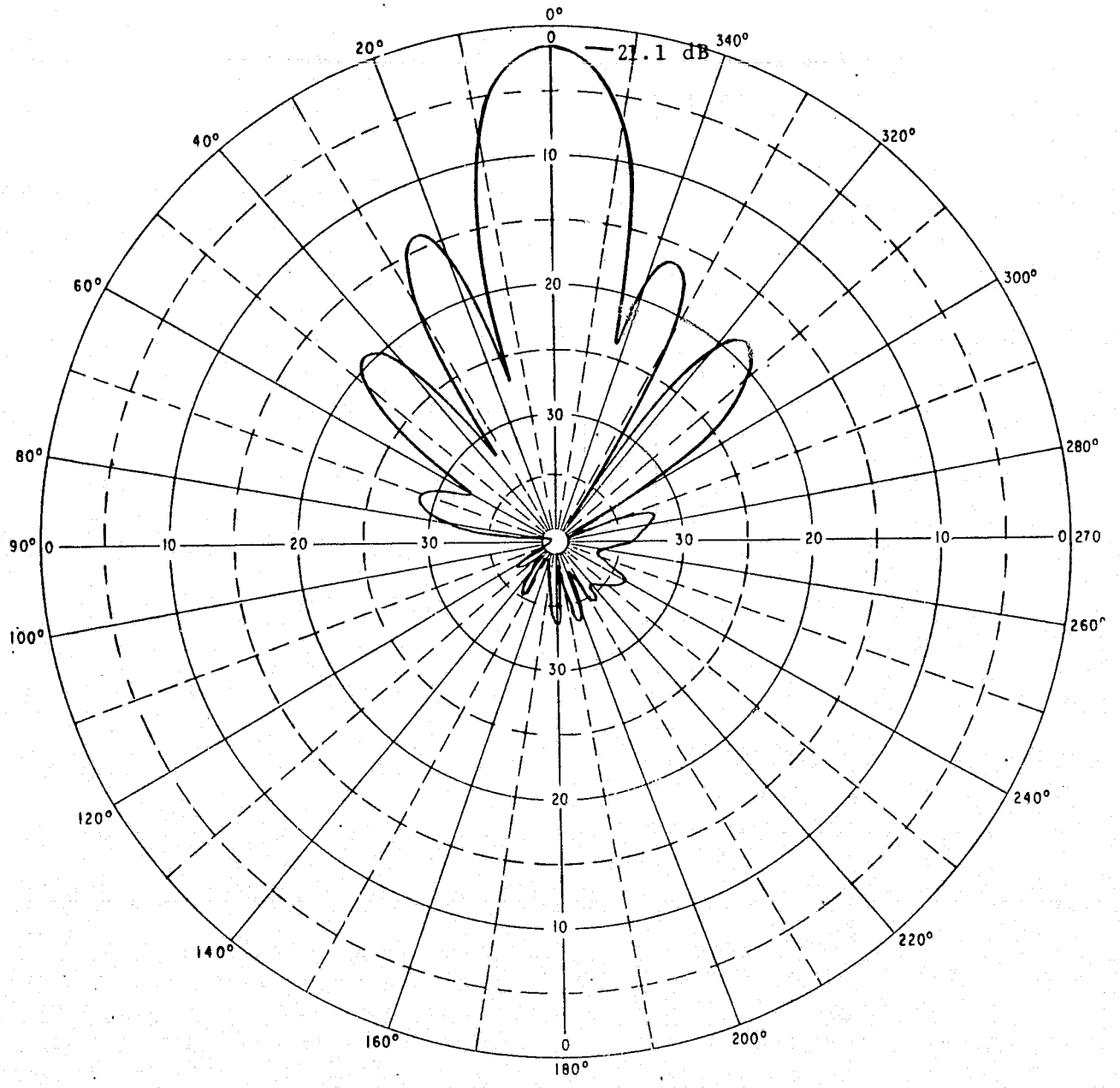

Figure B-1.5. E-Plane Pattern of 4 x 4 L-Band Array

-16 dB; further refinement should reduce this to -20 dB. Since the array is a resonant series structure, it cannot be made much larger. Panels would have to be connected together in a corporate coaxial feed on the back of the array as shown in Figure B1.6.

3. Build a section of the L-Band array to demonstrate the feasibility of the dual polarized feed system.

   The array in Figure B1.2 is the feasibility model for the dual polarized feed system. Its performance is described above.

4. Project performance of the full L-Band array based on performance of sub-array.

   As a result of the work completed on the subarray, the performance of the full L-Band array can be summarized below:

Theoretical Gain Full L-Band Aperture at 1.3 GHz			37.94 dB
Losses in Subarray		0.2 dB	
Coax Losses		0.45 dB	
Panel Interconnect Losses		0.05 dB	
Mismatch Losses		0.14 dB	
Phase Errors Losses		0.1 dB	
Total Losses		0.94 dB	0.94 dB
Net Gain			37.0 dB
Efficiency	81%		
Full Aperture Beamwidth	1° x 5.4°		
Sidelobes	-12.5 dB or as required		
Peak Power	6 kW (not demonstrated)		
Pointing Accuracy	±0.5° (not demonstrated)		
Bandwidth	35 MHz under 1.3:1 50 MHz under 1.5:1		
Cross-Polarization	-20 dB (not demonstrated)		

5. Select material with minimum loss tangent for X-Band Array.

   Three materials were considered: honeycomb, foam and cross-linked styrene. The loss tangent of the latter is known to be 0.0005

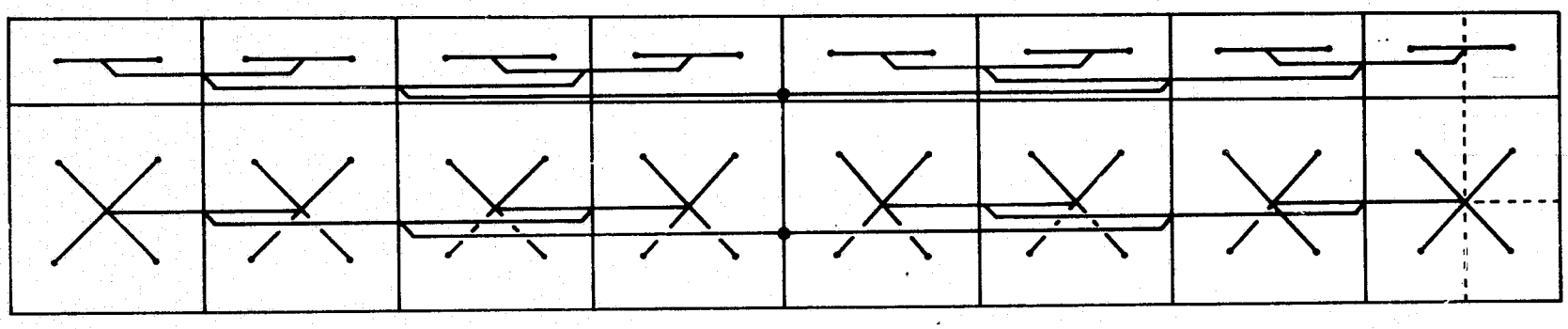

NOTE: COAXIAL LAYOUT SHOWN FOR ONE POLARIZATION. THE LAYOUT FOR THE OTHER POLARIZATION WOULD LIE VIRTUALLY ON TOP OF THE LAYOUT SHOWN

Figure B-1.6. Coaxial Corporate Feed Network for L-Band Array

(one third the loss tangent of teflon fiberglass). The effective loss tangents for the other two were unknown, and therefore much of the X-Band work was aimed at determining the usefulness of the honeycomb, and foam in an X-Band array. Quarter inch honeycomb was used on a 16 element array which had a 95% efficiency. However, 1/4 inch proved to be too thick for larger arrays having multiple transmission line bends. Eighth inch honeycomb still needs to be investigated. Eighth inch foam showed promise as an array substrate but was too heavily loaded with epoxy during fabrication and the resulting array efficiency was only 50% for a 128 element array. This array should be fabricated again using much less epoxy. The best hollow core material should then be compared with a low loss solid material such as the crosslinked styrene.

6. Determine maximum allowable thickness for X-Band array substrate.

Although some work done on 1/4 inch honeycomb showed promise, the success was limited to linear arrays as in Figure B1.7. The use of more complex transmission line circuits in a planar array caused unwanted coupling and excessive line radiation. Eighth inch subtrates were found to be controllable provided that sufficient care is given to the avoidance of coupling problems. Therefore 1/8 inch is the recommended maximum allowable thickness.

7. Design, fabricate and test 24 in. x 24 in. all microstrip X-Band array.

The first step in the development of the microstrip X-Band array was designing a 16 element linear array. Sixteen linear arrays could then be arrayed to form the square array. The linear array is shown in Figure B1.7. The radiation pattern for this array, Figure B1.8, shows a peak gain of 19.9 dB. When this is compared to the maximum theoretical 21.1 dB gain, the efficiency is found to be 95%. The linear design is a resonant series fed array on 1/4 inch honeycomb. The 1/4 inch thickness did not permit good control of the aperture distribution, and resulting errors are reflected in the side lobe structure of the array. The errors could not be entirely eliminated and would have been worse for the more complex feed network of a planar array.

EFFICIENCY EXCEEDS 95% FOR X-BAND ARRAY

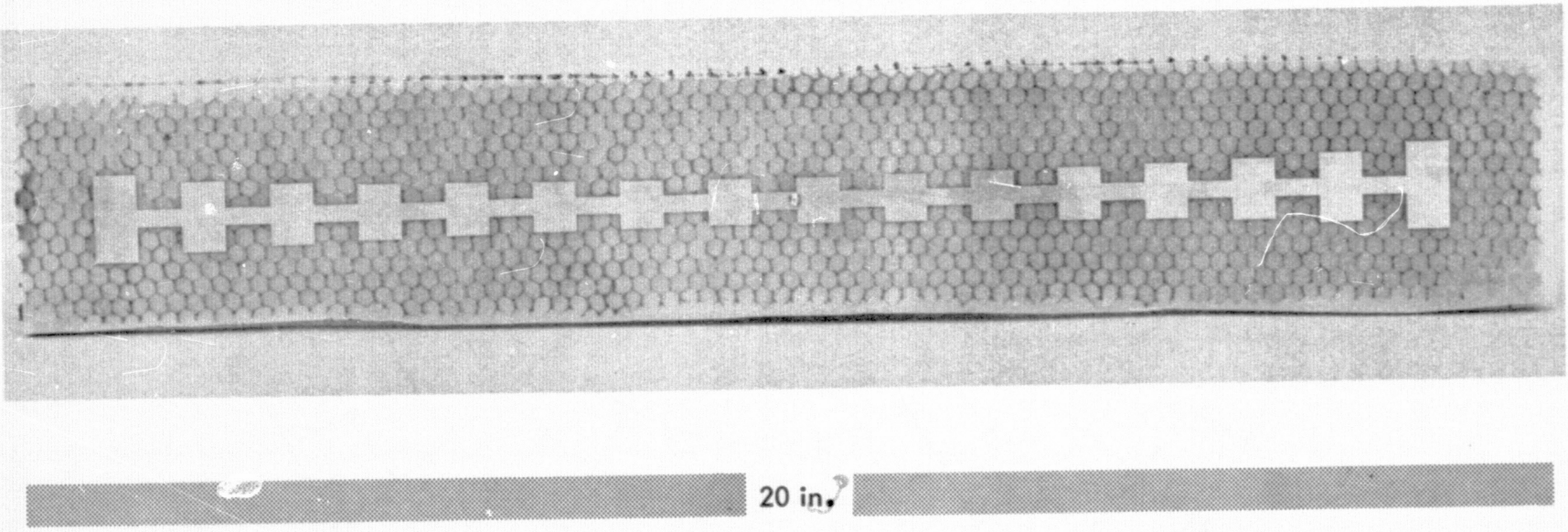

Figure B-1.7. X-Band Linear Array

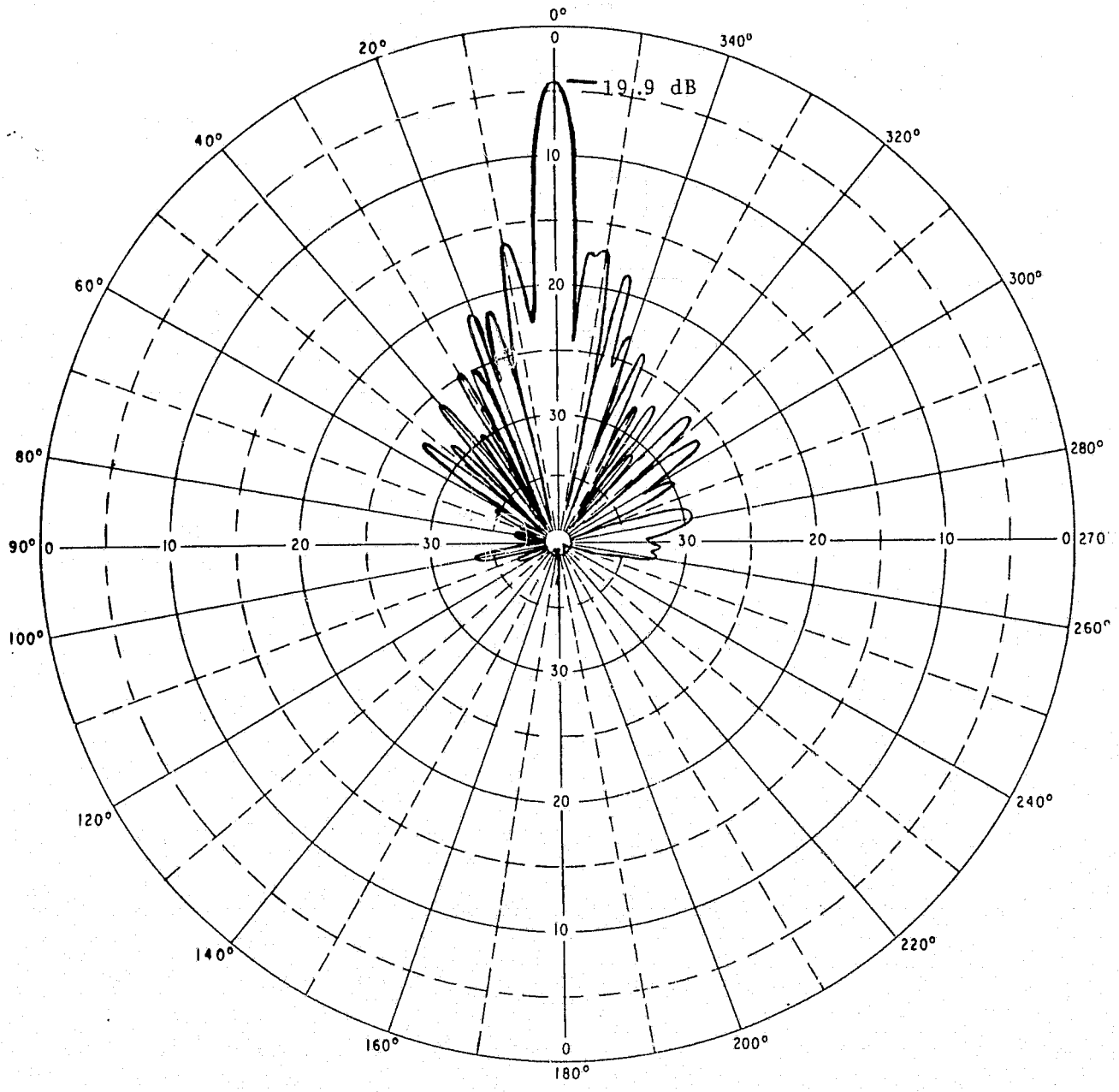

Figure B-1.8. E-Plane Pattern for Linear X-Band Array

It was, thus, decided to reduce the thickness to 1/8 inch and to get better control of the aperture by using a corporate feed network. The corporate network is not too crowded here because any one aperture has only one polarization. Figure B1.9 shows the planar array that developed from these deisgn changes. The H-plane pattern shown in Figure B1.10 indicates good aperture control. Feed errors in the E-plane resulted in a less satisfactory pattern, Figure B.1.11, but this can be corrected. The foam substrate was too heavily loaded with epoxy which lowered the gain to 26.4 dB, equivalent to a 50% efficiency.

9. Project performance of the full X-Band array based on performance of sub-array.

Although the X-Band array was not completely optimized, enough data was gathered to project an efficiency of 90% for planar sub-array. Other projections that can be derived are listed below:

Theoretical Gain of Full X-Band Aperture			46.2 dB
Losses in Sub-Array (90% efficiency)		0.5 dB	
Waveguide Losses		1.0 dB	
Panel Interconnect Losses		0.2 dB	
Mismatch Losses		0.2 dB	
Phase Error Losses		0.3 dB	
Total Losses		2.2 dB	
Net Gain			44.0 dB
Efficiency	60%		
Full Aperture Beamwidth	0.15° x 5.1°		
Sidelobes	-12.5 dB or as required		
Peak Power	20 kW (not demonstrated)		
Pointing Accuracy	±0.5° (not demonstrated)		
Bandwidth	35 MHz under 1.1:1		
Cross Polarization	-20 dB		

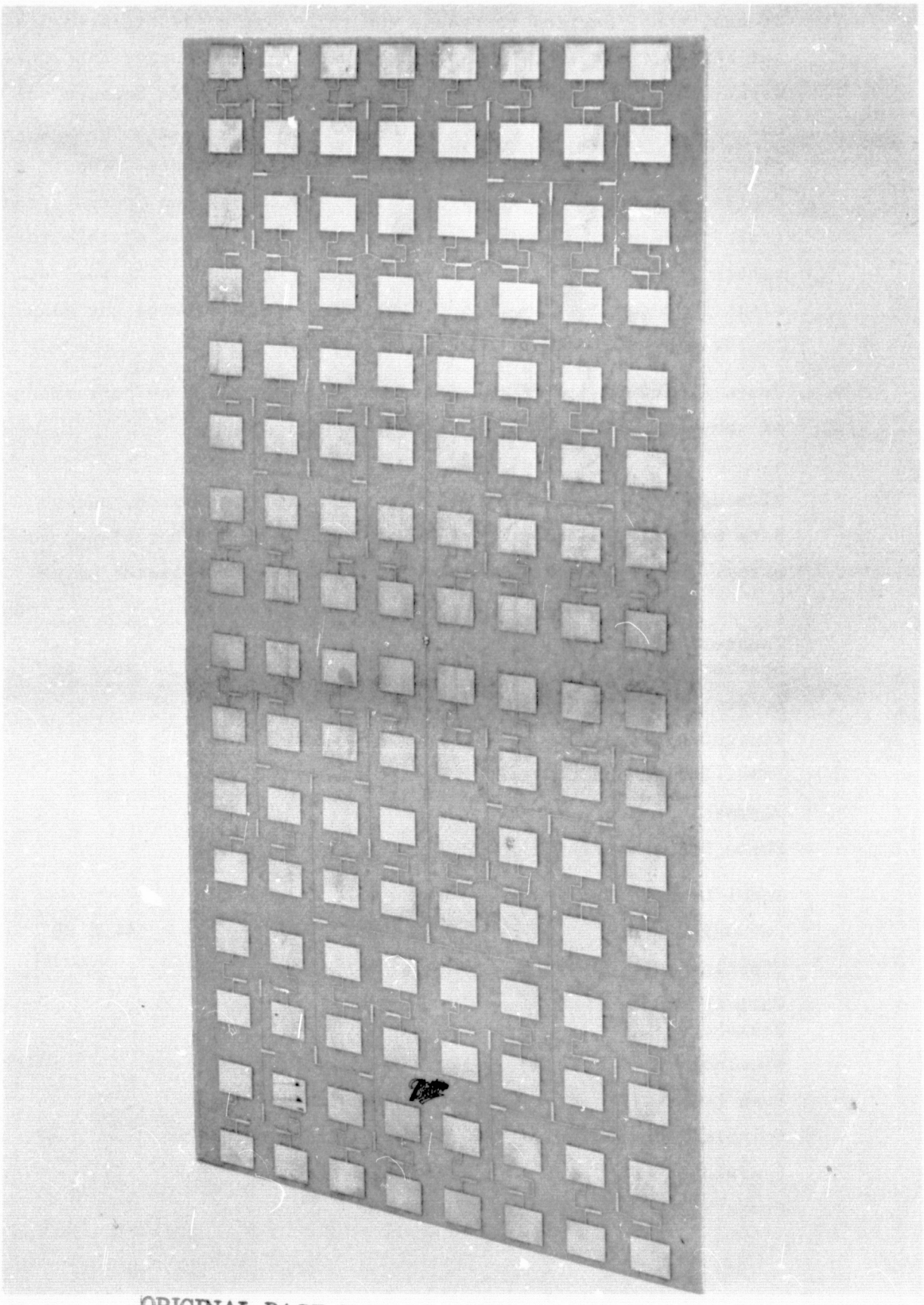

Figure B-1.9. X-Band Planar Array

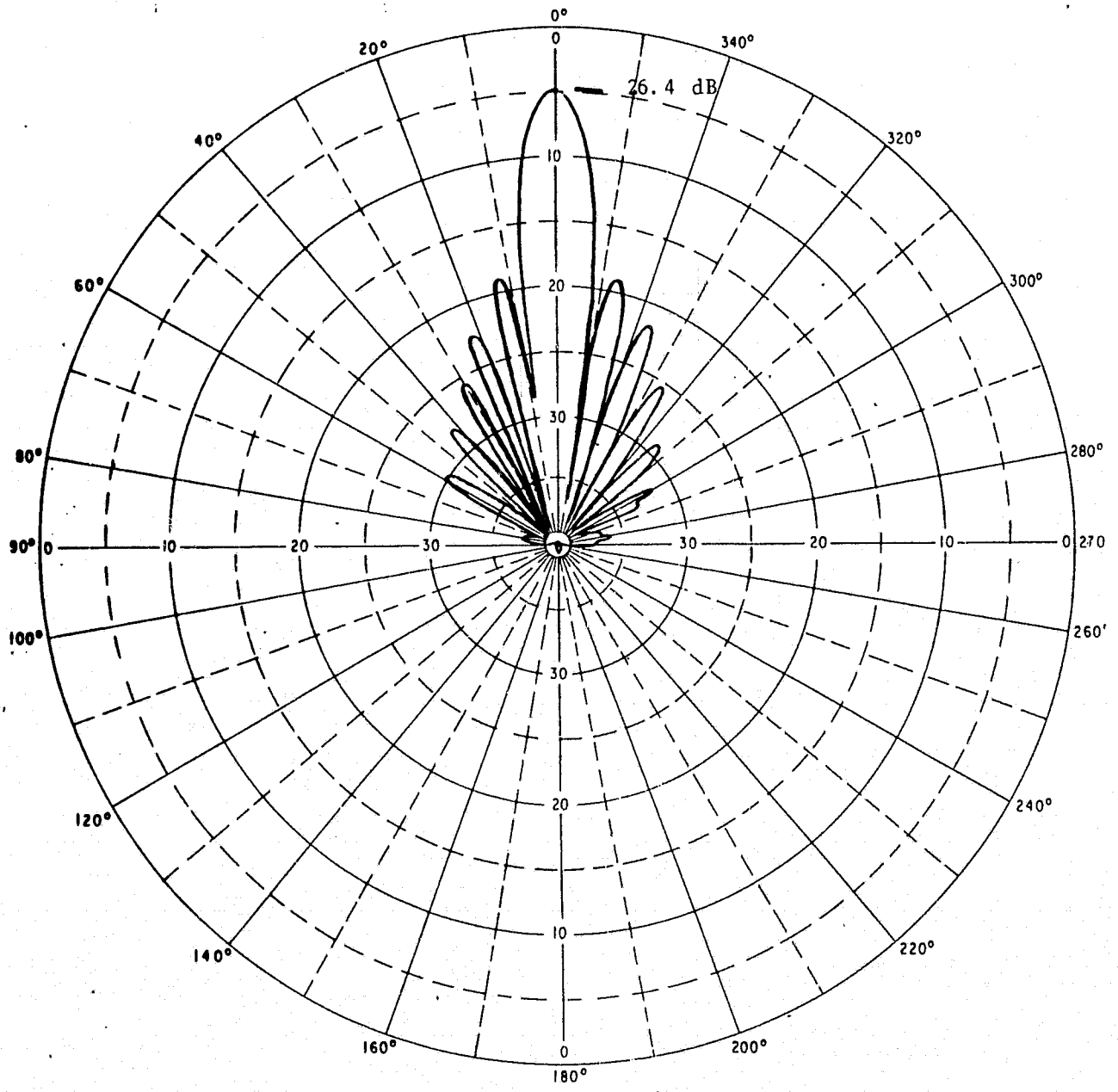

Figure B-1.10. H-Plane Pattern for Planar X-Band Array

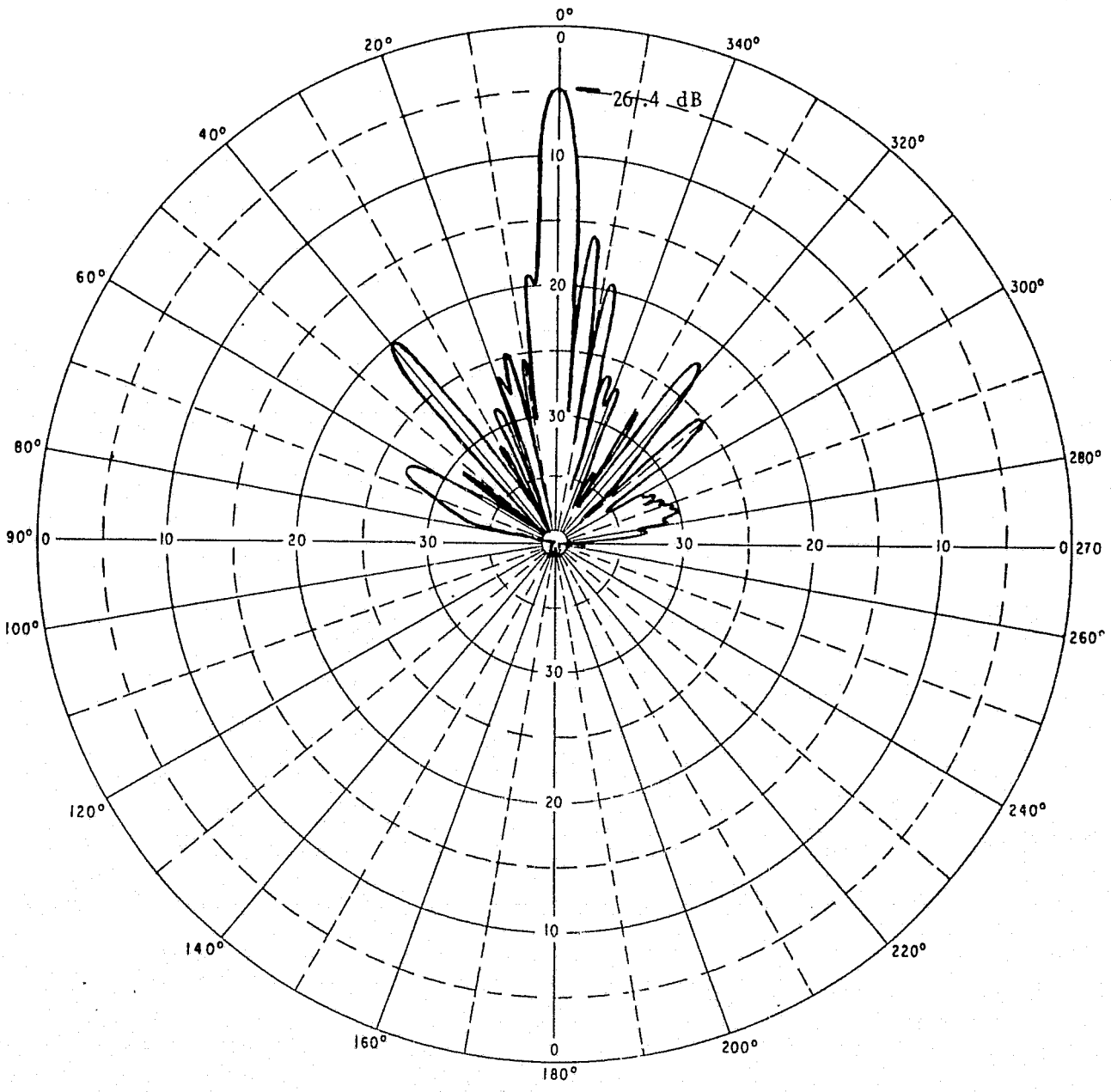

Figure B-1.11. E-Plane Pattern for Planar X-Band Array

B4.0 CONCLUSIONS

A dual polarization, microstrip, L-Band array with 95% efficiency has been designed, fabricated, and tested. Based on this test array a full 1.5m x 12m array can be expected to have 80% efficiency. Similarly a microstrip, linear, X-Band array has demonstrated 95% efficiency. This can reasonably be projected to 90% for a 256-element planar array, but was not proven in this study. Based on the available data, the full 0.36m x 12m array can be expected to have 60% efficiency. Some optimization of the X-Band work is still required, and in addition, a detailed analysis of the power handling problem should be considered.

APPENDIX C

ENVIRONMENT OF RESEARCH INSTITUTE OF MICHIGAN, STUDY OF AN OPTICAL PROCESSING SYSTEM

ERIM
FORMERLY WILLOW RUN LABORATORIES, THE UNIVERSITY OF MICHIGAN

STUDY OF AN OPTICAL PROCESSING SYSTEM FOR THE EARTH RESOURCES SHUTTLE IMAGING RADAR

114000-1-F

Prepared for the
Jet Propulsion Laboratory
4800 Oak Grove Drive
Pasadena, California 91103

Contract 954209
(Subcontract under NASA Contract NAS 7-100)
(Task Order No. RD-164)

July 1975

Radar and Optics Division
Environmental Research Institute of Michigan
P. O. Box 618
Ann Arbor, Michigan 48107

C. 3

CONTENTS

1
INTRODUCTION

The NASA earth resources satellite and shuttle program planned for flights in the 1980's will provide a space-borne experimentation and observation system. This satellite system will carry several sensors, including an image-forming radar designed to map large swaths of the earth's surface under all-weather conditions. In order to provide, from orbital altitudes, the resolving capability required for this task, special radar configurations and data processing techniques must be employed.. Radar systems having these properties are known, within the technical community, as Synthetic Aperture Radars (SAR's). This type of radar has undergone extensive development during the past twenty years under Department of Defense sponsorship.

An investigation of the optical system requirements for the Earth Resources Shuttle Imaging Radar (ERSIR) was carried out at ERIM. This document is a final report of that study. The purpose of the study was to determine the design parameters and feasibility of an on-board optical recorder and the associated ground-based processor. This study was based upon ERSIR design parameters supplied by JPL engineers. In addition, special problem areas such as range walk were examined and possible solutions were indicated along with recommendations for required developments in the recording and processing system for efficient data processing.

The purpose of this report is to outline a program of sound cost effectiveness for preparation of a SAR data processing facility dedicated to the NASA shuttle-satellite program. Data processing can be accomplished with available state-of-the-art optical data processing technology applied specifically to the

shuttle SAR image gathering task. Equipment used will be comprised of an optical recorder located on-board the spacecraft for recording of the SAR video signals and a ground-based data processing facility. The recorder will be designed and fabricated for this mission. Two specific development plans warrant consideration for the ground-based data processing facility. First, with some modification, a present ERIM processing facility can be dedicated to this task. Alternatively, a new facility can be built for this purpose.

ERIM involvement in the development effort would be comprised of the following:

1. Finalization of the data processing system requirements and preparation of system and sub-system design specifications. This system includes the optical recorder and the ground-based optical processing facility with image display and image tape storage provisions.

2. System and sub-system fabrication and test.

3. Participation in SAR flight experiments in support of the NASA program objectives for the SAR sensor evaluation and image analysis. This effort will be directed toward data obtained from the space-borne SAR. It can also include, however, SAR flight experiments using an ERIM aircraft equipped with its high quality multichannel SAR system which would serve to aid in definition of a sound SAR design for space-borne use.

4. SAR data processing and image data preparation services to be provided if ERIM based facilities are utilized.

ERIM's proposed program rests on the following major considerations:

1. ERIM's data processing facilities, which are unique in the nation, could be made available to the SAR-Shuttle program without additional capital investment.
2. ERIM's large store of experience can be applied to design problems to assure a comprehensive approach to system design, parameter selection analysis and data processing.
3. ERIM's multi-channel SAR system which can generate high quality data can be used to simulate the shuttle SAR at low cost.

In addition to these considerations, a formal involvement by ERIM in the program would allow an easy transfer of technology and results from on-going DoD sponsored programs in which ERIM has been heavily involved.

2
DATA PROCESSING SYSTEM

Design considerations for a coherent optical processing system to be used for generating terrain imagery from synthetic aperture radar data gathered with a satellite-borne SAR are discussed in this section. The radar sensor design parameters used as an input for data processing considerations discussed here were provided by the radar system designers from the Jet Propulsion Laboratory.

The optical processing system will be comprised generally of the following: 1) Data Recorder for conversion of radar video signals to a two-dimensional (spatial) recording on photographic film. This film is used as the input to the data processor. A line scan recorder which scans across the film width as the film is transported past the writing beam would be used. Both laser and CRT recorders have been developed for this type of use. 2) Data Processor which serves to convert the recorded input radar video data to the output may by appropriate optical processing. It will consist of an input film (with its transport) on which the imagery is recorded for later viewing and analysis. Currently available processor designs may be adaptable to meet the subject data processing requirements. 3) Map Display and Storage which allows the user to view and manipulate map data provided from the optical processor. Two configurations for the display will be used. First the map imagery (obtained at the processor output) is recorded on film which can be viewed directly and copied as photographic prints. This approach can be implemented for very large dynamic ranges using holographic recording principles. Second, the map imagery will be converted into an electronic signal which is digitized and recorded on magnetic tapes for

later TV display or computer analysis. Both of these approaches have been developed at ERIM. 4) Interface Converter which takes the normally available radar receiver signal and converts it to a signal suitable for optical recording and processing.

In this section, pertinent radar signal properties and the radar sensor geometry are reviewed and the data processing system is discussed. Specific choices for radar and mapping geometry parameters were made by the JPL and served as a basis for definition of a data processing system by ERIM.

2.1 RADAR DATA

The radar signal transmitted by the SAR is a sequence of pulses s_{on} with repetition period T, pulse length T_r, carrier frequency ω_c and frequency or phase modulation defined by a phase function $\theta(t)$. This signal may be written as

$$s_{on}(t) = a_o(t - nT)\cos[\omega_c(t - nT) + \theta(t - nT)]$$

The received signal from a point target at the vector range $\bar{r}$ and at angles α and β relative to the radar boresight, as in Figs. 1 and 2, experiences path transmission attenuation and reflection represented together by a factor $\tilde{\sigma}$, antenna two way gain denoted as $g(\alpha,\beta)$, and transmission path delay $2r/c$; giving a received signal s_{in} of the form

$$s_{in}(t,r) = \tilde{\sigma}\, a_o(t - nT - \frac{2r}{c})g(\alpha,\beta)\cos[\omega_c(t - nT - \frac{2r}{c}) + \theta(t - nT - \frac{2r}{c})]$$

At a point in the receiver we have the signal S_n which is essentially the same as s_{in} except for amplification and that it has been shifted from its original carrier ω_c to a lower frequency denoted ω_o. For convenience we will let $t - nT \equiv t'$ and write s_n as

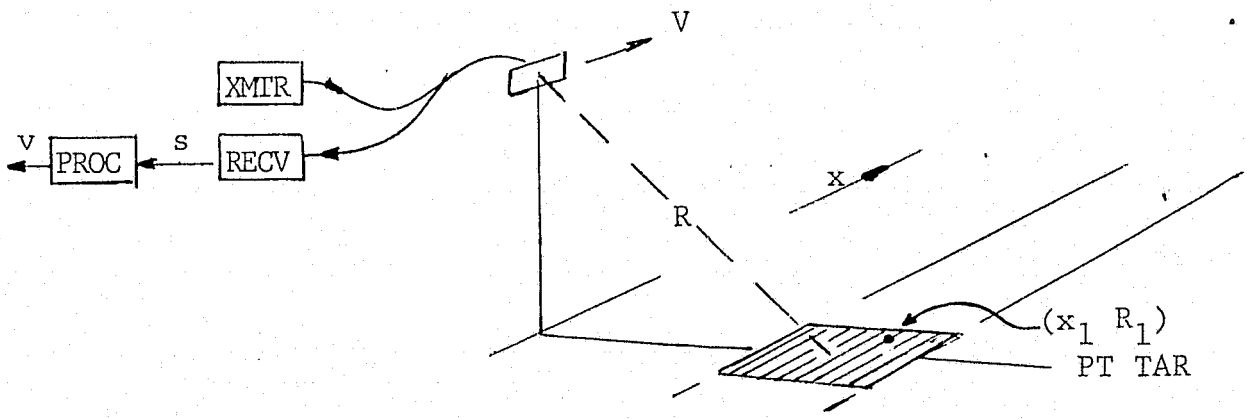

Figure 1. Side-Looking SAR

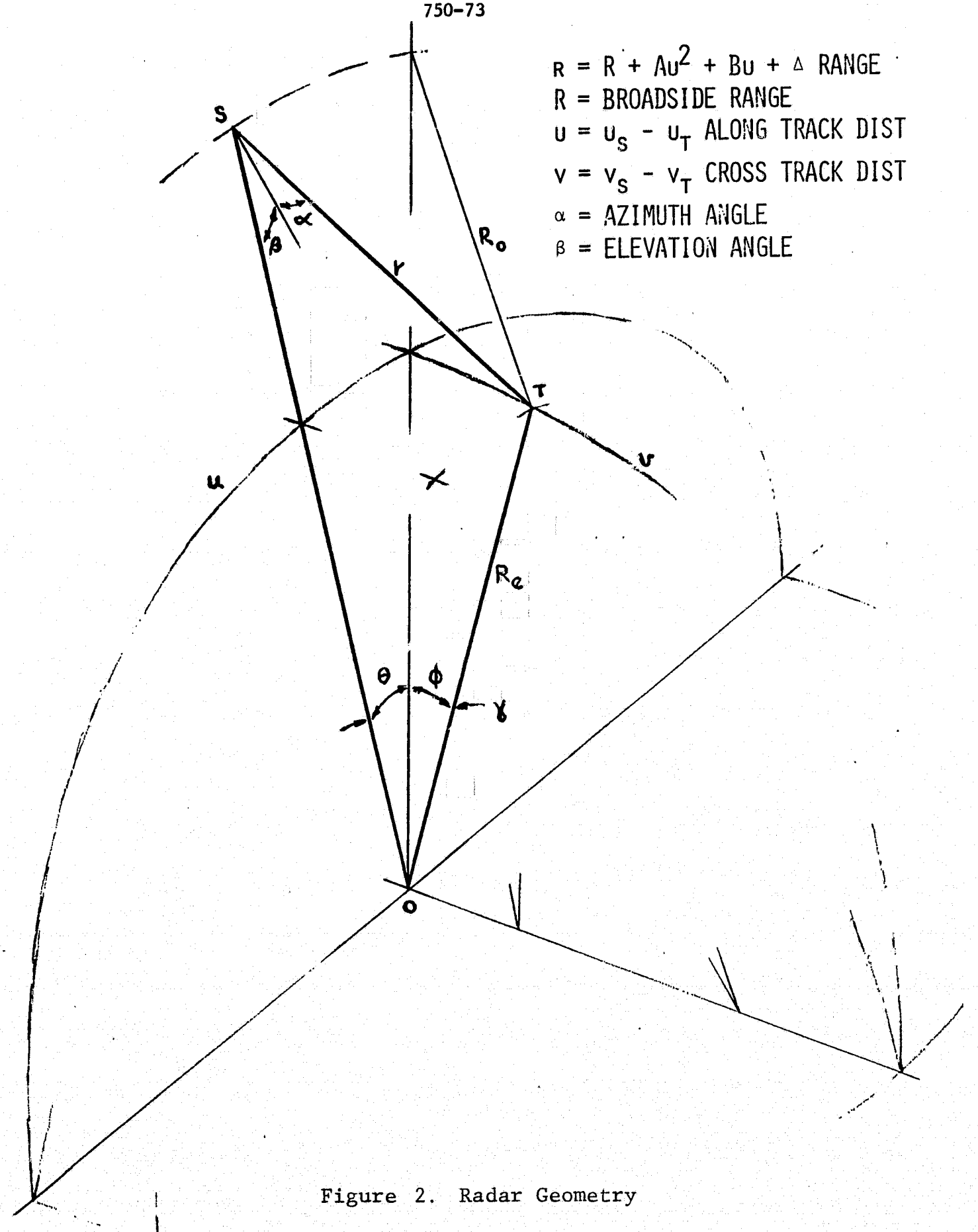

Figure 2. Radar Geometry

$$s_n(t,r) = \tilde{\sigma}\, a(t,r)g(\alpha,\beta)\cos\,\phi(t',r)$$

where

$$\phi(t',r) = \omega_o t' - \frac{2r}{\lambda} + \theta(t' - \frac{2r}{c})$$

$$a(t',r) = a(t' - \frac{2r}{c})$$

$$t' = t - nT$$

This expression retains the dispersed (uncompressed) range data represented by the original pulse envelope $a(t',r)$ and the frequency (or phase coding) θ. If pulse (range) compression were accomplished electronically in the receiver our expression for s_n would change simply by substituting a compressed pulse envelope expression for $a(t',r)$ and letting $\theta = 0$ except for some phase.

The signal s_n is recorded on film and processed in the optical processor to generate map imagery. For digital electronic processing s_n may be converted into its I and Q components, digitized and recorded on magnetic tapes and then processed with an electronic digital processor. For digital processing the offset frequency would usually not be required during data processing.

The expected values for radar parameters are summarized in Table 1. These data were provided by the radar system designers.

TABLE I
BASELINE PARAMETERS

SLANT RANGE INTERVAL

$\Delta R \leq 50$ KM	S-R INCREMENT
$\Delta t \simeq 320$ μsec	T INCREMENT
$\Delta t \cdot B_r \simeq 5800$	TIME · BANDWIDTH

SLANT RANGE

$\rho_r = 8.6$ m	RESOLUTION
$\bar{\rho}_r = \rho_r, 2\rho_r, 4\rho_r$	RESOLUTION (MI)
$B_r = 17.38$ MHz	BANDWIDTH
$f_o = B_r/2$	OFFSET FREQUENCY
$T_r = 23$ μsec (21 μsec)	PULSE LENGTH
$F = 1570$ to 1900	PRF

AZIMUTH

$\rho_a = 6.3$ m	RESOLUTION
$\bar{\rho}_a = 4\rho_a, 8\rho_a$	RESOLUTION (MI)
$B_a = 1200$ Hz	BANDWIDTH
$T_a \simeq .8$ sec $(\simeq .15$ sec$)_x$	APERTURE
$\Delta\alpha = 1.1^o(.172^o)_x$	BEAMWIDTH

EXPECTED GEOMETRY

$H = 185,278,370$ KM	ALTITUDE
$S = 40 - 100$ KM	GROUND SWATH
$\beta_o = 25^o, 38^o, 50^o$	ELEVATION

TABLE I
BASELINE PARAMETERS
(continued)

RANGE

$$r = R + Au^2 + Bu + \Delta$$

$$A = \left[\frac{(R_e + h_s)R_e}{R_e^2}\right] \cdot \frac{1}{2R}$$

$$B = \left[\frac{(R_e + h_s)R_e}{R_e^2}\right] 2v_o \tan\Omega \quad \frac{1}{2R}$$

$$\tan\Omega = \frac{V_v}{V_u}$$

$$\Delta \leq 5 \times 10^{-3} \text{ M}$$

$$Au^2 \leq 32 \text{ M}$$

$$Bu \leq 360 \text{ M } (3.5^o \text{ tilt max})$$

DATA RECORDING

4 channels (λ_1, λ_2, P_1, P_2)

900 sec/pass x 6 passes

18 MHz BW/channel

Selectable PRF/pass

2.1.1 SIGNAL PROPERTIES RELATED TO PROCESSING

The salient properties of the radar signal at the receiver output, as they relate to processing required to obtain imagery, can best be recognized after reformulation of the expression for s_n into two factors which will be dependent on slant range and along track distance. In complex notation, the receiver output for the return from a point target is

$$s_n(t',r) = \tilde{\sigma}\, a(t' - \frac{2r}{c}) g(\alpha) g(\beta) \exp -j \left[-\frac{2r}{\lambda} + \omega_o t' + \theta(t' - \frac{2r}{c}) \right]$$

where the antenna two way amplitude gain g is shown factored according to azimuth (α) and elevation or slant range (β) directions. We will factor $s_n(t',r)$ into range and azimuth terms s_r and s_a as follows

$$s_n(t',r) = s_r(t',r) \cdot s_a(r)$$

These range and azimuth terms are; for range,

$$s_r = a_r \exp -j \left[\theta_r \right]$$

with

$$a_r = \tilde{\sigma}\, a(t' - \frac{2r}{c}) g(\beta)$$

$$\theta_r = \omega_o t' + \theta(t' - \frac{2r}{c})$$

and for azimuth

$$s_a = a_a \exp -j \left[\theta_a \right]$$

with

$$a_a = g(\alpha) = g\left(\frac{u}{R}\right)$$

$$\theta_a = -\frac{2r}{\lambda}$$

Typically we have a range envelope a_r much shorter than the azimuth envelope a_a, and range frequencies $\frac{d\theta}{dt}$ much greater than azimuth frequencies $\frac{d\theta_a}{dt}$.

As discussed in Section 2.2 on system geometry, the instantaneous range r (for a spherical earth) that appears in the radar signal s_n can be expressed as

$$r = R + Au^2 + Bu + \Delta$$

with

$$A \simeq \frac{(R_e + h_s)(R_e + h_t)}{R_e^2} \frac{1}{2R}$$

$$B \simeq \frac{(R_e + h_s)(R_e + h_t)}{R_e^2} \frac{V_{ut}}{V} \frac{v_o}{R}$$

$$\Delta \simeq 0$$

Here R is slant range (in the plane normal to the radar flight path) and u is the along track or azimuth distance. The term Au^2 is due to the difference in target and radar along track positions, and Bu is due to a changing target to radar cross track distance. In the terms A and B we have R_e the earths radius, h_s and h_t the satellite and target local altitudes, V the satellite velocity, V_{ut} the target velocity in the cross track direction, and v_o the target cross track position at broadside to the satellite track. When the target is stationary the term Bu is zero because B is zero. The term Δ consists of all terms remaining in the binomial expansion used to obtain the above expression for r. As seen in the geometric data tabulated in Section 2.2, Δ is very small for the cases of interest and will therefore be dropped.

Substituting the expansion for r into the expression for the azimuth signal s_a gives

$$s_a = a_a(u) \exp -j\left[\theta_a(u)\right]$$

with

$$a_a(u) = g\left(\frac{u}{R}\right)$$

$$\theta_a = -\frac{2A}{\lambda} u^2 - \frac{2B}{\lambda} u - \frac{2}{\lambda} R$$

The quadratic phase $\frac{2A}{\lambda} u^2$ corresponds to a linear frequency modulation. For its time domain representation we take $u = Vt$, with V the along track distance rate of change, giving a corresponding quadratic phase term $\frac{2AV^2}{\lambda} t^2$. The coefficient of the t^2 (or u^2) term is a linear f.m. constant which we will denote as k_a for the azimuth dimension where, for the time domain, we have

$$k_a = -\frac{4AV^2}{\lambda}$$

The azimuth bandwidth over a synthetic aperture time interval T_a (corresponding to an aperture length L_a and beamwidth $\Delta\alpha$) will be

$$\begin{aligned} B_a &= k_a T_a \\ &= k_a \frac{L_a}{V} \\ &= k_a \frac{R\Delta\alpha}{V} \end{aligned}$$

In addition, however, note the frequency shift $\frac{2B}{\lambda}$ in $\frac{2Bu}{\lambda}$, which in the temporal domain becomes $\frac{2BVt}{\lambda}$, and the fixed phase $\frac{2uR}{\lambda}$. The total expected bandwidth for the azimuth signal will be $B_a + \frac{2BV}{\lambda}$, unless antenna steering or clutter tracking is used to force B to zero.

For the range dimension signal $s_r(t',r)$ a linear frequency modulation function (chirp) will be considered with the modulation constant k_r, thus

$$s_r(t',r) = a_r(t',r) \exp -j\theta_r(t',r)$$

with

$$a_r = a(t' - \frac{2r}{c}) \tilde{\sigma} g(\beta)$$

$$\theta_r = \frac{k_r}{2} (t' - \frac{2r}{c})^2 + \omega_o t'$$

$$t' = t - nT$$

$$r = R + Au^2 + Bu$$

Here again $r = R + Au^2 + Bu$ occurs in the envelope and phase terms above, however, we will not make this substitution for r at this point. The bandwidth B_r for the chirp modulation over a pulse length T_r seconds long will be

$$B_r = k_r T_r$$

With the use of an offset frequency $\omega_o = 2\pi f_o$ the total video bandwidth for the range dimension will be essentially $\frac{1}{2}B_r + f_o$. Using the theoretically minimum offset value of $f_o = \frac{1}{2}B_r$ we have a total video bandwidth for the range dimension of B_r (neglecting relatively small contributions which can arise from a varying r in s_r). Note that for practical reasons we must have a small offset in addition to $\frac{1}{2}B_r$ if we wish to process the entire data bandwidth. This is required to separate the data from the dc contributions and low frequency noise.

2.1.2 MATCHED FILTER PROCESSING

Processing of the SAR video signal $s_n(t',r)$ is a matched phase filter procedure. For this process the signal, in terms of its range and azimuth components s_r and s_a, is passed through a data processing system which can be characterized by a filter impulse response p which is matched in phase to the signal to be processed. We will consider the processing step without regard to hardware implementation in this section. For the range dimension the processor is matched to the transmitted linear FM modulation thus the phase matched impulse response required is

$$p_r = \exp\ j\left[\theta(-t)\right]$$

$$= \exp\ j\ \frac{k_r}{2}\ t^2$$

and for point target azimuth data with the processor matched to the azimuth linear FM we have impulse response

$$p_a = \exp\ j\left[\theta_a(-u)\right]$$

$$= \exp\ j\ \frac{k_a}{2}\ u^2$$

The output of the data processor, denoted v, will then be the convolution of s and p. For range processing of point target data we have in the range dimension

$$v_r(t) = \int s_r(\tau) p_r(t - \tau) \quad d\tau$$

$$v_r(t) = \tilde{\sigma}\, g(\beta) \int_{\tau_1}^{\tau_2} a_r(\tau) \exp\left[-j\left(\frac{k_r}{2}\tau^2 + \omega_o\tau\right)\right] \exp\left[j\frac{k_r}{2}(t-\tau)^2\right] d\tau$$

$$= \tilde{\sigma}\, g(\beta) e^{-j\frac{k_r}{2}t^2} \int_{\tau_1}^{\tau_2} a_r(\tau) \exp\left[-j(k_r t + \omega_o)\tau\right] d\tau$$

where

$$\tau_1 = -\frac{T_r}{2} \; ; \; \tau_2 = +\frac{T_r}{2}$$

$$t \equiv \left(t' - \frac{2r}{c}\right) = \left[t' - \frac{2}{c}(R + Au^2 + Bu)\right]$$

The convolution integral reduces to a Fourier transform of the pulse envelope $a_r(\tau)$ with the frequency variable being the quantity $k_r t$ and with a shift or offset ω_o. The limits of integration are defined by the pulse length T_r for the case of a point target. After the convolution integration is accomplished the dummy variable t is replaced by $\left[t' - \frac{2r}{c}\right]$. The phase term outside the integral can be neglected since the processed imagery is viewed in terms of $|v_r|$ or $|v_r|^2$.

Similarly, azimuth processing of the point signal history will give

$$v_a(u) = \int s_a(\tau) p_a(u - \tau)\, d\tau$$

$$= \int_{\tau_1}^{\tau_2} g\left(\frac{\tau}{R}\right) \exp\left[-j\left(\frac{k_a}{2}\tau^2 + \frac{2B\tau}{\lambda}\right)\right] \exp\left[j\frac{k_a}{2}(u - \tau)^2\right] d\tau$$

$$= e^{-j\frac{k_a}{2}u^2} \int_{\tau_1}^{\tau_2} g\left(\frac{\tau}{R}\right) \exp\left[-j\left(k_a u + \frac{2B}{\lambda}\right)\tau\right] d\tau$$

where

$$\tau_1 = -\frac{L_a}{2};\quad \tau_2 = \frac{L_a}{2}$$

Again we have the processed output in its azimuth dimension being the Fourier transform of the signal amplitude, $a_a = g$. The frequency variable is $k_a u$ and there is a frequency shift or offset $\frac{2B}{\lambda}$. The limits of integration are defined as plus and minus half the size of the azimuth dimension patch ($L_a = R\Delta\alpha$) illuminated by the antenna.

The resultant mapping of a point target will be the data processor output, v, which is

$$v = v_r \cdot v_a$$

2.1.3 RANGE AND AZIMUTH DATA COUPLING

The radar data measurement co-ordinates for any one target point are slant range R and along track or azimuth distance u, where $u = u_s - u_t$ the relative along track distance between the radar (satellite) and the target point. Implicite in the earlier discussion of data processing in Section 2.1.2 was that a point target signal history

$$s = s_r \cdot s_a$$

has a range term s_r with a propagation path delay $\frac{2r}{c}$ which is essentially constant over the duration of the azimuth term s_a as defined by the antenna azimuth beamwidth. In this case we take range as the constant $r = R$ in the range term s_r, while retaining the more exact form $r = R + Au^2 + Bu$ for range in the azimuth term s_a because over its extended duration its phase can experience a significant variation.

When the above assumption that $\frac{2r}{c} \simeq \frac{2R}{c}$ in s_r cannot be made then the range term experiences a shift in its envelope and also a variation in phase from pulse to pulse as a target passes through the radar beam. Thus, coupling between range and azimuth data occurs and matched filter processing, where the processor response is phase matched to the radar data with no coupling can give results with degraded resolution unless compensating provisions are made.

Judging when range-azimuth coupling exists to an extent which can affect the output map quality can be done in terms of the variation of radar to target range. Denoting the systems

resolution as ρ_r and ρ_a for range and azimuth respectively, we require that the change in range r over the radar azimuth aperture $-\frac{1}{2} L_a \leq u \leq \frac{1}{2} L_a$ be less than $\frac{1}{2}\rho_r$, i.e.,

$$r - R \leq \frac{1}{2}\rho_r$$

for $$-\frac{1}{2}L_a \leq u \leq \frac{1}{2}L_a$$

Recall that $r = R + Au^2 + Bu$ thus giving

$$r - R = Au^2 + Bu$$

The quadratic term Au^2 is denoted as range curvature and the linear term Bu is denoted as range walk. The range walk term is present only when the target or earth has a cross track movement relative to the radar, as caused by earths rotation for example.

The expected values for range change r - R, obtained from the tabulated data of Section 2.2, is summarized in Table 2 below for several orbit altitudes and several azimuth apertures (beamwidth $\Delta\alpha$). The data is given separately for range curvature and range walk. It can be seen that range curvature may require a modest amount of compensation while range walk (shown for the worst case of a polar orbit) will require a compensating provision.

TABLE II

Range Curvature (Total Aperture)

$\leq$ 32 M

Range Curvature (Sub-Apertures)

	H = 185 Km	H = 278 Km	H = 370 Km
1/8	$\leq$ 4m	$\leq$ 6m	$\leq$ 7m
1/4	$\leq$ 8m	$\leq$ 12m	$\leq$ 13m
1/2	$\leq$ 13m	$\leq$ 20m	$\leq$ 24m
1	$\leq$ 17m	$\leq$ 25m	$\leq$ 32m

Range Walk (Total Aperture)

$\leq 3.5^{o}$ variable azimuth tilt

2.2 RADAR GEOMETRY

The important two dimensional properties of the radar data become evident upon interpretation of radar to target geometry. Figure 2 shows the range r from the satellite radar to a point on the earth surface. The position of the radar (S) and the target point (T) are described in a spherical coordinate system which is fixed relative to the plane of the satellite orbit and with its origin at the earth's center, point O. Surface distance in the along track and cross track directions are defined by the coordinate variables u and v on a reference sphere equivalent to the spherical non-rotating earth. These distance coordinates lie on two orthogonal great circles. The great circle path for u is the projection of the satellite orbit path onto the reference (earth) sphere having the nominal earth radius R_e = 6,378.3 kilometers (KM). The surface distance variable v lies on a great circle whose plane is perpendicular to the plane of the satellite orbit. The angular position of any point in the spherical coordinates will be designated by the spherical angle θ in the u-plane (orbit plane) and the angle ϕ in the v plane.

Thus, in spherical coordinates the position of a point is defined by its radial distance from the earth's center and its spherical angle position, (ϕ,θ) or its surface position (u,v).

For a satellite altitude h_s and a target altitude h_t we get target and satellite position coordinates as follows:

Satellite: $R_e + h_s;\ \theta_s,\ \phi_s;\ u_s,\ v_s$

Target: $R_e + h_t;\ \theta_t,\ \phi_t;\ u_t,\ v_t$

Target movement due to earth's rotation would be described by changing target position coordinates. We will take the worst case speed of a surface point at the equator to be 465 meters/seconds (M/s).

The satellite orbit path and its trace on our reference sphere describe a great circle whereas the intersection of a fixed range line r from the satellite to the reference sphere will describe a "small circle" on the sphere. A great circle is one in which the plane of the circle contains the center of the sphere (point O) whereas a small circle does not contain point O.

The earth's surface swath that is mapped when the SAR antenna is fixed in position will not be a great or small circle path. Because of earth's rotation we map a curved path on the earth surface which is cyclic with each pass around the earth.

Expressions and data for several important geometric parameters will be reviewed here. Range r can be solved from the triangle formed by points o, S and T of Figure 2 with the following expression

$$r = \left[(r_e + h_s)^2 + (r_e + h_t)^2 - 2(R_e + h_s)(R_e + h_t)\cos\gamma\right]^{\frac{1}{2}}$$

where

$$\cos\gamma = \cos\theta \cos\phi$$

$$\theta = \theta_s - \theta_t \qquad \text{and} \qquad \phi = \phi_s - \phi_t$$

$$= \frac{u_s - u_t}{R_e} \qquad = \frac{v_s - v_t}{R_e}$$

We will assume $h_t = 0$ for the present considerations.

It will be convenient to write the range r in a form more suitable for analysis and computation as follows

$$r = \Big[R^2 + 4ab\cos\phi_o \sin^2\frac{\theta}{2} + 2ab\sin\phi_o\sin\phi + 4ab\cos\phi_o\sin^2\frac{\phi}{2} - 4ab\sin\phi_o\sin\phi\sin^2\frac{\theta}{2} - 8ab\cos\phi_o\sin^2\frac{\phi}{2}\sin^2\frac{\theta}{2}\Big]^{\frac{1}{2}}$$

where

$$R^2 = a^2 + b^2 - 2ab\cos\phi_o$$

$$a = R_e + h_s$$

$$b = R_e + h_t$$

$$\phi_o = \frac{v_o}{R_e} \; ; \; \phi = \frac{v}{R_e} \; ; \; \theta = \frac{u}{R_e}$$

Here R is the broadside range to the target when $\alpha = 0$. The angle ϕ_o is taken as a bias position for this angle with deviations from ϕ_o being defined by ϕ.

The range change Δr, relative to the broadside range R, will be

$$\Delta r = r - R$$

The first order approximation r', for the range r, is taken as

$$r' = R + \frac{ab}{2R_o}\theta^2 \cos\phi_o + \frac{ab}{R_o}\phi \sin\phi_o$$

The higher order range change Δ, which is the variation in range not included in the approximation r', is given by

$$\Delta = r' - r$$

The elevation angle β, measured to the target in the broadside plane up from the radar local vertical, is given by

$$\beta = \tan^{-1}\left[\frac{\sin(\phi_o + \phi)}{\frac{h_s}{R_e} + 1 - \cos(\phi_o + \phi)\cos\theta}\right]$$

The azimuth angle α, measured to the target in a plane normal to the broadside plane, is given by

$$\alpha = \tan^{-1}\left[\frac{\cos(\phi_o + \phi)\sin\theta}{\left\{\sin^2(\phi_o + \phi) + \left[\frac{h_s}{R_e} + 1 - \cos(\phi_o + \phi)\cos\theta\right]^2\right\}^{\frac{1}{2}}}\right]$$

The broadside slant range increment ΔR (corresponding to a ground swath Δv) will be bounded by max and min broadside ranges R_2 and R_1 respectively, giving

$$\Delta R = R_2 - R_1$$

The elevation beam width $\Delta\beta$ which is bounded by range lines R_2 and R_1 and which projects onto the ground swath Δv is

$$\Delta\beta = \beta_2 - \beta_1$$

$$\beta_2 = \beta(\phi_2)$$

$$\beta_1 = \beta(\phi_1)$$

The time increment Δt corresponding to the range increment ΔR is

$$\Delta t = \frac{2\Delta R}{c}$$

$$c = 2.99778 \times 10^8 \text{ meters/sec}$$

The grazing angle ψ, measured at the target location between the local ground tangent and the range line to the target, is given in terms of the geocentric angle γ as

$$\psi = \tan^{-1}\left[\frac{\cos\gamma - \cos\gamma_H}{\sin\gamma}\right]$$

The geocentric angle γ, and its horizon value γ_H for a target on the horizon line of sight, are given as

$$\gamma = \cos^{-1}\left[\cos(\phi_o + \phi)\cos\theta\right]$$

$$\gamma_H = \cos^{-1}\left[\frac{R_e}{R_e + h_s}\right]$$

A ground swath will have a cross track width Δv which is bounded by the max and min cross track distances v_2 and v_1 respectively, giving

$$\Delta v = v_2 - v_1$$

The derivative of broadside range R relative to cross-track ground distance v is

$$\frac{dR}{dv} = \cos\psi$$

Representative geometric data has been computed in two basic sets: along-track data and cross-track data. For along track data we have r, Δr, Δ, β, α, γ, ψ as a function of along-track distance u with h_s, v_o and D as parameters. For cross-track data we have R_2, ΔR, Δt, $\Delta\beta$, β_2, ψ_1 and $\frac{dR}{dv}\Big]_{R_2}$ as a function of v_2 with h_s and Δv as parameters. The parameter D defines the ratio cross-track to along track speed between radar and target.

Examples of computed geometric data are included in tables herein for the following cases:

Cross Track Data Parameters

Altitude: h_s = 185 KM, 278 KM, 370 KM

h_t = 0

Ground Swath: Δv = 70 KM

Along Track Data Parameters

Altitude: h_s = 185 KM; 278 KM, 370 KM

h_t = 0

Speed Ratio: D = 0, 0.063

Cross-Track Distance: v_o = as shown

GEOMETRIC PARAMETERS (CROSS TRACK)

ALTITUDE: 185. KM GROUND SWATH: 70. KM

CROSS TRACK MAX (KM)	SLANT RANGE MAX (KM)	SLANT RANGE INCR (KM)	TIME INCR (US)	ELEV BEAM WIDTH (DEG)	ELEV ANGL MAX (DEG)	GRAZE ANGL MIN (DEG)	SLT/CRS MIN
90.	206.300	20.191	134.706	19.695	25.864	63.327	0.111
100.	210.985	23.499	156.776	19.083	28.291	60.811	0.165
110.	216.045	26.648	177.784	18.413	30.606	58.406	0.217
120.	221.455	29.628	197.665	17.700	32.809	56.113	0.268
130.	227.188	32.434	216.384	16.959	34.902	53.930	0.317
140.	233.222	35.063	233.926	16.201	36.887	51.856	0.363
150.	239.534	37.518	250.302	15.439	38.767	49.885	0.407
160.	246.102	39.802	265.539	14.682	40.547	48.016	0.449
170.	252.906	41.921	279.676	13.939	42.230	46.243	0.488
180.	259.928	43.882	292.764	13.215	43.821	44.562	0.524
190.	267.150	45.696	304.861	12.516	45.325	42.968	0.558
200.	274.557	47.369	316.026	11.844	46.746	41.457	0.589
210.	282.135	48.912	326.322	11.203	48.090	40.024	0.618
220.	289.869	50.335	335.811	10.592	49.360	38.664	0.644
230.	297.747	51.645	344.555	10.014	50.561	37.373	0.669
240.	305.759	52.853	352.613	9.467	51.697	36.147	0.692
250.	313.894	53.966	360.039	8.952	52.773	34.981	0.712
260.	322.143	54.993	366.886	8.467	53.791	33.873	0.732
270.	330.497	55.939	373.203	8.010	54.757	32.818	0.749
280.	338.948	56.814	379.036	7.582	55.672	31.813	0.766
290.	347.490	57.621	384.424	7.180	56.540	30.855	0.781
300.	356.116	58.368	389.408	6.803	57.364	29.941	0.795
310.	364.819	59.060	394.021	6.449	58.147	29.069	0.808
320.	373.595	59.700	398.295	6.118	58.891	28.235	0.819
330.	382.438	60.295	402.260	5.807	59.599	27.437	0.830
340.	391.344	60.847	405.942	5.516	60.272	26.674	0.840
350.	400.308	61.360	409.364	5.242	60.914	25.942	0.850
360.	409.327	61.837	412.548	4.985	61.525	25.241	0.858
370.	418.397	62.282	415.515	4.744	62.108	24.568	0.867
380.	427.515	62.696	418.282	4.518	62.664	23.922	0.874
390.	436.678	63.084	420.866	4.305	63.195	23.301	0.881
400.	445.883	63.445	423.280	4.104	63.703	22.704	0.888
410.	455.128	63.784	425.539	3.916	64.188	22.129	0.894
420.	464.409	64.101	427.655	3.738	64.652	21.576	0.899
430.	473.726	64.399	429.639	3.570	65.096	21.042	0.905
440.	483.075	64.678	431.501	3.412	65.521	20.527	0.909
450.	492.455	64.940	433.250	3.263	65.928	20.030	0.914
460.	501.865	65.186	434.895	3.122	66.318	19.550	0.918
470.	511.302	65.418	436.443	2.989	66.692	19.086	0.923
480.	520.765	65.637	437.901	2.863	67.051	18.637	0.926
490.	530.252	65.843	439.277	2.744	67.396	18.203	0.930
500.	539.763	66.038	440.575	2.631	67.726	17.782	0.933
600.	635.919	67.495	450.298	1.768	70.412	14.199	0.958
700.	733.458	68.378	456.187	1.229	72.269	11.443	0.973
800.	831.820	68.942	459.951	0.872	73.582	9.231	0.983

GEOMETRIC PARAMETERS (CROSS TRACK)

ALTITUDE: 278. KM GROUND SWATH: 70. KM

CROSS TRACK MAX (KM)	SLANT RANGE MAX (KM)	SLANT RANGE INCR (KM)	TIME INCR (US)	ELEV BEAM WIDTH (DEG)	ELEV ANGL MAX (DEG)	GRAZE ANGL MIN (DEG)	SLT/CRS MIN
90.	292.809	14.059	93.795	13.786	17.900	71.292	0.075
100.	296.175	16.491	110.020	13.575	19.732	69.370	0.112
110.	299.852	18.865	125.857	13.336	21.520	67.492	0.149
120.	303.828	21.174	141.265	13.073	23.262	65.660	0.185
130.	308.091	23.414	156.208	12.789	24.956	63.876	0.220
140.	312.630	25.580	170.660	12.487	26.601	62.141	0.254
150.	317.433	27.669	184.598	12.170	28.197	60.456	0.288
160.	322.488	29.679	198.006	11.842	29.742	58.821	0.321
170.	327.783	31.608	210.876	11.504	31.237	57.236	0.352
180.	333.308	33.456	223.202	11.161	32.682	55.702	0.383
190.	339.050	35.222	234.986	10.815	34.077	54.216	0.412
200.	344.999	36.908	246.232	10.468	35.424	52.780	0.440
210.	351.144	38.514	256.948	10.121	36.722	51.391	0.467
220.	357.475	40.042	267.145	9.778	37.974	50.050	0.493
230.	363.983	41.495	276.838	9.438	39.180	48.754	0.518
240.	370.658	42.875	286.042	9.105	40.342	47.502	0.541
250.	377.491	44.184	294.775	8.778	41.460	46.294	0.564
260.	384.474	45.425	303.054	8.460	42.537	45.128	0.585
270.	391.599	46.601	310.900	8.149	43.573	44.002	0.605
280.	398.858	47.715	318.330	7.848	44.570	42.915	0.624
290.	406.244	48.769	325.366	7.555	45.529	41.866	0.642
300.	413.750	49.767	332.025	7.273	46.453	40.852	0.659
310.	421.370	50.712	338.329	7.000	47.342	39.874	0.676
320.	429.098	51.606	344.294	6.737	48.197	38.929	0.691
330.	436.927	52.452	349.939	6.483	49.020	38.016	0.706
340.	444.853	53.253	355.283	6.240	49.812	37.133	0.719
350.	452.870	54.012	360.341	6.006	50.575	36.281	0.732
360.	460.974	54.729	365.131	5.781	51.310	35.456	0.745
370.	469.160	55.409	369.666	5.565	52.018	34.659	0.756
380.	477.423	56.053	373.963	5.358	52.700	33.887	0.767
390.	485.761	56.664	378.034	5.160	53.356	33.140	0.778
400.	494.169	57.242	381.894	4.970	53.990	32.417	0.788
410.	502.643	57.791	385.554	4.787	54.600	31.717	0.797
420.	511.181	58.311	389.026	4.613	55.188	31.039	0.806
430.	519.779	58.805	392.321	4.446	55.756	30.381	0.815
440.	528.434	59.274	395.449	4.286	56.304	29.744	0.823
450.	537.143	59.719	398.421	4.133	56.832	29.126	0.830
460.	545.904	60.143	401.245	3.986	57.342	28.526	0.837
470.	554.714	60.545	403.930	3.845	57.835	27.943	0.844
480.	563.571	60.928	406.485	3.711	58.311	27.378	0.851
490.	572.473	61.292	408.915	3.582	58.770	26.828	0.857
500.	581.418	61.639	411.230	3.458	59.214	26.294	0.863
600.	672.828	64.339	429.245	2.469	62.929	21.681	0.908
700.	766.895	66.077	440.833	1.806	65.636	18.076	0.937
800.	862.730	67.241	448.599	1.346	67.647	15.167	0.956

GEOMETRIC PARAMETERS (CROSS TRACK)

ALTITUDE: 370. KM GROUND SWATH: 70. KM

CROSS TRACK MAX (KM)	SLANT RANGE MAX (KM)	SLANT RANGE INCR (KM)	TIME INCR (US)	ELEV BEAM WIDTH (DEG)	ELEV ANGL MAX (DEG)	GRAZE ANGL MIN (DEG)	SLT/CRS MIN
90.	381.405	10.833	72.276	10.555	13.648	75.543	0.057
100.	384.031	12.747	85.039	10.458	15.093	74.009	0.085
110.	386.913	14.632	97.621	10.348	16.516	72.496	0.114
120.	390.045	16.487	109.997	10.225	17.917	71.005	0.142
130.	393.421	18.309	122.148	10.090	19.294	69.538	0.169
140.	397.034	20.094	134.056	9.944	20.646	68.097	0.196
150.	400.879	21.839	145.703	9.787	21.971	66.681	0.223
160.	404.949	23.544	157.075	9.622	23.270	65.292	0.250
170.	409.237	25.206	168.161	9.449	24.542	63.931	0.275
180.	413.736	26.823	178.950	9.269	25.785	62.598	0.301
190.	418.439	28.394	189.435	9.084	27.001	61.293	0.325
200.	423.340	29.920	199.610	8.894	28.187	60.016	0.350
210.	428.432	31.398	209.472	8.700	29.345	58.768	0.373
220.	433.708	32.829	219.019	8.503	30.474	57.549	0.396
230.	439.161	34.212	228.250	8.305	31.575	56.359	0.418
240.	444.785	35.549	237.166	8.105	32.647	55.197	0.439
250.	450.574	36.839	245.770	7.905	33.690	54.064	0.460
260.	456.521	38.082	254.066	7.705	34.706	52.958	0.480
270.	462.620	39.280	262.058	7.507	35.694	51.881	0.500
280.	468.865	40.433	269.753	7.310	36.655	50.830	0.518
290.	475.251	41.543	277.155	7.115	37.589	49.806	0.537
300.	481.771	42.610	284.273	6.922	38.497	48.808	0.554
310.	488.421	43.635	291.114	6.732	39.379	47.836	0.571
320.	495.194	44.620	297.686	6.546	40.236	46.889	0.587
330.	502.087	45.566	303.997	6.363	41.069	45.967	0.602
340.	509.094	46.474	310.055	6.183	41.877	45.069	0.617
350.	516.211	47.346	315.869	6.007	42.662	44.194	0.632
360.	523.433	48.182	321.448	5.836	43.425	43.341	0.645
370.	530.755	48.984	326.800	5.668	44.165	42.511	0.659
380.	538.174	49.753	331.933	5.505	44.884	41.703	0.671
390.	545.686	50.492	336.857	5.346	45.582	40.915	0.683
400.	553.287	51.199	341.580	5.191	46.260	40.147	0.695
410.	560.972	51.878	346.109	5.040	46.917	39.400	0.706
420.	568.740	52.529	350.453	4.894	47.556	38.671	0.717
430.	576.586	53.154	354.619	4.752	48.177	37.961	0.727
440.	584.508	53.753	358.615	4.614	48.779	37.269	0.737
450.	592.501	54.327	362.448	4.480	49.364	36.594	0.747
460.	600.565	54.879	366.126	4.350	49.932	35.936	0.756
470.	608.694	55.408	369.655	4.224	50.484	35.294	0.764
480.	616.888	55.915	373.041	4.103	51.020	34.668	0.773
490.	625.142	56.402	376.291	3.984	51.541	34.058	0.781
500.	633.456	56.870	379.411	3.870	52.047	33.462	0.788
600.	719.376	60.648	404.614	2.910	56.390	28.220	0.850
700.	809.200	63.222	421.791	2.216	59.691	24.021	0.892
800.	901.742	65.023	433.808	1.710	62.233	20.581	0.921

GEOMETRIC PARAMETERS (ALONG TRACK)

ALTITUDE: 185. KM CROSS TRACK DIST: 260. KM D= 0.0

ALONG TRACK DIST (M)	RANGE (KM)	RANGE CHG (M)	RANGE CHG-HO (M)	ELEV ANGL (DEG)	AZIM ANGL (DEG)	GEOC ANGL (DEG)	GRAZE ANGL (DEG)
0.	322.143	0.0	0.000	53.791	0.0	2.336	33.873
250.	322.143	0.100	0.000	53.791	0.044	2.336	33.873
500.	322.143	0.399	0.000	53.791	0.089	2.336	33.873
750.	322.144	0.898	0.000	53.791	0.133	2.336	33.873
1000.	322.145	1.596	0.000	53.791	0.178	2.336	33.873
1250.	322.145	2.493	0.000	53.791	0.222	2.336	33.873
1500.	322.147	3.591	0.000	53.791	0.267	2.336	33.873
1750.	322.148	4.887	0.000	53.791	0.311	2.336	33.872
2000.	322.149	6.383	0.000	53.791	0.355	2.336	33.872
2250.	322.151	8.079	0.000	53.791	0.400	2.336	33.872
2500.	322.153	9.974	0.000	53.791	0.444	2.336	33.872
2750.	322.155	12.068	0.000	53.791	0.489	2.336	33.872
3000.	322.157	14.362	0.000	53.791	0.533	2.336	33.871
3250.	322.160	16.855	0.000	53.791	0.578	2.336	33.871
3500.	322.162	19.548	0.001	53.791	0.622	2.336	33.871
3750.	322.165	22.440	0.001	53.791	0.666	2.336	33.870
4000.	322.168	25.532	0.001	53.791	0.711	2.336	33.870
4250.	322.172	28.823	0.001	53.791	0.755	2.336	33.869
4500.	322.175	32.313	0.002	53.791	0.800	2.336	33.869
4750.	322.179	36.003	0.002	53.791	0.844	2.336	33.868
5000.	322.183	39.892	0.002	53.791	0.888	2.336	33.868
5250.	322.187	43.981	0.003	53.791	0.933	2.336	33.867
5500.	322.191	48.269	0.004	53.791	0.977	2.336	33.867
5750.	322.196	52.757	0.004	53.791	1.022	2.336	33.866
6000.	322.200	57.444	0.005	53.791	1.066	2.336	33.865
6250.	322.205	62.330	0.006	53.791	1.111	2.336	33.865
6500.	322.210	67.415	0.007	53.791	1.155	2.336	33.864
6750.	322.216	72.700	0.008	53.791	1.199	2.336	33.864
7000.	322.221	78.185	0.009	53.791	1.244	2.336	33.863
7250.	322.227	83.868	0.011	53.791	1.288	2.336	33.862
7500.	322.233	89.751	0.013	53.791	1.333	2.337	33.861
7750.	322.239	95.833	0.014	53.791	1.377	2.337	33.861
8000.	322.245	102.115	0.016	53.791	1.421	2.337	33.860
8250.	322.252	108.596	0.018	53.791	1.466	2.337	33.859
8500.	322.258	115.276	0.021	53.791	1.510	2.337	33.858
8750.	322.265	122.155	0.023	53.791	1.555	2.337	33.857
9000.	322.272	129.234	0.026	53.791	1.599	2.337	33.856
9250.	322.279	136.511	0.029	53.790	1.643	2.337	33.855
9500.	322.287	143.989	0.032	53.790	1.688	2.337	33.854
9750.	322.295	151.665	0.036	53.790	1.732	2.337	33.853
10000.	322.302	159.540	0.040	53.790	1.777	2.337	33.852
20000.	322.781	637.687	0.632	53.787	3.549	2.342	33.790
40000.	324.686	2543.229	10.047	53.773	7.071	2.363	33.545
60000.	327.837	5694.498	50.373	53.751	10.537	2.397	33.147
80000.	332.199	10056.016	157.088	53.720	13.923	2.444	32.611
100000.	337.724	15580.854	377.121	53.679	17.208	2.502	31.955

GEOMETRIC PARAMETERS (ALONG TRACK)

ALTITUDE: 185. KM CROSS TRACK DIST: 100. KM D= 0.0

ALONG TRACK DIST (M)	RANGE (KM)	RANGE CHG (M)	RANGE CHG-H0 (M)	ELEV ANGL (DEG)	AZIM ANGL (DEG)	GEOC ANGL (DEG)	GRAZE ANGL (DEG)
0.	210.985	0.0	0.000	28.291	0.0	0.898	60.811
250.	210.986	0.152	0.000	28.291	0.068	0.898	60.811
500.	210.986	0.610	0.000	28.291	0.136	0.898	60.811
750.	210.987	1.372	0.000	28.291	0.204	0.898	60.810
1000.	210.988	2.438	0.000	28.291	0.272	0.898	60.810
1250.	210.989	3.810	0.000	28.291	0.339	0.898	60.809
1500.	210.991	5.486	0.000	28.291	0.407	0.898	60.808
1750.	210.993	7.467	0.000	28.291	0.475	0.898	60.807
2000.	210.995	9.753	0.000	28.291	0.543	0.898	60.806
2250.	210.998	12.343	0.000	28.291	0.611	0.899	60.805
2500.	211.001	15.239	0.001	28.291	0.679	0.899	60.803
2750.	211.004	18.439	0.001	28.291	0.747	0.899	60.802
3000.	211.007	21.943	0.001	28.291	0.815	0.899	60.800
3250.	211.011	25.753	0.002	28.291	0.882	0.899	60.798
3500.	211.015	29.867	0.002	28.291	0.950	0.899	60.796
3750.	211.020	34.285	0.003	28.291	1.018	0.899	60.794
4000.	211.024	39.009	0.004	28.291	1.086	0.899	60.791
4250.	211.029	44.037	0.005	28.291	1.154	0.899	60.789
4500.	211.035	49.369	0.006	28.291	1.222	0.899	60.786
4750.	211.040	55.006	0.007	28.291	1.290	0.899	60.783
5000.	211.046	60.948	0.009	28.291	1.357	0.899	60.780
5250.	211.053	67.194	0.011	28.291	1.425	0.900	60.777
5500.	211.059	73.745	0.013	28.291	1.493	0.900	60.774
5750.	211.066	80.600	0.015	28.291	1.561	0.900	60.770
6000.	211.073	87.759	0.018	28.290	1.629	0.900	60.767
6250.	211.081	95.223	0.021	28.290	1.697	0.900	60.763
6500.	211.088	102.992	0.025	28.290	1.764	0.900	60.759
6750.	211.096	111.064	0.029	28.290	1.832	0.900	60.755
7000.	211.105	119.441	0.034	28.290	1.900	0.900	60.751
7250.	211.114	128.123	0.039	28.290	1.968	0.901	60.746
7500.	211.122	137.108	0.045	28.290	2.036	0.901	60.742
7750.	211.132	146.398	0.051	28.290	2.103	0.901	60.737
8000.	211.141	155.992	0.058	28.290	2.171	0.901	60.732
8250.	211.151	165.889	0.065	28.290	2.239	0.901	60.727
8500.	211.161	176.091	0.074	28.290	2.307	0.902	60.722
8750.	211.172	186.597	0.083	28.290	2.374	0.902	60.717
9000.	211.183	197.407	0.092	28.290	2.442	0.902	60.712
9250.	211.194	208.521	0.103	28.290	2.510	0.902	60.706
9500.	211.205	219.939	0.115	28.290	2.578	0.902	60.700
9750.	211.217	231.661	0.127	28.290	2.645	0.903	60.694
10000.	211.229	243.686	0.141	28.290	2.713	0.903	60.688
20000.	211.958	973.063	2.245	28.287	5.414	0.916	60.326
40000.	214.851	3865.801	35.429	28.275	10.728	0.967	58.949
60000.	219.588	8602.334	175.433	28.255	15.855	1.048	56.876
80000.	226.052	15066.747	538.173	28.226	20.723	1.150	54.345
100000.	234.101	23115.881	1266.805	28.190	25.283	1.270	51.570

GEOMETRIC PARAMETERS (ALONG TRACK)

ALTITUDE: 185. KM CROSS TRACK DIST: 260. KM D= 0.063

ALONG TRACK DIST (M)	RANGE (KM)	RANGE CHG (M)	RANGE CHG-HO (M)	ELEV ANGL (DEG)	AZIM ANGL (DEG)	GEOC ANGL (DEG)	GRAZE ANGL (DEG)
0.	322.143	0.0	0.000	53.791	0.0	2.336	33.873
250.	322.156	13.192	-0.000	53.793	0.044	2.336	33.871
500.	322.170	26.584	-0.000	53.795	0.089	2.336	33.870
750.	322.183	40.176	-0.001	53.796	0.133	2.336	33.868
1000.	322.197	53.967	-0.002	53.798	0.178	2.336	33.866
1250.	322.211	67.958	-0.003	53.799	0.222	2.336	33.864
1500.	322.225	82.149	-0.004	53.801	0.266	2.336	33.862
1750.	322.239	96.539	-0.005	53.802	0.311	2.337	33.861
2000.	322.254	111.129	-0.006	53.804	0.355	2.337	33.859
2250.	322.269	125.918	-0.008	53.805	0.400	2.337	33.857
2500.	322.284	140.907	-0.009	53.807	0.444	2.337	33.855
2750.	322.299	156.095	-0.010	53.809	0.488	2.337	33.853
3000.	322.314	171.482	-0.011	53.810	0.533	2.337	33.851
3250.	322.330	187.070	-0.013	53.812	0.577	2.338	33.849
3500.	322.346	202.856	-0.014	53.813	0.622	2.338	33.847
3750.	322.362	218.842	-0.015	53.815	0.666	2.338	33.845
4000.	322.378	235.027	-0.016	53.816	0.710	2.338	33.842
4250.	322.394	251.411	-0.017	53.818	0.755	2.338	33.840
4500.	322.411	267.995	-0.017	53.819	0.799	2.338	33.838
4750.	322.428	284.778	-0.017	53.821	0.843	2.339	33.836
5000.	322.445	301.760	-0.017	53.822	0.888	2.339	33.834
5250.	322.462	318.942	-0.017	53.824	0.932	2.339	33.832
5500.	322.479	336.322	-0.016	53.825	0.976	2.339	33.829
5750.	322.497	353.902	-0.015	53.827	1.021	2.339	33.827
6000.	322.515	371.680	-0.014	53.829	1.065	2.340	33.825
6250.	322.533	389.658	-0.012	53.830	1.109	2.340	33.822
6500.	322.551	407.835	-0.010	53.832	1.154	2.340	33.820
6750.	322.569	426.210	-0.007	53.833	1.198	2.340	33.818
7000.	322.588	444.785	-0.004	53.835	1.242	2.340	33.815
7250.	322.607	463.559	0.000	53.836	1.287	2.341	33.813
7500.	322.625	482.531	0.005	53.838	1.331	2.341	33.810
7750.	322.645	501.702	0.010	53.839	1.375	2.341	33.808
8000.	322.664	521.072	0.015	53.841	1.420	2.341	33.805
8250.	322.684	540.641	0.022	53.842	1.464	2.341	33.803
8500.	322.703	560.409	0.029	53.844	1.508	2.342	33.800
8750.	322.723	580.375	0.037	53.845	1.552	2.342	33.798
9000.	322.743	600.540	0.046	53.847	1.597	2.342	33.795
9250.	322.764	620.903	0.056	53.848	1.641	2.342	33.792
9500.	322.784	641.466	0.066	53.850	1.685	2.342	33.790
9750.	322.805	662.226	0.078	53.851	1.729	2.343	33.787
10000.	322.826	683.185	0.090	53.853	1.774	2.343	33.784
20000.	323.827	1683.844	1.867	53.912	3.538	2.354	33.655
40000.	326.768	4624.968	23.092	54.022	7.025	2.385	33.281
60000.	330.933	8789.803	97.244	54.123	10.437	2.430	32.765
80000.	336.276	14132.824	269.847	54.214	13.750	2.487	32.125
100000.	342.742	20598.864	596.070	54.295	16.948	2.555	31.381

GEOMETRIC PARAMETERS (ALONG TRACK)

ALTITUDE: 185. KM CROSS TRACK DIST: 100. KM D= 0.063

ALONG TRACK DIST (M)	RANGE (KM)	RANGE CHG (M)	RANGE CHG-HO (M)	ELEV ANGL (DEG)	AZIM ANGL (DEG)	GEOC ANGL (DEG)	GRAZE ANGL (DEG)
0.	210.985	0.0	0.000	28.291	0.0	0.898	60.811
250.	210.993	7.843	-0.000	28.295	0.068	0.898	60.807
500.	211.001	15.992	-0.002	28.298	0.136	0.899	60.803
750.	211.010	24.447	-0.004	28.302	0.204	0.899	60.799
1000.	211.019	33.207	-0.007	28.306	0.271	0.899	60.794
1250.	211.028	42.272	-0.011	28.310	0.339	0.899	60.790
1500.	211.037	51.644	-0.016	28.313	0.407	0.899	60.785
1750.	211.047	61.320	-0.021	28.317	0.475	0.899	60.780
2000.	211.057	71.302	-0.027	28.321	0.543	0.900	60.775
2250.	211.067	81.590	-0.033	28.324	0.611	0.900	60.770
2500.	211.078	92.183	-0.040	28.328	0.679	0.900	60.764
2750.	211.088	103.081	-0.048	28.332	0.746	0.900	60.759
3000.	211.100	114.285	-0.056	28.336	0.814	0.900	60.753
3250.	211.111	125.793	-0.065	28.339	0.882	0.901	60.748
3500.	211.123	137.607	-0.074	28.343	0.950	0.901	60.742
3750.	211.135	149.726	-0.083	28.347	1.018	0.901	60.736
4000.	211.148	162.150	-0.093	28.350	1.085	0.901	60.729
4250.	211.160	174.879	-0.103	28.354	1.153	0.902	60.723
4500.	211.173	187.913	-0.113	28.358	1.221	0.902	60.716
4750.	211.187	201.252	-0.123	28.362	1.289	0.902	60.710
5000.	211.200	214.896	-0.133	28.365	1.356	0.902	60.703
5250.	211.214	228.845	-0.143	28.369	1.424	0.903	60.696
5500.	211.228	243.098	-0.153	28.373	1.492	0.903	60.689
5750.	211.243	257.656	-0.163	28.376	1.560	0.903	60.681
6000.	211.258	272.519	-0.173	28.380	1.627	0.903	60.674
6250.	211.273	287.686	-0.183	28.384	1.695	0.904	60.66
6500.	211.289	303.157	-0.192	28.388	1.763	0.904	60.659
6750.	211.304	318.933	-0.201	28.391	1.830	0.904	60.651
7000.	211.320	335.013	-0.209	28.395	1.898	0.904	60.643
7250.	211.337	351.398	-0.217	28.399	1.966	0.905	60.634
7500.	211.353	368.087	-0.224	28.402	2.033	0.905	60.626
7750.	211.370	385.080	-0.231	28.406	2.101	0.905	60.618
8000.	211.388	402.376	-0.237	28.410	2.169	0.906	60.609
8250.	211.405	419.977	-0.242	28.413	2.236	0.906	60.600
8500.	211.423	437.882	-0.246	28.417	2.304	0.906	60.591
8750.	211.441	456.091	-0.249	28.421	2.371	0.907	60.582
9000.	211.460	474.603	-0.252	28.424	2.439	0.907	60.573
9250.	211.479	493.419	-0.253	28.428	2.507	0.907	60.564
9500.	211.498	512.539	-0.253	28.432	2.574	0.908	60.554
9750.	211.517	531.962	-0.251	28.435	2.642	0.908	60.544
10000.	211.537	551.688	-0.248	28.439	2.709	0.908	60.535
20000.	212.574	1588.430	2.103	28.585	5.398	0.927	60.025
40000.	216.071	5085.867	45.815	28.869	10.667	0.989	58.395
60000.	221.387	10401.808	221.636	29.143	15.723	1.077	56.140
80000.	228.395	17409.249	656.573	29.407	20.500	1.186	53.499
100000.	236.943	25958.086	1500.730	29.660	24.959	1.311	50.672

GEOMETRIC PARAMETERS (ALONG TRACK)

ALTITUDE: 278. KM CROSS TRACK DIST: 260. KM D= 0.0

ALONG TRACK DIST (M)	RANGE (KM)	RANGE CHG (M)	RANGE CHG-H0 (M)	ELEV ANGL (DEG)	AZIM ANGL (DEG)	GEOC ANGL (DEG)	GRAZE ANGL (DEG)
0.	384.474	0.0	0.000	42.537	0.0	2.336	45.128
250.	384.475	0.085	0.000	42.537	0.037	2.336	45.128
500.	384.475	0.339	0.000	42.537	0.074	2.336	45.128
750.	384.475	0.763	0.000	42.537	0.112	2.336	45.128
1000.	384.476	1.356	0.000	42.537	0.149	2.336	45.128
1250.	384.477	2.119	0.000	42.537	0.186	2.336	45.128
1500.	384.477	3.051	0.000	42.537	0.223	2.336	45.127
1750.	384.479	4.153	0.000	42.537	0.261	2.336	45.127
2000.	384.480	5.424	0.000	42.537	0.298	2.336	45.127
2250.	384.481	6.865	0.000	42.537	0.335	2.336	45.127
2500.	384.483	8.475	0.000	42.537	0.372	2.336	45.127
2750.	384.485	10.255	0.000	42.537	0.409	2.336	45.126
3000.	384.487	12.204	0.000	42.537	0.447	2.336	45.126
3250.	384.489	14.323	0.000	42.537	0.484	2.336	45.126
3500.	384.491	16.611	0.000	42.537	0.521	2.336	45.125
3750.	384.494	19.069	0.000	42.536	0.558	2.336	45.125
4000.	384.496	21.696	0.001	42.536	0.596	2.336	45.124
4250.	384.499	24.493	0.001	42.536	0.633	2.336	45.124
4500.	384.502	27.459	0.001	42.536	0.670	2.336	45.123
4750.	384.505	30.594	0.001	42.536	0.707	2.336	45.123
5000.	384.508	33.899	0.001	42.536	0.744	2.336	45.122
5250.	384.512	37.374	0.002	42.536	0.782	2.336	45.122
5500.	384.515	41.018	0.002	42.536	0.819	2.336	45.121
5750.	384.519	44.831	0.003	42.536	0.856	2.336	45.121
6000.	384.523	48.814	0.003	42.536	0.893	2.336	45.120
6250.	384.527	52.966	0.004	42.536	0.931	2.336	45.119
6500.	384.532	57.288	0.004	42.536	0.968	2.336	45.119
6750.	384.536	61.779	0.005	42.536	1.005	2.336	45.118
7000.	384.541	66.440	0.006	42.536	1.042	2.336	45.117
7250.	384.546	71.270	0.007	42.536	1.079	2.336	45.116
7500.	384.551	76.269	0.008	42.536	1.117	2.337	45.116
7750.	384.556	81.438	0.009	42.536	1.154	2.337	45.115
8000.	384.561	86.776	0.010	42.536	1.191	2.337	45.114
8250.	384.567	92.284	0.011	42.536	1.228	2.337	45.113
8500.	384.572	97.961	0.012	42.536	1.265	2.337	45.112
8750.	384.578	103.807	0.014	42.536	1.303	2.337	45.111
9000.	384.584	109.823	0.016	42.536	1.340	2.337	45.110
9250.	384.590	116.008	0.018	42.536	1.377	2.337	45.109
9500.	384.597	122.362	0.019	42.536	1.414	2.337	45.108
9750.	384.603	128.886	0.022	42.536	1.451	2.337	45.107
10000.	384.610	135.579	0.024	42.536	1.489	2.337	45.106
20000.	385.016	542.030	0.383	42.533	2.975	2.342	45.040
40000.	386.638	2163.555	6.095	42.524	5.933	2.363	44.779
60000.	389.326	4851.071	30.640	42.508	8.858	2.397	44.355
80000.	393.057	8582.687	95.910	42.486	11.733	2.444	43.779
100000.	397.803	13328.985	231.323	42.458	14.546	2.502	43.069

GEOMETRIC PARAMETERS (ALONG TRACK)

ALTITUDE: 278. KM CROSS TRACK DIST: 100. KM D= 0.0

ALONG TRACK DIST (M)	RANGE (KM)	RANGE CHG (M)	RANGE CHG-HO (M)	ELEV ANGL (DEG)	AZIM ANGL (DEG)	GEOC ANGL (DEG)	GRAZE ANGL (DEG)
0.	296.175	0.0	0.000	19.732	0.0	0.898	69.370
250.	296.175	0.110	0.000	19.732	0.048	0.898	69.370
500.	296.175	0.440	0.000	19.732	0.097	0.898	69.369
750.	296.176	0.991	0.000	19.732	0.145	0.898	69.369
1000.	296.177	1.762	0.000	19.732	0.193	0.898	69.369
1250.	296.178	2.752	0.000	19.732	0.242	0.898	69.368
1500.	296.179	3.963	0.000	19.732	0.290	0.898	69.367
1750.	296.180	5.395	0.000	19.732	0.338	0.898	69.367
2000.	296.182	7.046	0.000	19.732	0.387	0.898	69.366
2250.	296.184	8.918	0.000	19.732	0.435	0.899	69.365
2500.	296.186	11.010	0.000	19.732	0.484	0.899	69.364
2750.	296.188	13.321	0.000	19.732	0.532	0.899	69.362
3000.	296.191	15.854	0.000	19.732	0.580	0.899	69.361
3250.	296.194	18.606	0.001	19.732	0.629	0.899	69.360
3500.	296.197	21.578	0.001	19.732	0.677	0.899	69.358
3750.	296.200	24.771	0.001	19.732	0.725	0.899	69.356
4000.	296.203	28.184	0.001	19.732	0.774	0.899	69.354
4250.	296.207	31.816	0.002	19.732	0.822	0.899	69.352
4500.	296.211	35.669	0.002	19.732	0.870	0.899	69.350
4750.	296.215	39.742	0.003	19.732	0.919	0.899	69.348
5000.	296.219	44.036	0.003	19.732	0.967	0.899	69.346
5250.	296.224	48.549	0.004	19.732	1.015	0.900	69.343
5500.	296.228	53.282	0.005	19.732	1.064	0.900	69.341
5750.	296.233	58.236	0.006	19.732	1.112	0.900	69.338
6000.	296.238	63.409	0.007	19.732	1.160	0.900	69.335
6250.	296.244	68.803	0.008	19.732	1.209	0.900	69.332
6500.	296.249	74.416	0.009	19.732	1.257	0.900	69.329
6750.	296.255	80.250	0.011	19.732	1.305	0.900	69.326
7000.	296.261	86.304	0.013	19.732	1.354	0.900	69.323
7250.	296.268	92.577	0.014	19.732	1.402	0.901	69.320
7500.	296.274	99.071	0.017	19.732	1.450	0.901	69.316
7750.	296.281	105.784	0.019	19.732	1.499	0.901	69.313
8000.	296.288	112.718	0.021	19.732	1.547	0.901	69.309
8250.	296.295	119.872	0.024	19.732	1.595	0.901	69.305
8500.	296.302	127.245	0.027	19.732	1.644	0.902	69.301
8750.	296.310	134.838	0.031	19.732	1.692	0.902	69.297
9000.	296.318	142.652	0.034	19.732	1.740	0.902	69.293
9250.	296.326	150.685	0.038	19.732	1.789	0.902	69.288
9500.	296.334	158.938	0.043	19.732	1.837	0.902	69.284
9750.	296.342	167.410	0.047	19.732	1.885	0.903	69.280
10000.	296.351	176.103	0.052	19.732	1.934	0.903	69.275
20000.	296.879	705.785	0.837	19.730	3.862	0.916	68.994
40000.	298.980	2805.194	13.294	19.724	7.688	0.967	67.919
60000.	302.450	6275.075	66.522	19.714	11.441	1.048	66.274
80000.	307.242	11067.034	206.916	19.700	15.090	1.150	64.218
100000.	313.295	17120.366	495.181	19.681	18.611	1.270	61.899

GEOMETRIC PARAMETERS (ALONG TRACK)

ALTITUDE: 278. KM CROSS TRACK DIST: 260. KM D= 0.064

ALONG TRACK DIST (M)	RANGE (KM)	RANGE CHG (M)	RANGE CHG-H0 (M)	ELEV ANGL (DEG)	AZIM ANGL (DEG)	GEOC ANGL (DEG)	GRAZE ANGL (DEG)
0.	384.474	0.0	0.000	42.537	0.0	2.336	45.128
250.	384.486	11.368	-0.000	42.538	0.037	2.336	45.126
500.	384.497	22.906	-0.001	42.540	0.074	2.336	45.124
750.	384.509	34.613	-0.002	42.542	0.112	2.336	45.122
1000.	384.521	46.490	-0.003	42.543	0.149	2.336	45.120
1250.	384.533	58.538	-0.004	42.545	0.186	2.336	45.118
1500.	384.545	70.755	-0.006	42.547	0.223	2.336	45.116
1750.	384.558	83.141	-0.008	42.548	0.261	2.337	45.114
2000.	384.570	95.698	-0.010	42.550	0.298	2.337	45.112
2250.	384.583	108.424	-0.013	42.552	0.335	2.337	45.110
2500.	384.596	121.320	-0.016	42.553	0.372	2.337	45.108
2750.	384.609	134.386	-0.018	42.555	0.409	2.337	45.106
3000.	384.622	147.621	-0.022	42.557	0.447	2.337	45.104
3250.	384.635	161.026	-0.025	42.558	0.484	2.338	45.102
3500.	384.649	174.601	-0.028	42.560	0.521	2.338	45.100
3750.	384.663	188.345	-0.032	42.562	0.558	2.338	45.097
4000.	384.677	202.259	-0.036	42.563	0.595	2.338	45.095
4250.	384.691	216.342	-0.039	42.565	0.632	2.338	45.093
4500.	384.705	230.595	-0.043	42.567	0.670	2.338	45.090
4750.	384.719	245.018	-0.047	42.568	0.707	2.339	45.088
5000.	384.734	259.610	-0.051	42.570	0.744	2.339	45.086
5250.	384.749	274.372	-0.055	42.572	0.781	2.339	45.083
5500.	384.764	289.303	-0.059	42.573	0.818	2.339	45.081
5750.	384.779	304.404	-0.063	42.575	0.856	2.339	45.079
6000.	384.794	319.674	-0.067	42.577	0.893	2.340	45.076
6250.	384.810	335.114	-0.071	42.578	0.930	2.340	45.074
6500.	384.825	350.723	-0.074	42.580	0.967	2.340	45.071
6750.	384.841	366.501	-0.078	42.582	1.004	2.340	45.068
7000.	384.857	382.449	-0.081	42.583	1.041	2.340	45.066
7250.	384.873	398.566	-0.085	42.585	1.078	2.341	45.063
7500.	384.889	414.852	-0.088	42.587	1.116	2.341	45.061
7750.	384.906	431.308	-0.091	42.588	1.153	2.341	45.058
8000.	384.922	447.933	-0.094	42.590	1.190	2.341	45.055
8250.	384.939	464.728	-0.096	42.592	1.227	2.341	45.053
8500.	384.956	481.691	-0.099	42.593	1.264	2.342	45.050
8750.	384.973	498.824	-0.101	42.595	1.301	2.342	45.047
9000.	384.991	516.126	-0.103	42.597	1.338	2.342	45.044
9250.	385.008	533.598	-0.104	42.598	1.376	2.342	45.041
9500.	385.026	551.238	-0.105	42.600	1.413	2.343	45.039
9750.	385.043	569.047	-0.106	42.602	1.450	2.343	45.036
10000.	385.061	587.026	-0.106	42.603	1.487	2.343	45.033
20000.	385.919	1444.547	0.499	42.668	2.968	2.354	44.895
40000.	388.438	3963.324	11.592	42.793	5.906	2.386	44.494
60000.	392.010	7535.584	54.028	42.911	8.796	2.431	43.939
80000.	396.607	12132.808	156.525	43.021	11.627	2.488	43.246
100000.	402.194	17719.788	353.689	43.125	14.383	2.556	42.434

GEOMETRIC PARAMETERS (ALONG TRACK)

ALTITUDE: 278. KM CROSS TRACK DIST: 100. KM D= 0.064

ALONG TRACK DIST (M)	RANGE (KM)	RANGE CHG (M)	RANGE CHG-HO (M)	ELEV ANGL (DEG)	AZIM ANGL (DEG)	GEOC ANGL (DEG)	GRAZE ANGL (DEG)
0.	296.175	0.0	0.000	19.732	0.0	0.898	69.370
250.	296.181	5.745	-0.000	19.735	0.048	0.898	69.366
500.	296.187	11.711	-0.002	19.738	0.097	0.899	69.363
750.	296.193	17.898	-0.004	19.741	0.145	0.899	69.360
1000.	296.199	24.307	-0.006	19.744	0.193	0.899	69.356
1250.	296.206	30.936	-0.010	19.747	0.242	0.899	69.353
1500.	296.213	37.785	-0.014	19.750	0.290	0.899	69.349
1750.	296.220	44.856	-0.019	19.752	0.338	0.899	69.345
2000.	296.227	52.148	-0.024	19.755	0.387	0.900	69.341
2250.	296.235	59.661	-0.030	19.758	0.435	0.900	69.337
2500.	296.242	67.394	-0.037	19.761	0.483	0.900	69.333
2750.	296.250	75.348	-0.045	19.764	0.532	0.900	69.329
3000.	296.259	83.523	-0.053	19.767	0.580	0.900	69.325
3250.	296.267	91.919	-0.062	19.770	0.628	0.901	69.320
3500.	296.276	100.536	-0.071	19.773	0.677	0.901	69.315
3750.	296.284	109.373	-0.081	19.776	0.725	0.901	69.311
4000.	296.293	118.432	-0.092	19.778	0.773	0.901	69.306
4250.	296.303	127.710	-0.103	19.781	0.822	0.902	69.301
4500.	296.312	137.210	-0.114	19.784	0.870	0.902	69.296
4750.	296.322	146.930	-0.126	19.787	0.918	0.902	69.291
5000.	296.332	156.871	-0.139	19.790	0.967	0.902	69.285
5250.	296.342	167.033	-0.152	19.793	1.015	0.903	69.280
5500.	296.352	177.415	-0.165	19.796	1.063	0.903	69.274
5750.	296.363	188.018	-0.179	19.799	1.112	0.903	69.268
6000.	296.374	198.841	-0.193	19.801	1.160	0.903	69.263
6250.	296.385	209.885	-0.207	19.804	1.208	0.904	69.257
6500.	296.396	221.149	-0.222	19.807	1.256	0.904	69.251
6750.	296.408	232.634	-0.237	19.810	1.305	0.904	69.245
7000.	296.419	244.340	-0.252	19.813	1.353	0.905	69.238
7250.	296.431	256.266	-0.268	19.816	1.401	0.905	69.232
7500.	296.443	268.412	-0.284	19.819	1.450	0.905	69.225
7750.	296.456	280.778	-0.300	19.822	1.498	0.905	69.219
8000.	296.468	293.365	-0.316	19.824	1.546	0.906	69.212
8250.	296.481	306.173	-0.332	19.827	1.594	0.906	69.205
8500.	296.494	319.200	-0.349	19.830	1.643	0.906	69.198
8750.	296.507	332.448	-0.365	19.833	1.691	0.907	69.191
9000.	296.521	345.916	-0.382	19.836	1.739	0.907	69.184
9250.	296.535	359.605	-0.398	19.839	1.787	0.907	69.177
9500.	296.549	373.513	-0.415	19.842	1.836	0.908	69.169
9750.	296.563	387.642	-0.431	19.845	1.884	0.908	69.162
10000.	296.577	401.991	-0.448	19.847	1.932	0.908	69.154
20000.	297.331	1156.021	-0.624	19.961	3.856	0.927	68.757
40000.	299.883	3708.328	11.709	20.186	7.664	0.989	67.476
60000.	303.797	7621.697	72.225	20.405	11.389	1.077	65.674
80000.	309.019	12844.376	232.675	20.619	15.001	1.187	63.509
100000.	315.486	19311.288	558.134	20.828	18.476	1.312	61.122

GEOMETRIC PARAMETERS (ALONG TRACK)

ALTITUDE: 370. KM CROSS TRACK DIST: 260. KM D= 0.0

ALONG TRACK DIST (M)	RANGE (KM)	RANGE CHG (M)	RANGE CHG-HO (M)	ELEV ANGL (DEG)	AZIM ANGL (DEG)	GEOC ANGL (DEG)	GRAZE ANGL (DEG)
0.	456.521	0.0	0.000	34.706	0.0	2.336	52.958
250.	456.521	0.072	0.000	34.706	0.031	2.336	52.958
500.	456.521	0.289	0.000	34.706	0.063	2.336	52.958
750.	456.522	0.651	0.000	34.706	0.094	2.336	52.958
1000.	456.522	1.158	0.000	34.706	0.125	2.336	52.958
1250.	456.523	1.809	0.000	34.706	0.157	2.336	52.958
1500.	456.524	2.605	0.000	34.706	0.188	2.336	52.958
1750.	456.525	3.546	0.000	34.706	0.219	2.336	52.958
2000.	456.526	4.631	0.000	34.706	0.251	2.336	52.958
2250.	456.527	5.861	0.000	34.706	0.282	2.336	52.957
2500.	456.528	7.236	0.000	34.706	0.313	2.336	52.957
2750.	456.530	8.756	0.000	34.706	0.345	2.336	52.957
3000.	456.532	10.420	0.000	34.706	0.376	2.336	52.957
3250.	456.533	12.229	0.000	34.706	0.408	2.336	52.956
3500.	456.535	14.183	0.000	34.706	0.439	2.336	52.956
3750.	456.537	16.281	0.000	34.706	0.470	2.336	52.955
4000.	456.540	18.525	0.000	34.706	0.502	2.336	52.955
4250.	456.542	20.912	0.000	34.706	0.533	2.336	52.955
4500.	456.545	23.445	0.001	34.706	0.564	2.336	52.954
4750.	456.547	26.122	0.001	34.706	0.596	2.336	52.954
5000.	456.550	28.944	0.001	34.706	0.627	2.336	52.953
5250.	456.553	31.911	0.001	34.706	0.658	2.336	52.953
5500.	456.556	35.022	0.001	34.706	0.690	2.336	52.952
5750.	456.559	38.279	0.002	34.706	0.721	2.336	52.951
6000.	456.563	41.679	0.002	34.706	0.752	2.336	52.951
6250.	456.566	45.225	0.002	34.706	0.784	2.336	52.951
6500.	456.570	48.915	0.003	34.706	0.815	2.336	52.950
6750.	456.574	52.750	0.003	34.706	0.846	2.336	52.949
7000.	456.578	56.729	0.004	34.706	0.878	2.336	52.948
7250.	456.582	60.853	0.004	34.706	0.909	2.336	52.947
7500.	456.586	65.122	0.005	34.706	0.940	2.337	52.947
7750.	456.591	69.536	0.005	34.706	0.972	2.337	52.946
8000.	456.595	74.094	0.006	34.706	1.003	2.337	52.945
8250.	456.600	78.797	0.007	34.706	1.034	2.337	52.944
8500.	456.605	83.644	0.008	34.706	1.066	2.337	52.943
8750.	456.610	88.636	0.009	34.706	1.097	2.337	52.942
9000.	456.615	93.773	0.010	34.706	1.128	2.337	52.941
9250.	456.620	99.054	0.011	34.706	1.160	2.337	52.940
9500.	456.626	104.480	0.012	34.706	1.191	2.337	52.939
9750.	456.631	110.051	0.013	34.706	1.222	2.337	52.938
10000.	456.637	115.766	0.015	34.706	1.254	2.337	52.937
20000.	456.984	462.889	0.235	34.704	2.506	2.342	52.875
40000.	458.370	1848.748	5.749	34.697	5.002	2.363	52.626
60000.	460.670	4149.233	18.887	34.686	7.477	2.397	52.219
80000.	463.872	7350.714	59.276	34.670	9.922	2.444	51.666
100000.	467.956	11454.668	143.442	34.650	12.328	2.502	50.980

GEOMETRIC PARAMETERS (ALONG TRACK)

ALTITUDE: 370. KM CROSS TRACK DIST: 100. KM D= 0.0

ALONG TRACK DIST (M)	RANGE (KM)	RANGE CHG (M)	RANGE CHG-HD (M)	ELEV ANGL (DEG)	AZIM ANGL (DEG)	GEOC ANGL (DEG)	GRAZE ANGL (DEG)
0.	384.031	0.0	0.000	15.093	0.0	0.898	74.009
250.	384.031	0.086	0.000	15.093	0.037	0.898	74.009
500.	384.031	0.344	0.000	15.093	0.075	0.898	74.009
750.	384.032	0.775	0.000	15.093	0.112	0.898	74.008
1000.	384.032	1.377	0.000	15.093	0.149	0.898	74.008
1250.	384.033	2.152	0.000	15.093	0.186	0.898	74.008
1500.	384.034	3.099	0.000	15.093	0.224	0.898	74.007
1750.	384.035	4.218	0.000	15.093	0.261	0.898	74.007
2000.	384.037	5.509	0.000	15.093	0.298	0.898	74.006
2250.	384.038	6.973	0.000	15.093	0.336	0.899	74.005
2500.	384.040	8.608	0.000	15.093	0.373	0.899	74.004
2750.	384.042	10.416	0.000	15.093	0.410	0.899	74.003
3000.	384.043	12.396	0.000	15.093	0.448	0.899	74.002
3250.	384.046	14.548	0.000	15.093	0.485	0.899	74.001
3500.	384.048	16.872	0.000	15.093	0.522	0.899	74.000
3750.	384.050	19.368	0.000	15.093	0.559	0.899	73.998
4000.	384.053	22.037	0.001	15.093	0.597	0.899	73.997
4250.	384.056	24.877	0.001	15.093	0.634	0.899	73.995
4500.	384.059	27.890	0.001	15.093	0.671	0.899	73.993
4750.	384.062	31.075	0.001	15.093	0.709	0.899	73.992
5000.	384.066	34.432	0.002	15.093	0.746	0.899	73.990
5250.	384.069	37.961	0.002	15.093	0.783	0.900	73.988
5500.	384.073	41.662	0.002	15.093	0.820	0.900	73.986
5750.	384.077	45.535	0.003	15.093	0.858	0.900	73.984
6000.	384.081	49.581	0.003	15.093	0.895	0.900	73.981
6250.	384.085	53.798	0.004	15.093	0.932	0.900	73.979
6500.	384.089	58.188	0.004	15.093	0.970	0.900	73.977
6750.	384.094	62.750	0.005	15.093	1.007	0.900	73.974
7000.	384.099	67.483	0.006	15.093	1.044	0.900	73.972
7250.	384.103	72.389	0.007	15.093	1.081	0.901	73.969
7500.	384.109	77.467	0.008	15.093	1.119	0.901	73.966
7750.	384.114	82.717	0.009	15.093	1.156	0.901	73.963
8000.	384.119	88.139	0.010	15.093	1.193	0.901	73.960
8250.	384.125	93.733	0.011	15.093	1.231	0.901	73.957
8500.	384.131	99.500	0.013	15.093	1.268	0.902	73.954
8750.	384.137	105.438	0.014	15.093	1.305	0.902	73.951
9000.	384.143	111.548	0.016	15.093	1.342	0.902	73.947
9250.	384.149	117.830	0.018	15.093	1.380	0.902	73.944
9500.	384.155	124.284	0.020	15.093	1.417	0.902	73.940
9750.	384.162	130.911	0.022	15.093	1.454	0.903	73.937
10000.	384.169	137.709	0.025	15.093	1.491	0.903	73.933
20000.	384.582	550.539	0.395	15.092	2.981	0.916	73.707
40000.	386.229	2197.442	6.294	15.088	5.944	0.967	72.841
60000.	388.958	4926.768	31.640	15.082	8.873	1.048	71.507
80000.	392.747	8715.923	99.023	15.073	11.751	1.150	69.821
100000.	397.566	13534.569	238.784	15.063	14.566	1.270	67.894

GEOMETRIC PARAMETERS (ALONG TRACK)

ALTITUDE: 370. KM CROSS TRACK DIST: 260. KM D= 0.065

ALONG TRACK DIST (M)	RANGE (KM)	RANGE CHG (M)	RANGE CHG-H0 (M)	ELEV ANGL (DEG)	AZIM ANGL (DEG)	GEOC ANGL (DEG)	GRAZE ANGL (DEG)
0.	456.521	0.0	0.000	34.706	0.0	2.336	52.958
250.	456.531	9.839	-0.000	34.708	0.031	2.336	52.957
500.	456.541	19.824	-0.001	34.709	0.063	2.336	52.955
750.	456.551	29.953	-0.002	34.711	0.094	2.336	52.953
1000.	456.561	40.228	-0.003	34.713	0.125	2.336	52.951
1250.	456.572	50.648	-0.005	34.714	0.157	2.336	52.949
1500.	456.582	61.213	-0.007	34.716	0.188	2.336	52.947
1750.	456.593	71.922	-0.009	34.717	0.219	2.337	52.945
2000.	456.604	82.777	-0.012	34.719	0.251	2.337	52.943
2250.	456.615	93.777	-0.015	34.721	0.282	2.337	52.941
2500.	456.626	104.922	-0.018	34.722	0.313	2.337	52.939
2750.	456.637	116.213	-0.022	34.724	0.345	2.337	52.937
3000.	456.649	127.648	-0.026	34.726	0.376	2.337	52.935
3250.	456.660	139.228	-0.030	34.727	0.407	2.338	52.933
3500.	456.672	150.953	-0.035	34.729	0.439	2.338	52.931
3750.	456.684	162.823	-0.039	34.730	0.470	2.338	52.929
4000.	456.696	174.838	-0.044	34.732	0.501	2.338	52.927
4250.	456.708	186.998	-0.050	34.734	0.533	2.338	52.925
4500.	456.720	199.303	-0.055	34.735	0.564	2.339	52.922
4750.	456.733	211.753	-0.061	34.737	0.595	2.339	52.920
5000.	456.745	224.347	-0.067	34.738	0.627	2.339	52.918
5250.	456.758	237.087	-0.073	34.740	0.658	2.339	52.915
5500.	456.771	249.972	-0.079	34.742	0.689	2.339	52.913
5750.	456.784	263.001	-0.085	34.743	0.721	2.339	52.911
6000.	456.797	276.175	-0.092	34.745	0.752	2.340	52.908
6250.	456.811	289.495	-0.098	34.746	0.783	2.340	52.906
6500.	456.824	302.959	-0.105	34.748	0.815	2.340	52.904
6750.	456.838	316.568	-0.112	34.750	0.846	2.340	52.901
7000.	456.851	330.321	-0.119	34.751	0.877	2.340	52.899
7250.	456.865	344.220	-0.126	34.753	0.909	2.341	52.896
7500.	456.879	358.263	-0.133	34.754	0.940	2.341	52.894
7750.	456.894	372.451	-0.140	34.756	0.971	2.341	52.891
8000.	456.908	386.784	-0.148	34.758	1.002	2.341	52.888
8250.	456.922	401.262	-0.155	34.759	1.034	2.342	52.886
8500.	456.937	415.884	-0.162	34.761	1.065	2.342	52.883
8750.	456.952	430.651	-0.169	34.762	1.096	2.342	52.880
9000.	456.967	445.563	-0.177	34.764	1.128	2.342	52.878
9250.	456.982	460.620	-0.184	34.766	1.159	2.342	52.875
9500.	456.997	475.821	-0.191	34.767	1.190	2.343	52.872
9750.	457.012	491.167	-0.198	34.769	1.221	2.343	52.870
10000.	457.028	506.657	-0.205	34.770	1.253	2.343	52.867
20000.	457.766	1244.713	-0.247	34.834	2.502	2.354	52.734
40000.	459.931	3410.199	4.983	34.956	4.985	2.386	52.349
60000.	463.005	6483.502	28.644	35.074	7.439	2.431	51.814
80000.	466.968	10446.652	88.706	35.186	9.856	2.488	51.144
100000.	471.798	15277.172	207.648	35.294	12.226	2.557	50.354

GEOMETRIC PARAMETERS (ALONG TRACK)

ALTITUDE: 370. KM CROSS TRACK DIST: 100. KM D= 0.065

ALONG TRACK DIST (M)	RANGE (KM)	RANGE CHG (M)	RANGE CHG-HD (M)	ELEV ANGL (DEG)	AZIM ANGL (DEG)	GEOC ANGL (DEG)	GRAZE ANGL (DEG)
0.	384.031	0.0	0.000	15.093	0.0	0.898	74.009
250.	384.036	4.553	-0.000	15.095	0.037	0.898	74.006
500.	384.040	9.279	-0.001	15.098	0.075	0.899	74.004
750.	384.045	14.177	-0.003	15.100	0.112	0.899	74.001
1000.	384.050	19.249	-0.005	15.102	0.149	0.899	73.998
1250.	384.056	24.493	-0.008	15.105	0.186	0.899	73.995
1500.	384.061	29.910	-0.012	15.107	0.224	0.899	73.992
1750.	384.067	35.500	-0.016	15.109	0.261	0.899	73.989
2000.	384.072	41.263	-0.021	15.112	0.298	0.900	73.986
2250.	384.078	47.198	-0.026	15.114	0.336	0.900	73.983
2500.	384.084	53.307	-0.033	15.116	0.373	0.900	73.979
2750.	384.091	59.588	-0.039	15.118	0.410	0.900	73.976
3000.	384.097	66.041	-0.046	15.121	0.447	0.900	73.972
3250.	384.104	72.668	-0.054	15.123	0.485	0.901	73.969
3500.	384.111	79.467	-0.063	15.125	0.522	0.901	73.965
3750.	384.118	86.439	-0.072	15.128	0.559	0.901	73.961
4000.	384.125	93.584	-0.081	15.130	0.597	0.901	73.957
4250.	384.132	100.901	-0.091	15.132	0.634	0.902	73.953
4500.	384.139	108.391	-0.102	15.135	0.671	0.902	73.949
4750.	384.147	116.054	-0.113	15.137	0.708	0.902	73.945
5000.	384.155	123.890	-0.125	15.139	0.746	0.902	73.940
5250.	384.163	131.898	-0.137	15.142	0.783	0.903	73.936
5500.	384.171	140.079	-0.150	15.144	0.820	0.903	73.932
5750.	384.180	148.432	-0.163	15.146	0.857	0.903	73.927
6000.	384.188	156.958	-0.176	15.149	0.895	0.903	73.922
6250.	384.197	165.657	-0.190	15.151	0.932	0.904	73.918
6500.	384.206	174.528	-0.205	15.153	0.969	0.904	73.913
6750.	384.215	183.572	-0.220	15.156	1.007	0.904	73.908
7000.	384.224	192.789	-0.235	15.158	1.044	0.905	73.903
7250.	384.233	202.178	-0.251	15.160	1.081	0.905	73.897
7500.	384.243	211.740	-0.267	15.162	1.118	0.905	73.892
7750.	384.253	221.474	-0.284	15.165	1.156	0.905	73.887
8000.	384.262	231.381	-0.301	15.167	1.193	0.906	73.881
8250.	384.273	241.460	-0.318	15.169	1.230	0.906	73.876
8500.	384.283	251.712	-0.336	15.172	1.267	0.906	73.870
8750.	384.293	262.136	-0.354	15.174	1.305	0.907	73.865
9000.	384.304	272.733	-0.372	15.176	1.342	0.907	73.859
9250.	384.315	283.502	-0.391	15.179	1.379	0.907	73.853
9500.	384.326	294.444	-0.410	15.181	1.416	0.908	73.847
9750.	384.337	305.558	-0.429	15.183	1.453	0.908	73.841
10000.	384.348	316.845	-0.448	15.186	1.491	0.909	73.835
20000.	384.941	909.498	-1.238	15.278	2.978	0.928	73.514
40000.	386.948	2916.561	1.828	15.459	5.933	0.989	72.478
60000.	390.035	6004.218	26.168	15.638	8.848	1.078	71.009
80000.	394.178	10147.040	97.211	15.814	11.708	1.187	69.226
100000.	399.343	15312.140	247.844	15.986	14.499	1.312	67.234

2.3 OPTICAL RECORDING

SAR video data which is to be optically processed is first recorded as a spatial signal on a long strip of photographic film (transparency). The writing beam of the recorder scans across the film width (y-direction) as the film is transported in the orthogonal x-direction past the scan line. The radar return from individual transmitted pulses is recorded so as to extend over the width of the film. Successive pulses occur side by side extending in the direction of the film length as shown in Figure 3.

2.3.1 RECORDING PARAMETERS

The scan speed V_y for the writing beam across the film width and the film speed V_x are selected to scale the radar signal bandwidths to that of the recorder. We will denote the recorder spatial bandwidth as B_y and B_x. With radar signal bandwidth B_r for the chirp or other modulation, used with an offset f_o; and azimuth (Doppler) bandwidth B_a, we require the recording speeds

$$V_y = \frac{1}{B_y}\left(\frac{B_r}{2} + f_o\right) \text{ and } V_x = \frac{1}{B_x}\left(\frac{B_a}{2}\right)$$

It should be noted that any offset frequency (carrier) in the signal to be recorded must be included, as shown, in the definition of the video signal bandwidth.

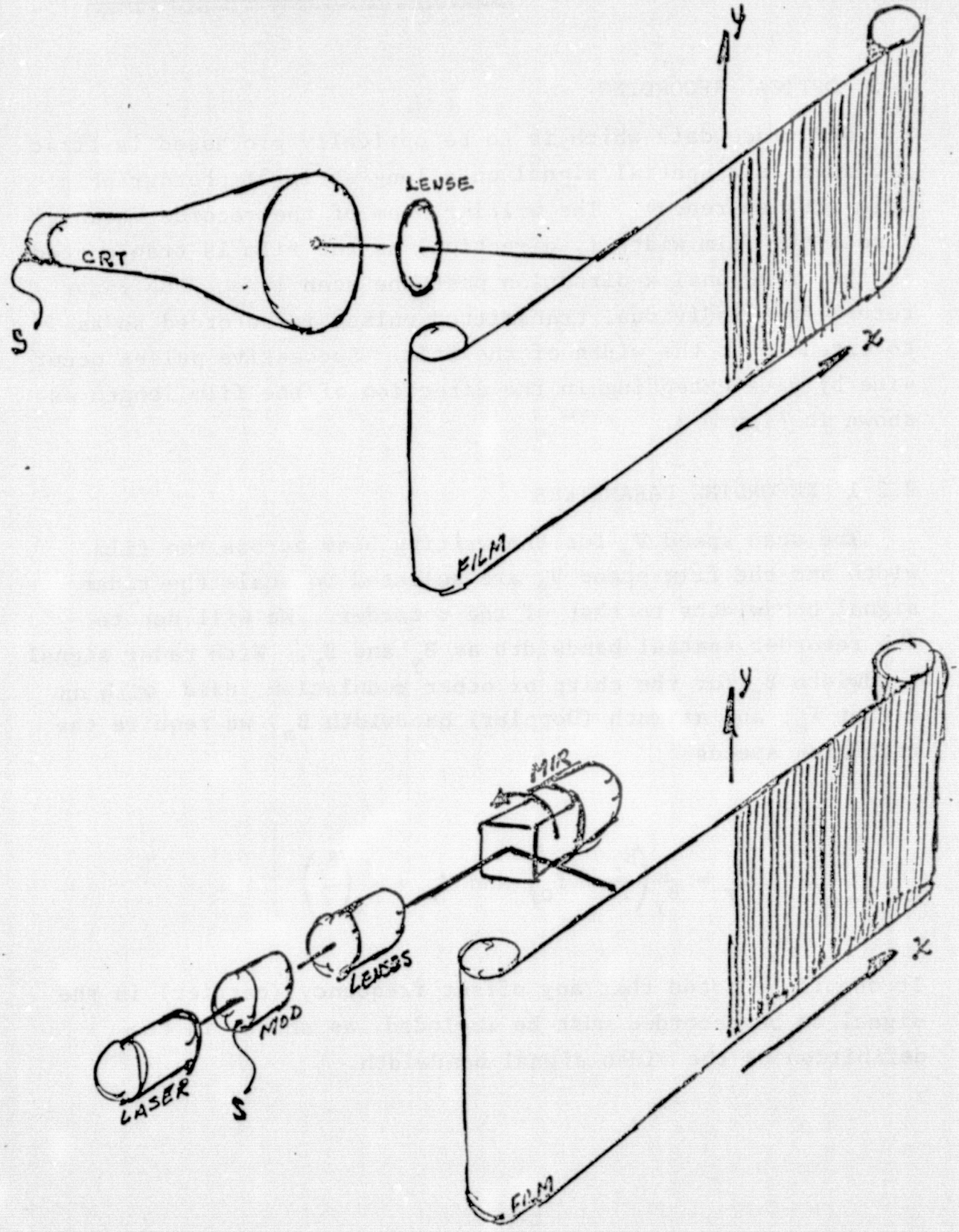

FIGURE 3. CRT/FILM AND LASER/FILM RECORDERS, FUNCTIONAL DIAGRAMS.

The radar measurement coordinates, slant range and azimuth distance, will be scaled to the recording film coordinates y and x respectively. Denoting the range and azimuth scale factors as q and p, respectively, we require

$$q = \frac{V_r}{V_y} \text{ and } p = \frac{V}{V_x}$$

where $V_r = c/2$ is the two way propagation velocity of the radar signal and V is the along-track velocity of the radar platform. Common units must be used for these velocities.

The video signal variables from the time domain when scaled to the spatial domain become:

$$(t' - \frac{2r}{c}) \rightarrow (y - \frac{r}{q}) \frac{2q}{c}$$

$$(u_s - u_t) \rightarrow (x - \frac{u_t}{p}) \, p$$

The recorded scan line length (or approximate film width) Y is a scaled representation of the slant range interval ΔR and is expressed as

$$Y = \Delta R(\frac{1}{q})$$

The film length X, for an along track strip map run of T_x seconds will be

$$X = V_x T_x (\frac{1}{p})$$

2.3.2 RECORDED SIGNAL PROPERTIES

The analog form of the radar signal is recorded on film. This signal is of course bi-polar and must have a DC or bias level added to it prior to optical recording in order to fit the non-bipolar response of the recording film. The expression for the video signal when scaled to the spatial variables in recording will be

$$s_r = a_r(y-y_t)e^{-j\left[\frac{1}{2}k'_r(y-y_t)^2 + w'_o\, y\right]}$$

$$s_a = a_a(x-x_t)e^{-j\left[\frac{1}{2}k'_a(x-x_t)^2 + w'_a(x-x_t)\right]}$$

with $\quad k'_r = \frac{4q^2}{c^2}\, k_r,\ k'_a = p^2\, k_a,\ w'_o = \frac{2q}{c}\, w_o,\ w'_a = \frac{2Bp}{\lambda}$

For a single point target the analog form of the radar signal being recorded will be the familiar sampled, and approximately linear FM (quardatic phase) signal in its azimuth (along-track) dimension. In the range dimension the signal will be essentially a repeat of the transmitted signal modulation (unless it has been electronically compressed) with time delay defined by transmission path length between target and radar. If the transmitted signal is linearly frequency modulated then the two dimensional recording for a point target signal history will be a two-dimensional linear FM signal with the appearance of a set of concentric rings which are typically asymmetric x to y as shown in Figure 4. Optically, this recorded pattern is classified as a Fresnel zone plate. If the frequency spectrum of the radar signal was not centered on zero frequency the recorded data will be an off center section of a zone plate as shown in Figure 5.

If the radar data has been compressed in range prior to optical recording then the recorded point target history

FIGURE 4. ZONE PLATE, TWO-DIMENSIONAL

FIGURE 6. ZONE PLATE, ONE-DIMENSIONAL

Range offset

Azimuth offset

Range-Azimuth offset

FIGURE 5. ZONE PLATE, TWO-DIMENSIONAL, OFFSET

will be a line comprised of a one-dimensional zone plate in the x or azimuth dimension as shown in Figure 6.

The sketch of a point target history given in Figures 4, 5, and 6 is for the case where the range from the radar to the point target is essentially constant as the target passes through the radar antenna pattern. For many SAR applications the radar to target range departs from being a constant by an insignificant amount (less than a resolution element size). However, for the antenna azimuth beamwidth and range values expected for some spaceborne SAR, and for the case of non-stationary targets, departures from constant range of several resolution elements may occur over the azimuth data aperture. This change in range from a constant value will typically be dominated by a quadratic and/or linear variation, although higher order changes do exist.

Non-constant range during a point target signal history can affect the signal in mainly two ways: envelope shift and frequency or phase shift. We will discuss some of the envelope shift properties a bit further. Significant departure from constant range is referred to as range curvature (or quadratic envelope shift) and range walk (or linear envelope shift) for quadratic and linear range changes respectively. A sketch of a point target signal recording which includes these distortions is shown in Figure 7 for range curvature and for range walk. The sketch of these distortions in Figure 7 is shown in considerably exaggerated proportions. The amount of curvature and walk will vary with range or the y dimension of the recording film. Curvature will be slightly greater at far range than at near range, over a fixed size azimuth beamwdith. Walk due to a target cross track velocity component can be considerably greater at far range than at near range.

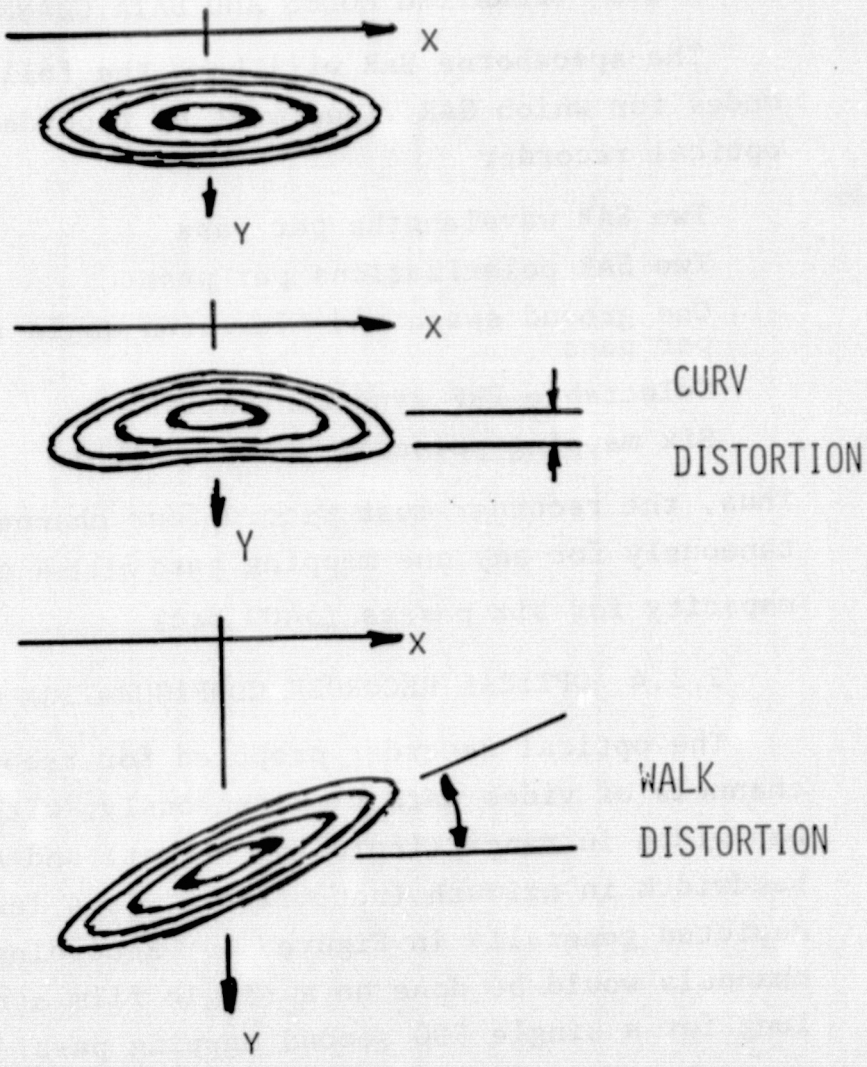

RECORDED POINT TARGET (ZONE PLATE) SIGNALS

Figure 7

2.3.3 OPERATING MODES AND DATA CHANNELS

The spaceborne SAR will have the following operating modes for which SAR video must be recorded by a spaceborne optical recorder

Two SAR wavelengths per pass

Two SAR polarizations per pass

One ground swath and elevation angle (out of 3 possible) per pass

Selectable PRF synchronization

Six mapping passes (900 sec each)

Thus, the recorder must record four channels of data simultaneously for any one mapping pass with a total recording capacity for six passes (5400 sec).

2.3.4 OPTICAL RECORDER CONFIGURATION

The optical recorder proposed for recording four separate channels of video data simultaneously, with an 18 MHz temporal bandwidth in range (including offset) and a 600 Hz temporal bandwidth in azimuth (not offset), is a laser/film device depicted generally in Figure 8. Recording of the four data channels would be done on a single film strip 10" wide and 60' long for a single 900 second mapping pass (or 360' long for six passes). Though a single film strip is used each data channel within the recorder would have a separate scanner and intensity modulator for the writing laser beam. An acousto-optic scanner with a flat scanning field would be used. An electro-optic light intensity modulator would provide for modulation of the laser writing beam in proportion to the radar video signal.

RECORDER CONFIGURATION:

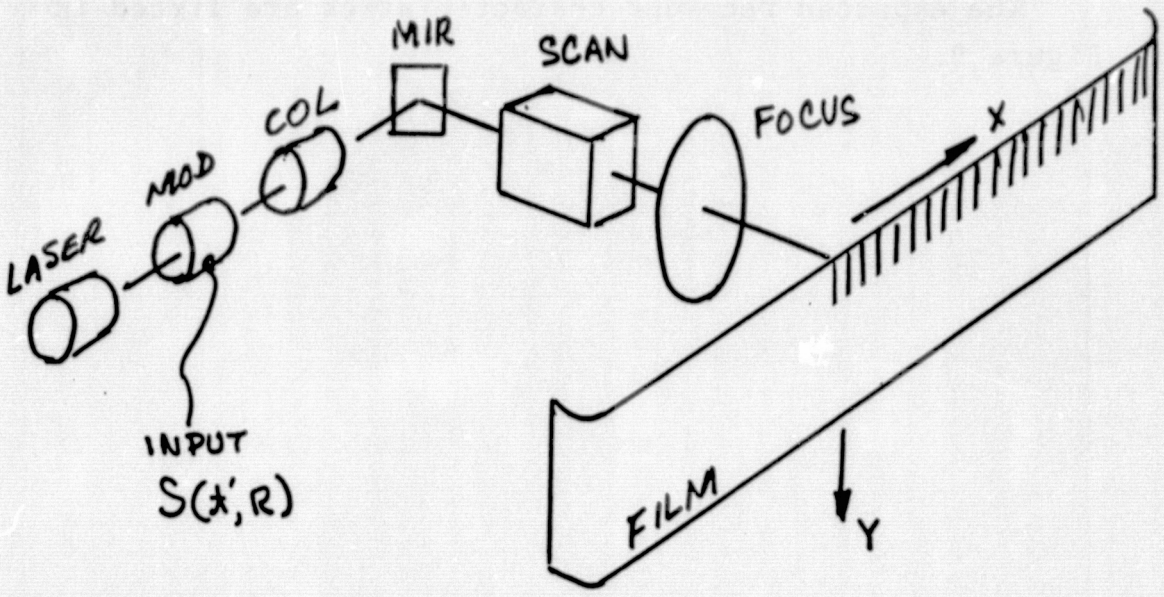

$q = 8.4 \times 10^5$ $p = 3.8 \times 10^5$

$\frac{B_a}{2} = 600$ Hz, $B_x = 30$ c/mm, $V_x = 20$ mm/sec

$B_r = 18$ MHz, $B_y = 100$ c/mm, $V_y = 1.8 \times 10^5$ mm/sec

Film: 10" wide x 60'/900 sec pass

Four adjacent channels

One channel shown

Figure 8.

An optical recorder of this type requires engineering development; however, the technology required has been well developed in various laser recorder programs and needs only to be directed toward the specific requirements herein.

The expected recorder characteristics are listed in Figure 9.

1 Spaceborne Unit (4-chan)

Laser/Film

Acousto-Optic Scanner

Electro-Optics Modulator

Flat Film Plane

Focus Lens

3" Wide Film x 360'/6 passes

B_x = 30 c/mm, B_y = 100 c/mm

Wt: 350 lb

Size: 4' x 1.6' x 2'

Power: 500 w

Figure 9. Recorder Configuration

2.4 OPTICAL PROCESSING

Data recorded on photographic film with the optical recorder is converted to map data by the coherent optical processor. The underlying concept involved is the same matched phase filter procedure described in terms of the electronic version of the radar video data in Section 2.1.2. A coherent optical processor, by nature of the hardware and physical principles involved, offers such unique features as instantaneous processing over large space-bandwidth product area signals such as those inherent with SAR data, and immediate viewing of map data at the processor output without use of special display devices.

In the spatial coordinates of the recorded data the radar signal for a point target is

$$s = s_r \cdot s_a$$

$$s_r = a_r(y-y_t)e^{-j\left[\frac{1}{2}k'_r(y-y_t)^2 + w'_{oy}\right]}$$

$$s_a = a_a(x-x_t)e^{-j\left[\frac{1}{2}k'_a(x-x_t)^2 + w'_a(x-x_t)\right]}$$

The optical processor with the matched phase response p_r and p_a provides an output $v(x,y)$ which can be written as

$$v = v_r \cdot v_a$$

$$v_r = \int s_r(y - y_t)p_p(y)\, dy$$

$$v_a = \int s_a(x - x_t)p_a(x)\, dx$$

The required processor response for the linear frequency modulation in s_r and s_a, when using light with wavelength λ_o, is

$$p_r = e^{j \frac{\pi}{\lambda_o z_r} y^2}$$

with

$$z_r = \frac{2\pi}{\lambda_o k'_r}$$

and

$$p_a = e^{j \frac{\pi}{\lambda_o z_a} x^2}$$

with

$$z_a = \frac{2\pi}{\lambda_o k'_a}$$

This process indicated by the above integrals for v is accomplished by illuminating the recorded signal (film) with a coherent plane wave of light as sketched in Figure 10. The point target signal history acts as an astigmatic Fresnel zone plate causing the light passing through it to focus. The light does not focus to a single point since the focal lengths differ in the range (y direction) and azimuth (x direction)

PROCESSING CONCEPT

$$V_R(Y_T) = \int S_R(Y - Y_T)\, P_R(Y)\, DY \qquad \text{RANGE}$$

$$V_A(X_T) = \int S_A(X - X_T) P_A(X)\, .\, DX \qquad \text{AZIMUTH}$$

MATCHED PHASE FILTER FUNCTIONS

$$P_R = E^{J \frac{\pi}{\lambda_o Z_R} Y^2} \qquad Z_R = \frac{2}{\lambda_o K_R'} \qquad \text{RANGE}$$

$$P_A = E^{J \frac{\pi}{\lambda_o Z_A} X^2} \qquad Z_A = \frac{2\pi}{\lambda_o K_A'} \qquad \text{AZIMUTH}$$

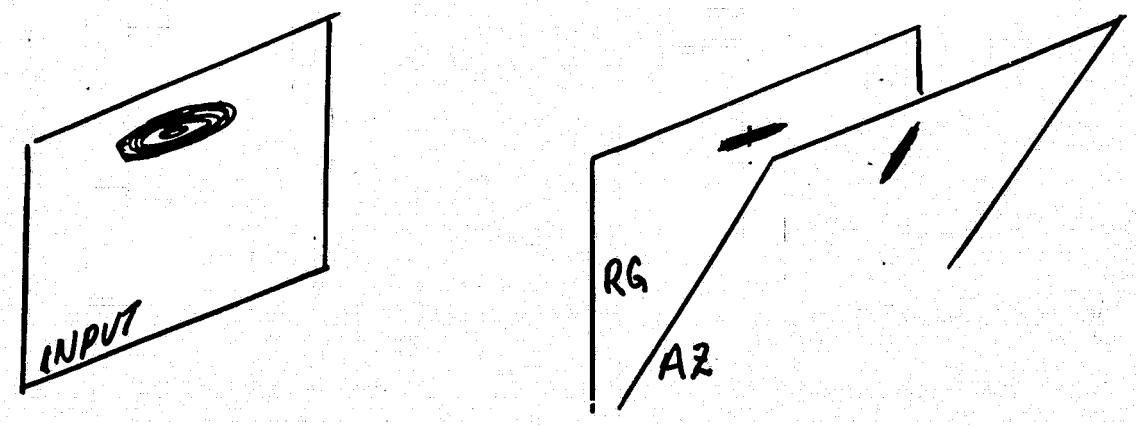

Figure 10.

as indicated by the focal length expressions z_r and z_a above. Rather, focus occurs at separate planes for each dimension, as shown in Figure 10. As suggested in Figure 10, the azimuth focal plane is tilted relative to the range focal plane. This is an inherent property of the radar signal caused by the fact that the azimuth focal length z_a is dependent on radar to target slant range which, of course, varies over the swath being mapped.

Functionally, optical processing consists of utilizing the optical focusing properties of the recorded radar data as described above, together with appropriate optical components which serve (a) to cause the range and azimuth focal planes to coincide at the output (map) plane of the processor; (b) to compensate if needed for any peculiarities inherent in the radar signal such as range curvature and range walk; and, (c) to provide added functions such as mixed integration, map coordinate conversion from slant range to ground range, or aperture weighting.

The proposed optical processor is the decoupled tilted-plane type depicted in its top and side views in the sketch of Figure 11. It is comprised of an input (radar signal) film, liquid gate and transport, a spherical followed by a cylindrical telescopic lense set, an output map film and transport, a collimated laser light source, and components not shown which serve auxilliary functions such as mixed integration and spatial filtering. The input signal film, which would contain four separate data channels across the film width, would be processed a single channel at a time. Each data channel has a maximum width of 58 mm. Figure 12 lists expected processor design parameters.

The two spherical lenses form a spherical telescope which images the focussed data from the y or range dimension

OPTICAL PROCESSOR
(DE-COUPLED, TILTED)

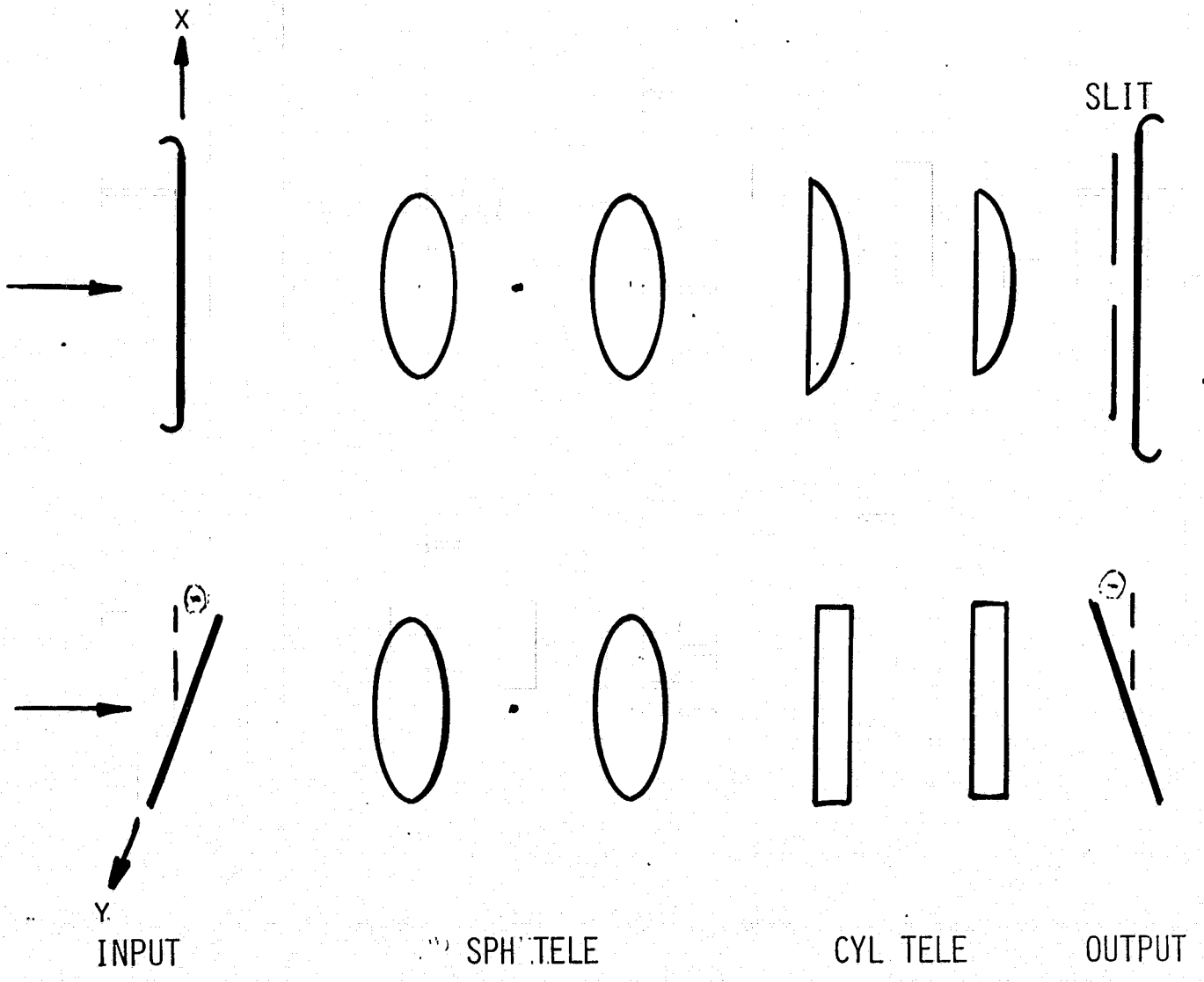

Figure 11.

Wavelength (Light)

$$\lambda_o = .632\ \mu m$$

Input Aperture

$$x = 40\ mm,\ y = 70\ mm$$

Spatial Bandwidth

$$B_x = 100\ c/mm,\ B_y = 100\ mm$$

Aspect Ratio

$$K = \frac{q}{p} = 2.2$$

Tilt Angle

$$\theta = \sin \frac{\lambda}{2q\lambda_o} \left(\frac{K^2}{K^2 - 1} \right) = \begin{cases} 16^o (L) \\ 2.2^o (X) \end{cases}$$

Magnification

$$M_x = \frac{1}{K},\ M_y = 1$$

Single Data Channel Processing

Mixed Integration

Curvature & Walk Correction

Figure 12. Optical Processing Parameters

onto the output film plane with a lateral magnification M_y of unity. The two cylindrical lenses form a cylindrical telescope with a lateral magnification in azimuth of M_x and a corresponding axial magnification of M_x^2. The combined affect of axial magnification with a tilt of the film planes by a prescribed angle θ brings the range and azimuth focal planes into co-incidence at the processor output plane.

The inherent focal lengths of the recorded data and the required tilt for the processor film planes are dependent on radar wavelength. The adjustment required in the processor to accommodate L and X band data is straight forward and consists of a change in film plane tilt angle θ and a small axial shift of the input film plane relative to the lenses.

2.4.1 MIXED INTEGRATION

Mixed integration of processed radar data has been specified as a requirement by the radar systems designer. It will serve to smooth or lowpass filter the resultant map data while also affecting resolution and signal to clutter ratio. Several types of hardware implementation of mixed integration are possible in the optical processor. The results obtained, though different in some detailed aspects for the various hardware implementations, will not differ significantly in the final map data obtainable. The basic provision in mixed integration is a summation of the processor output over corresponding sub-apertures of the input radar data. The basis

for accomplishing this operation lies in low pass filtering in the spatial frequency domain or making the spatial impulse response broader.

In the frequency domain, this can be accomplished by sub-aperture or low pass filtering of the spatial frequency spectrum of the recorded radar data. Denoting the signal spectrum as S(w), the sub-aperture filter function as H(w), and the processor matched filter response (corresponding to p) as P(w), we have a map output v that can be written in x and y dimensions as

$$v(x,y) = \mathcal{F}^{-1}\left[H(w_x,w_y) \cdot H.(w_x,w_y)\ P(w_x,w_y)\right]$$

The operator $\mathcal{F}^{-1}$ indicates the inverse Fourier transform operation. The initial Fourier transform is normally available in the processor, without special provisions, at the plane between the spherical elements of the spherical telescope. $H(w_x,w_y)$ is realized simply as a window or aperture whose size is selected based upon the desired sub-aperture size or mixed integration factor. The above expression for the output v(x,y) after sub-aperture filtering represents the case for a single sub-aperture that is fixed in position. Shifting the aperture for $H(w_x,w_y)$ about the signal spectrum will be indicated by $H(w_x,w_y) \rightarrow H(w_x-w_1,\ w_y-w_2)$ where w_1 and w_2 characterize the position shift, thus we have

$$v(x,y) = \mathcal{F}^{-1}\left[S(w_x,w_y)\ H(w_x-w_1,\ w_y-w_2)\ P(w_x,w_y)\right]$$

Finally, as is typically the case, we observe the light intensity $|v|^2$ at the processor output (map) plane and therefore realize a summation of intensities for all position of H(w). Thus, a non-coherent (intensity) summation for data from the coherent sub-apertures defined by H is obtained and can be written as

$$|v(x,y)|^2 = \int_{w_x,w_y} \left| \mathcal{F}^{-1} \left[S(w_x,w_y)\ H(w_x-w_1,\ w_y-w_2)\ P(w_x,w_y) \right] \right|^2$$

In the spatial domain mixed integration is obtained by convolving the output intensity $|v|^2$ with an aperture function h. This operation can be expressed as

$$|v(x,y)|^2 = |s(x,y)\ p(x,y)|^2 * h(x,y)$$

where * denotes convolution and $|s * p|^2$ is the light intensity output normally available without mixed integration. The width and shape of the aperture function h is readily selectable.

The equivalent sub-apertures used in mixed integration process can be scanned in a continuous, or a stepwise manner. It can be shown that the continuous (overlapping) scan gives a slightly greater mixed integration affect than does a non-overlapping stepwise scan; however, the difference can be accounted for in the design so that a specified mixed integration affect can be provided.

2.4.2 RANGE CURVATURE AND WALK COMPENSATION

Departure of the radar point target signal from its undistored two-dimensional linear FM form can occur when the radar to target range departs from a constant value by more than $\pm \frac{1}{4}\rho_r$ during a point target signal history. In terms of radar to target range r we have

$$r = R + Au^2 + Bu$$

$$Au^2 \geq \pm \frac{1}{4}\rho_r \quad \text{Curvature}$$

$$Bu \geq \pm \frac{1}{4}\rho_r \quad \text{Walk}$$

The significant aspects of such distortion are a change in shape of the two dimensional point target history due to envelope shift; and, a change in the frequency of the azimuth portion (s_a) of the radar signal in proportion to range walk.

A quadratically varying envelope shift due to range curvature causes the signal to lie on a curved rather than straight, constant range, path. A linear envelope shift due to range walk causes the signal to lie on a path that is tilted relative to a straight, constant range, path. See Figure 7.

Curvature distortion will be less than four range resolution elements and a corrective compensation can readily be implemented in the optical processor. The distortion will not be constant over the ground swath being mapped, therefore, a small departure from full compensation may be experienced over a swath interval. The several methods of curvature correction possible are:

Frequency plane correction holographic filter.
Processing lens compensation.
Recording format compensation.
Chirp modulation balancing compensation.

An example of the compensation realized with a frequency plane correction filter for a one-dimensional signal is shown in Figure 13.

Envelope shift distortion due to range walk is readily compensated for by a rotation of the azimuth lens of the optical processor and the output plane as indicated in Figure 14. Range walk can be characterized by a rotation of a point target signal history through an angle Ω in radar space and Ω_f in recording space. The angle Ω_f is a scaled equivalent of the departure of the radar antenna boresight in azimuth from the zero doppler position in the presence of earth's rotation. At the equator Ω can reach $\pm 3.5^{o}$ for a polar orbit.

The presence of range walk due to earth's rotation also gives rise to an azimuth offset frequency ω_a' as noted in Section 2.3.2 and it should be removed prior to optical recording by antenna steering or a clutterlock. In addition, azimuth spectrum wander to antenna azimuth drift should be removed with a clutterlock before recording.

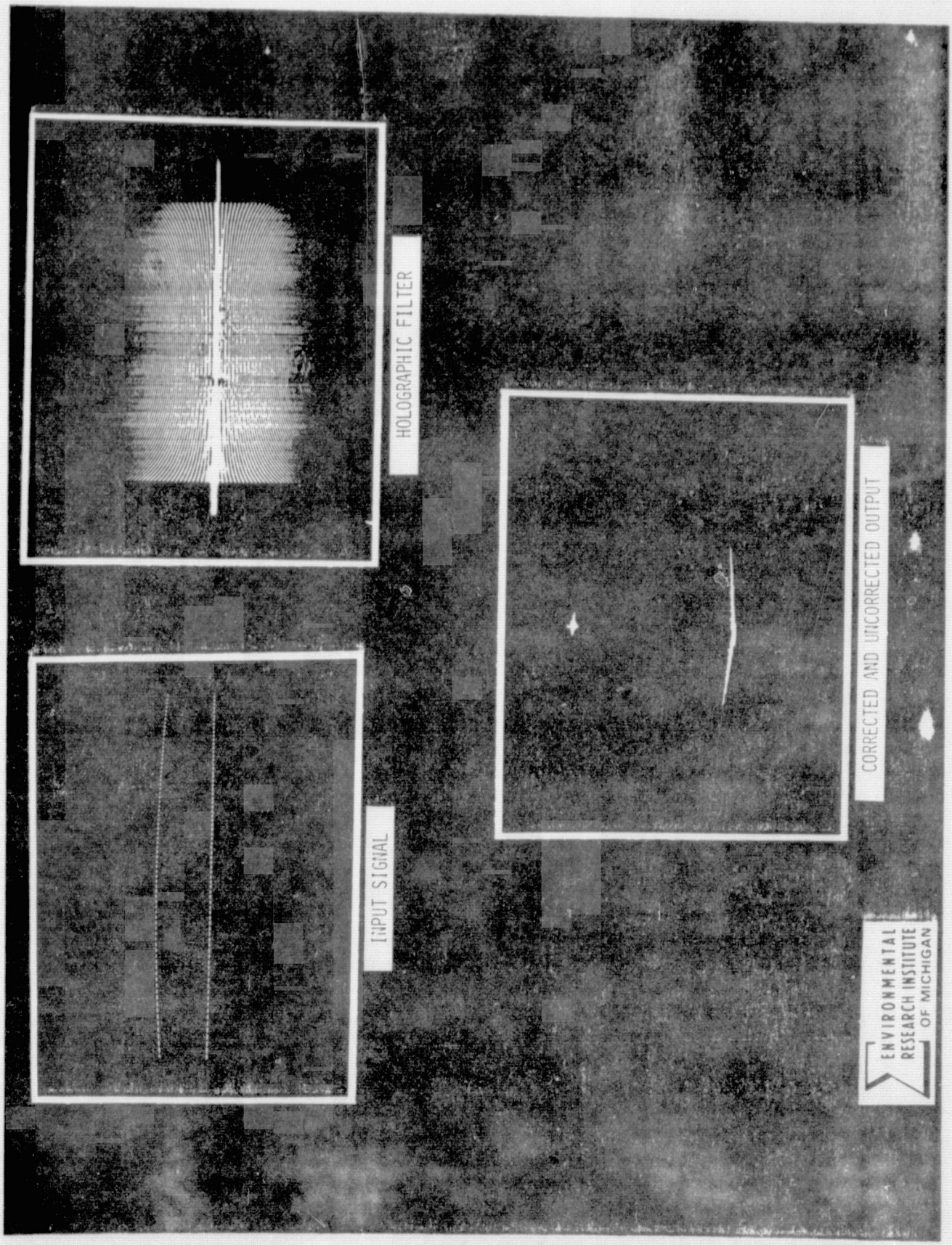

Figure 13(a)

Figure 13(b)

RANGE WALK COMPENSATION

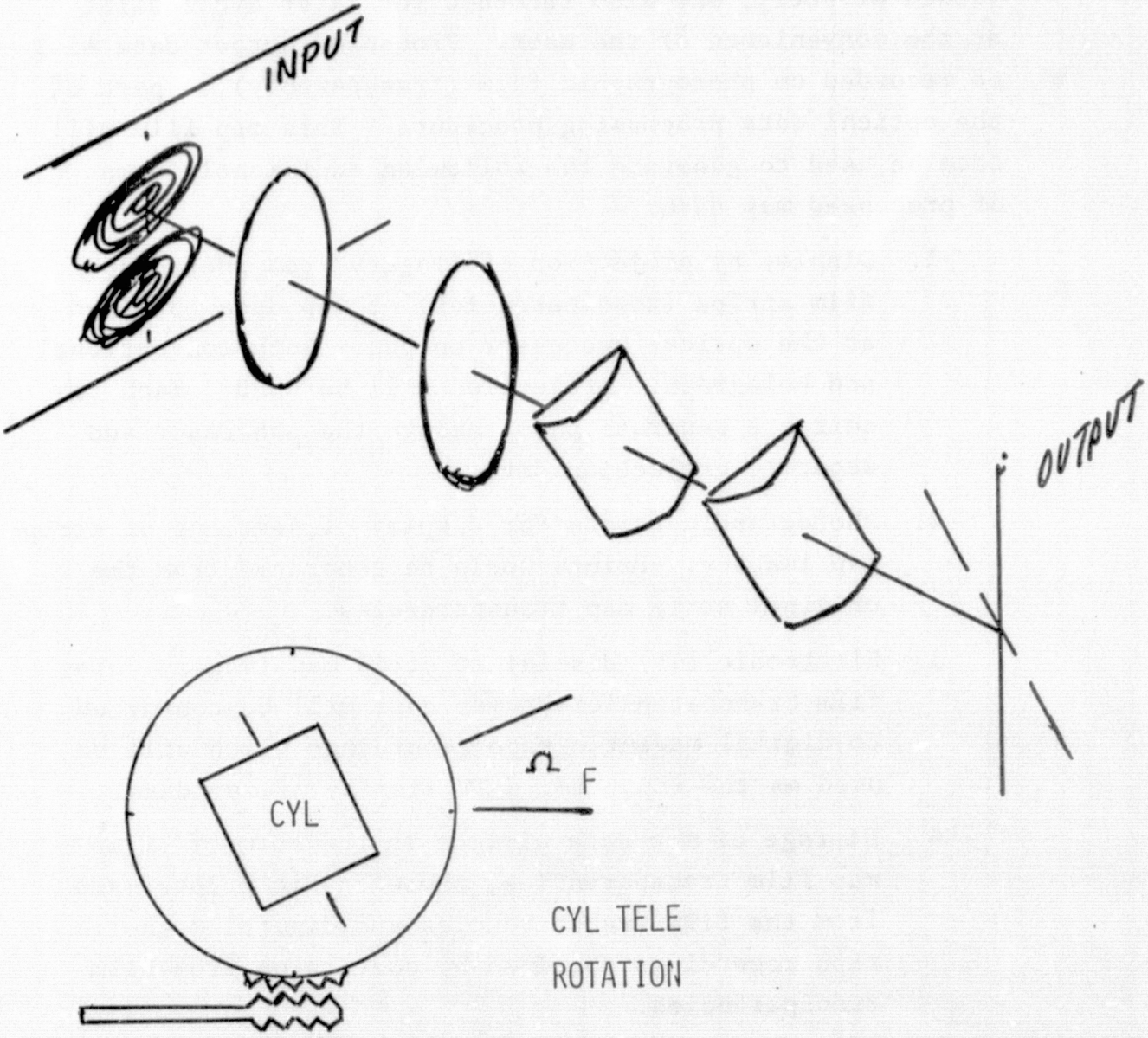

Figure 14

2.5 MAP DISPLAY AND STORAGE

The processed map data, available at the optical processor output as a light intensity distribution, can be viewed directly, and also recorded for later availability at the convenience of the user. Processor output data will be recorded on photographic film (transparency) as part of the optical data processing procedure. This map film will then be used to generate the following additional forms of processed map data:

1. Display by projection of imagery from photographic film strips (transparencies) of map data obtained at the optical processor output. Both conventional and holographic projection will be used. Each requires a separate pass through the processor and separate projection devices.
2. Photographic prints for display of sections of strip map imagery. Prints would be generated from the original strip map transparencies.
3. Electronic (TV) display of strip map imagery. The film transparencies of map data will be converted to digital magentic tape recordings which will be used as the input for a TV display of map data.
4. Storage of map data will be in the form of strip map film transparencies, photographic prints made from the film transparencies and digital magnetic tape recordings obtained by conversion from film transparencies.

   (a) Optical data processing to obtain the initial strip map film transparencies is done

on a single data channel basis. With four data channels per pass, 60' of signal film per pass and six passes; a total of about 1440' of signal film requires optical processing. This could be accomplished in as little as two days, including development of the output film transparencies.

(b) Preparation of photographic prints from the original map transparencies would be accomplished on a frame-wise basis where each frame would comprise (at most) map data for a full swath of a single data channel with an along track azimuth length about equal to the swath width, at a magnification of 5 to 10 times. Greater magnification of selected smaller map sections could also be provided but with some loss of resolution. Prints for about 6% of the full six pass data set (1440' of signal film) would correspond to a selected 90' of the original signal film. This would correspond to a minimum of 300 frames or prints. Preparation of 10 copies of 300 prints, would require about 2 to 4 days.

(c) Magnetic tape storage of map data requires conversion of map data transparencies to digitized electronic signal which would then be recorded on magnetic tapes. Using an image dissector which scans across the film width as the film moves past, will allow conversion of the film data over about 3000 resolvable elements per scan in range. Conversion of 1' of output map

film over a 3000 element portion of its swath. (Together with digitization and magnetic tape recording of the electronic output) will require about one hour of scan line when using a scan speed of 50 μsec per sample point of the scanned imagery. This could be accomplished with a modified version of the present ERIM Image Dissector and Digitization facility. Using a 9-track, 1600 bpi, 2400 ft length magnetic tape, and with an 8-bit word for each of the sample points in the scanned imagery, we require about 2 such magnetic tapes for each one foot of map film length.

A one-foot long by 3000 element wide section of map data would correspond to an earth's surface section of approximately 20 to 40 km of swath and 300 km of strip map length (depending somewhat upon the geometry mode of the SAR).

3
PROGRAM PLAN

The proposed program for a dedicated Shuttle-SAR optical data processing system development and related support activities is comprised of the major tasks listed below. Included in each task description is a preliminary cost estimate for the task and an approximate calendat period required to perform the task.

1) Optical data processing system parameter analysis and preparation of system and subsystem design specifications. ($80,000 - 9 Months).

2) Newly fabricated data processing subsystems; and, system integration and testing. This would include: spaceborne optical recorder and its interface, optical processor, film copier and printer, map data digitizer and recorder, map data film projector, TV display and controller, and miscellaneous instrumentation. This would follow task 1 above. ($1,700,000 - 30 to 36 Months).

3) Data processing services for each four channel x 360' long signal film set. This includes the processor output map transparencies, prints of about 6% of the map data, and digitizing and tape recording of about 1% of the map data, with a seven-day turn around time. It assumes use of the above type of system.
($14,000 - 7 Days).

4) Support for spaceborne SAR system performance analysis and image of analysis after the system is spaceborne.
($70,000 - 12 Months).

It should be noted that as an alternative to task 2 as shown, use of a modified version of the ERIM data processing facility could reduce costs to less than half of that indicated.

APPENDIX D

GOODYEAR AEROSPACE CORPORATION, SPACE SHUTTLE SYNTHETIC APERTURE RADAR FINAL REPORT

GOODYEAR AEROSPACE

CORPORATION

ARIZONA DIVISION

SPACE SHUTTLE SYNTHETIC APERTURE RADAR -

FINAL REPORT

Contract No. JPL-953053
Contract Work Order No. 10

Submitted to
California Institute of Technology
Jet Propulsion Laboratory
4800 Oak Grove Drive
Pasadena, California 91103

GERA-2113
Code 99696

12 August 1975

ABSTRACT

This report presents the results of a feasibility study performed to investigate a digital signal processor for real-time operation with a synthetic aperture radar system aboard the Space Shuttle. This report includes pertinent digital processing theory, a description of the proposed system, and size, weight, power, scheduling, and development estimates.

TABLE OF CONTENTS

LIST OF ILLUSTRATIONS

LIST OF TABLES

SECTION I - INTRODUCTION

This report presents the results of a study program in which the feasibility of developing a digital signal processor to be an integral part of the Space Shuttle Synthetic Aperture Radar (SAR) was determined. The study examined the geometries and beam tracking corrections associated with an orbital radar mapping system, the technologies available for implementing the processor, the architecture of the processor, tradeoffs which can influence the design, and such factors as the size, weight, and power consumption of a representative design. A program schedule and cost have also been derived. Costs for the processor configuration derived here have been estimated using components which semiconductor manufacturers' representatives have forecast to be readily available by 1977. Obviously, dramatic breakthroughs (or setbacks) such as the semiconductor industry has continually experienced, could influence these estimates. However, digital signal processors for synthetic aperture radar systems having complexities comparable to the Space Shuttle Synthetic Radar task are presently being developed. Therefore, it is felt that advances in the semiconductor field will not affect the performance achievable with a digital signal processor, but could impact the hardware by which it is implemented and the cost of the development.

Table I, which was supplied by Jet Propulsion Laboratory, presents the radar characteristics for which this processor has been configured. Table II defines the variables used in this report.

The processor configuration described in this report is capable of processing L-band and X-band radar data at a real-time rate. Although the range dimension processing for the two radar frequencies is virtually identical, the azimuth dimension hardware required for the L-band processing exceeds that necessary for X-band by more than a factor of six. As the L-band operations dominate the processing to such a degree, this mode will be used for all design within this report, and the X-band will be considered as a fallout from the design.

TABLE I - RADAR CHARACTERISTICS (ALTITUDE = 185 KM)

Parameters	L-band			X-band		
Frequency (GHz)	1.3			8.33		
Wavelength (m)	0.23			0.036		
Quantization (bits)	6			6		
Azimuth looks (image)	4 or 8			4 or 8		
Range looks (image)	1, 2, 4			1, 2, 4		
Presum number	1			1		
Transmitted pulse width (μs)	23.0			21.0		
Range ambiguity (dB)	20			20		
Azimuth ambiguity (dB)	22.5			22.5		
Image dynamic range (dB)	50			50		
Image grayscale resolution (dB)	1			1		
Spatial resolution (m) nominal	25, 50			25, 50		
Antenna azimuth dimension (m)	12			12		
Bandwidth* (MHz) (I and Q each)	17.38			17.38		
Receive time (μs)	329			329		
Off-nadir angle (deg)	25	38	50	25	38	50
Antenna elevation dimension (m)	0.65	1.55	2.2	0.12	0.24	0.36
PRF	1860	1615	1900	1850	1615	1900
Swath width (km)	100	78.1	62.6	100	78.1	62.6
Range compression ratio	400	400	400	365	365	365
Length of azimuth channels (m)	1188	1414	1704	186	221	267
Range to swath center (km)	205	244	294	205	244	294

*Assumes 26 percent broadening of main response of the compressed pulse.

TABLE II - VARIABLES AND ABBREVIATIONS

ACF = azimuth compression filter

A/D = analog-to-digital

α = orbit inclination with respect to equator

β = antenna beamwidth

B = bandwidth

C = speed of light

δR_g = ground range resolution

δR_s = slant range resolution

ϵ = beamwidth required for one synthetic aperture

f_d = doppler frequency

γ = compliment of the doppler cone angle

h = spacecraft altitude

I = in-phase (real) data component

K = sidelobe weighting factor

λ = radar wavelength

L_{syn} = synthetic aperture length

N = number of bits in a digital word

Φ = signal phase

ϕ = off-nadir angle

PRF = pulse repetition frequency

TABLE II - VARIABLES AND ABBREVIATIONS (CONT)

ψ = azimuth pointing angle

Q = quadrature (imaginary) data component

RAM = random access memory

RCF = range compression filter

ROM = read-only memory

R_g = ground range

R_s = slant range

ρ = radius of earth = 6367.7 km

τ = transmitter pulse length

θ_g = angle between slant range vector and surface of earth

V_E = tangential velocity of earth at equator = 463.07 m/s

V_{REL} = velocity of spacecraft relative to earth

W_a = azimuth resolution

W_r = range resolution

Twelve-bit complex words (6-bit I and Q) have been selected for the azimuth compression memory. Twelve-bit complex samples are large enough to preserve the input dynamic range without having small signal suppression or spurious target generation effects result. Because range compression and azimuth filtering have been performed prior to this storage, the dominant noise source will be the rounding of the samples to six bits. Quantization noise has a uniform distribution; thus, it is readily shown that the dynamic range of the signals stored in this memory (peak signal-to-rms quantization noise) is 40.8 dB.

Specifications require that 50 dB of dynamic range be available for both frequencies at the processor output. The increase in dynamic range when azimuth compression is performed is

$$\text{dynamic range increase} = 10 \log \frac{K^2 \lambda R_s}{2W_a^2} \text{ dB} \quad . \tag{1}$$

Equation (1) exceeds 10 dB for all operating modes. An additional 3-dB increase in dynamic range will also be obtained when the four azimuth looks are summed. Thus, greater than 50-dB dynamic range will be available at the processor output.

All memories in this report are semiconductor devices. Although discs, drums, etc., were considered, it appears that in the time frame of this design semiconductors will provide the most cost-effective storage for synthetic aperture processing.

Finally, this report describes a processor capable of real-time operation for all radar data at one frequency and polarization. Cost savings are possible by designing the equipment to process the data at a fraction of real time, to process only a fraction of the range swath per pass of the data, or to process only one or two azimuth looks per pass of the data. The viability of such tradeoffs will be determined by user requirements, however, and will not be considered further in this report.

SECTION II - SIGNAL PROCESSOR DESIGN

1. AZIMUTH MEMORY REQUIREMENTS

The majority of the storage in the digital signal processor is that required to perform azimuth compression and to combine azimuth looks. From Table I, it is seen that the longest synthetic aperture to be processed is 1704 meters, which occurs when the off-nadir angle is 50 degrees at L-band. In the digital signal processor, the azimuth spacing will be reduced to the minimum possible, i.e., one complex sample per the reciprocal of the required bandwidth. Because of the 26-percent excess spatial bandwidth, this becomes 19.84 meters per sample for 25-meter resolution. Dividing the synthetic aperture length by this sample spacing results in a maximum of 86 samples per look to be processed. For 38 degrees off-nadir, 72 samples are necessary, and for 25 degrees off-nadir, 60 samples are necessary. The number of range samples in each PRF is the product of the A/D converter rate and the receiver time, less the number of samples in an uncompressed range pulse; hence, 5353 range gates will be required to store each PRF after range compression. In summary, the memory size is seen to be dictated by the off-nadir angle requiring the maximum storage, which is the 50-degree case, for which 460,358 complex word storage locations are required for each look. Because each complex word is 12 bits, and because four looks are to be processed, the azimuth compression memory will require 22.1 megabits of storage.

In addition to the azimuth compression storage, it is necessary to provide a delay of three synthetic aperture lengths to store processed data until corresponding looks at the same target are available. Because detected data are being stored, a sample spacing of one-half the desired resolution should be maintained. As the data have been converted to ground range, the 50-degree off-nadir angle mode will require the largest amount of storage, a total of 2.454 megawords. Nine-bit words will be adequate for this task.

2. COMPENSATION FOR ANTENNA POSITION

The radar antenna is not stabilized. Thus, to properly focus the data, corrections must be made in the processor to compensate for the antenna's deviations about the desired pointing angle. Compensation for shuttle roll (which will introduce dopplers caused by the separation of the antenna from the spacecraft) and center of gravity acceleration and for orbit characteristics will require data to be input to the processor from external sources.

The actual off-nadir angle of the antenna beam can be estimated by measuring the average return power as a function of range. The effects of the earth's rotation require relatively straightforward calculations which can be performed by a minicomputer.

The azimuth pointing angle of the antenna must be determined by a clutterlock because it can deviate by as much as 2 degrees from the yaw angle of the shuttle. Because this exceeds the 3-dB antenna beamwidth by a factor of 4 in L-band and a factor of 26 at X-band, and the PRF is adequate for sampling only the doppler within the antenna beam, the number of beamwidths of displacement must be calculated. In addition, pitch rotation of the antenna (which will cause the azimuth and elevation patterns to interchange) will add a linearly changing doppler offset as a function of the range to the clutterlock signal.

A straightforward technique for resolving the ambiguity and determining the pitch and yaw angles requires that the clutterlock be range gated. Because the intersection of a cone of constant doppler with the earth (for a flat, nonrotating earth approximation) is a hyperbola, the doppler frequency in the center of the beam will change as a function of range (except when the antenna is pointed perpendicular to the plane of the orbit). Figure 1 illustrates the intersection of the pointing angle vector to a line of constant doppler (isodop).

The cone angle of the isodop which the azimuth yaw vector intersects was calculated by a computer program. Analysis of the computer data verified that sufficient curvature exists to resolve the antenna pointing ambiguity. To initialize the clutterlock, a portion

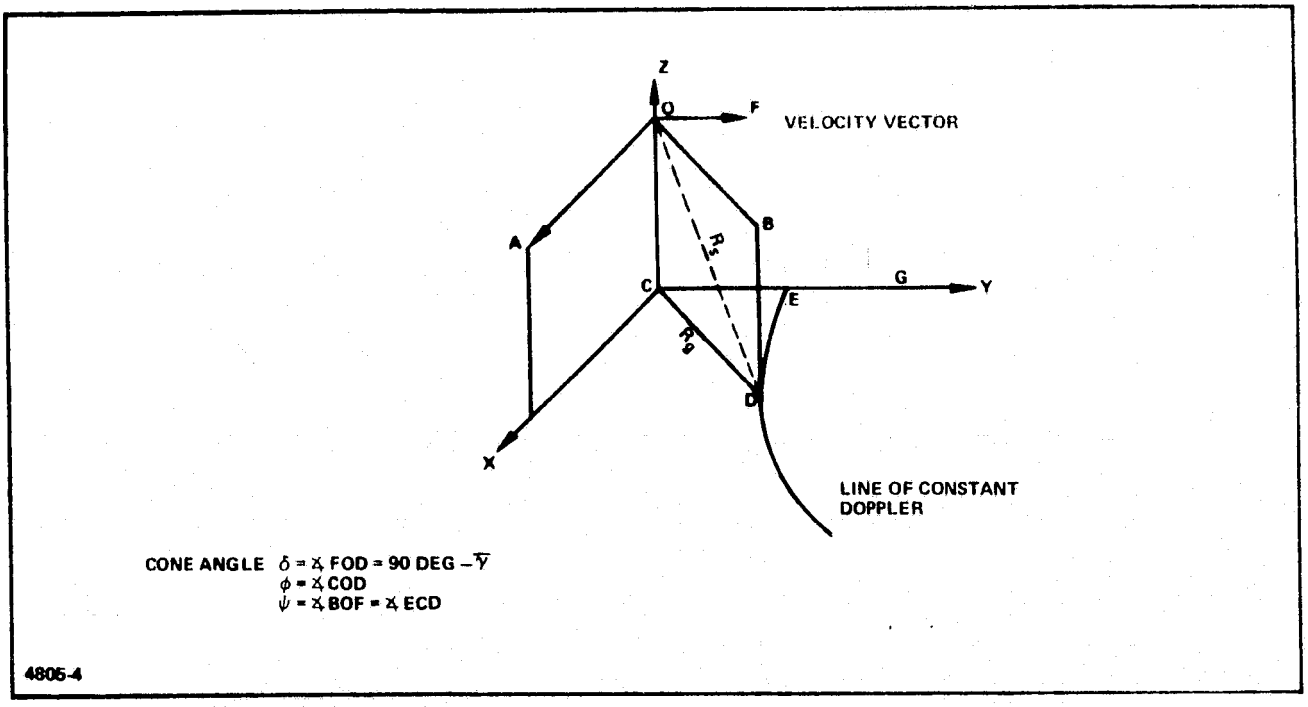

Figure 1 - Cone Angle Geometry

of the data tape equivalent to a few synthetic apertures may be recorded in an auxiliary storage and "run backward;" i.e., PRF number N, N - 1, . . . , 1. The final values in the clutterlock thus become the initial conditions when the data tape is processed.

After the pitch and yaw angles have been resolved, the clutterlock will continue to track the motion of the beam. It would appear to be beneficial to process the L-band data first, because of the lower number of ambiguities from which the pointing angle must be determined. The clutterlock signal from this processing could then be stored and used to provide additional aid for the X-band signals.

The doppler frequency at the center of the antenna beam as a function of γ, the complement of the cone angle, is given by

$$f_d = \frac{2V}{\lambda} \cos \gamma \quad , \tag{2}$$

where

$$\gamma = \arccos(\sin\psi \sin\phi) \quad .$$

Hence, for a given value of ψ, the doppler in the center of the antenna beam across the range swath is given by

$$\Delta f_d = \frac{2V}{\lambda} \sin\psi \left| \sin\phi_{max} - \sin\phi_{min} \right| \quad . \tag{3}$$

Table III presents the doppler frequency for various values of ϕ and ψ. The pitch angle has been assumed to be zero, although similar tables may be readily derived for nonzero values.

TABLE III - TABULATED DOPPLER FREQUENCIES (L-BAND)

Yaw angle, ψ (deg)	0.5	1.0	2.5	5.0	7.5	10.0
Off-nadir angle, ϕ (deg)						
15	152.7	306.6	768.3	1530.5	2291.4	3048.4
20	202.4	404.9	1012.1	2021.6	3028.3	4028.4
25	249.8	500.7	1250.0	2498.4	3741.2	4978.1
30	295.9	591.9	1479.6	2956.2	4426.6	5889.0
35	339.7	679.5	1697.4	3379.5	5078.4	6755.3
40	380.0	761.2	1902.1	3800.3	5690.9	7571.1
45	419.1	836.9	2092.4	4179.7	6260.4	8328.2
50	453.4	906.8	2254.7	4528.2	6782.4	9022.1
55	485.3	969.5	2423.9	4842.3	7282.2	9648.2
60	512.6	1025.1	2562.3	5119.7	7667.5	10199.7

3. COMPENSATION FOR ROTATION OF THE EARTH

To properly clutterlock and focus synthetic aperture radar data, a correction must be made for the rotational velocity of the earth (463.07 m/s at the equator). Figure 2 illustrates the extremes of relative velocity as a function of the orbit altitude for various orbit inclinations.

In addition, target motion will be caused by rotation of the earth. A target at near range will have a lower relative radial velocity component than a target at far range because of the slant range geometry. Thus, a correction signal must be generated which varies as a function of range. This is illustrated for a polar orbit in Figure 3. Over the period of a synthetic aperture at L-band at a 25-degree off-nadir angle, a target at far range will change in slant range by approximately 30 meters more than one at near range. As this exceeds eight range gates (slant range), a range slippage correction which varies as a function of range will also be required. The variation in range slippage is illustrated in Figure 3.

Note that corrections similar to the above must also be made if the spacecraft deviates from a circular orbit.

4. RANGE WALK AND RANGE CURVATURE

The definitions and geometries of range walk and range curvature are presented in Figure 4. Range curvature, which is proportional to the amount of quadratic phase error measured about a best linear fit for a synthetic aperture, is given by

$$\text{range curvature} = \frac{(L_{syn})^2}{8R_s} \quad ,$$

where L_{syn} is the synthetic aperture length, and R_s is the slant range to the target.

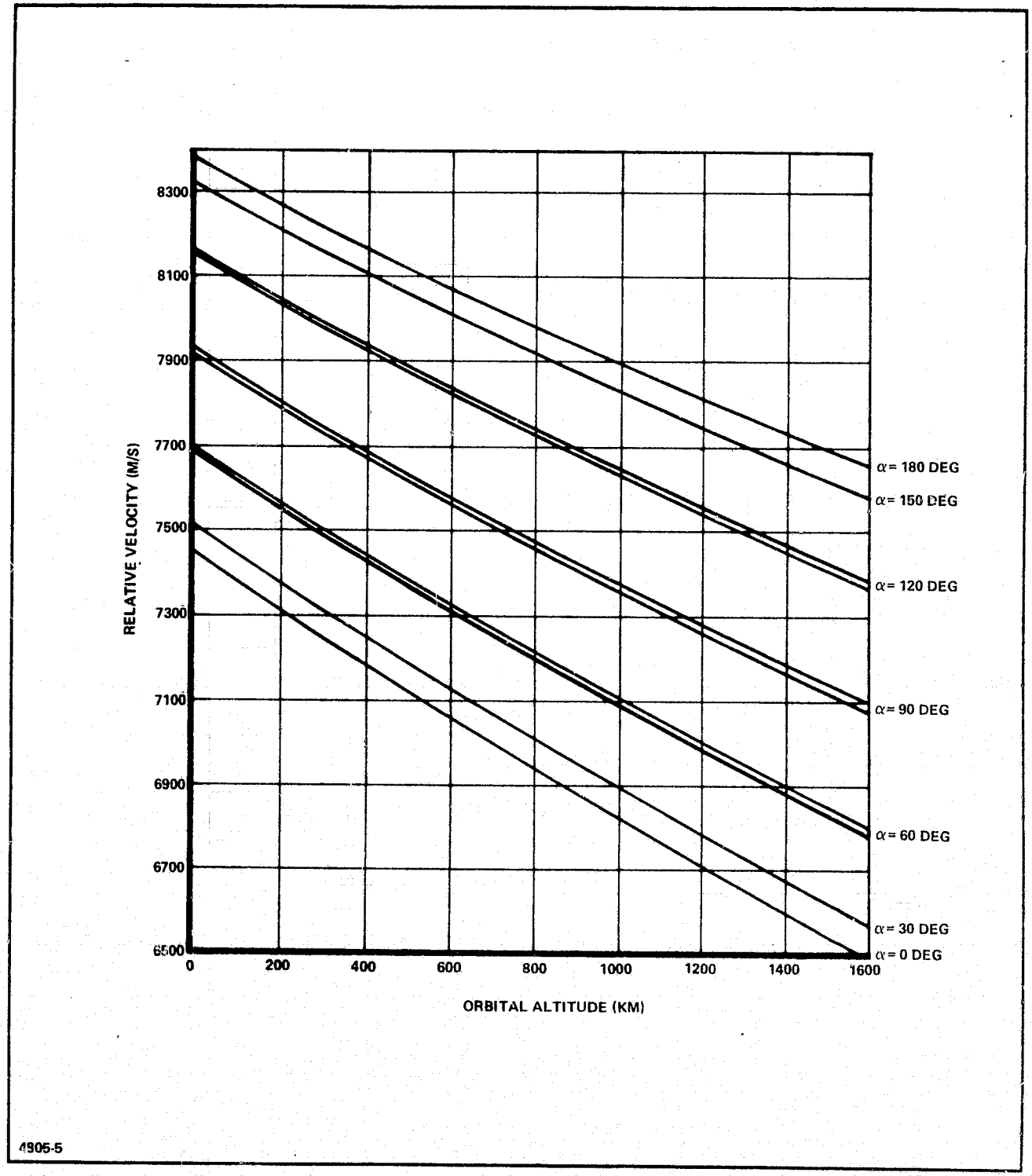

Figure 2 - Relative Velocity versus Orbital Altitude

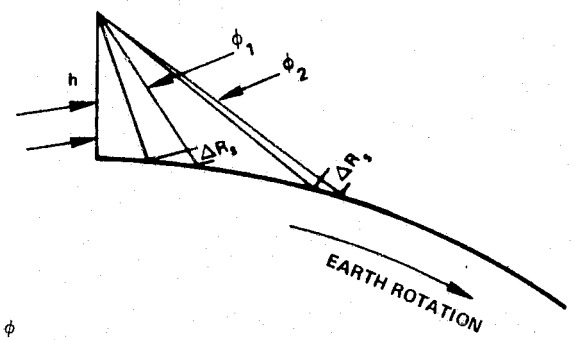

$\Delta V_g = \Delta V_s \text{ SINE } \phi$

FOR L-BAND MAPPING AT EQUATOR				
OFF-NADIR ANGLE (DEG)	SYNTHETIC APERTURE TIME (S)	NEAR RANGE TARGET VELOCITY (M/S)	FAR RANGE TARGET VELOCITY (M/S)	Δ RANGE SLIPPAGE PER SYNTHETIC APERTURE (M)
25	0.149	60.44	262.28	30.1
38	0.186	269.30	332.90	11.8
50	0.223	348.33	378.35	6.7

VARIABLE RANGE SLIPPAGE IS REQUIRED TO COMPENSATE FOR THE EARTH'S ROTATION.

4805-6

Figure 3 - Variation in Range Slippage

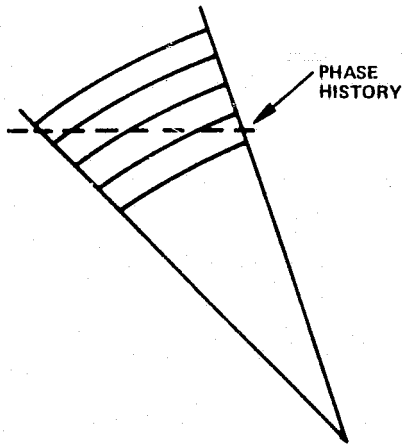

RANGE WALK

RANGE WALK IS CAUSED BY THE PHASE HISTORY LYING IN MORE THAN ONE RANGE GATE DUE TO THE ANTENNA BEAM OR LOOK ANGLE SKEW. RANGE WALK CORRECTION IS A LINEAR PHASE ADJUSTMENT.

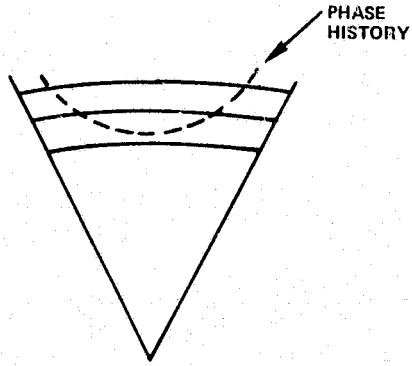

RANGE CURVATURE

RANGE CURVATURE EFFECTS OCCUR WHEN THE VARIATION OF A SECTION OF A PARABOLIC PHASE HISTORY ABOUT A STRAIGHT LINE APPROXIMATION APPROACHES OR EXCEEDS A RANGE RESOLVABLE ELEMENT.

4805-7

Figure 4 - Range Walk and Range Curvature Definitions

From the values in Table 1, the maximum range curvature occurs at L-band for a 50-degree off-nadir angle and equals 1.23 meters. The slant range samples are spaced by 8.63 meters. Analysis has shown that the effect of this 14-percent displacement upon resolution and sidelobes is virtually negligible.

The correction for range walk will be performed as two distinct operations which will be referred to as fine and coarse range slippage. Fine range slippage is the resampling of the data such that a given return remains at the same position relative to the new data samples. Coarse range slippage advances (or retards) the data by an integer number of range gates. These operations are illustrated in Figure 5.

For a squinted beam, the per sample range change, ΔR, is given by the equation

$$\Delta R = \frac{V \sin \psi \sin \phi}{PRF} \quad . \tag{4}$$

Note that ψ will differ for each of the four azimuth looks, and that both ψ and Φ change with range.

5. REQUIRED NUMBER OF AZIMUTH REFERENCE FUNCTIONS

It has been shown that 5353 range samples are to be processed for each of the four looks. The generation of 21,412 different reference functions would require an enormous amount of hardware. Fortunately, this is not necessary.

Analysis has shown that satisfactory results may be achieved if the azimuth phase history and azimuth compression reference functions are mismatched by no more than 45-degree peak phase error. Therefore, as the phase, ϕ, is given by

$$\Phi = \frac{4\pi R_s}{\lambda} \approx \Phi_o + \frac{2\pi X^2}{\lambda R_{s0}} \quad , \tag{5}$$

where R_{s0} is the slant range to the center of the azimuth phase history, the peak phase error occurs when

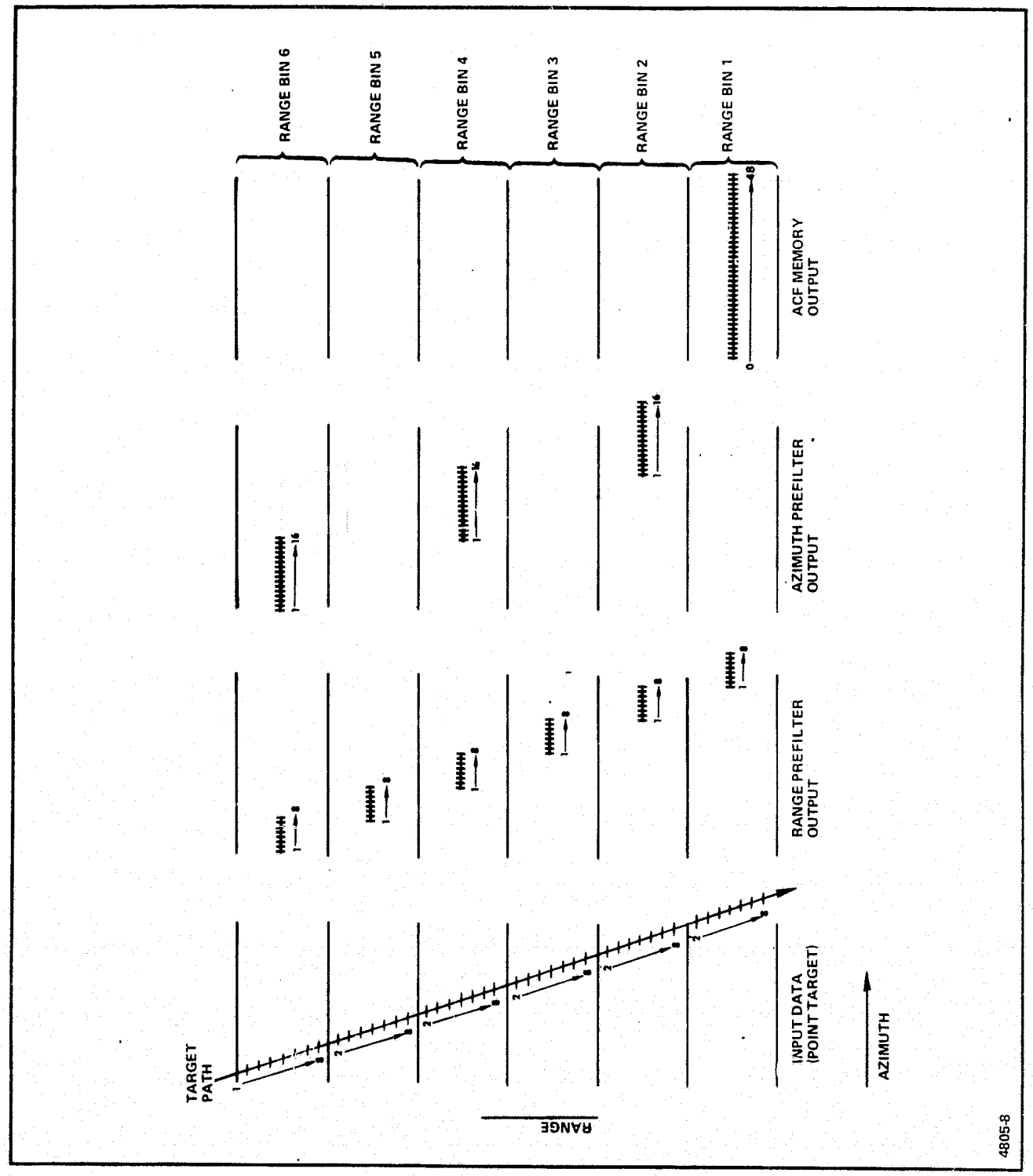

Figure 5 - Range Slippage Correction

$$X = \frac{1}{2}L_{syn} = \frac{1.26\lambda R_{s0}}{4W_a} \quad . \tag{6}$$

Then,

$$\Delta\Phi = \frac{2\pi X^2}{\lambda R_{s0}^2}\left(\frac{\Delta R_s}{2}\right) = \frac{(1.26)^2\lambda\pi}{16W_A^2}\Delta R_s = \frac{\pi}{4} \quad , \tag{7}$$

$$\Delta R_s = \frac{4W_A^2}{(1.26)^2\lambda} \quad ,$$

where ΔR_s is the slant range interval for which one azimuth reference function may be utilized.

For the L-band processing, ΔR_s = 6800 meters. Hence, fewer than 10 reference functions will suffice for processing each azimuth look.

6. SLANT RANGE TO GROUND RANGE CONVERSION

Slant range to ground range conversion is an interpolation process which will transform evenly spaced data points from a straight line into evenly spaced data points on a circle. This geometry is illustrated in Figure 6. This process will be performed after azimuth compression to minimize storage requirements.

The ground and slant range samples have the approximate relationship

$$\delta R_g = \delta R_s \sec\theta_g \quad . \tag{8}$$

The angle θ_g is calculated from the relationship

$$\frac{\sin(90 \text{ deg} + \theta_g)}{h + \rho} = \frac{\sin(\phi)}{\rho} \quad . \tag{9}$$

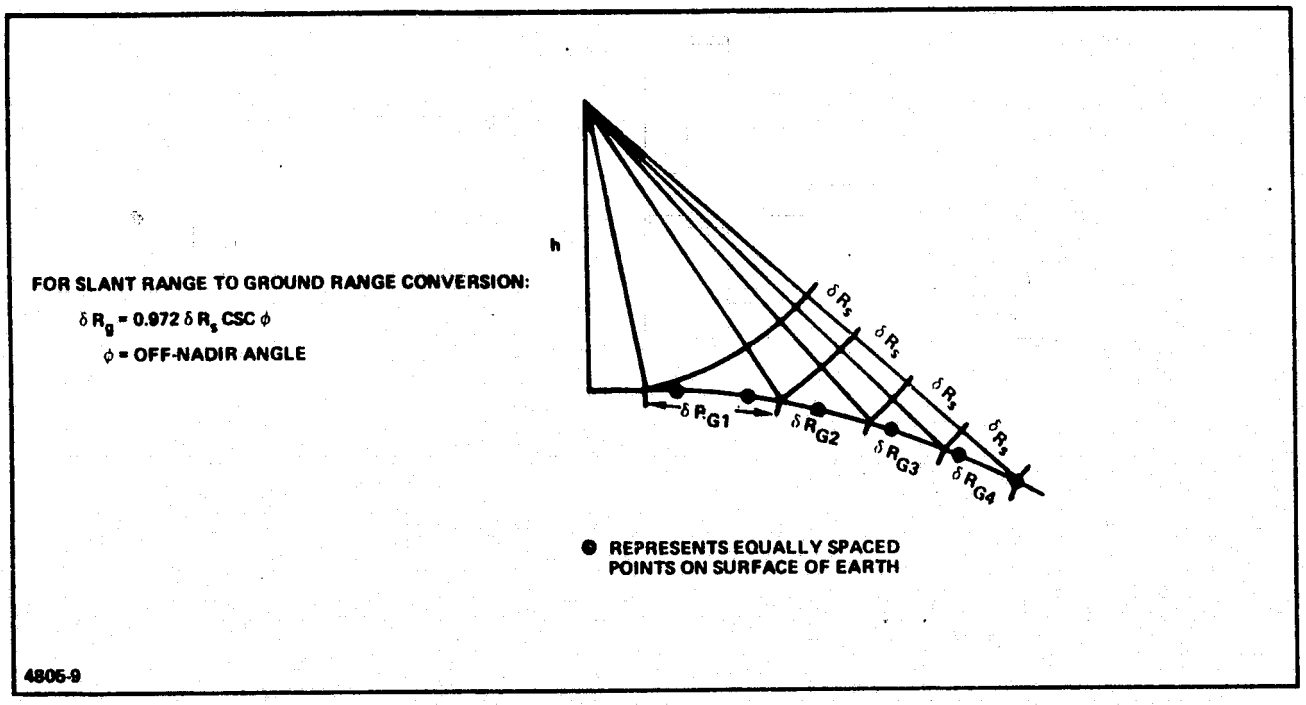

Figure 6 - Slant Range to Ground Range Conversion

For a 185-km orbit, θ_g is given by

$$\theta_g = \cos^{-1}(1.029 \sin \phi) \quad . \tag{10}$$

Thus,

$$\delta R_g = 0.972\ R_s \operatorname{cosec} \phi \quad ; \tag{11}$$

where the instantaneous value of ϕ is given by

$$\phi = \cos^{-1}\left[\frac{R_s^2 + h^2 + 2\rho h}{2R_s(h + \rho)}\right] \quad . \tag{12}$$

The slant range to ground range conversion will resample the data to produce ground range samples spaced by 12.5 meters prior to detection. Data at near range will have proportionately poorer resolution. Data at far range, for which the ground range resolution will be better than that specified, will be effectively filtered to 25-meter resolution with one and a fraction range looks when the resampling process is performed.

7. PROCESSOR OUTPUT SAMPLING RATE

The spectra of the processor output before and after detection are presented in Figure 7. As can be seen, the detection process doubles the signal bandwidth; thus, it is desirable to double the output sampling rate in both the range and azimuth dimensions to preserve the processed resolution.

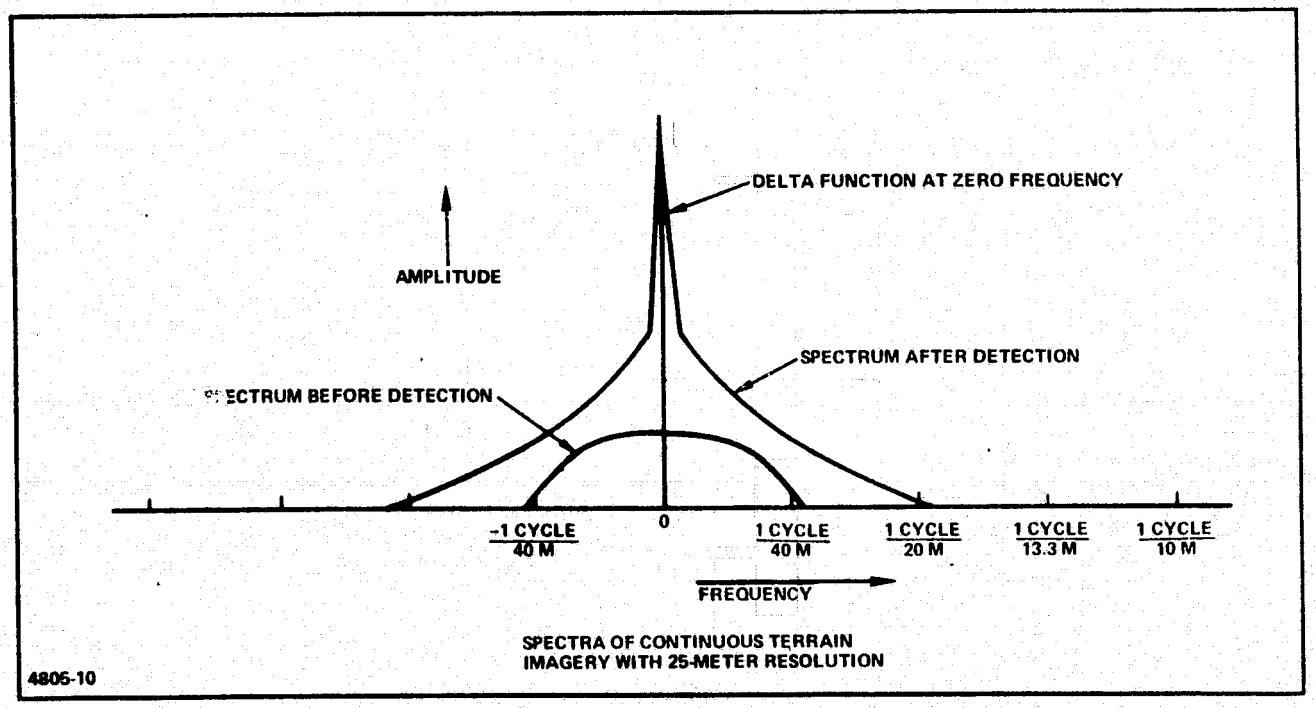

Figure 7 - Spectra of Continuous Terrain Imagery with 25-Meter Resolution

Although it would be possible to reduce the size of the 22.9 megabit azimuth look storage if larger sampling spaces were used, the resultant savings would have little effect on the overall system cost, and the mean resolution of the system would be reduced. Thus, 12.5 meter sample spacing is recommended for the data after detection.

8. AZIMUTH MULTIPLE LOOKS

When processing synthetic aperture radar data, all or part of the doppler bandwidth may be processed for resolution. If the total bandwidth is used for resolution, the resultant processed signal contains all the information about the target which can be obtained (assuming the system is linear). Therefore, a multiple-look system can never gather more information about any target than a one-look system having the same bandwidth (when the system is linear).

If the bandwidth is divided into sections, several signals may be derived from the total bandwidth, each of which when processed yields proportionately less resolution. When the target is composed of random features, the pieces of the total bandwidth will be statistically identical but uncorrelated. When the target is regular on a scale larger than the maximum resolution length, the pieces of the bandwidth will be correlated and nonstatistical in nature. Thus, combining the multiple looks will result in a better image than any look by itself.

Two methods for the production of multiple looks, illustrated in Figure 8, are:

1. Filtering to form multiple bandwidth sections, with each section processed coherently and the results detected and summed
2. Processing for ultimate resolution and low-pass filtering detected outputs to the desired resolution.

Studies have shown that these two methods of producing multiple looks are virtually identical in terms of the quality of the resulting image.

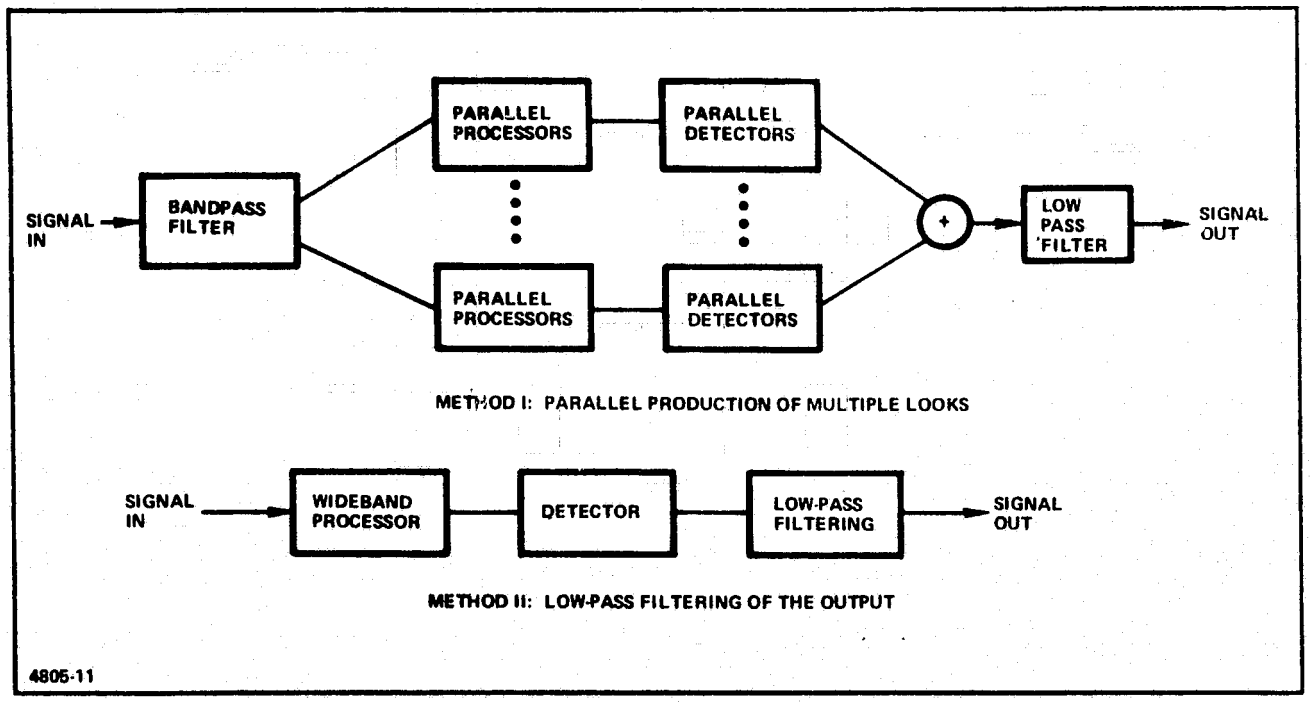

Figure 8 - Two Methods Used for Producing Multiple Looks

For the processor to be discussed in Section IV, Method 1 will be employed for the azimuth four-look mode, because this method requires the least amount of storage to be utilized in the azimuth compression filter. Method 2 will be employed when more than four azimuth looks and more than one range look are desired (with a corresponding decrease in resolution). Implementation of Method 2 requires very little additional hardware to implement when configured with the four-look processor.

SECTION III - PROCESSOR SIGNAL FLOW

Figure 9 is included to show the sequence of the operations required to process the data and the flow of the image and navigation data throughout the processor. The hardware and algorithms to be used to perform these operations will be detailed in Section IV. Although some of the operations listed will be performed simultaneously, while the performance of others may be distributed throughout many subunits, the general order and location in which they are shown is correct. It is hoped that this diagram will assist the reader in comprehending the overall operation of the digital signal processor.

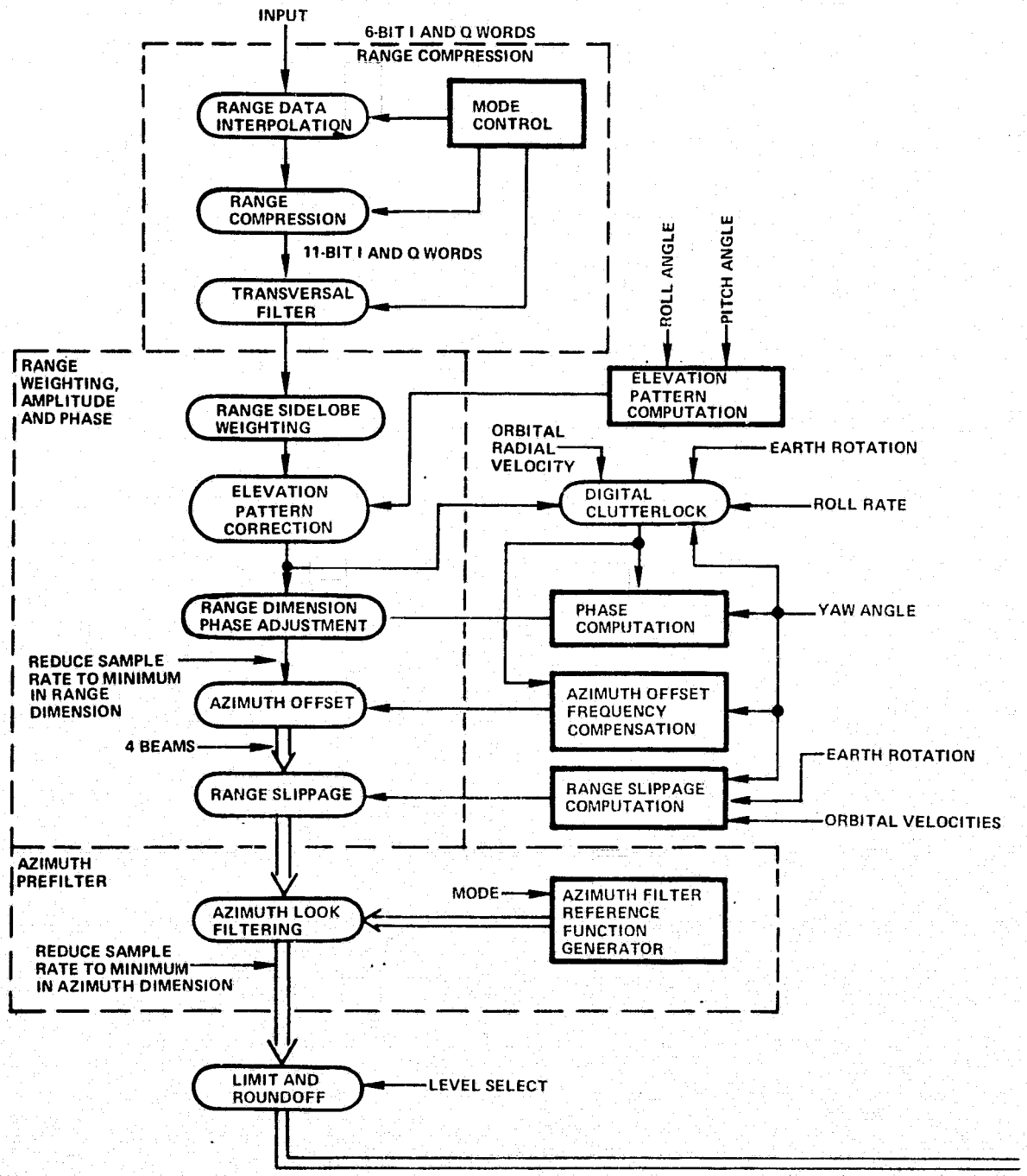

Figure 9. Space Shuttle SAR Processing Flow (Sheet 1 of 2)

4805-2

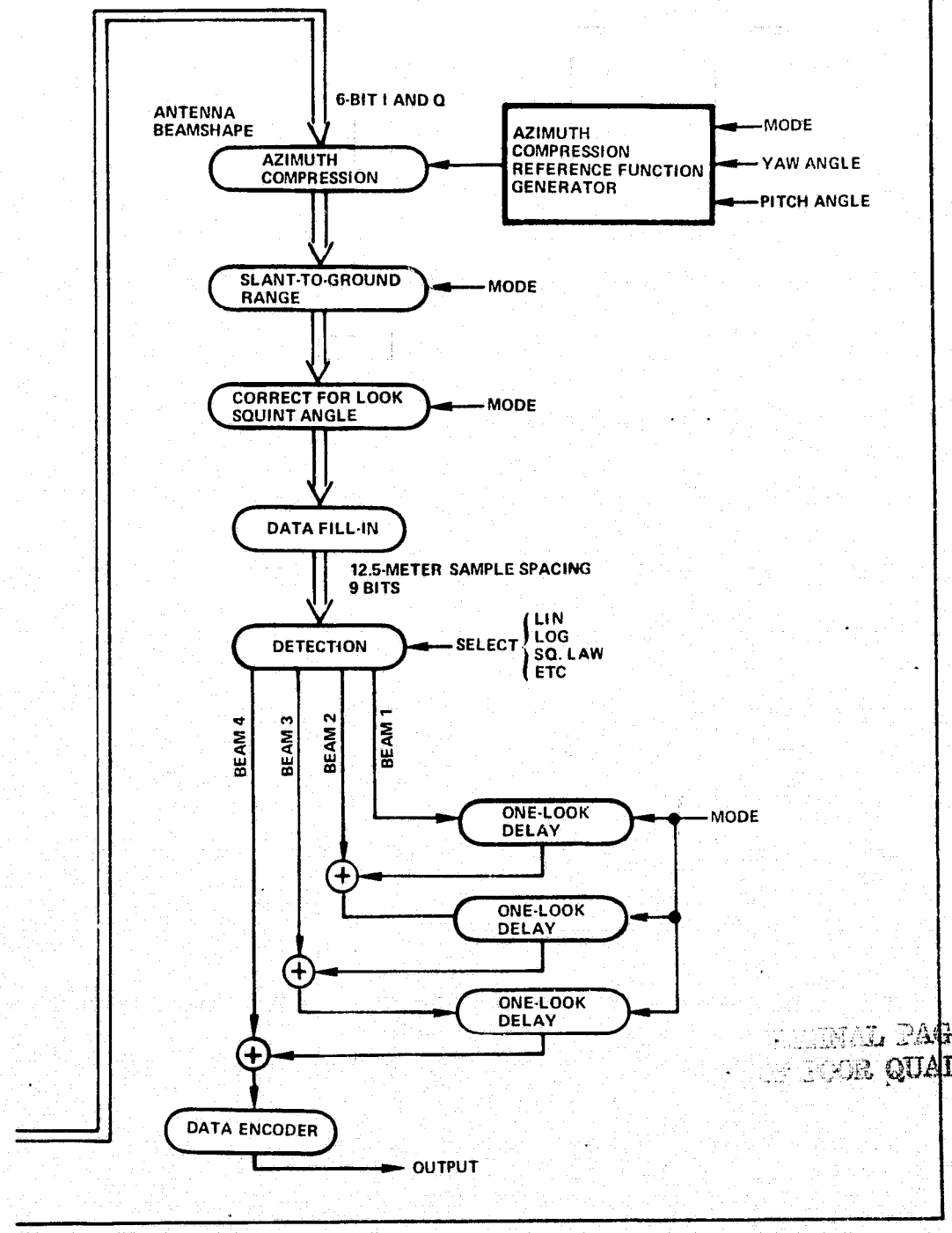

Figure 9. Space Shuttle SAR Processing Flow (Sheet 2 of 2)

SECTION IV - PROCESSOR DESCRIPTION

1. INTRODUCTION

In this section, a digital signal processor capable of producing imagery with the desired resolution and number of looks at a real-time rate will be configured. The algorithms and the order in which they are implemented have been shown by experience to produce adequate performance and can be implemented with hardware designs balanced in speed, size, power, maintainability, and cost. The processor is designed to handle data recorded on tape with a 100-percent duty cycle.

The system has been designed about the parameters detailed in Sections I and II. Growth of the system for higher orbit altitudes is discussed at the end of this section. The sizing has been performed about components (primarily memory elements) which have high probabilities of being available within the next two to three years.

Figure 10 is an overall block diagram of the digital signal processor.

2. RANGE COMPRESSION FILTER

The range compression filtering is the first operation to be performed by the digital signal processor. Although compression requirements increased the dynamic range, and a correspondingly larger word size is required for storage of each sample, factors such as phase corrections and clutterlock accuracies make collapsing of the range pulse desirable at this point.

An iterative range compression algorithm has been selected for this analysis. As illustrated in Figure 11(A), the parabolic phase of a chirp signal is approximated by a piecewise linear approximation in the range compression filter (RCF), with the resulting phase error shown in Figure 11(B). Each straight line segment can be implemented by an iterative filter having linear phase. Noise buildup in the filter is avoided by allowing only 0, 90, or 180 degree phase shifts within the loops. This choice results in a very small

number of complex multiplications (four if $B\tau = 400$) being required for each output data point. This is because all time samples of the matched filter function for $B\tau = 400$ have phases divisible by 18 degrees, and with proper presumming only multiplications by the sines of 18 degrees, 36 degrees, 54 degrees, and 72 degrees are necessary (0 degrees and 90 degrees being trivial operations).

Range compression ratios with the property described above have square roots which are integer divisible by four. The algorithm can be employed with a pulse having any dispersion ratio smaller than that of the filter by simply adjusting the sampling rate of the digitized signal to match the frequency versus time slope of the filter. If the signal has a time-bandwidth product, $B\tau$ and the filter $B'\tau'$, then the sampling rate increase is a factor of $\left((B'\tau')/B\tau\right)^{1/2}$. This can be accomplished by either an increase in the A/D conversion rate of this factor or by an interpolation filter (which has been included in the sizing of this processor).

If the transmitted waveform were a "stairstep" chirp signal, it and the RCF would be matched. For a linear chirp signal, the phase error illustrated in Figure 11(B) occurs. The results of this mismatch are "paired-echo" images of the collapsed pulse. Thus, a transversal filter is necessary to generate a delayed, phase shifted, and attenuated signal which is added to the output to remove these sidelobes. This has also been included in the estimate.

The range pulse compression algorithm described in this section has been shown to require an interpolation circuit to match the FM rate of the signal and the RCF, and a transversal filter to remove the sidelobes caused by phase mismatch. The transversal filter may be eliminated if the transmitted waveform were a stairstep chirp instead of a linear chirp. The interpolation network may be eliminated either by the choice of $B\tau$ products whose square roots are exactly divisible by four (e.g., 64, 144, 256, 400, 596, etc.), or by the approximately 5-percent increase in the A/D conversion rate. These devices have been included in the estimate, however, to provide the user with virtually any compression ratio desired (assuming in this design it is less than 400).

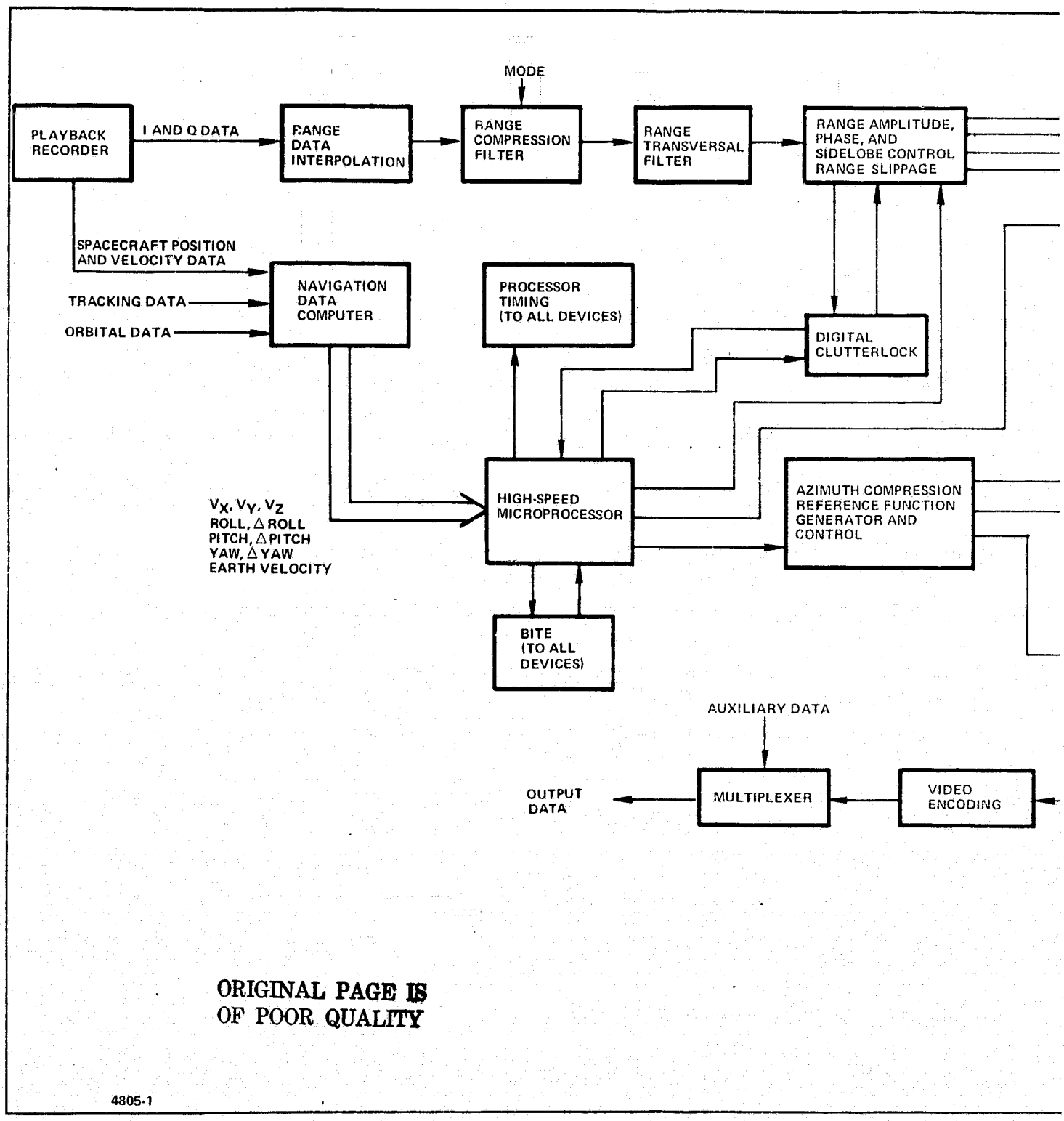

ORIGINAL PAGE IS
OF POOR QUALITY

Figure 10. Space Shuttle SAR Processor Block Diagram (Sheet 1 of 2)

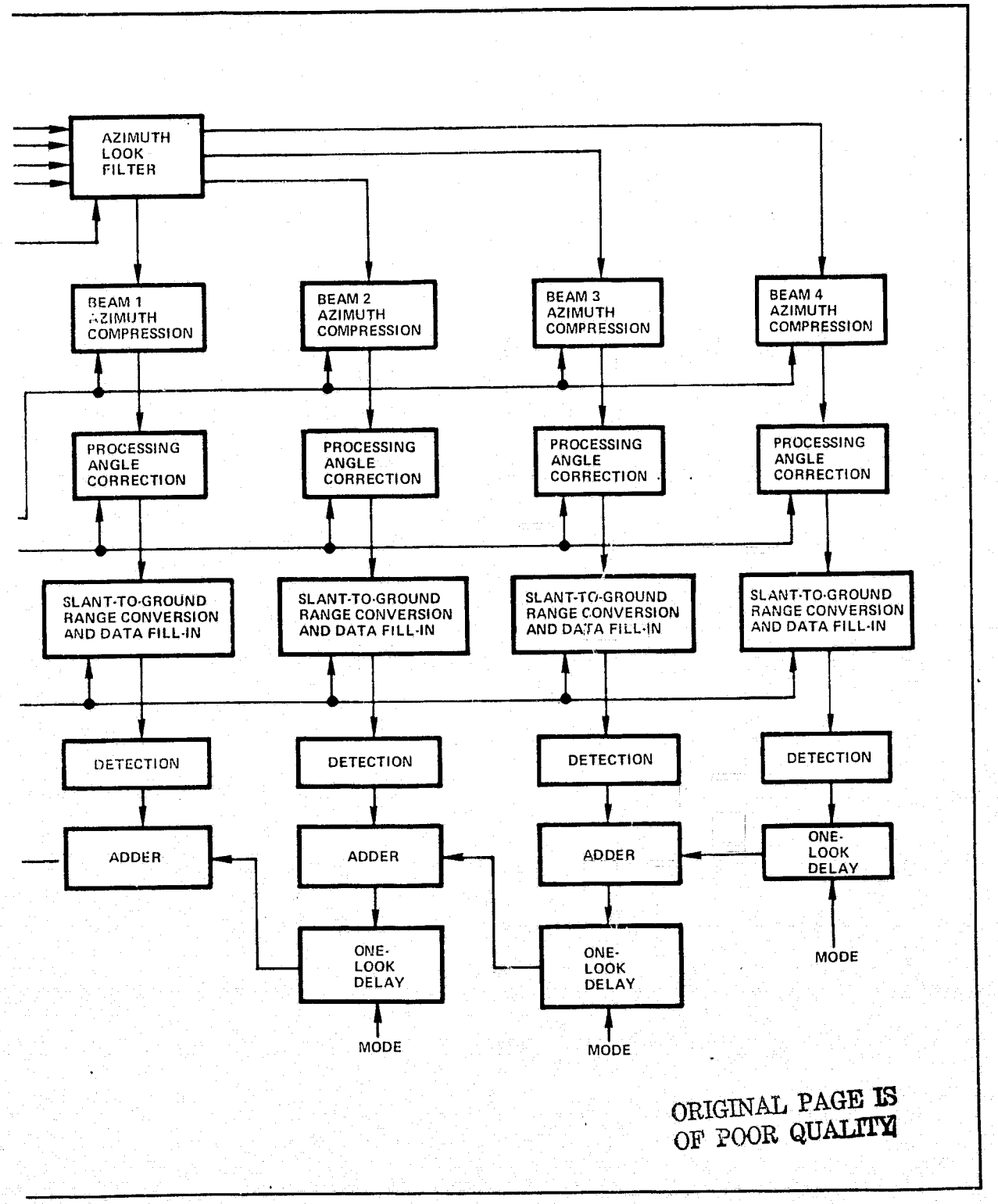

Figure 10. Space Shuttle SAR Processor Block Diagram (Sheet 2 of 2)

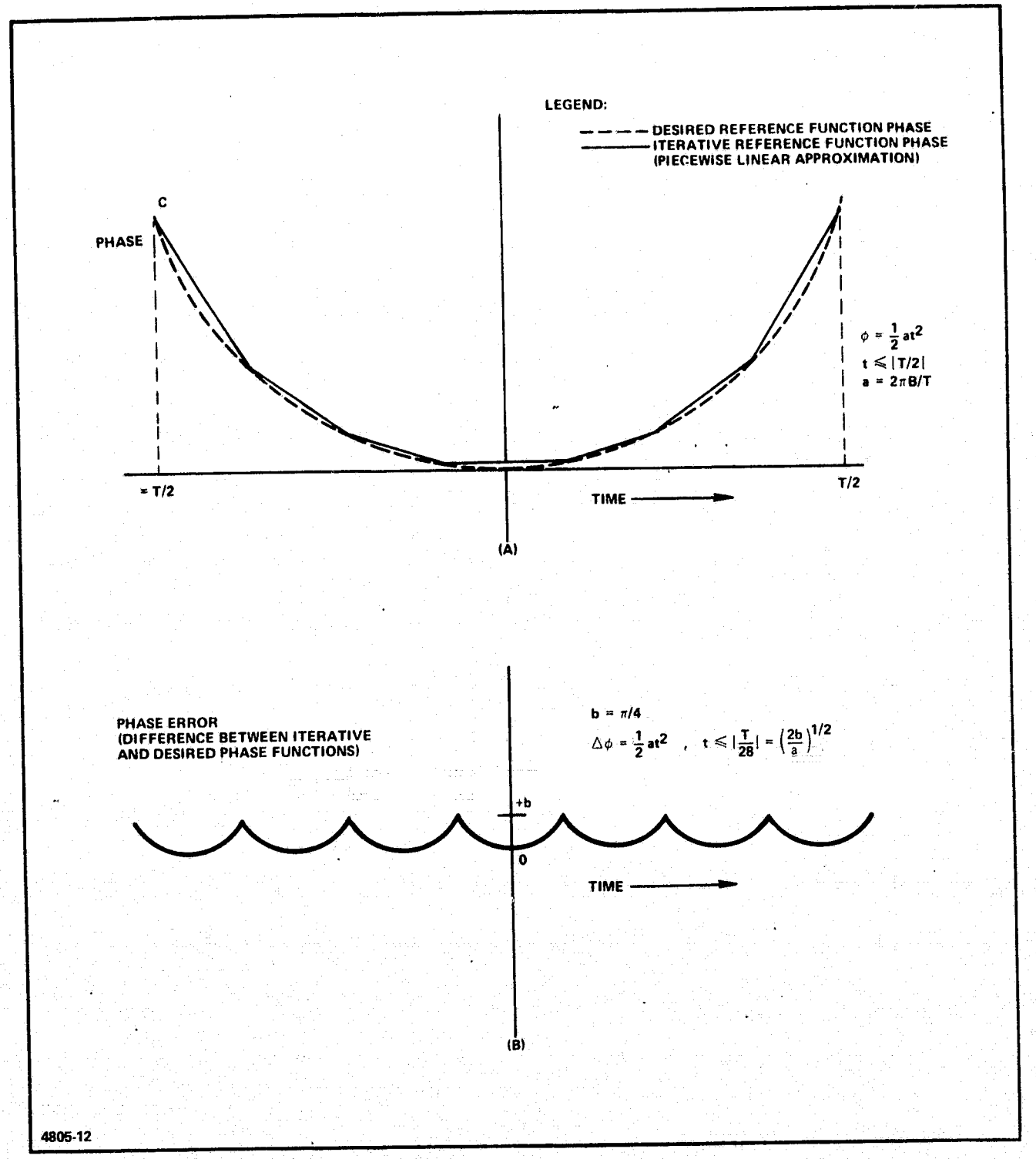

Figure 11- Reference Function for an Iterative Range Compression Filter

It is estimated that the RCF will require 30 printed circuit boards, utilize 2250 integrated circuits, and consume 750 watts.

3. RANGE AMPLITUDE, PHASE, AND SIDELOBE CONTROL FILTER

This unit is essentially a very high-speed array of complex multipliers, storage, and read only memories (ROM's). Its purposes include:

1. Weighting of the range compressed signal for sidelobe control
2. Adjustment of amplitude across the range swath for antenna elevation pointing angle correction
3. Application of the required phase correction to each range cell as dictated by the clutterlock and navigation computer
4. Performance of range slippage
5. Offsetting the azimuth spectrum for azimuth look filtering
6. Reduction of the range dimension sampling rate (if increased in the range compression filtering).

The complexity of the algorithm used for range sidelobe control will be dictated by the peak and integrated sidelobe specifications.

Fine range slippage requires a range dimension interpolation. It is performed by storing samples of the weighting function spaced at much finer intervals than the data samples. Then, as illustrated in Figure 12, the center of the stored function is aligned with the point at which a data point is to be reconstructed, and reference function points are accessed from addresses corresponding to existing data. A digital convolution is performed, resulting in the interpolated data point.

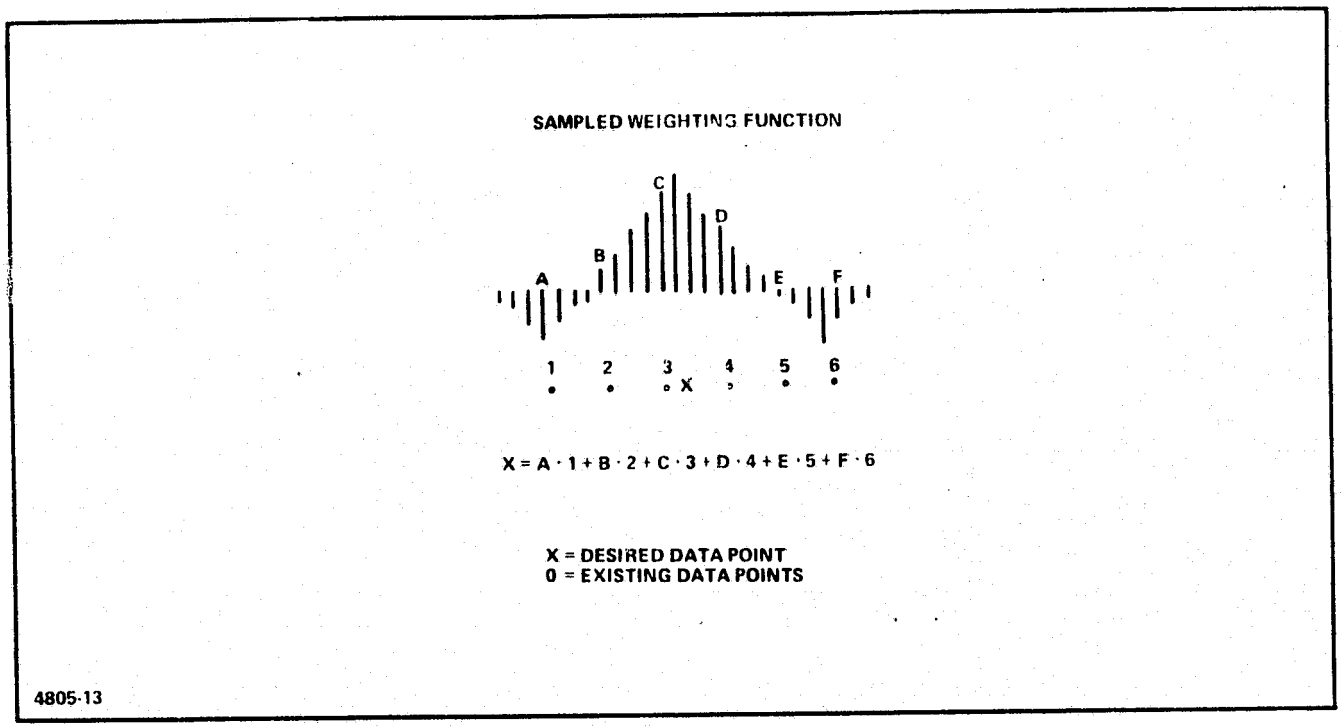

Figure 12 - Digital Interpolation

Offsetting the spectrum in azimuth is a phase adjustment, i.e., a vector rotation. One complex multiplication per output data point is necessary to perform this task. The azimuth offset operation allows all four azimuth looks to be formed by low-pass filtering operations by translating the desired center frequency of each azimuth look to zero. A generalized block diagram is shown in Figure 13.

It is estimated that the range amplitude, phase, and sidelobe control filter will require 10 boards, 600 integrated circuits, and consume 300 watts.

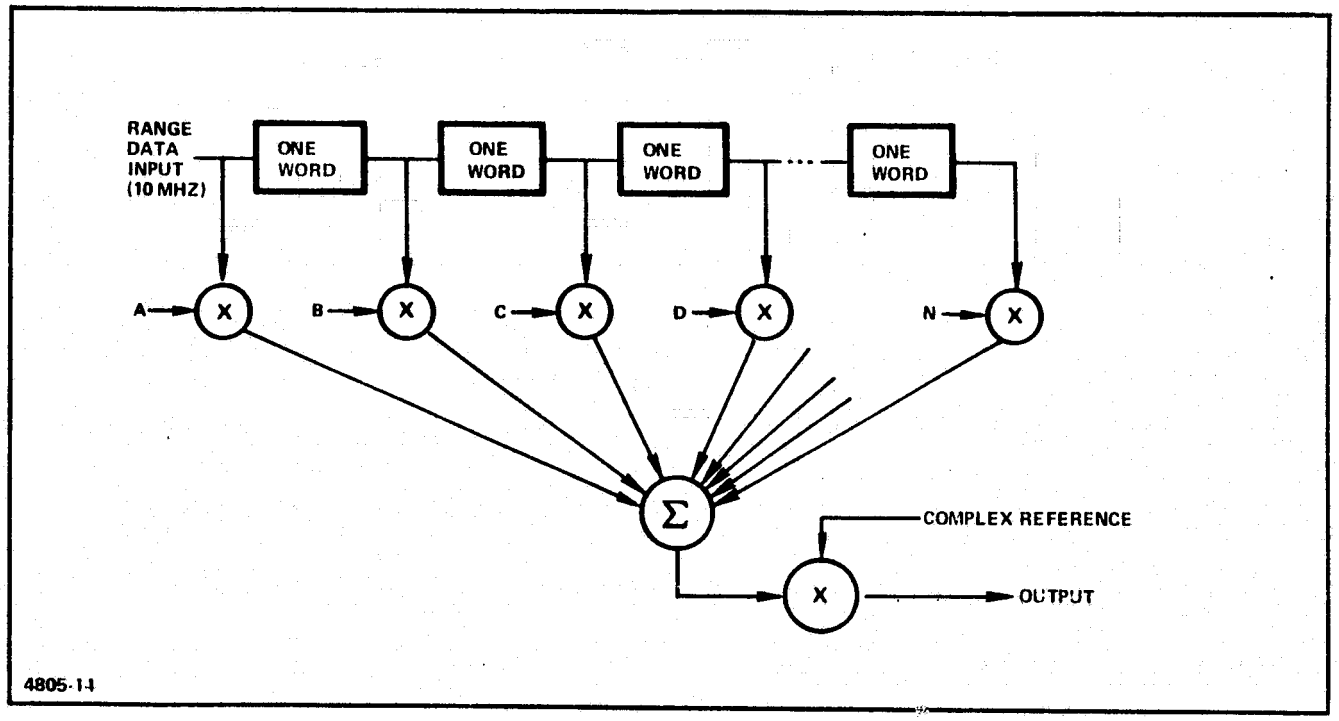

Figure 13 - Range Filter Block Diagram

4. AZIMUTH PREFILTER

The azimuth prefilter consists of a bank of four nonrecursive low-pass filters, each filter separating, shaping, and weighting the spectrum for one of the azimuth looks. The data rate will be reduced to the minimum (approximately one complex sample for every 20 meters of spacecraft travel) at the filter output to maintain the minimum azimuth compression filter memory size. In addition to the filtering, coarse range slippage (i.e., integer range gate slippage) is also performed in this unit.

The azimuth prefilter will be implemented with "integrate and dump" filter sections. This type of filter, illustrated in Figure 14, digitally convolves N contiguous data points with an N-point low-pass filter function and outputs one data point. Therefore, if the input data rate is sampled at the Nyquist rate, and if the bandwidth is to be decreased by a factor of four, then N/4 sections must be time-multiplexed to maintain an adequate sampling rate.

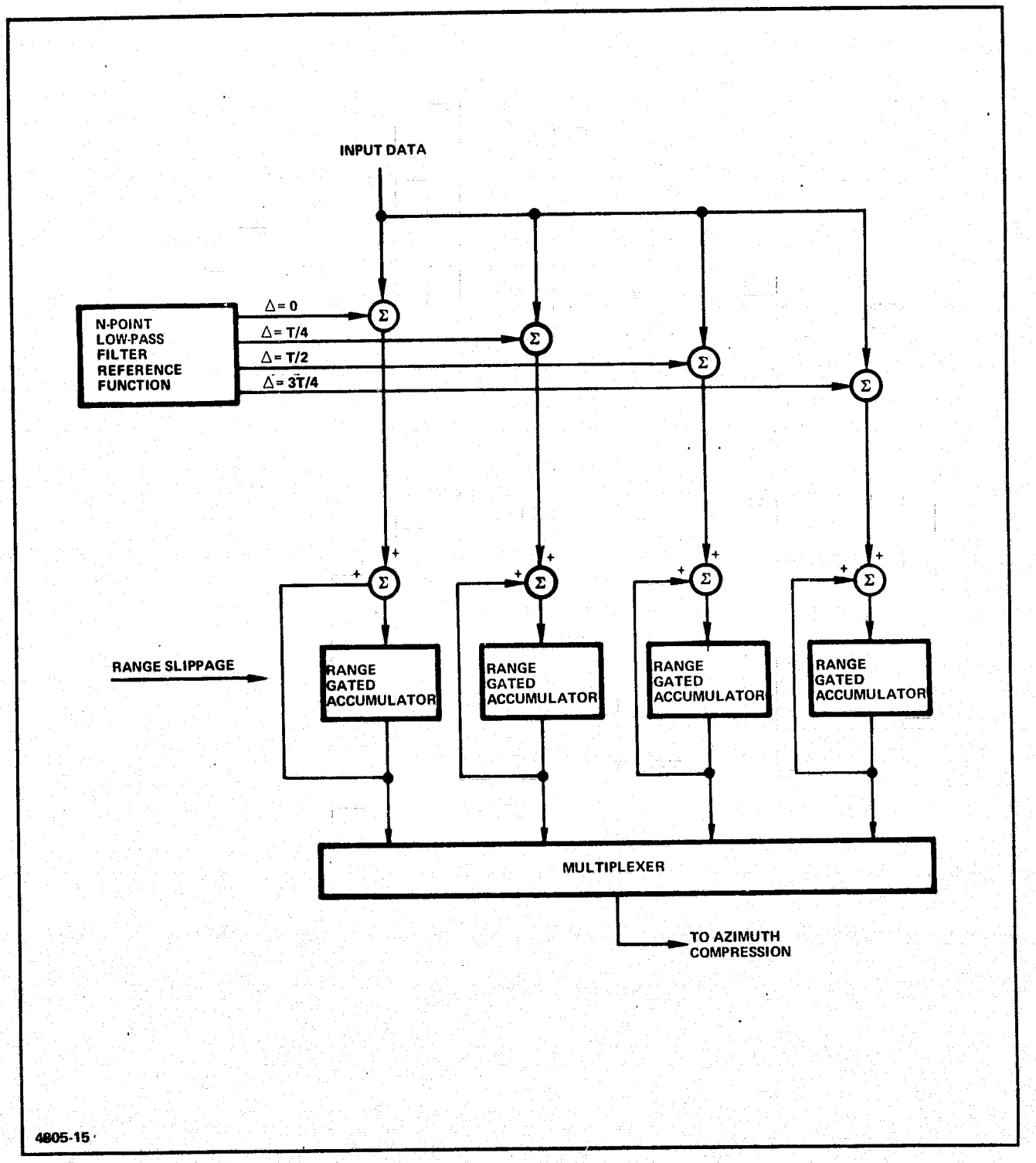

Figure 14 - Azimuth Prefilter (One of Four Sections)

Every data point entering a filter section is multiplied by N/4 evenly spaced samples of the low-pass function, and each product is added to the sum stored in one of the N/4 accumulators. After N products have been summed in any accumulator, its contents are dumped, it is cleared, and a new convolution is initiated. Thus, for every N azimuth sample input, the contents of each accumulator is dumped once.

To obtain the required sidelobe levels after azimuth compression, the filter will include a weighting function, as was done in the range dimension. Because pulse weighting and pulse compression are linear operations, weighting may be performed prior to collapsing with no detrimental effects. (In fact, weighting of the low-pass filter reference function actually reduces the complexity of the design of this device, because passband droop is now a desirable feature.)

The azimuth prefilter reference function will have only an in-phase component. Any operations requiring complex multiplications to implement will be done in the azimuth compression filter. This will simplify the arithmetic in the unit, both for the generation of the filter function, and for the hardware required to perform the convolution.

The value of N required for the azimuth prefilter will be determined by the processor integrated sidelobe specifications. Because the output data rate is being reduced by a factor of four, the power in the filter's stop band will lay over its passband threefold. Thus, a sharp transition band and low passband ripple are very desirable. Four filter sections have been assumed for this estimate, allowing for the use of a 16-point reference function.

The azimuth prefilter must handle data at the same rate as all devices preceding it, because the rate is not reduced until the data are output. Therefore, 10-MHz operation is necessary. This unit is estimated to require 30 boards with 1600 integrated circuits, and will require 750 watts.

5. AZIMUTH COMPRESSION FILTER

The azimuth compression filter (ACF) is the largest unit within the digital signal processor. It consists of an input data buffer, the 22.1 megabit azimuth compression memory, the azimuth compression reference function generator, 344 complex multipliers, four 86-point summing networks, range and azimuth interpolation networks which produce ground range samples spaced by 12.5 meters and align the azimuth looks for addition, and detectors. Each ACF section compresses data by convolving them with the proper matched filter reference function, as illustrated in Figure 15. After each compression, the data are shifted by one position, a new range sweep is entered, and the process is repeated.

In addition to the parabolic phase function necessary to compress the azimuth phase history for each of the looks, the reference function used in the ACF must account for such factors as the antenna beam shape (including such factors as those introduced by spacecraft pitch), any further weighting required for sidelobe control, changes in the ground sample positions (caused by acceleration, earth rotation, etc.), and antenna slewing. The ability of the convolution processor to continually modify the ACF reference function to optimize the processing is a major advantage of this algorithm.

The ACF reference function is complex; i.e., it has an in-phase and quadrature component. It can be expressed as

$$h(X) = f(X)\, e^{j\Phi(X)} = f(X)\left[\cos \Phi(X) + j \sin \Phi(X)\right] \quad , \qquad (13)$$

where

$h(X)$ = the complex reference function

$f(X)$ = an amplitude shaping function

$\Phi(X)$ = a real phase function

X = the azimuth coordinate

and $j = (-1)^{1/2}$.

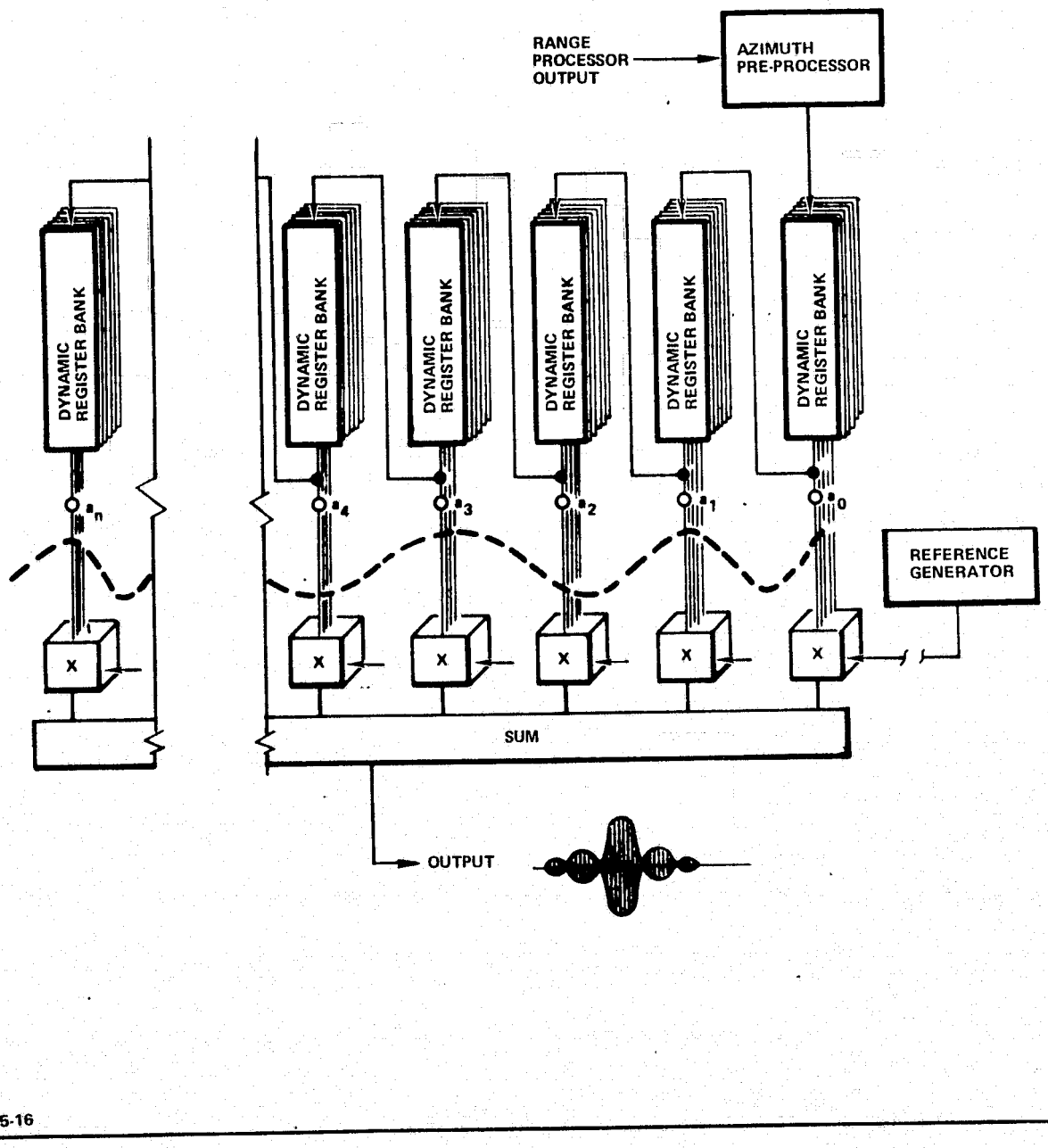

Figure 15 - SAR Processor Using the Convolution Algorithm

For the geometry illustrated in Figure 16, the phase term in the reference function is given by

$$\Phi(X) = \frac{4\pi}{\lambda} R(X)$$

$$= \frac{4\pi}{\lambda} R_o + \cos \psi_o X + \left[\frac{\sin^2 \psi_o}{2R_o}\right] X^2 + \left[\frac{\cos \psi_o \sin^2 \psi_o}{2R_o^2}\right] X^3 \quad , \qquad (14)$$

where

$R(X)$ = the slant range to the target

R_o = the slant range to the center of the synthetic aperture

ψ_o = the yaw angle plus the squint angle of the look.

The constant term can be ignored. The linear term in X, which does not depend on range, is corrected for in the range filtering. The cubic term is orders of magnitude smaller than the squared term and can be neglected. The phase function therefore becomes

$$\Phi(X) = \frac{2\pi R_o}{\lambda}\left(\frac{X \sin \psi_o}{R_o}\right)^2 \quad . \qquad (15)$$

The number of range cells for which this phase function may be used was analyzed in Section II, paragraph 5.

Upon completion of the azimuth compression, a two-dimensional interpolation must be performed. This interpolation will

1. Generate data points spaced by 12.5 meters in both range and azimuth
2. Remove the squint angle from the four azimuth looks for proper addition.

Figure 17 illustrates this process.

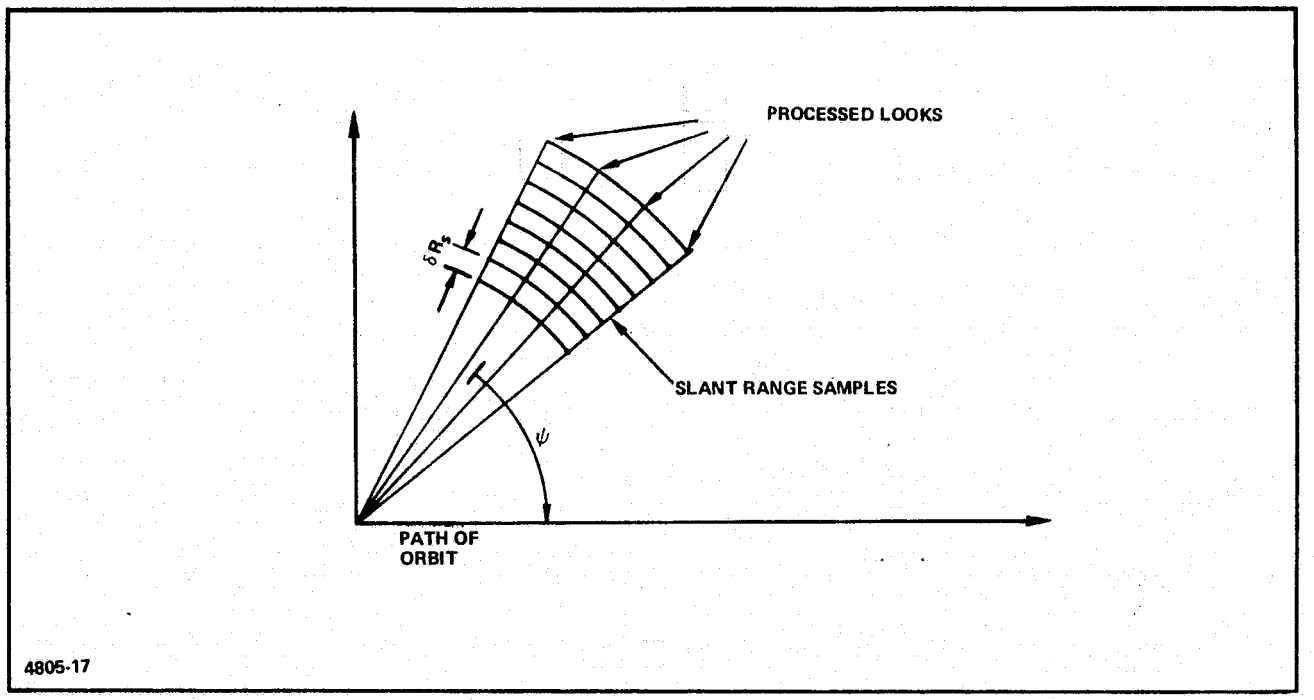

Figure 16 - Phase Term in Reference Function

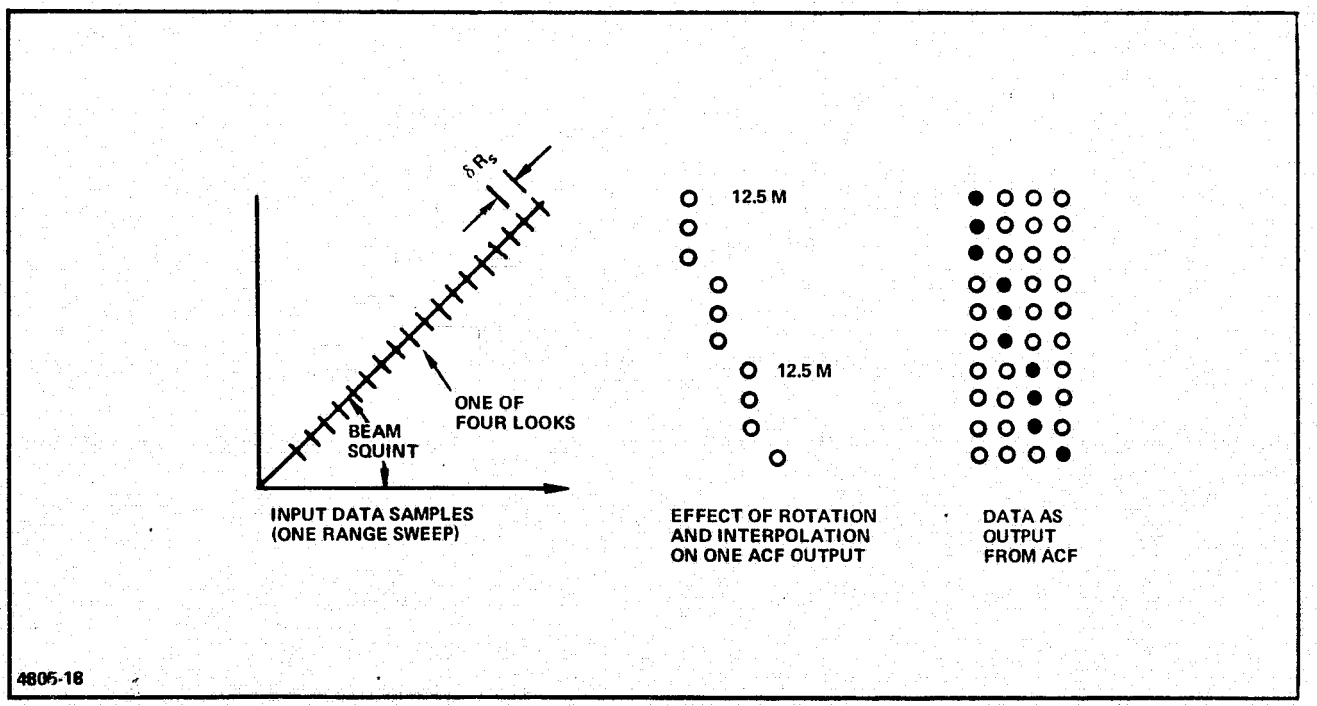

Figure 17 - Postcompression Coordinate Transformation

The slant-to-ground range conversion process was described in Section II, paragraph 6. The azimuth interpolation is a similar process in an orthogonal coordinate, although the azimuth resampling does not change the sample spacing (the sample spacing interpolation is performed in the azimuth compression filter), but only removes the processing angle.

At the completion of the interpolation processes, the signals will be detected typically by forming $(I^2 + Q^2)^{1/2}$. After azimuth look summation, the data will be encoded.

The ACF described in this section is estimated to require 180 boards. It will require 9250 integrated circuits, assuming 1350 charge-coupled devices (CCD's) (16,384-bit memories) will form the bulk storage illustrated in Figure 15. The unit is estimated to require 4350 watts.

6. AZIMUTH LOOK SUMMATION

As was described in Section II, paragraph 1, a 22-megabit cache storage is required for retaining looks until corresponding data points are available for addition. This memory required a 33.7-megabit per second access rate (9-bit words) for real-time operation. Considering the size, speed, and mode dependence of the memory accessing, a solid-state storage has been sized for the digital signal processor.

This memory has been estimated using a 64k-bit CCD, projected to be available within three years (see Section V, paragraph 1). The storage would require 336 of these devices.

The azimuth look summation circuitry is estimated to require 10 circuit boards, contain 400 integrated circuits, and consume 400 watts.

7. DIGITAL CLUTTERLOCK

Figure 18 is the basic block diagram for the proposed digital clutterlock. ROM's will be used to determine the magnitude and phase of each range compressed data point. The change in phase from sample to sample for a particular range, $\Delta\phi$, is determined by

subtraction. Next, $\Delta\phi$ is compared with the average phase change for a given range, $\overline{\Delta\phi}$, to determine the rate of change of the phase. (A constant rate of change would imply the antenna is not slewing in azimuth.) The difference in the sample value and the average value are accumulated, this process effectively filtering statistical noise. Overflow of the accumulator (either positive or negative) will cause $\overline{\Delta\phi}$ to be modified. The loop time constant will be on the order of the travel time across a small number of null-to-null azimuth beamwidths.

The amplitude circuitry serves to warn the clutterlock that the data are being received from a low return area or radar shadow and may not have sufficient signal-to-noise, or that a land-water boundary has been crossed and rapid phase change will be expected.

The range gated $\overline{\Delta\phi}$ and $\bar{A}$ estimates will be used to generate a "best fit" curve. The allowable curves are generated by computation of the zero frequency paths for the possible antenna ambiguities and rotations, as explained in Section II, paragraph 2. This information is used to track the antenna ambiguity and antenna rotation during the processing and to generate the required azimuth phase and amplitude correction signals. The information may also be stored to aid in processing of other polarizations or frequencies.

The digital clutterlock will receive computational assistance from the microprocessor and a general-purpose minicomputer. It is estimated to require 10 boards, 600 integrated circuits, and consume 200 watts.

8. PROCESSOR COMPUTATION AND CONTROL DEVICES

A high-speed microprocessor is used to control the digital signal processor. It is used to generate filter reference function coefficients and perform other varied computations which must be made periodically, as well as interface the digital signal processor with external equipment. It is estimated that the microprocessor required for this application will require 10 circuit boards, 600 integrated circuits, and consume 250 watts.

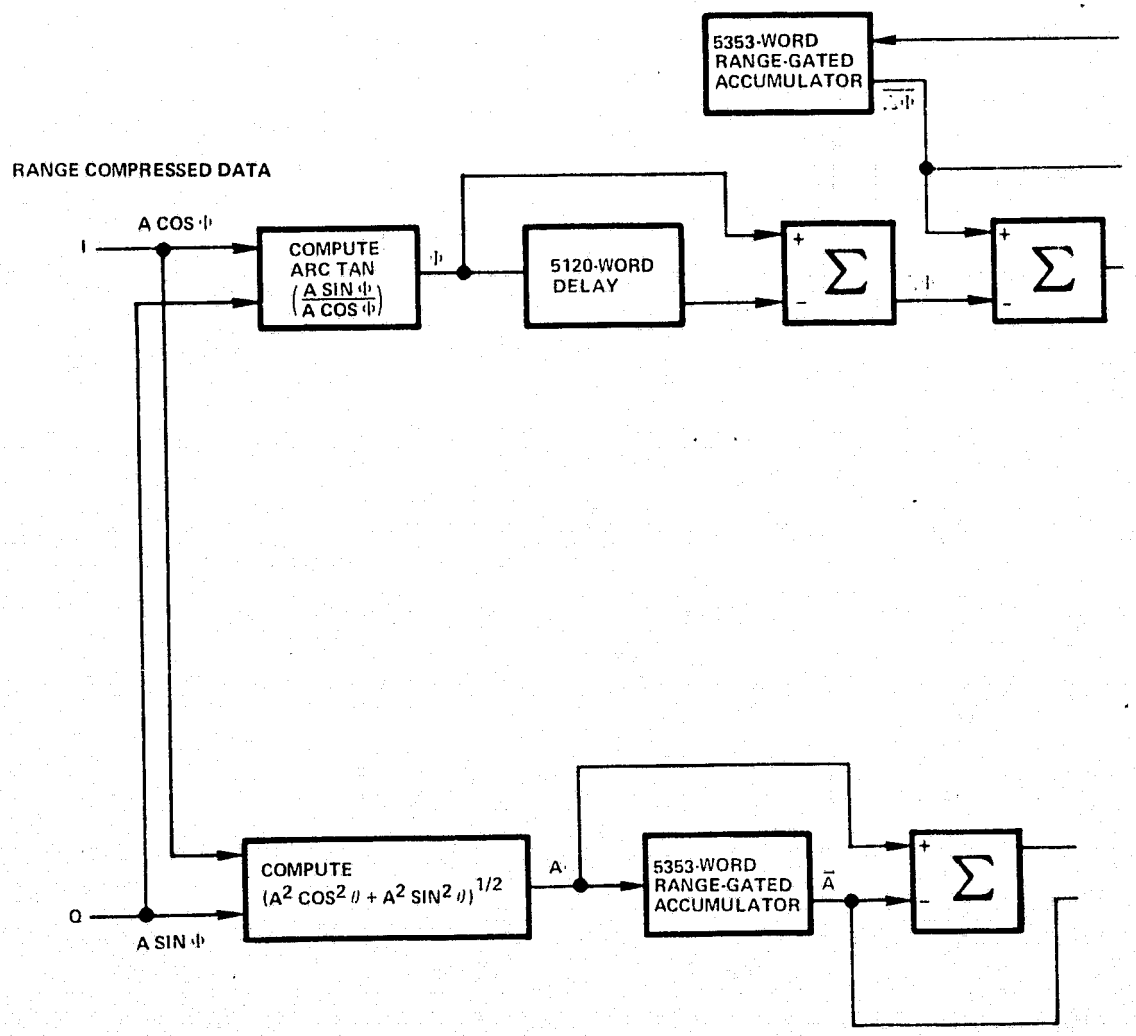

ORIGINAL PAGE IS
OF POOR QUALITY

4805-3

Figure 18. Digital Phase Clutterlock (Sheet 1 of 2)

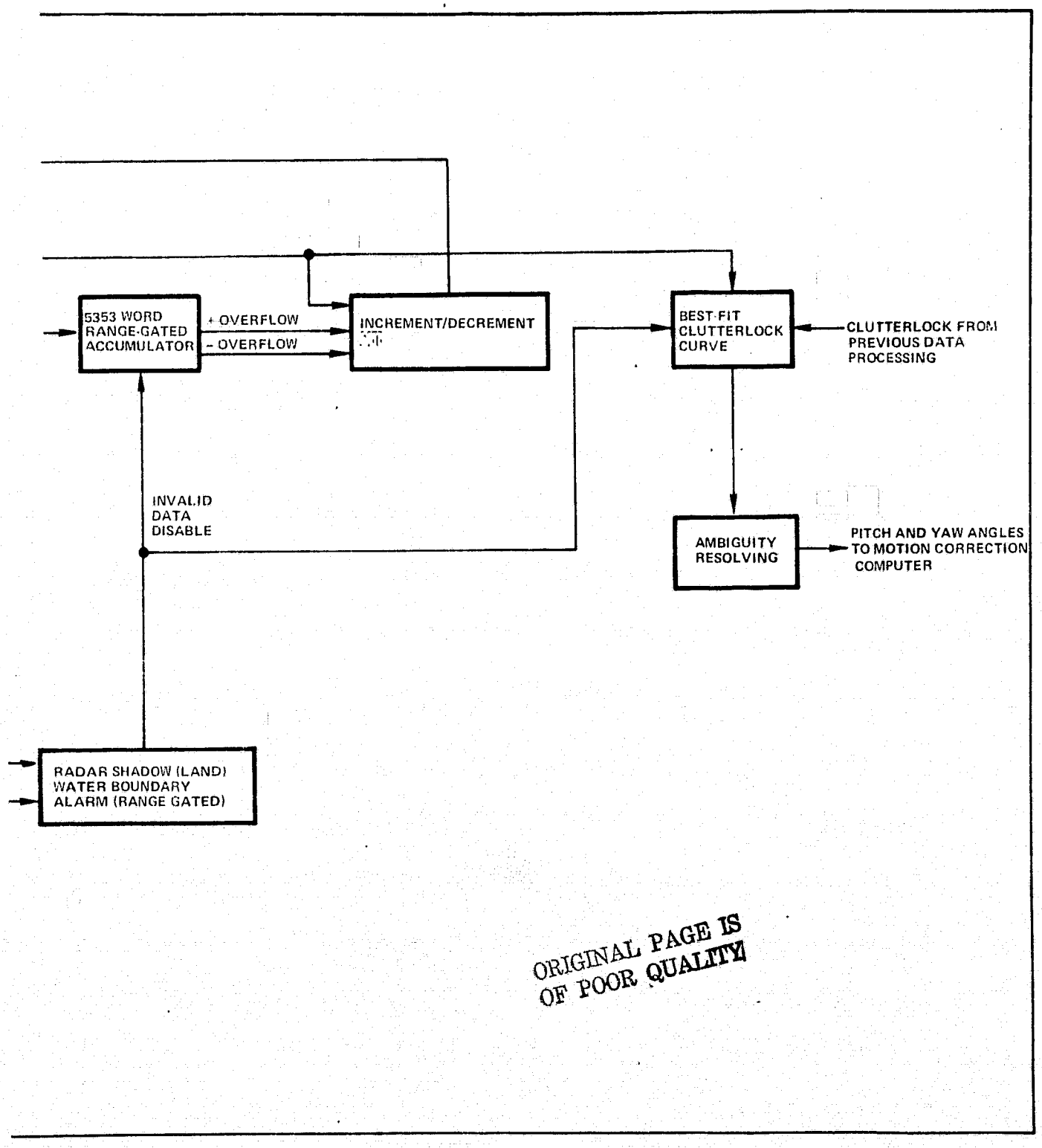

Figure 18. Digital Phase Clutterlock (Sheet 2 of 2)

An associated minicomputer will serve a variety of purposes from generation of test signals while off-line to performing calculations involving spacecraft position, velocity, acceleration, and attitude while on-line. It should be able to utilize information from the data tapes as well as data from ground-based tracking stations, thus interfacing the processor with auxiliary data devices.

Any of a host of commercially available small computers are available for this task. The specifics of the machine depend much upon the various uses for which it is intended (especially when off-line). Typically, such a machine requires 1500 watts.

9. BUILT-IN TEST EQUIPMENT (BITE)

For a digital signal processor of this magnitude, rapid fault isolation is imperative. A testing philosophy which processes radar data in multiple locations while the processor is on-line and comparing the processed outputs has proven to be an excellent method of accomplishing this task. A well-designed BITE system, using the concept, will isolate a fault to a replaceable unit, which may be replaced immediately and repaired when time permits.

The BITE will make extensive use of integrated circuit microprocessors, utilizing their inherent power to perform calculations identical to those performed by the processor (but at a reduced rate of speed and with a greatly reduced number of integrated circuits) and to compare the results with sampled processor values.

For this processor, it is estimated that the BITE will require 20 circuit boards, 1200 integrated circuits, and consume 450 watts.

10. SUMMARY OF PROCESSOR COMPONENTS

Processor components in the space shuttle radar are summarized below:

Unit	No. of boards	No. of IC's	Power
Range compression filter	30	2,250	750
Range amplitude, phase and sidelobe control	10	600	300
Azimuth prefilter	30	1,600	750
Azimuth compression filter	180	9,250	4,350
Azimuth look summation	10	400	400
Digital clutterlock	10	600	200
Microprocessor	10	600	250
BITE	20	1,200	450
General-purpose minicomputer	-	-	1,500
Total	300	16,500	8,950

It is estimated that the processing system and all peripheral equipment will be packaged in three racks, sized 6-1/2 feet by 2-1/2 feet by 2 feet, and have a total weight of 3000 pounds.

The processor estimate has been based on previously described CCD memory devices and predominantly Schottky logic, with a reduced size and power consumption factor based on anticipated advances in LSI devices described in Section V.

11. PROCESSOR GROWTH

The processor described in Section IV could be used with minor modifications (primarily time constants) to process data from 278- and 370-km orbits. The four-look operation would be retained, and the resulting azimuth resolutions would be 30.65 and 35.36 meters for the respective orbits. Maintaining 25-meter resolution with fewer looks would be possible, but the modification is more complex.

If 25-meter resolution is to be maintained, the size of the ACF and azimuth look summation networks will increase linearly with range. Thus, for operation at 370-km altitude, it is anticipated that an additional 190 circuit boards will be necessary, thereby increasing the processor size by over 60 percent.

SECTION V - TECHNOLOGY SURVEY

1. GENERAL

A portion of this program was spent examining new memory and logic technologies which may influence the processor design. Emphasis was placed upon determining the advancements which had a high probability of resulting in major new products available within the next three years. In this section, the results of the technology survey will be presented. Table IV lists the names and addresses of individuals contacted.

2. MEMORY TECHNOLOGY

The most promising technology for producing large memory devices with high data rates is the CCD. This technology should be used to mass produce memory devices of 16k bits and larger, having data rate of 10 MHz, and dissipating a mere 10 μW per bit within the next year. The per-bit price for commercial devices has been projected to be less than one-tenth cent per bit in three to five years.

Digital CCD's having 16,384 bits have recently been announced by Intel, Fairchild, and Bell-Northern. Intel's device is constructed as 64 parallel, 256-bit multiplexed shift registers with single data input and data output pins. It requires four phased clock signals. The read/modify/write cycle time is 620 ns. The Fairchild device is organized as four parallel 4096-bit devices, each composed of 32 parallel 128-bit multiplexed shift registers. Each section has a read/modify/write cycle time of 300 ns. The device only requires one clock. The Bell-Northern device is organized as four parallel 4096-bit shift registers. It requires two phased clocks. The Northern-Bell device is in a 16-pin package, Intel in an 18-pin package, and Fairchild a 24-pin package. The Fairchild and Bell-Northern devices would be preferable for the proposed processor.

TABLE IV - CONTACTS WITH SEMICONDUCTOR MANUFACTURERS AND CONTRACTORS

Organization	Name	Technology	Address/phone
Texas Instruments	Richard Horton	I^2L	713-494-5115
	Jerald McGee	I^2L	713-494-5115
Motorola	James Bunkley	I^2L	602-244-3714
	Robert Jenkins	EFL	602-962-3346
TRW	Barry Dunbridge	EFL	TRW Systems Group, One Space Park, Redondo Beach, CA 90278
RCA	Albert Sheng	I^2L/SOS	201-722-3200 (2612)
	Raymond Minet	CCD	717-397-7661 (2294)
	Michael Diagostino	SOS	201-722-3200 (2507)
Fairchild	Frank Bower	CCD	415-493-7250 or 8001
Intel	Kenneth Kwong	CCD	408-246-7501
	Donald Bryson	CCD	408-246-7501
Air Force Avionics Laboratory	Ronald Belt	CCD	513-255-2459
	Millard Mier	Magnetic Bubbles	513-255-2459
	Stewart Cummins	Magnetic Bubbles	513-255-2459
Bell-Northern Research	William Coderre	CCD/SOS	613-596-4439, Manager, Technology Liaison, Dept. 5G20, Bell-Northern Research, P.O. Box 3511, Station C, Ottawa, Canada KIY487

It should be emphasized, however, that CCD development is oriented toward the computer industry, and that CCD's will require operating conditions with temperatures below 70 deg C. Thus, for a ground station processor, they appear to be an excellent memory device, but for spacecraft operation, both component qualification and careful thermal design will be necessary, both of which could prove extremely expensive.

Conventional MOS technology appears to be rushing to meet the challenge of CCD's. The announcement of a 16,384-bit MOS random access memory (RAM) was hinted at by several manufacturers, but a formal announcement will probably not be made during 1975. Prices of these devices have been projected to be competitive with CCD's.

Magnetic bubble technology was discussed with the Air Force Avionics Laboratory. This technology does not appear imminent enough for the proposed processor timetable.

Integrated injection logic (I^2L) is a bipolar technology which may also be a viable alternative within the next few years. A 4096-bit RAM using this technology is anticipated by the end of this year, and much larger devices are projected. I^2L has very high packing densities, requires relatively low power, and has a -55-degree to +125-degree Celsius temperature range.

3. LOGIC TECHNOLOGIES

During the next three to five years, small, medium, and large scale integration (SSI, MSI, and LSI) high-speed logic families will probably continue to utilize Schottky and low-power Schottky TTL and ECL. These logic families are very large, readily available, familiar to designers, and have reached near minimum cost. Although new devices will be emerging, they will probably be improvements on and extensions of existing logic families.

Three new technologies which are being heralded for very large scale integration devices are integrated injection logic (I^2L), emitter follower logic (EFL), and silicon-on-sapphire CMOS (SOS). Texas Instruments appears to have the largest I^2L development program.

A four-bit microprocessing element, the SBP0400, has already been introduced, and the company projects a full line of computer products within three years. Among the advantages of I^2L technology are extremely high packing density (a factor of 10 above TTL), static operation, TTL compatibility, a -55-deg to +125-deg C temperature range, and a virtually constant propagation power product.

The SOS technology is being most strongly pursued by RCA. A large number of LSI devices are also projected for introduction within a year. If successfully produced, SOS CMOS circuits promise Schottky TTL speeds with one to two order of magnitudes less power consumption. The SOS technology should be faster because of the lower parasitic capacitance of the sapphire substrate and have higher densities than conventional CMOS by at least a factor of two.

The major obstacle to SOS technology appears to be the cost of the sapphire substrate, which presently is 10 times that of conventional silicon. RCA feels, however, that eventual demand for these devices will greatly lower production costs, making them competitive with conventional CMOS.

The EFL technology has been referred to as a "Cinderella" and a "sleeper." This pre-TTL configuration is being studied by such companies as TRW and Motorola. EFL circuits have the same cell size as I^2L but promise much higher speeds. EFL may be the longest in development of these technologies, because Motorola says no marketable products are presently in development, and TRW has produced only customized devices.

SECTION VI - PROCESSOR COSTING AND SCHEDULING

1. GENERAL

Paragraph 2 of this section presents costing of the design and development of a ground-based processor described in Section IV in terms of man-hours and material dollars and a program schedule (two years) over which the program would last. Paragraph 3 discusses factors which must be considered if a spaceborne processor is to be constructed.

2. GROUND-BASED PROCESSOR

Table V lists costs of developing a ground-based processor system. Figure 19 is the program schedule. A manloading estimate for this program is shown at the bottom of the figure. This processor has been costed on the basis of a laboratory environment, the use of commercial grade components, and commercial design and development practices. The playback recorder has not been included in the cost estimate.

3. SPACEBORNE PROCESSING SYSTEM

Costing and scheduling of the development of a spaceborne processing system is extremely speculative with the information available at this time. When the design parameters become better defined, it is felt that these numbers may be factored into the data presented in Table V to estimate the actual cost.

Discussions with engineers involved in the development of previous spacecraft systems have tended to project a three-year development program is possible (although a highly coordinated effort is required). This estimate is speculative as many parameters affecting the program are not defined.

TABLE V - GROUND-BASED PROCESSOR COSTING

Item	Hours (senior)	Hours (junior)	Computer	Material (dollars)
Program administration	7,000	7,000	200	
Systems studies	6,000	1,500	200	
Design and development	8,500	31,000	500	100,000
System fabrication	7,000	41,000	50	200,000
System integration and testing	3,000	6,000	50	
Acceptance testing	400	800		
Documentation	4,000	8,500		
Installation and checkout	100	500		
Operation and maintenance training	500	500		
Total	36,500	96,800	1,000	300,000

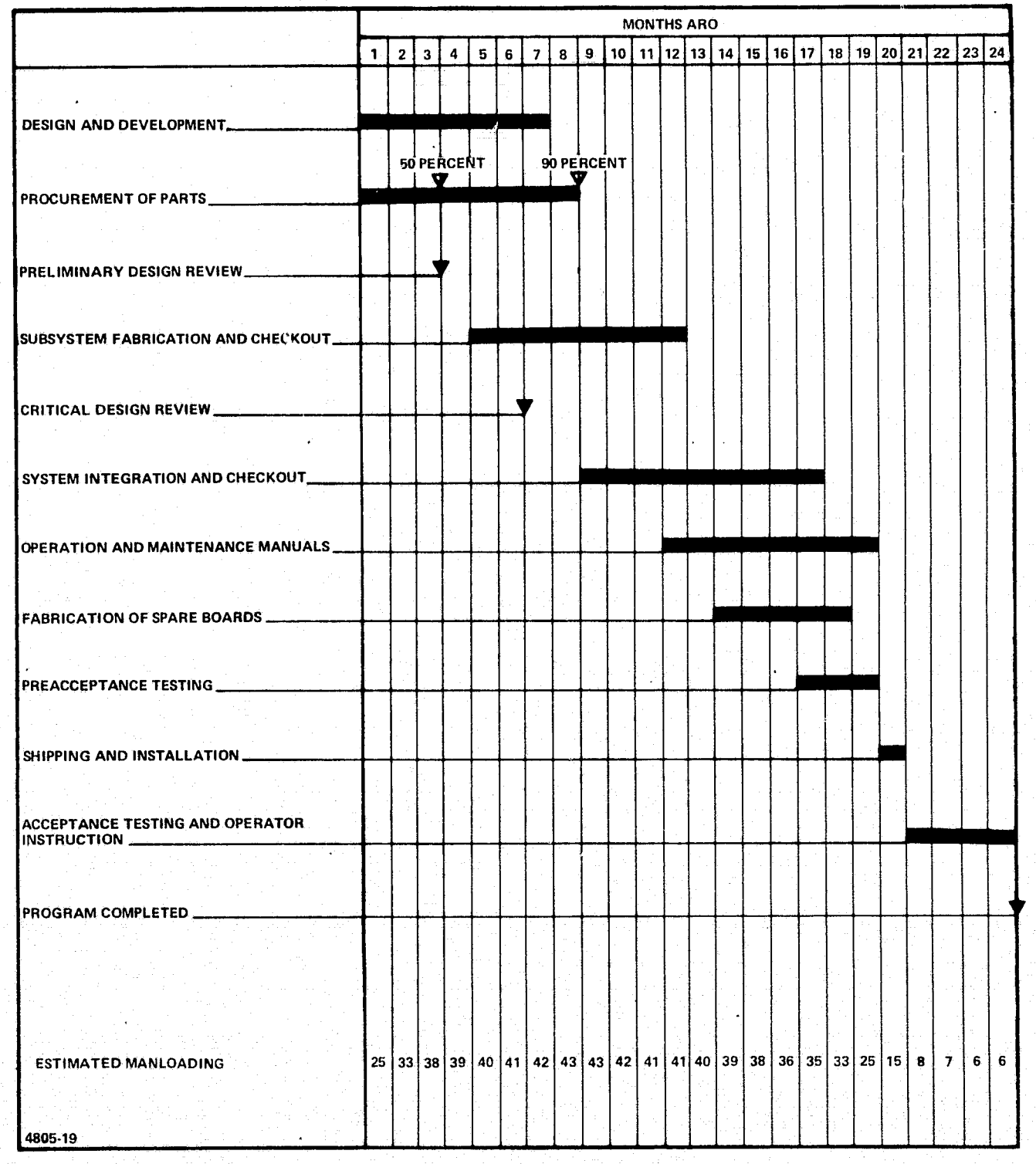

Figure 19 - Space Shuttle SAR Digital Signal Processor Development Schedule (Ground-Based Processor)

Thus, although a spaceborne processing system could most certainly be developed, its extended program time and much higher cost must be carefully weighed against the benefits it could produce.

SECTION VII - CONCLUSIONS

A digital signal processor for producing imagery made from a spaceborne radar operating at L- and X-band is indeed feasible. Indeed, more complex processors than this are presently being built. The processor may be deployed either as a ground-based system, fed by tape recorded and/or data linked data, or as a piece of equipment in the manned laboratory area of the shuttle.

The increased cost of a spaceborne processor plus the increased development time (based on experience with previous spaceborne hardware) weigh heavily against this option. Unless real-time operation for any possible orbit (i.e., the need for processing data exists when a data link to a ground-based processor is not available) is absolutely necessary, the cost effectiveness of this option seems very low.

The technology to build this processor exists today. Future advances in memory and LSI will be able to reduce its size, cost, power consumption, etc., but as the complete capability of the radar is being utilized, no improvement in performance will result.

NASA — JPL — Coml., L.A., Calif.